Tampere University

SUVI HOLMSTEDT

Conversion of Biomass-Based Compounds into Added-Value Chemicals

Synthetic Modifications of Quinic Acid

Tampere University Dissertations 466

Tampere University Dissertations 466

SUVI HOLMSTEDT

Conversion of Biomass-Based Compounds into Added-Value Chemicals

Synthetic Modifications of Quinic Acid

ACADEMIC DISSERTATION
To be presented, with the permission of
the Faculty of Engineering and Natural Sciences
of Tampere University,
for public discussion in the Auditorium RG202
of the Rakennustalo building, Korkeakoulunkatu 5, Tampere,
on 24th September, at 12 o'clock.

ACADEMIC DISSERTATION
Tampere University, Faculty of Engineering and Natural Sciences
Finland

Responsible supervisor	Assistant Professor Nuno R. Candeias University of Aveiro Portugal	
Supervisor and Custos	Professor Arri Priimägi Tampere University Finland	
Pre-examiners	Professor Vittorio Pace University of Turin Italy	Associate Professor with Habilitation Teresa Pinho e Melo University of Coimbra Portugal
Opponent	Associate Professor Christian Marcus Pedersen University of Copenhagen Denmark	

The originality of this thesis has been checked using the Turnitin OriginalityCheck service.

Copyright ©2021 author

Cover design: Roihu Inc.

ISBN 978-952-03-2086-7 (print)
ISBN 978-952-03-2087-4 (pdf)
ISSN 2489-9860 (print)
ISSN 2490-0028 (pdf)
http://urn.fi/URN:ISBN:978-952-03-2087-4

PunaMusta Oy – Yliopistopaino
Joensuu 2021

ACKNOWLEDGEMENTS

The research presented in this thesis was carried out in the Laboratory of Chemistry and Bioengineering at Tampere University (previously Tampere University of Technology) during the years 2017–2021. I would like to kindly acknowledge The Finnish Cultural Foundation (decision 00190336) for personal grant, the Academy of Finland (Decisions no. 294067 and 326416) and Fundação para a Ciência e Tecnologia (SRFH/QUI-QOR/1131/2020) for funding this research and securing the continuation of this project.

My profoundest gratitude goes to my supervisor, Assistant Professor Nuno R. Candeias. I am grateful for all the support, guidance, and understanding over these years. You have found the right words in the moments of desperation and made me feel worth something. I am grateful that you let me to do mistakes, learn and understand and to grow independent while knowing I'm not alone. Over the years, depending on the situation you have adapted multiple roles such as supervisor, psychologist and friend, which is a true skill of how to lead people. I would also like to thank my second supervisor Professor Arri Priimägi for adopting me into your group with open arms after Nuno's transition to Aveiro.

Professor Vittorio Pace and Associate Professor Teresa Pinho e Melo are sincerely thanked for the pre-examination of this thesis. Thank you for your valuable comments. I would also like to thank all the collaborators of my research work. Also, many thanks to all staff at the department of Chemistry and Advanced materials.

I would like to express my gratitude to Professor Petri Pihko for sparking the interest towards organic chemistry and total synthesis back in the days. Your supporting words during the years as well as hiking tips have kept me positive. To my dear colleagues at laboratory: thank you for making the enjoyable atmosphere! Especially I would like to thank everybody in RedLabs. Very special thanks to Rafael Vale for your friendship, Tuesday burgers, refreshing challenges, practical jokes and all the help. I would also like to thank Dr. Benedicta Assoah for encouraging words and fruitful discussions at the office. Also, many thanks to my lab mates Dr. Jagadish Salunke, Dr. Rakesh Puttreddy, Kim Kuntze and others for the warm and fun atmosphere in the lab and at lunchtime. Great thanks to Dr. Suvi Lehtimäki for making the lab functional!

Very special thanks to my ex-colleagues and friends Dr. Juha Siitonen, Dr. Sami Kortet and Saara Riuttamäki. Our annual "pikkujoulu conferences" and active WhatsApp-group have given me joy and encouragement. You have been the best listeners and peer-support of all! Thanks to my Jyväskylä-girls for relaxing weekend get-togethers, care and support. Of the friends from Tampere, I would like to express my special thanks to Jenni and Sini. Sauna evenings with Jenni and adventures in the forest and nightlife with Sini have helped me to recover in the middle of busy and stressing moments. All the rest of the friends, thank you for the support, joy, love and care!

Last but not least, I want to give my sincerest acknowledgements to my family. Mom and dad, thank you for letting me be myself and make my own decisions while enjoying your support.

”Two roads diverged in a wood, and I —,
I took the one less traveled by,
and that has made all the difference."

— Robert Frost

Lämmin kiitos kaikille, jotka ovat olleet läsnä näiden vuosien varrella, kannustaneet ja kuunnelleet. Olen onnellinen, kiitollinen ja ylpeä.

Tampere, July 30th, 2021
Suvi Holmstedt

ABSTRACT

Fossil-based resources currently provide the energy and feedstock chemicals to sustain our ways of living. A transition from crude oil to biorenewables is essential to provide sustainable energy sources and alternative routes for fine chemicals in the future. Such transition is challenging due to the over-functionalized nature of biomass-based molecules, as they have an oxygen-containing group in almost every carbon. In turn, the fossil-based chemicals we currently use are under-functionalized, therefore the methods for exploiting these resources are very different. In light of this, selected current methods for defunctionalization of biomass-based molecules are surveyed in this thesis, followed by review on the synthetic manipulation of quinic acid, a biomass-derived cyclitol.

Quinic acid occurs widely in plants and microorganisms and can serve as starting material in the synthesis of chiral compounds. This thesis studies the valorization of quinic acid and is focused on the removal of hydroxyl groups permitting the formation of chiral building blocks for use in the synthesis of natural products.

The use of tris(pentafluorophenyl)borane combined with hydrosilanes is a contemporary tool in the site selective deoxygenation of biomass-derived feedstocks and was explored in the valorization of quinic acid. The borane-catalyzed hydrosilylation through a silyloxonium intermediate led to formation of unforeseen synthetic fragments by diversification of reaction conditions. The divergent defunctionalization provided access to chiral aldehydes, alcohols and tetrahydrofuran derivatives and eventually expanded to the formal synthesis of homocitric acid. The deoxygenation mechanism was rationalized by Density Functional Theory calculations.

O,O-Silyl migrations across quinic acid derivatives were observed during the deoxygenation experiments. Such migrations were further studied and optimized, resulting in selective formation of silylated regioisomers. The migration reactions were observed to be dependent on the reaction conditions and silyl substituents. One of the regioisomers obtained was further modified to build the first total synthesis of an African ant cyclitol and the formal synthesis of kidney disease drug VS-105.

A redesigned concise total synthesis of epimeric natural carbasugars isolated from *Streptomyces lincolnensis* is presented in this thesis. The synthesis had as key steps the regioselective reduction of quinic acid and the epimerization of one of the intermediates to create a divergent point.

Lastly, several quinic acid derivatives were synthesized, and their biological properties briefly assessed, leading to the identification of a particular derivative as a promising lead for the development of glioblastoma multiforme chemotherapeutic agents.

The findings presented in this thesis deepen the versatility of quinic acid as a chiral scaffold. Although quinic acid has been used as a chiral pool molecule for decades, application of modern synthetic methods provides a powerful tool for diversification of common intermediates. The protocols presented also expand the group of chiral fragments that can be obtained from biorenewables. The facility of creating a divergent point also enables studying how structural modification of quinic acid derivatives correlates with the bioactivity.

TIIVISTELMÄ

Energiantuotantoon ja kemikaalien valmistukseen käytettävät raaka-aineet ovat pääosin fossiilisia. Tulevaisuudessa nämä on korvattava biopohjaisilla raaka-aineilla. Siirtymä on kuitenkin haastava, sillä biomassapohjaiset molekyylit ovat erittäin funktionalisoituja eli lähes jokainen hiiliatomi muodostaa sidoksen happea sisältävään funktionaaliseen ryhmään. Tällä hetkellä käyttämämme fossiilipohjaiset kemikaalit ovat puolestaan alifunktionalisoituja, joten resurssien hyödyntämismenetelmät ovat hyvin erilaiset. Tässä väitöskirjassa tutkitaan menetelmiä biomassapohjaisten molekyylien, kuten kiinihapon defunktionalisoimiseksi ja käyttämiseksi synteesissä.

Kiinihappoa esiintyy laajasti kasveissa sekä mikro-organismeissa ja sitä voidaan käyttää lähtöaineena kiraalisten molekyylien synteesissä. Tämän väitöskirjan kokeellisessa osuudessa tutkittiin kiinihapon käyttöä synteesin lähtöaineena ja keskityttiin erityisesti hydroksyyliryhmien selektiiviseen poistamiseen. Näin saadaan aikaiseksi yksinkertaistettuja kiraalisia fragmentteja, joita voidaan käyttää luonnonainesynteesissä.

Tris(pentafluorofenyyli)boraanin käyttö silyylihydridien kanssa on nykyaikainen menetelmä happea sisältävien funktionaalisten ryhmien poistamiseen biomassapohjaisista molekyyleistä. Tässä väitöskirjassa tätä menetelmää tutkittiin käyttäen lähtöaineena kiinihappoa. Reaktio-olosuhteita muuttamalla boraanikatalysoitu hydrosilylointi tuotti uusia synteettisiä fragmentteja silyylioksonium-välituotteen kautta. Haarauttava defunktionalisointimenetelmä tuotti kiraalisia aldehydejä, alkoholeja, tetrahydrofuraanijohdannaisia sekä homositruunahapon muodollisen synteesin. Reaktiomekanismia tutkittiin tiheysfunktionaaliteorian avulla.

Deoksygenaatiokokeiden aikana havaittiin kiinihappojohdannaisten *O,O*-silyylivaelluksia. Vaellusreaktioiden tutkiminen ja optimointi johti regioisomeerien selektiiviseen muodostumiseen. Vaellusten havaittiin riippuvan reaktio-olosuhteista ja käytetyistä silyylisubstituenteista. Yhtä regioisomeeriä käytettiin lähtöaineena afrikkalaisista muurahaisista eristetyn luonnonaineen kokonaissynteesissä sekä munuaislääke VS-105:n muodollisessa synteesissä.

Tässä väitöskirjassa on myös esitetty *Streptomyces lincolnensis* -bakteerista eristettyjen epimeeristen karbasokerien lyhyt kokonaissynteesi. Synteesin keskeisinä vaiheina oli kiinihapon regioselektiivinen pelkistys sekä välituotteen epimerisointi toiseksi luonnonaineeksi.

Väitöskirjan viimeisessä osassa on esitetty useiden kiinihappojohdannaisten synteesi ja lyhyt arviointi niiden biologisista ominaisuuksista. Tämän avulla tunnistettiin potentiaalinen johdannainen glioblastooma multiformen kemoterapeuttiseen hoitoon.

Tämä väitöskirjatutkimus monipuolistaa kiinihapon käyttöä kiraalisten molekyylien lähtöaineena. Vaikka kiinihappoa on käytetty synteesin lähtöaineena vuosikymmenten ajan, työssä esitettyjen modernien menetelmien soveltaminen mahdollistaa yhden välituotteen haarauttamisen useiksi uusiksi tuotteiksi. Näin voidaan laajentaa biomassasta saatavien kiraalisten fragmenttien monimuotoisuutta. Synteesin haarauttaminen mahdollisti myös molekyylikirjastojen rakentamisen. Niiden avulla tutkittiin, miten kiinihappojohdannaisten rakenteelliset erot vaikuttavat niiden bioaktiivisuuteen.

CONTENTS

ACKNOWLEDGEMENTS......iii

ABSTRACT......v

TIIVISTELMÄ......vii

ABBREVIATIONS......xi

ORIGINAL PUBLICATIONS......xv

AUTHOR'S CONTRIBUTION......xvii

1 INTRODUCTION TO VALORIZATION OF BIOMASS......1
  1.1 Carbohydrates and carbacycles in nature......3

2 DEOXYGENATION OF BIOLOGICALLY SOURCED POLYOLS......5
  2.1 Catalytic deoxygenation of biomass-derived feedstocks......5
  2.2 Partial deoxygenation of polyols......8
  2.3 Conclusions on biomass deoxygenation......11

3 SYNTHETIC APPLICATIONS OF QUINIC ACID......13
  3.1 Production and availability of quinic acid......13
  3.2 Reactions of quinic acid......14
    3.2.1 Protection of hydroxyl groups......14
    3.2.2 Deoxygenation of quinic acid......20
    3.2.3 Oxidative C–C cleavage......23
  3.3 Quinic acid in total syntheses......26
  3.4 Use of quinic acid in medicinal chemistry......30

4 MATERIALS AND METHODS......35
  4.1 Compound characterization......35
  4.2 Computational details......36
  4.3 Experimental section......37
    4.3.1 General procedure for $B(C_6F_5)_3/R_3SiH$ deoxygenation......37
    4.3.2 General procedure for Malaprade reaction......38

4.3.3 General procedure for silyl migration reaction 39
4.3.4 Gilman reaction 40

5 $B(C_6F_5)_3$-CATALYZED DEOXYGENATION OF QUINIC ACID DERIVATIVES 43
5.1 Aim of the study 43
5.2 Initial studies 43
5.3 Deoxygenation studies 46
5.4 Valorization of deoxygenation products 48
5.5 Mechanistic insight 50

6 *O,O*-SILYL GROUP MIGRATIONS IN QUINIC ACID DERIVATIVES: TOWARDS DIVERGENT SYNTHESIS 55
6.1 Aim of the study 55
6.2 Silyl group migration in quinic acid derivatives and the effect of the protecting groups 55
6.3 Total synthesis of African ant cyclitol 58
6.4 Formal synthesis of VS-105 62

7 CONCISE TOTAL SYNTHESIS OF NATURAL CARBASUGARS 65
7.1 Aim of the study 65
7.2 Isolation of the carbasugars and previous total synthesis 65
7.3 Total synthesis of natural carbasugars isolated from *S. lincolnensis* 67

8 QUINIC ACID DERIVATIVES: ANTICANCER EFFECT ON GLIOBLASTOMA 73
8.1 Aim of the study 73
8.2 Preliminary biological screening 73
8.3 Quinic acid amides 74
8.4 Cytotoxicity results 76

9 CONCLUSIONS 77

REFERENCES 79

PUBLICATIONS 93

ABBREVIATIONS

Ac	acetyl
AD-mix-β	catalyst, mixture of reagents containing phthalazine adduct with dihydroquinidine
AIBN	2,2’-azobis(2-methylpropionitrile)
Amberlyst-15	polystyrene based ion exchange resin
aq.	aqueous
Ar	aryl
$BAr_{3,5\text{-}CF3}$	tris(3,5-difluorophenyl)borane
Bn	benzyl
Boc	*tert*-butoxycarbonyl
BOM	benzyloxymethyl acetal
Bu	butyl
Bz	benzoyl
cat.	catalyst
Cp	cyclopentyl
CSA	camphorsulfonic acid
Cy	cyclohexyl
DAHP	3-deoxy-D-arabinoheptulosonate 7-phosphate
DBU	1,8-diazabicyclo[5.4.0]undec-7-ene
DFT	density functional theory
DHQ	3-dehydroquinate, 3-dehydroquinic acid
DIBAL-H	diisobutylaluminium hydride
DMAP	4-dimethylaminopyridine
DMF	dimethylformamide
DMP	Dess-Martin periodinane
DMSO	dimethylsulfoxide
DODH	deoxydehydration
E	*entgegen,* stereodescriptor for double bonds, following the Cahn–Ingold–Prelog priority rules, the higher priority groups are on opposite sides of the double bond

equiv.	equivalents
Et	ethyl
HBCat	catecholborane
HDO	hydrodeoxygenation
HMDS	hexamethyldisilazane
i	iso
IC_{50}	half maximal inhibitory concentration
im	imidazole
KHMDS	hexamethyldisilazane potassium salt
LN299	human brain glioblastoma cell line
*m*CPBA	*meta*-chloroperbenzoic acid
Me	methyl
MOM	methoxymethyl ether
Ms	methanesulfonyl (mesyl)
MS	molecular sieves
n	normal; linear chain
n.d.	not determined
n.r.	no reaction
NBS	*N*-bromosuccinimide
NMI	*N*-methylimidazole
NMR	nuclear magnetic resonance spectroscopy
nOe	nuclear Overhauser effect
NOESY	nuclear Overhauser effect spectroscopy
NP	nanoparticle
Ns	nitrobenzenesulfonyl
OAc	acetate
OMe	methoxy
p	para
PCC	pyridinium chlorochromate
PDC	pyridinium dichromate
Pg	protecting group
Ph	phenyl
Pr	propyl
pyr	pyridine
quant.	quantitative
R	a general abbreviation for an atom or a group of atoms

r.t.	room temperature
R_f	retardation factor
Si	a general abbreviation for R_3Si-group
SiH	a general abbreviation for R_3SiH
t-/*tert-*	tertiary
TBAF	tetrabutylammonium fluoride
TBDMS	*tert*-butyldimethylsilyl
TBDPS	*tert*-butyldiphenylsilyl
TCDI	thiocarbonyldiimidazole
Tebbe's reagent	μ-Chloro[di(cyclopenta-2,4-dien-1-yl)]dimethyl(μ-methylene)titaniumaluminum
TEMPO	(2,2,6,6-tetramethylpiperidin-1-yl)oxyl
Tf	trifluoromethanesulfonate
TFA	trifluoroacetic acid
TFAA	trifluoroacetic acid anhydride
THF	tetrahydrofuran
TLC	thin layer chromatography
TMS	trimethylsilyl
Ts	*p*-toluenesulfonyl (tosyl)
UHP	urea hydrogen peroxide
Z	*zusammen*, stereodescriptor for double bonds, following the Cahn–Ingold–Prelog priority rules, the higher priority groups are on same side of the double bond

ORIGINAL PUBLICATIONS

Publication **I** Suvi Holmstedt, Lijo George, Alisa Koivuporras, Arto Valkonen, and Nuno R. Candeias. Deoxygenative Divergent Synthesis: En Route to Quinic Acid Chirons. *Organic Letters,* **2020**, *22*, 8370−8375.

Publication **II** Suvi Holmstedt, Alexander Efimov, and Nuno R. Candeias. *O,O*-Silyl Group Migrations in Quinic acid derivatives: An Opportunity for Divergent Synthesis. *Organic Letters,* **2021**, *23*, 3083−3087.

Publication **III** Suvi Holmstedt and Nuno R. Candeias. A Concise Synthesis of Carbasugars Isolated from *Streptomyces Lincolnensis. Tetrahedron*, **2020**, *76*, 131346.

Publication **IV** Akshaya Murugesan*, Suvi Holmstedt*, Kenna C. Brown*, Alisa Koivuporras, Ana S. Macedo, Nga Nguyen, Pedro Fonte, Patricia Rijo, Olli Yli-Harja, Nuno R. Candeias, and Meenakshisundaram Kandhavelu. Design and synthesis of novel quinic acid derivatives: in vitro cytotoxicity and anticancer effect on glioblastoma. *Future Medicinal Chemistry*, **2020**, *12*, 1891-1910. *Equal contribution.

AUTHOR'S CONTRIBUTION

I Suvi Holmstedt designed and carried out the synthesis and characterization of the compounds, interpreted the results, and drafted the manuscript. Lijo George and Alisa Koivuporras contributed to the synthesis and characterization of some compounds. Arto Valkonen performed the X-ray crystallographic studies. Nuno R. Candeias performed the DFT calculations, supervised the work and revised the manuscript. All co-authors contributed to the writing of the manuscript.

II Suvi Holmstedt designed and carried out the synthesis and characterization of the compounds, interpreted the results and prepared the manuscript. Alexander Efimov measured the HRMS. Nuno R. Candeias supervised the work and revised the manuscript. All co-authors contributed to the writing of the manuscript.

III Suvi Holmstedt designed and carried out the synthesis and characterization of the compounds, interpreted the results, and drafted the manuscript. Nuno R. Candeias performed the DFT calculations, supervised the work and revised the manuscript.

IV Suvi Holmstedt designed and carried out the synthesis including the characterization of the compounds. Alisa Koivuporras contributed to the synthesis of some compounds. Nuno R. Candeias supervised the synthetic work. Biological studies were done by the group of Meenakshisundaram Kandhavelu (Molecular signaling group) and external collaborators. The manuscript was written in collaboration with the co-authors.

1 INTRODUCTION TO VALORIZATION OF BIOMASS

Biomass is a term for matter of organic origin, which can be turned into energy sources. Well-known commodities from biomass are biofuels and -gases, but biomass is also a valuable source of small functionalized chiral molecules. Nature-derived enantiopure building blocks are useful for organic synthesis and constitute a group of molecules called chiral pool. In general, chiral pool means a set of compounds which are abundant and available from natural sources, but the broader definition also includes molecules procurable from resolution of racemates, chemical or enzymatic enantioselective procedures, and natural derivatives succinctly manipulated.[1] Natural molecules such as carbohydrates, amino acids and carbacycles among others can be used as starting materials in organic synthesis to provide the carbon skeletons of the target molecules and most importantly, the chirality.

Most synthesis targets invariably bear from at least one to dozens of stereocenters, and their installation is undoubtedly the most difficult part of organic chemistry.[2] Starting the synthesis from chiral pool molecules can avoid the difficulty in the construction of some of the stereogenic centres in the target molecule. The chiral pool is a powerful tool for building complex molecules as its use improves the efficiency in organic synthesis.[3, 4] Resorting to the chiral pool might circumvent the use of expensive and hazardous chemical transformations. For instance, asymmetric catalysis often requires expensive and toxic transition metal -based catalysts and screening of the reaction conditions.[5] On the other hand, one cannot always find a suitable chiral pool molecule that has close structural relation or stereoconfiguration to the target, and asymmetric catalysis might be a solution. Hence, both chiral pool and asymmetric catalysis should be considered when optimizing organic syntheses.[6]

Natural organisms, such as plants, animals, and fungi, produce secondary metabolites for multiple purposes, such as self-protection.[7-10] While these secondary metabolites can often be potential drugs, their therapeutical use might be infeasible due to the small amounts available from natural sources. The synthetic preparation of such natural molecules from simple building blocks is called total synthesis. The synthesis of a previously prepared intermediate, which has a known pathway to the target molecule such as natural product or drug molecule, is called formal synthesis. The production of natural products in desirable scale, the diversification and optimization of the structure aiming at superior biological activity are among the benefits of total synthesis. The main requirements of total synthesis are the efficiency, *i.e.* high chemical yield and step economy, as well as the atom economy and minimum waste.[11] Use of chiral building blocks derived from chiral pool (chirons) is highly recommendable as it allows fulfilling these requirements and provides a resource-efficient biomass use (one of the main principles of circular bioeconomy).

Obviously, the valorization of highly functionalized biomass-based molecules is challenging and requires development and endeavor.[3] From a synthetic chemist's perspective, a better nomination for biomass-based molecules could be "*too highly functionalized molecules*". Handling those molecules is challenging due to the overmuch functionality (mainly OH-groups), namely regarding their polarity and the reactions that are tolerated by the presence of such functional groups. Additionally, the same functional groups can influence the chemoselectivity of reactions.[12] Over the years, we have learned to construct complex structures from simple building blocks, but do we know how to efficiently deconstruct the complexity? And can we do it only partly, or selectively?

This thesis will focus on the recent development in the valorization of biomass-derived compounds, with the main research objective being the selective deoxygenation of hydroxyl groups of quinic acid and expand the utility of such polyol in the total syntheses of natural products.

After presenting the class of biomass-derived molecules that are most relevant to this thesis, a survey on methods for removal of oxygen-containing groups from polyols is introduced in Chapter 2. In Chapter 3, the most pertinent synthetic transformations of chiral pool molecule, quinic acid, are presented to underlie the experimental part of this work. Chapter 4 briefly presents the methods and materials used in thesis, although details can be found in Publications **I–IV** and its respective supplementary materials. Chapter 5 introduces the divergent deoxygenative synthesis strategy to chirons derived from quinic acid. In Chapter 6 a study of *O,O*-silyl group migrations in quinic acid derivatives and the use of these synthetic intermediates are discussed. Chapter 7 comprises a concise total synthesis of two natural carbasugars, followed by a discussion on the synthesis of a potential chemotherapeutic agent derived from quinic acid for treatment of glioblastoma multiforme in Chapter 8.

1.1 Carbohydrates and carbacycles in nature

Biomass consists primarily of carbohydrates, which can be divided into monosaccharides and di-, oligo- or polysaccharides, where monosaccharide units are joined together.[13] Monosaccharides and disaccharides are commonly referred as sugars. The basic unit of carbohydrates contains carbon, hydrogen and oxygen, usually as six-membered ring with empirical formula $(CH_2O)_n$ where $n \geq 3$. Monosaccharides can exist in three isomeric structures, from which the 6-membered pyranose form is usually the most stable (Scheme 1). The cyclic forms can exist as two anomeric structures, according to the relative orientation of the hydroxyl group in the anomeric carbon. Those can be interconverted by isomerization and this is called mutarotation. In the pyranose forms, the anomer is called α if the 1-OH is on the same face as the hydroxymethyl unit (CH_2OH) and β if it is on the opposite face. These isomeric forms of sugars affect deeply their reactivity, and the presence of the oxygen atom in the ring differentiates the synthetic manipulation of sugars from other natural polyols introduced in following chapters.

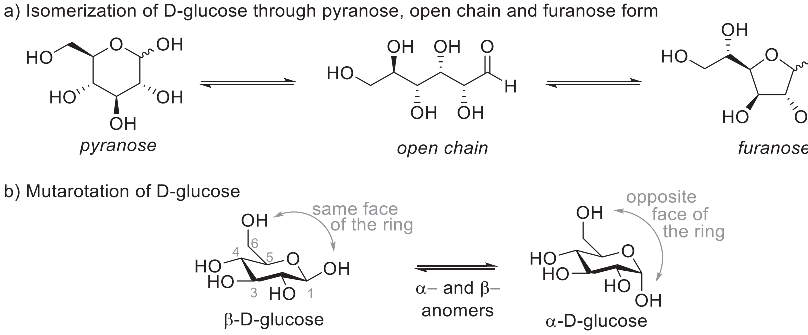
a) Isomerization of D-glucose through pyranose, open chain and furanose form
pyranose
open chain
furanose
b) Mutarotation of D-glucose
same face of the ring
β-D-glucose
α– and β– anomers
opposite face of the ring
α-D-glucose

Scheme 1. a) Isomerization of D-glucose. b) Mutarotation of D-glucose.

Carbohydrates have various biological functions including metabolism, energy storage, and acting as structural components of glycoproteins, glycolipids and other conjugates.[14] Compounds structurally similar to carbohydrates are good alternatives when improving their biological properties. These types of molecules are called carbohydrate mimetics. Carbasugars, previously called pseudo-sugars, have a similar structure to sugars but lacking an oxygen in the ring, thus precluding the isomerization through open chain form (Figure 1). Carbasugars are not very abundant in nature but are biologically interesting since they can mimic sugars in biological processes.[14,15]

When the oxygen from the pyranose or furanose ring of sugars is substituted by a methylene unit (such as in carbasugars) the molecule is classified as carbacycle. This broad term refers to any compound that is cyclic and has only carbons in the ring structure (Figure 1. 1). Simple examples of carbacycles could be cyclopentane, cyclohexane and benzene. However, carbacycles found from natural sources are usually more complex (see molecules **1**–**5**), containing three-dimensionally arranged functional groups such as OH-bearing stereogenic centers. Examples of such compounds are cyclitols (also called as pseudo-carbasugars), that are also under the wide carbacycle classification.[15] Cyclitols are cyclic polyols with three or more hydroxyl groups attached to different carbons of the carbacycle core and may contain other functional groups like amine and carboxyl groups (Figure 1. 1).

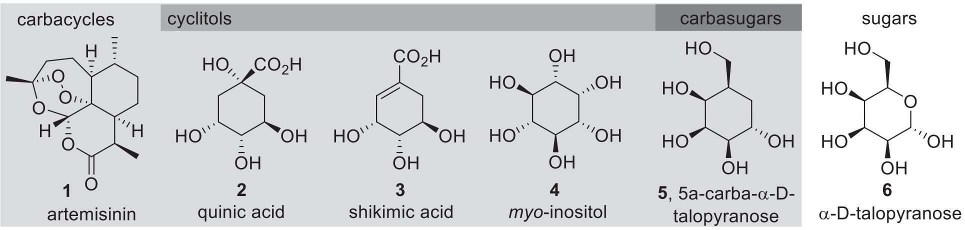

Figure 1. Classification and examples of carbacycles, cyclitols, carbasugars and sugars. Antimalarian drug artemisinin **1** is a carbacycle because of all-carbon ring. Quinic acid **2**, shikimic acid **3**, *myo*-inositol **4** and 5a-carba-α-D-talopyranose **5** are carbacycles and cyclitols *i.e.* cyclic polyols. 5a-Carba-α-D-talopyranose **5** is also a carbasugar due to its relative structure of sugar α-D-talopyranose **6**.

Functionalized carbacycles are widely found in nature, either directly as one carbacycle unit or more often as subunit of larger natural products.[14, 16] As mentioned before, these polyols may have important biological activity themselves, but some of the most abundant ones can be used to synthesize diverse chiral fragments or even complex chiral natural products. This thesis will focus on the diversification of natural cyclitol quinic acid (**2**). Chapter 3 will introduce this highly valuable feedstock chemical, its transformations and use in total syntheses and finally our efforts towards its valorization.

2 DEOXYGENATION OF BIOLOGICALLY SOURCED POLYOLS

The urgent global need for transition from fossil-based resources towards renewable energy sources and sustainable fine chemical production sources has challenged the chemistry community.[17-19] Despite the rather short transition time, the efforts done in developing methods for removing oxygen from biologically sourced primary chemicals (e.g. polyols) have afforded a notable diversity of secondary target molecules. Chapter 2.1 shortly summarizes the methods that can be used in C–O bond cleavage to yield industrially important chemicals. Chapter 2.2 focuses on the partial deoxygenation of C–O bonds to produce advanced building blocks.

2.1 Catalytic deoxygenation of biomass-derived feedstocks

The aim of this chapter is to introduce methods for the transformation of primary chemicals from biomass-based feedstocks into secondary target molecules. The recent efforts done in the conversion of biomass into fuels and feedstock chemicals is showed by the 20% annual increase of the publications on this topic.[20, 21] In most cases the secondary products are simple molecules derived from extensive C–O bond cleavage. This section will not cover the literature comprehensively, but instead briefly introduce the most common strategies for the removal of oxygenated functionalities from common biomass-based feedstocks, namely (Scheme 2): hydrogenation, dehydration, deoxydehydration and hydrodeoxygenation.

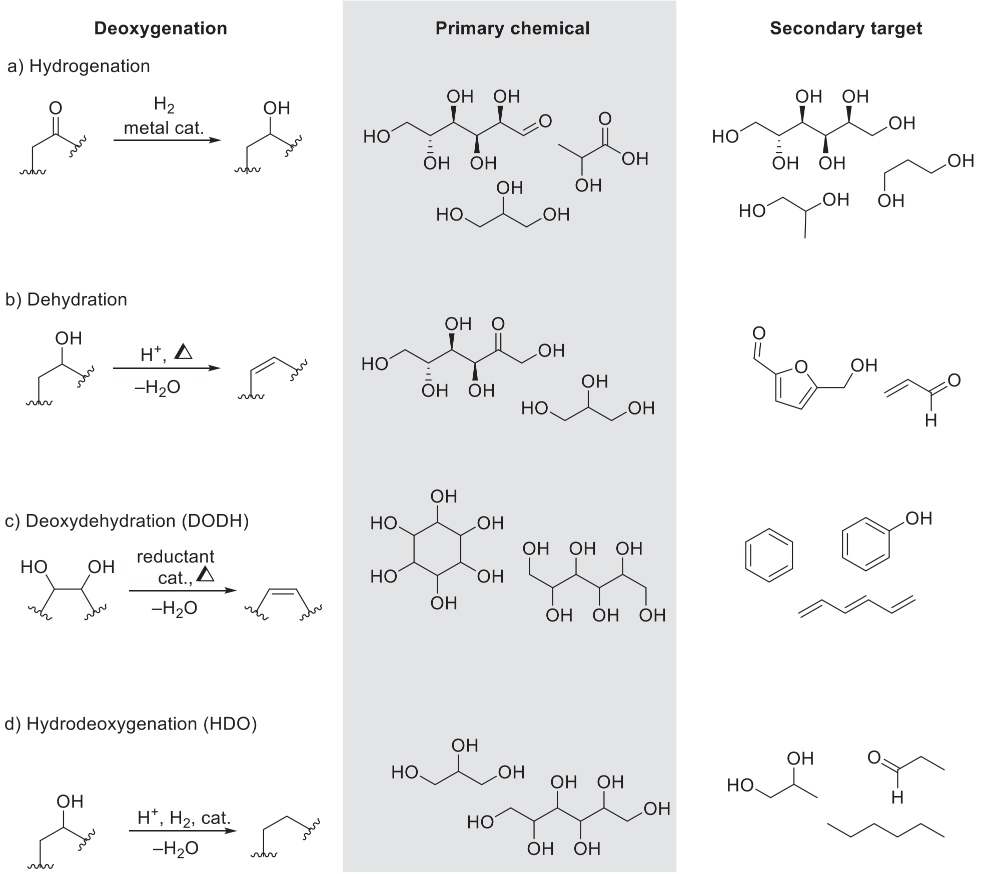
Deoxygenation
Primary chemical
Secondary target
a) Hydrogenation
H2
metal cat.
b) Dehydration
H+, Δ
–H2O
c) Deoxydehydration (DODH)
reductant
cat., Δ
–H2O
d) Hydrodeoxygenation (HDO)
H+, H2, cat.
–H2O

Scheme 2. Methods for C–O bond cleavage of biomass-based polyols: a) hydrogenation; b) dehydration; c) deoxydehydration and d) hydrodeoxygenation and examples primary chemicals and their secondary target molecules.

The homogeneous and heterogeneous catalytic hydrogenation methods of unsaturated substrates are usually selective and effective (Scheme 2. Scheme 2a).[22] However, the difficult recovery of homogenous catalysts in biorefineries benefit the use of heterogeneous catalysts. Raney nickel is widely used as catalyst in the hydrogenation of sugars into hexitols. Also, platinum- and ruthenium-based catalysts are alternatives for Raney nickel, due to their high activity. The metal-catalyzed hydrogenation of sugars has been industrially used for the production of sugar alcohols such as sorbitol and mannitol, while xylose has been converted into xylitol and furfural.[20] Hydrogenation of biomass-based carboxylic acids, such as lactic acid, succinic acid and levulinic acid yields C_3, C_4 and C_5 building block chemicals, respectively.[18] In addition, the ionic hydrogenation of glycerol, a by-product of biodiesel production, is a path to produce 1,3-propanediol, an important building block in polymer chemistry.[19]

The dehydration of bio-based chemicals produces building blocks with alkene units, which can be further converted into alkanes *via* hydrogenation (Scheme 2b).[18] Industrially, dehydration is carried out at high temperatures under strongly acidic conditions. As examples, the dehydration of glycerol yields important industry chemical acrolein, a source material of 1,3-propanediol and acrylic acid[23] and sugar dehydration (xylose and glucose) can lead to furfural and 5-hydroxymethyl furfural.[24]

Deoxydehydration (DODH) removes two adjacent hydroxyl groups from vicinal diols yielding alkene unit (Scheme 2c). Due to the *cis*-diol specificity, rhenium-catalyzed DODH yields secondary targets with high selectivity. Toste *et al.* reported full deoxydehydration of natural polyols with CH_3ReO_3 catalyst in combination with simple alcohols as external reductants.[25] These improved conditions yielded simple hydrocarbons by cleaving all or most of C–O bonds from biomass-based polyols such *myo*-inositol, glycol, and sorbitol.

Hydrodeoxygenation reactions use molecular hydrogen to cleave the C–O bond, involving a dehydration followed by hydrogenation or hydrogenolysis (Scheme 2d). Depending on the reaction pathway, glycerol hydrodeoxygenation yields C3 alcohols or carbonyl compounds.[26] The acid-catalyzed double-dehydration of sugar alcohols followed by hydrogenolysis can produce deoxygenated C6 targets up to fully deoxygenated hexane.[27]

The presence of hydroxyl and alkene functions in the common products of the reactions presented in Scheme 2 (right-hand side column) allows further functionalization. However, when considering the synthesis of complex molecules such as drugs and natural products, the secondary target molecules displayed in Scheme 2 are too simple: the above-described methods usually lead to over-defunctionalization of the biomass-derived molecules, as most of such methods are stereoablative. Synthesis of advanced intermediates bearing stereogenic centers from biomass-based molecules requires milder methods, controllability, and site-selectivity. The next chapter will introduce the achievements in that area.

2.2 Partial deoxygenation of polyols

The seminal works on the $B(C_6F_5)_3$-catalyzed hydrosilylation by Yamamoto and Piers[28-30] has found to be very functional in the selective C–O bond cleavage of silmple alcohols and complex polyols. Scheme 3 describes the catalytic cycle of hydrosilylation of a hydroxyl function. The C–O bond cleavage with this catalytic system is feisty towards primary and secondary alcohols but reports of tertiary hydroxyl cleavage are few and the substrate scope strictly limited[29, 31] Besides alcohols, also carbonyl functionalities are reduced into alcohols, and further, up to alkanes.

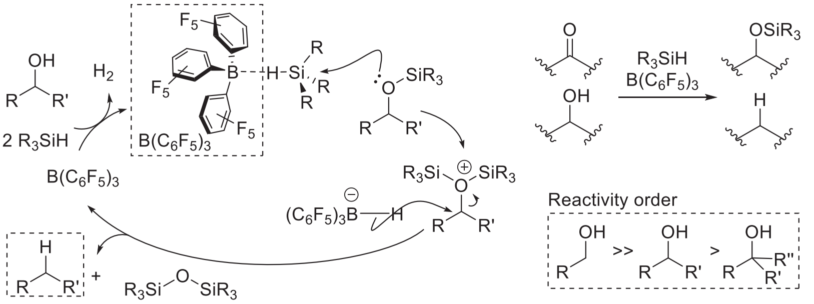

Scheme 3. Catalytic cycle for $B(C_6F_5)_3/R_3SiH$ deoxygenation of alcohols, R=alkane, R'=H or alkane

As demonstrated by Gagné, silyl hydrides can provide extensive deoxygenation of silylated sugars (Scheme 4a). Initially an iridium-catalyst[32] and later $B(C_6F_5)_3$,[33] yielded different ratios of hexanes in presence of excess of Et_2SiH_2 (Scheme 4a). $B(C_6F_5)_3$-catalyzed reaction was notably faster and efficient, which allowed the use of less reactive tertiary silanes. By manipulating the reaction conditions, a partial deoxygenation of glucose **9** and glucitol **11** derivatives into 1,6-deoxy glucitol **10** was conducted (Scheme 4b). The silyl protecting groups as well as the size of the silyl hydride revealed to be pivotal for the chemoselectivity. These findings launched an extensive campaign on $B(C_6F_5)_3$-catalyzed partial deoxygenation of sugar derivatives.

a) Iridium- and $B(C_6F_5)_3$-catalyzed hydrosilylative reduction of glucose to hexanes

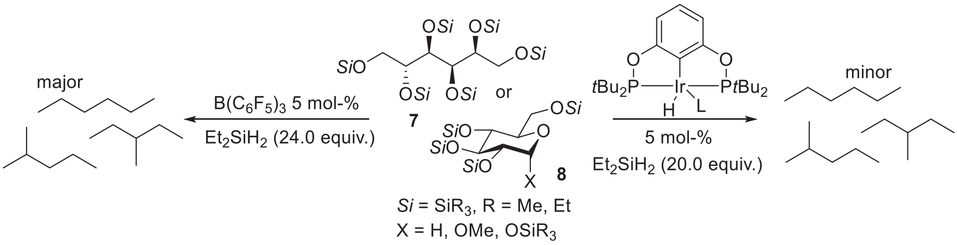
major
$B(C_6F_5)_3$ 5 mol-%
Et_2SiH_2 (24.0 equiv.)
SiO
OSi OSi
OSi
OSi OSi
7
or
OSi
SiO
SiO
SiO
O
X
8
Si = SiR_3, R = Me, Et
X = H, OMe, $OSiR_3$
O
O
tBu2P
Ir
PtBu2
H
L
5 mol-%
Et_2SiH_2 (20.0 equiv.)
minor

b) Initial findings of partial deoxygenation of sugar derivatives catalyzed by $B(C_6F_5)_3$

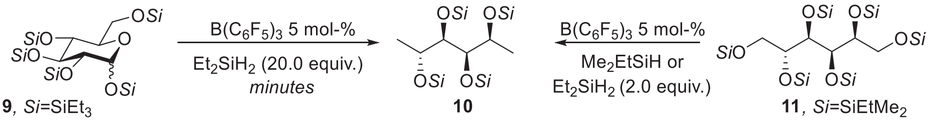
OSi
SiO
SiO
O
SiO
OSi
9, Si=$SiEt_3$
$B(C_6F_5)_3$ 5 mol-%
Et_2SiH_2 (20.0 equiv.)
minutes
OSi OSi
OSi OSi
10
$B(C_6F_5)_3$ 5 mol-%
Me_2EtSiH or
Et_2SiH_2 (2.0 equiv.)
OSi OSi
SiO
OSi
OSi OSi
11, Si=$SiEtMe_2$

Scheme 4. a) Full deoxygenation of carbohydrates to hexanes. b) Initial findings of partial deoxygenation of sugar derivatives.

An elaborated elegant fashion for partial and selective deoxygenation of C–O bonds in C_6O_6 polyols was later reported (Scheme 5).[34] Several silyl ethers derived from hexols (**12**) were reduced to trioxygenated species (**13**), while the selectivity of the reaction was rationalized by substrate-controlled cyclic silyloxonium intermediate (Scheme 5a). In cyclic 1,2-deoxy glucose **14** the reaction started with ring opening. Surprisingly, the cleavage of silyl-activated primary hydroxyl (at C6) was minor, and competing intramolecular cyclization took place (Scheme 5b). This intermediate led to unexpected deoxygenation of secondary hydroxyl over more reactive primary one (**15**).

Bicyclic dehydrated sugar derivatives (silylated isosorbide and isomannide (**17**)) were shown to produce diverse synthons depending on the choice and amounts of silyl reducing agent (Scheme 5c).[34] The deoxygenation of such sugar derivatives seemed to have a complex reaction mechanism *via* anchimeric assistance, to yield unexpected products chemoselectively. The manipulation of the reaction conditions and change of the substrate's protecting groups was shown to deeply impact the outcome of the reaction.

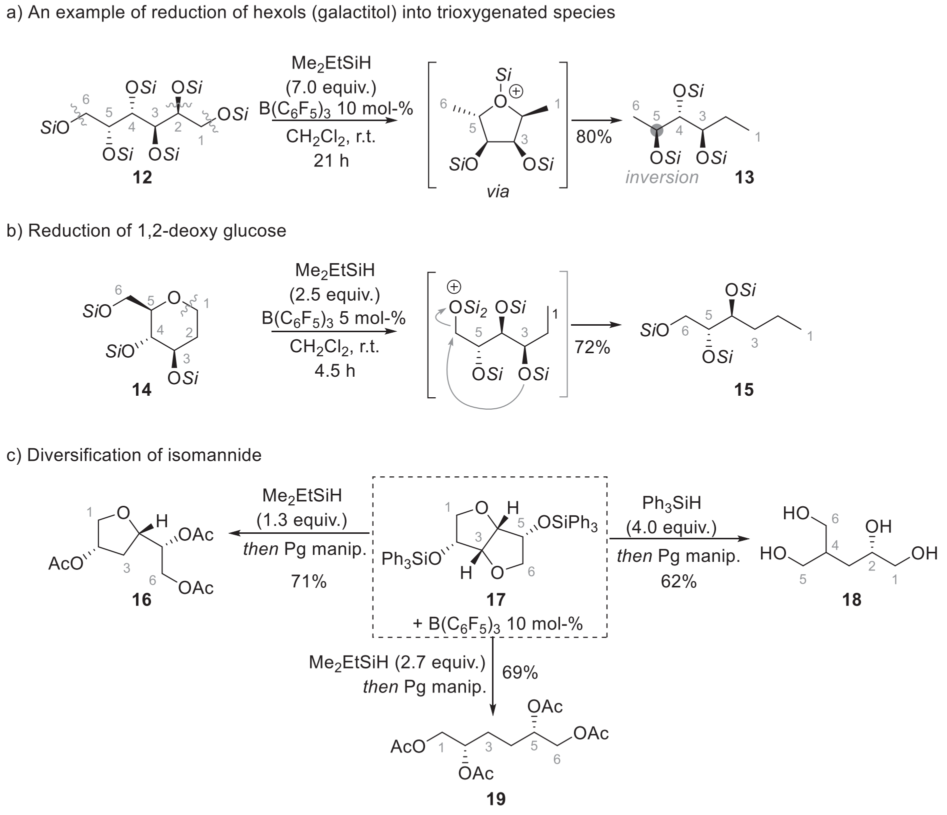
a) An example of reduction of hexols (galactitol) into trioxygenated species

b) Reduction of 1,2-deoxy glucose

c) Diversification of isomannide

12
Me2EtSiH
(7.0 equiv.)
B(C6F5)3 10 mol-%
CH2Cl2, r.t.
21 h
via
80%
inversion
13
14
Me2EtSiH
(2.5 equiv.)
B(C6F5)3 5 mol-%
CH2Cl2, r.t.
4.5 h
72%
15
16
Me2EtSiH
(1.3 equiv.)
then Pg manip.
71%
17
+ B(C6F5)3 10 mol-%
Ph3SiH
(4.0 equiv.)
then Pg manip.
62%
18
Me2EtSiH (2.7 equiv.)
then Pg manip.
69%
19

Scheme 5. Selected examples of Gagné's work on chemoselective partial deoxygenation of silylated sugar derivatives. a) Reduction of hexols. b) Reduction of 1,2-deoxy glucose. c) Diversification of isomannide.

Recently the site-selectivity of C–O bond cleavage in cyclic sugar derivatives (**20**) was demonstrated to depend on the fluoroarylborane catalyst (Scheme 6).[35] The choice of catalyst ($B(C_6F_5)_3$ or $BAr_{3,5\text{-}CF_3}$) changed the deoxygenation outcome with the less-hindered and less Lewis-acidic $BAr_{3,5\text{-}CF_3}$ cleaving preferentially the exocyclic C–O bond whereas $B(C_6F_5)_3$ catalyzed the endocyclic C–O bond cleavage (Scheme 6a).

Changing the site-selectivity of C–O bond cleavage of isosorbide **23** was carried out by varying the protecting group and the reductant amount (Scheme 6b).[36] Apart from previous reductions/deoxygenations, catecholborane (HBCat) was used as a hydride source. HBCat together with silyl or BCat-protecting groups enabled the chemoselective substrate manipulation after careful optimization. For example, when isosorbide was protected with BCat (**23-BCat**), catechol borane in presence of

10 mol-% $B(C_6F_5)_3$ reduced only primary positions (**24**), though excess of reductant was used (6.0 equiv.). Use of 2 equivalents of HBCat allowed the reduction of **23-SiEt$_3$** into **25** in 62% yield. Notably, the selectivity of the reaction changed when replacing the borane reducing agent by the hydrosilane (cf. **23→25** and **23→28**; Pg=$SiEt_3$, 2 equiv. of hydride source). With bulky triphenylsilyl protecting group (**23-SiPh$_3$**) the reduction cleanly yielded **27** using 1 equivalent of HBCat.

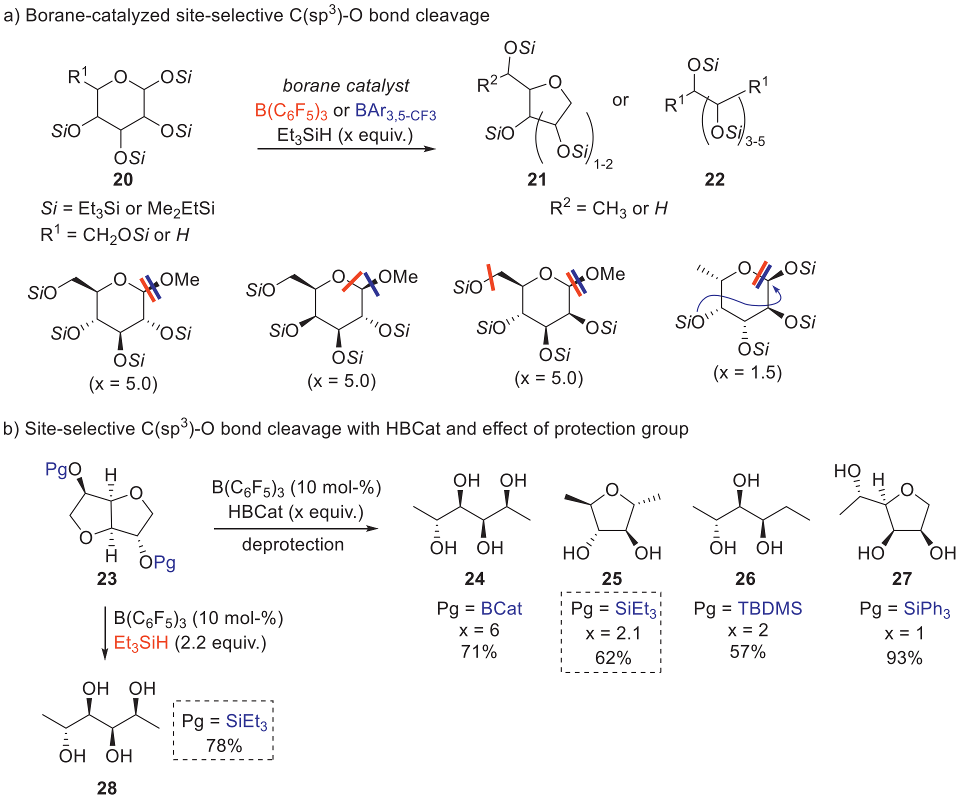
a) Borane-catalyzed site-selective C(sp3)-O bond cleavage
borane catalyst
B(C6F5)3 or BAr3,5-CF3
Et3SiH (x equiv.)
R1
OSi
SiO
20
Si = Et3Si or Me2EtSi
R1 = CH2OSi or H
R2
21
or
22
1-2
3-5
R2 = CH3 or H
OMe
(x = 5.0)
(x = 5.0)
(x = 5.0)
(x = 1.5)
b) Site-selective C(sp3)-O bond cleavage with HBCat and effect of protection group
PgO
H
OPg
23
B(C6F5)3 (10 mol-%)
HBCat (x equiv.)
deprotection
OH
HO
24
Pg = BCat
x = 6
71%
25
Pg = SiEt3
x = 2.1
62%
26
Pg = TBDMS
x = 2
57%
27
Pg = SiPh3
x = 1
93%
B(C6F5)3 (10 mol-%)
Et3SiH (2.2 equiv.)
28
Pg = SiEt3
78%

Scheme 6. a) Site-selectivity of two fluoroarylboranes. b) Protecting group influence in the deoxygenation of sugar-derivatives.

2.3 Conclusions on biomass deoxygenation

Reaching fuels and feedstock chemicals from natural sources has been accomplished through various processes. The methods described in Chapter 2.1 are mostly scalable and of industrial applicability, mainly leading to simple products. Notwithstanding the importance of such transformations due to their catalytic, protecting-group free and atom economic nature, they concurrently lead to loss of most functional groups and stereoinformation. While the products obtained with such methods might well serve the energy industry and the production of stock chemicals, transformations capable of partial deoxygenate biomass-derived molecules would be desirable when aiming at the syntheses of complex targets.

The research around the partial deoxygenation of biomass-based chemicals has provided ample information on how sugar derivatives behave in $B(C_6F_5)_3$-catalyzed C–O bond cleavage. Such extensive studies inspire to develop methods for the selective deoxygenation of quinic acid, hauling this research area forward. This field of chemistry is still developing and directing the reactivity to certain functional groups, as for example in the selective deoxygenation of secondary hydroxyls over primary ones, which still requires improvements. Despite the availability of some of those methods, the anchimeric assistance as the basis for selectivity render those processes substrate-dependent and hence not applicable to variable biomass-based molecules. In addition, the current available methods still demand for improving the atom economy and diminishing waste by obviating the use of protecting groups.

Considering the available methods for partial deoxygenation of biologically sourced polyols, the fluoroarylborane catalyzed $C(sp^3)$–O bond cleavage of silyl ethers serves as a versatile method to reduce the OH-functionalities in sugar derivatives. Previous extensive studies have revealed that the chemoselectivity of the deoxygenation can be manipulated by:

a. The amount of the reductant,
b. The electronic and stereochemical character of the reductant,
c. The electronic character of the borane catalyst ($B(C_6F_5)_3$ vs. $BAr_{3,5\text{-}CF3}$),
d. Protecting groups of the substrate, and most importantly
e. The substrate stereoconfiguration.

Despite the considerably large substrate scope of sugar-derivatives, the application of this method to other classes of biomass-based molecules has remained somewhat unexplored. Considering the well documented substrate-dependence outcome of the borane-catalyzed C–O cleavage of silyl ethers, studying the deoxygenation of other chiral pool molecules such as cyclitols is of significance in the quest for biomass-derived carbon skeletons for preparation of fine chemicals.

3 SYNTHETIC APPLICATIONS OF QUINIC ACID

3.1 Production and availability of quinic acid

Quinic acid was first isolated in the end of 18th century after being found as an impurity of quinine.[37] The structure of quinic acid was assigned by Fisher *et al.* in 1932,[38] and later confirmed by X-ray analysis.[39] Quinic acid and its acyl derivatives have been found to be abundant in many natural sources including coffee beans, cinchona tree's bark, other plants and fruits as well as food wastes.[16] Currently, quinic acid and some of its derivatives are commercially available with high enantiomeric purity.

Quinic acid **2** is a side product of the shikimate pathway (Scheme 7), which produces biologically important aromatic compounds, such as amino acids phenylalanine, tyrosine and tryptophan.[40] Shikimic acid **3** is an intermediate in the biosynthesis of aromatics in bacteria and plants, but the absence of its pathway in mammals forces those organisms to obtain the essential aromatic amino acids from their diet. The carbon source of this pathway is D-glucose **29**, which with transketolase enzyme forms D-erythrose-4-phosphate **30** (Scheme 7). Condensation with phosphoenol pyruvate **31** in the presence of DAHP synthase followed by DHQ synthase yields the common intermediate 3-dehydroquinic acid **33**. Lastly, quinic acid dehydrogenase reduces the 3-dehydroquinic acid to D-quinic acid **2**.

Depart from IUPAC rules of atom numbering, quinic acid's numbering shown in Scheme 7 (numbering of Publication **I** and **II**) will be used through this thesis. Publications **III** and **IV** use different atom numbering, which was either originated from the isolated natural products or introduction of substituents that alter the group precedence.

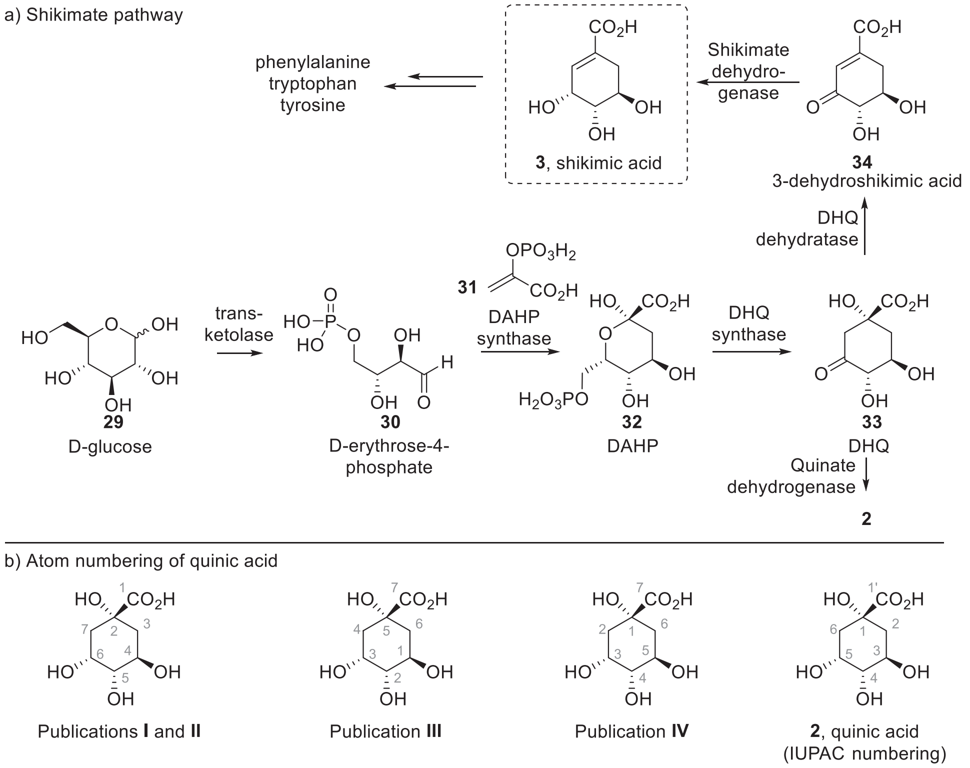
a) Shikimate pathway
phenylalanine
tryptophan
tyrosine
CO2H
HO
OH
OH
3, shikimic acid
Shikimate
dehydro-
genase
CO2H
O
OH
OH
34
3-dehydroshikimic acid
DHQ
dehydratase
HO
OH
HO
OH
OH
29
D-glucose
trans-
ketolase
O
HO–P
HO
O
OH
H
OH
O
30
D-erythrose-4-
phosphate
OPO3H2
31
CO2H
DAHP
synthase
HO
CO2H
O
H2O3PO
OH
OH
32
DAHP
DHQ
synthase
HO
CO2H
O
OH
OH
33
DHQ
Quinate
dehydrogenase
2
b) Atom numbering of quinic acid
Publications I and II
Publication III
Publication IV
2, quinic acid
(IUPAC numbering)

Scheme 7. a) Biosynthetic pathway of quinic acid and shikimic acid by shikimate pathway. b) Atom numbering of quinic acid used in this thesis and in the original Publications **I**–**IV**. DAHP = 3-deoxy- D-arabino-heptulosonic acid 7-phosphate; DHQ = 3-dehydroquinic acid.

3.2 Reactions of quinic acid

3.2.1 Protection of hydroxyl groups

The chemoselective modification of quinic acid often requires the protection of hydroxyl group(s), which can be also done for solubility enhancement in different solvents. Quinic acid **2** or quinide **35** (Scheme 8), are sparsely soluble in most organic solvents, although soluble in polar solvents such as water, alcoholic solvents and DMSO. Such limited solubility in organic solvent greatly restricts the transformations applicable to these cyclitols. This chapter introduces the one-step protection routes applied to quinic acid **2** or to quinide **35**. The purpose of this chapter is to give an overview of the reactivity order of quinic acid's hydroxyl groups in order to later perform selective synthetic transformations.

Quinic acid can go through an esterification reaction, either inter- or intramolecular. The intermolecular esterification of quinic acid with methanol (**36**, R=Me) has been reported with various acid catalysts, [41-43] although also other alcohols have been used (Scheme 8). The intramolecular esterification (*i.e.* lactonization) has raised more attention since this transformation effortlessly mask both carboxylic acid and secondary 4-OH moieties. Therefore, quinide **35** is commonly used as starting material as it still allows further manipulation of *cis*-hydroxyl groups or other chemical transformations. The lactonization occurs under acidic conditions[44,45] and the discovery of quinide **35** from natural sources indicates the spontaneous lactonization in biological environment.[46]

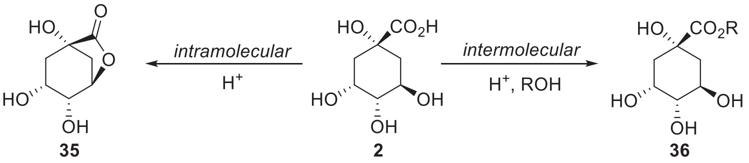

HO
O
O
HO
OH
35
intramolecular
H+
HO
CO2H
HO
OH
OH
2
intermolecular
H+, ROH
HO
CO2R
HO
OH
OH
36

Scheme 8. Intramolecular and intermolecular esterification of quinic acid.

The direct monoprotection of quinic acid **2** or its ester derivative **36** remains rare due to selectivity issues on equivalent hydroxyl groups. The formation of some regioisomers (chlorogenic acid derivatives **37**, Scheme 9) is more selective with cinnamoyl chlorides, but complex mixtures are generally achieved, as characterized by LC-MS.[47] Regioselective esterification of 5-OH (**38**) was achieved by enzymatic synthesis with *Candida antarctica* lipase A with different esters and anhydrides.[48]

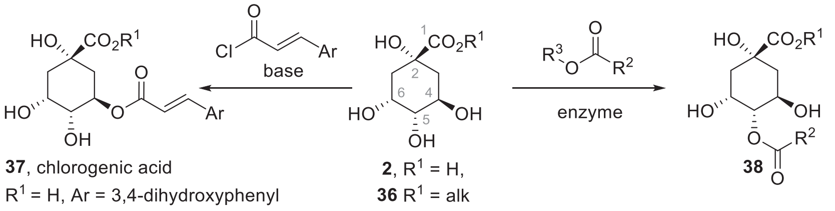

HO
CO2R1
O
HO
O
Ar
OH
37, chlorogenic acid
R1 = H, Ar = 3,4-dihydroxyphenyl
O
Cl
Ar
base
1
HO
CO2R1
2
6
4
HO
5
OH
OH
2, R1 = H,
36 R1 = alk
O
R3
O
R2
enzyme
HO
CO2R1
HO
OH
O
R2
38
O

Scheme 9. Selective monoesterification of quinic acid.

The monoprotection of quinide **35** favors the protection of C6-hydroxyl group. The locked conformation of the lactone places C6-hydroxyl group equatorial and C5-hydroxyl group in axial position. The reactivity of equatorial hydroxyl groups over axial ones has been also reported previously for carbohydrates and simpler cyclohexanol derivatives.[49, 50] The regioselectivity in the monosilylation of secondary hydroxyl groups can be controlled by the modification of the reaction conditions. Thermodynamic conditions favor the 5-OH silylation delivering a mixture of monosilylated compounds in a 1:2 ratio (**39**:**40**, 84% overall yield) at 90 °C (Table 1, entry 1). Contrastingly, the same reaction performed at 0 °C provides the isomers in a 97:3 ratio (**39**:**40**, 82% overall yield).[51] The type of silyl groups also impact the isomer ratio, as smaller TBDMS-group show great selectivity towards protection of C6-hydroxyl group (**39**-**TBDMS**) (Table 1, entry 3). In contrast, TBPDS-analog delivers only 30% of **39**-**TBDPS** (entry 4) together with **40**-**TBDPS** (20%). In this thesis study, the selective TBDPS-protection of 6-OH was achieved in 91% yield, clearly indicating the importance of the solvent (entry 5).

The monoprotection of quinide **35** can be extended beyond the selective silylation. Catalytic regioselective sulfonylation of C6 hydroxyl with tosyl chloride affords **39-Ts** exclusively (Table 1, entry 6)[52] and 6-OH protection with benzyl can be performed in a regioselective manner (**39-Bn**, entry 7).[53]

Table 1. Monoprotection of quinide **35**.

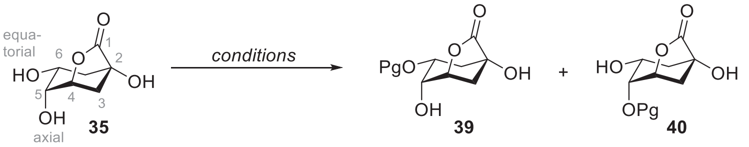

Entry	Conditions	Pg	Yield (%) (**39**/**40**)
1	TBDMS-Cl, DMAP, Et_3N, Bu_4NI, DMF, 90 °C	TBDMS	54 (**39**)
2	TBDMS-Cl, DMAP, Et_3N, Bu_4NI, DMF, 0 °C	TBDMS	80 (**39**)
3	TBPMS-Cl, imidazole, DMF	TBDMS	83 (**39**)
4	TBDPS-Cl, imidazole, DMF	TBDPS	30 (**39**)+ 20 (**40**)
5[a]	TBDPS-Cl, imidazole, CH_3CN	TBDPS	91 (**39**)
6	TsCl, NMI, chiral benzazaborole, Na_2CO_3	Ts	>99 (**39**)
7[b]	TsOH, DMF, C_6H_6, then Bu_2SnO/BnBr	Bn	81 (**39**)

[a] Unpublished data. [b] Reaction started from quinic acid, with simultaneous lactonization and protection.

A recent example of monoprotection of quinide **35** was presented by Li *et al.* as part of a site-divergent hydroxyl protection in polyols.[54] The selectivity of axial (C5) and equatorial (C6) hydroxyl propargylation varied according to the enantiomer of the ligand used along with copper catalyst. Both regioisomers **41** and **42** were synthesized with high selectivity and good yield (Scheme 10).

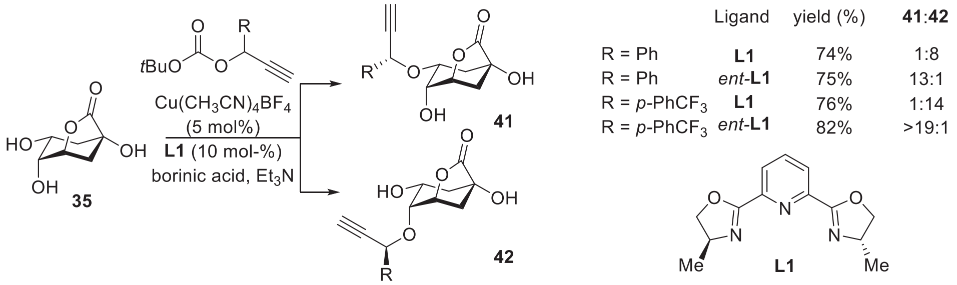

	Ligand	yield (%)	**41**:**42**
R = Ph	**L1**	74%	1:8
R = Ph	*ent*-**L1**	75%	13:1
R = *p*-PhCF$_3$	**L1**	76%	1:14
R = *p*-PhCF$_3$	*ent*-**L1**	82%	>19:1

Scheme 10. Site-selective propargylation of quinide **35**.

While protecting groups should be inert towards the reaction conditions they are submitted to, their presence can have a deep impact on the reactivity of the molecule. For instance, the protection of diols in the form of cyclic structures rigids the substrate, which hampers flexibility and restrain conformation changes. Occasionally, the impact of increased rigidity may be irrelevant or even beneficial for the subsequent synthetic steps.[55, 56] On the other hand, large acyclic protecting groups may favor other conformations and thus allow disparate reactivity.[57, 58] In the following paragraphs are presented examples of di- or triprotection of quinic acid's or quinide's hydroxyl groups.

In 2000, Gotor *et al.* exploited the protection of C4- and C6-hydroxyl groups of **43** and prepared TBDMS-derivative **44** in a single step (74 %, Scheme 11a)[59] This protection strategy allowed the synthetic manipulation of 5-OH in later stage. The singe-step acetylation of all secondary hydroxyl groups of **43** allowed the manipulation of tertiary hydroxyl in Panza's synthesis of carba-L-rhamnose and Bianco´s synthesis of a sialic acid derivative (Scheme 11a).[41, 60] Along with these, protection of all secondary hydroxyl groups of **43** can be done with TMS-group.[61]

Applying a single molecule to protect two hydroxyl groups simultaneously (*i.e.* cyclic protecting group) may improve the protection's regioselectivity in cases of polyols because the second protection is facilitated by the intramolecular attack. For example, selective 5,6-OH protection of **36** with acyclic groups is unknown, but facile protection of these two hydroxyls can be achieved with cyclic protecting groups such as dimethyl acetal **46**[62], benzylidene acetal **47**[63], orthoester **48**[64] and cyclohexane **49**[65] groups (Scheme 11b).

Protection of *trans*-diol (4,5-OH) can be performed by introduction of butane- or cyclohexane diacetal groups yielding bicyclic **50** or its tricyclic counterpart **51** (Scheme 11b). Protection of 4-OH and 5-OH gives access to functionalization of 6-OH and this protection strategy has been adapted in the syntheses of various natural products.[65-69]

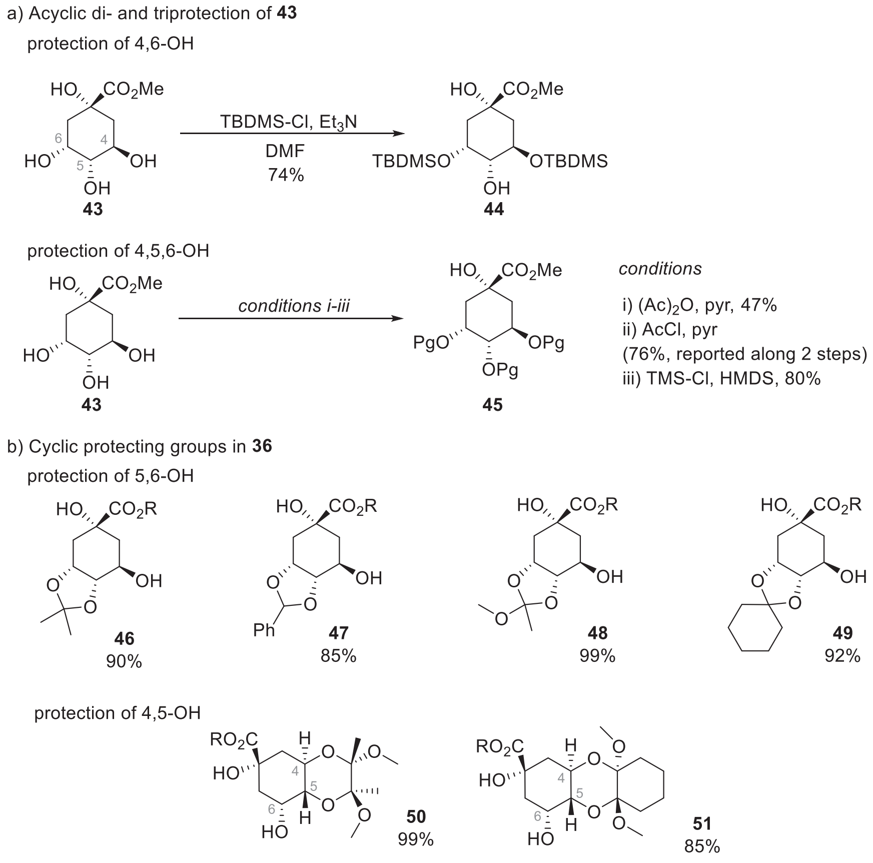
a) Acyclic di- and triprotection of 43
protection of 4,6-OH
HO
CO2Me
OH
6
4
5
43
TBDMS-Cl, Et3N
DMF
74%
TBDMSO
OTBDMS
44
protection of 4,5,6-OH
conditions i-iii
PgO
OPg
45
conditions
i) (Ac)2O, pyr, 47%
ii) AcCl, pyr
(76%, reported along 2 steps)
iii) TMS-Cl, HMDS, 80%
b) Cyclic protecting groups in 36
protection of 5,6-OH
CO2R
O
Ph
46
90%
47
85%
48
99%
49
92%
protection of 4,5-OH
RO2C
H
50
99%
51
85%

Scheme 11. a) Acyclic protecting groups of quinic acid hydroxyl groups. b) Cyclic protecting groups of quinic acid hydroxyl groups.

Vicinal *cis*-diol protection (5,6-OH) on quinide **35** with acyclic protecting groups has not been reported. Indeed, such kind of protection proved to be challenging when attempting the preparation of cytotoxic agents against glioblastoma (Chapter 8).

Quinide **35** silylation with TBDPS-Cl in presence of base provided the desired disilylated compound (**56**, Scheme 12b) in only 38% yield along with mono- and trisilylated analogues. Instead, the 5,6-diol protection has been performed in good yields with various cyclic protecting groups (single-step lactonization and 5,6-OH protection, compounds **52–55**) (Scheme 12a).[70-74] Such protection has also been previously achieved with triphosgene yielding **57**,[75] while for this thesis work the same product was obtained using the safer carbonyldiimidazole.[76] Sulfur-containing protection groups were additionally explored to yield sulfite **58** and sulfate **59**.[76]

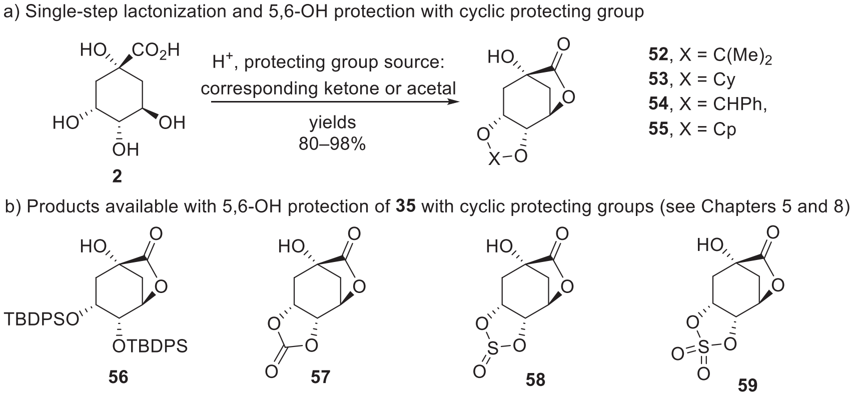
a) Single-step lactonization and 5,6-OH protection with cyclic protecting group

b) Products available with 5,6-OH protection of **35** with cyclic protecting groups (see Chapters 5 and 8)

HO
CO2H
HO
OH
OH
2
H+, protecting group source:
corresponding ketone or acetal
yields
80–98%
HO
O
O
O
X
O
52, X = C(Me)2
53, X = Cy
54, X = CHPh,
55, X = Cp
TBDPSO
OTBDPS
56
57
S
58
O=S=O
59

Scheme 12. Protection of vicinal 5,6-diol moiety of quinide **35** a) previously b) in this work.

The protection of all hydroxyl and carboxyl groups of **2** or **36** can be achieved by the installation of silyl (**60**),[77] methyl (**61**)[78] or acetyl groups (**62**)[79] (Scheme 13). The protection of the three hydroxyl groups of quinide (**35**) has been done by introduction of TMS (**63**)[77] and benzoyl (**64**)[46] groups. While small silanes are typically used in the OH-protection of quinic acid derivatives, larger silyl groups TBDPS and TBDMS (**65** and **66**, respectively) could be installed in high yields during the selective deoxygenation study (Chapter 5).[76]

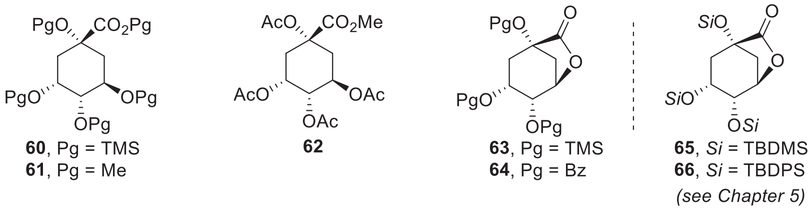
PgO
CO2Pg
PgO
OPg
OPg
60, Pg = TMS
61, Pg = Me
AcO
CO2Me
AcO
OAc
OAc
62
PgO
O
O
PgO
OPg
63, Pg = TMS
64, Pg = Bz
SiO
O
O
SiO
OSi
65, Si = TBDMS
66, Si = TBDPS
(see Chapter 5)

Scheme 13. Products available by full protection of quinic acid **2** and quinide **35**.

Scheme 14 collects the plausible structures available by selective or full protection of quinic acid in an attempt to summarize the available protecting strategies. The scarce or no use of protecting groups is preferred, albeit they might provide the only way to hide the reactivity of certain functionalities in highly functionalized molecules such as quinic acid. When aiming at the modification of polyols to produce added-value molecules, unexpected chemo- and regioselectivity and protecting group migrations (see Chapter 6) might present great opportunities for achieving regioisomers unavailable by direct protecting strategies.

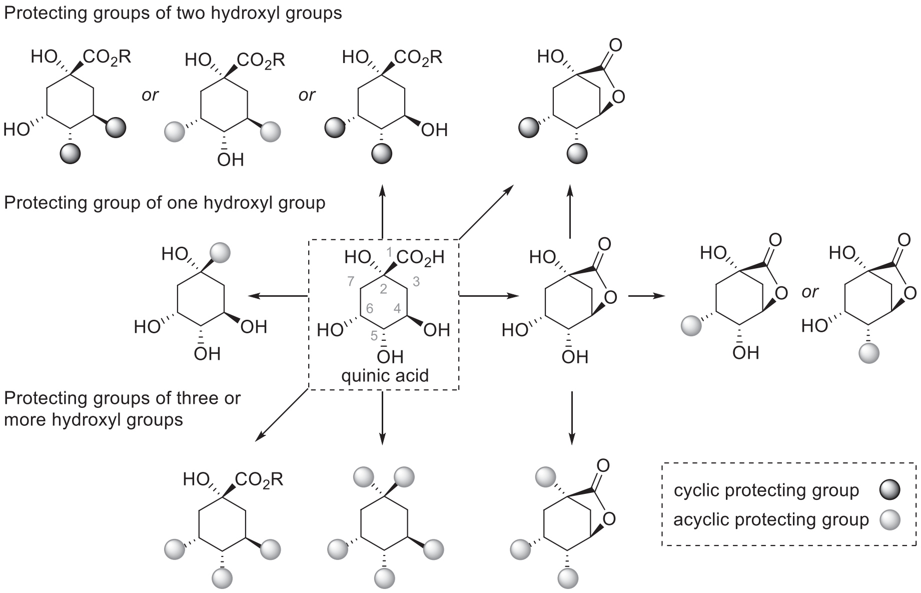
Protecting groups of two hydroxyl groups
HO
CO_2R
or
OH
O
Protecting group of one hydroxyl group
1
2
3
4
5
6
7
CO_2H
quinic acid
Protecting groups of three or more hydroxyl groups
cyclic protecting group
acyclic protecting group

Scheme 14. Quinic acid derivatives by single-step protection strategy. Protecting groups are presented in generic form.

3.2.2 Deoxygenation of quinic acid

As discussed in Chapter 2, the selective deoxygenation of naturally sourced polyols is a competitive tool for synthesizing chirons from abundant renewable matter. Despite the chiral pool strategies relying on natural carbacycles such as quinic acid, a toolbox for the deoxygenation of these natural polyols has remained unrevealed. However, the use of quinic acid in organic synthesis often requires removing some of the hydroxyl groups. Moreover, the development of new deoxygenation methods is important when considering the imperative transition from fossil-based to biomass-based feedstocks in the context of fine chemistry.

Practical, reliable and facile procedures for carbacycles' deoxygenation are somewhat limited. Heretofore, Barton–McCombie reaction has been a single method utilized for the selective C–O bond cleavage of quinic acid along with elimination–hydrogenation sequence (Scheme 15). Generally, Barton–McCombie reaction is very operable and high-yielding towards secondary as well as tertiary hydroxyl groups.[80] The drawbacks of this reaction are the two-step procedure and the use of toxic organotin hydride reagent.

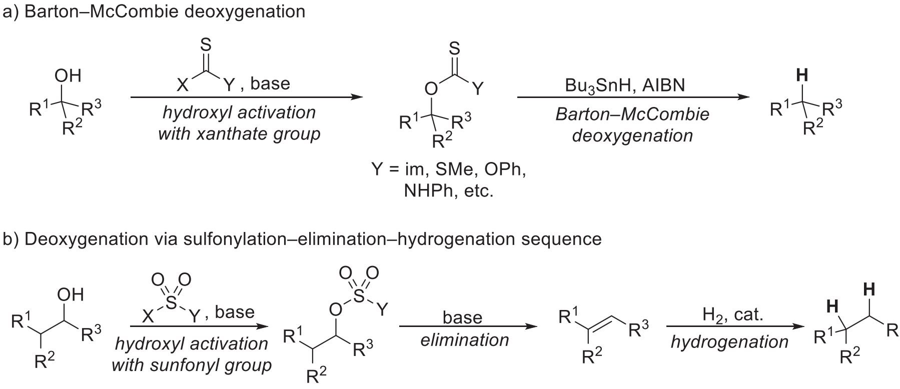
a) Barton–McCombie deoxygenation
OH
R1 R3 R2
X Y, base (S)
hydroxyl activation with xanthate group
O Y S
R1 R3 R2
Y = im, SMe, OPh, NHPh, etc.
Bu3SnH, AIBN
Barton–McCombie deoxygenation
H
R1 R3 R2
b) Deoxygenation via sulfonylation–elimination–hydrogenation sequence
OH
R1 R3 R2
X S Y, base (O O)
hydroxyl activation with sunfonyl group
O S Y
R1 R3 R2
base
elimination
R1 R3 R2
H2, cat.
hydrogenation
H H
R1 R3 R2

Scheme 15. General representation of the currently available methods for oxygen removal from quinic acid: a) Barton–McCombie reaction and b) sulfonylation–elimination–hydrogenation sequence.

Each hydroxyl group of quinic acid has been previously removed using the Barton–McCombie deoxygenation. The tertiary hydroxyl group of quinic acid was cleaved with Barton–McCombie deoxygenation in the total syntheses of (+)–palitantin[81] and immunosuppressant FK506[82] (**70**, Figure 2). Further, molecule's **70** secondary 4-OH was deoxygenated in the formal total synthesis of cyclohexane fragment of enacyloxins (**69**).[83] Moreover, secondary hydroxyls 5-OH or 6-OH were cleaved in the syntheses of 19-nor-vitamin D and several other vitamin D analogues (**67** and **68**).[84, 85]

Besides the reported Barton–McCombie deoxygenation of the tertiary hydroxyl of quinic acid, this functionality has been manipulated to allow the vicinal diol cleavage[86, 87] (**77** and **78**) and reduction of corresponding epoxide with $LiAlH_4$ (**76**).[88]

As presented in left hand side hoop of Figure 2, the complete selective deoxygenation of the carboxylic acid moiety is still a reverie (molecules **71** and **72**). Such method would be a handy tool to access chiral C7 fragments with a tertiary stereocenter bearing hydroxyl and methyl groups. This type of moiety embellishes several natural products (for example **76** as a subunit of aquayamycin[88]) but the straight deoxygenation of primary hydroxyl group in neopentyl alcohol derivatives is yet unknown.

The structures presented in right hand side hoop of Figure 2 are achieved by the elimination of hydroxyl groups or oxidative cleavage of the vicinal diols. Quinic acid can also be seen as a biomass-based alternative for the production of commodity chemicals, which are industrially used to produce other important feedstock chemicals. For example, the metal-free extensive oxygen removal has yielded biomass-based benzoic acid **73**[89] and hydroquinone **74**.[90]

The dehydration of 4-OH or 6-OH by sulfonylation of hydroxyl group followed by treatment with strong base has yielded key intermediates for total syntheses (e.g. **75** and **78**, Figure 2).[67, 91-93] Further, the double bond could be hydrogenated[91, 94] or used as a versatile platform for conjugate addition[92], α-functionalization[95, 96] and Diels–Alder reaction[97].

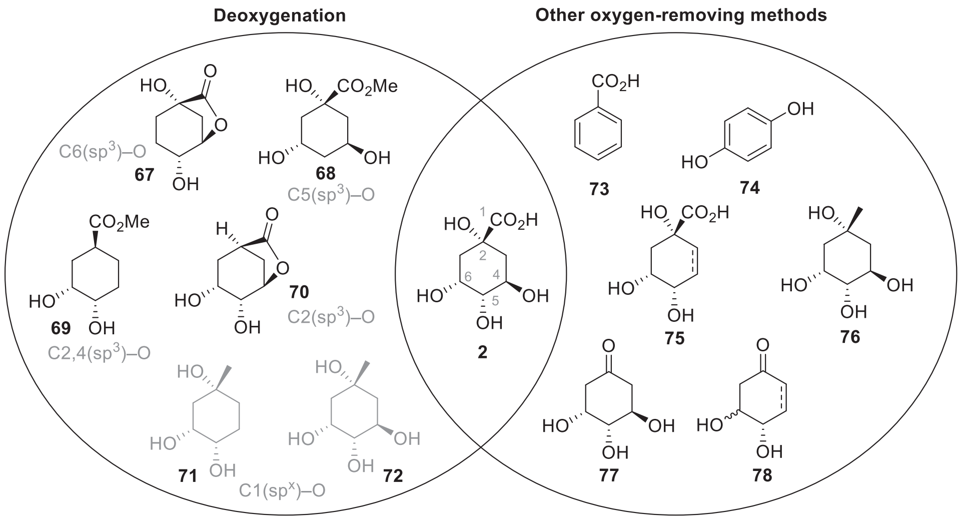

Figure 2. Structures of molecules obtained from removal of oxygenated functionalities from quinic acid. Structures are simplified and shown without protecting groups.

3.2.3 Oxidative C–C cleavage

Quinic acid can be considered as a starting material in reaching diverse skeletons besides carbacycles. The presence of the vicinal diol moieties provides access to oxidative C–C bond cleavage by Malaprade and other oxidative reactions. Such transformation delivers chiral acyclic building blocks upon C5–C6 cleavage, while reduction of C1 carboxylic acid moiety allows C1–C2 cleavage to provide chiral cyclohexanone derivatives (Scheme 16).

The Malaprade reaction consists on the glycol cleavage with a non-toxic and stable reagent periodic acid (or its salts).[98] It is relatively selective for 1,2-diols which can form cyclic periodate intermediate (*cis*-diols), leaving the other diol functions unmodified. Use of periodate absorbed in wet silica gel broadens the substrate scope dramatically due to the possibility of using non-polar solvents. Other iodine-based reagents as well as chromium, ruthenium and lead reagents are able to execute the glycol cleavage. Alternatively, use of $Pb(OAc)_4$ (known as Criegee reaction) can be considered. Although the use of lead is less robust than the periodic salts, it has enhanced reactivity and better solubility in organic solvents thus enabling the cleavage of cumbersome substrates.

While oxidative cleavage reactions of C1–C2 and C5–C6 diols of quinic acid derivatives have been documented (and will be presented next), the C3–C4 and C6–C7 cleavages have not been reported. Nevertheless, considering that elimination reactions of different hydroxyl groups (namely C4[67] and C6[99]) are widely known for quinic acid, the installation of C=C bonds prone for *syn*-dihydroxylation and further C–C cleavage would provide chiral linear C7 fragments.

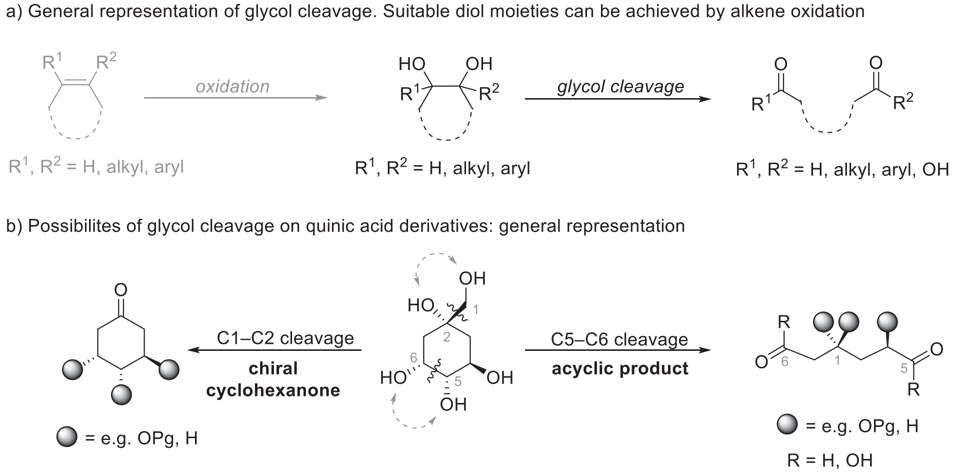
a) General representation of glycol cleavage. Suitable diol moieties can be achieved by alkene oxidation
R1
R2
oxidation
R1, R2 = H, alkyl, aryl
HO
OH
R1
R2
glycol cleavage
R1, R2 = H, alkyl, aryl
O
O
R1
R2
R1, R2 = H, alkyl, aryl, OH
b) Possibilites of glycol cleavage on quinic acid derivatives: general representation
O
= e.g. OPg, H
C1–C2 cleavage
chiral
cyclohexanone
OH
HO
1
2
6
HO
5
OH
OH
C5–C6 cleavage
acyclic product
R
O
6
1
5
O
R
= e.g. OPg, H
R = H, OH

Scheme 16. a) A general representation of glycol cleavage. b) Possibilities of oxidative C–C cleavage in quinic acid derivatives.

Maycock's and co-workers' total synthesis of (+)-negamycine **87** from quinic acid employed both C1–C2 and C5–C6 cleavages to achieve the linear structure of the natural product (Scheme 17).[100] The reduction of lactone **52** provided triol **79** and was followed by $NaIO_4$-mediated oxidative C–C cleavage to yield ketone **80** in 95% yield. Secondary C4 hydroxyl was protected with Bz-group, which promoted elimination as the cyclic rigid isopropylidene-group forced the molecule to adapt a boat conformation and triggered axial OBz-elimination. The temperature-controlled reduction of C2-ketone yielded 1:3 mixture of alcohols ((*S*)-**81** and (*R*)-**81**) and suppressed elimination. Isopropylidene removal yield *cis*-diol **83**, that was converted into a linear dialdehyde by Criegee cleavage and instantly reduced with $NaBH_4$ to form primary alcohol **84**. Regioselective protection of primary hydroxyl group at C5 was solved by base-mediated protecting group migration. The desired 1,4-Bz shift was achieved exclusively (**84**→**85**), and the migration reaction allowed the selective use of TBDMS- and BOM-protecting groups (**86**) in a later stage of the synthesis.

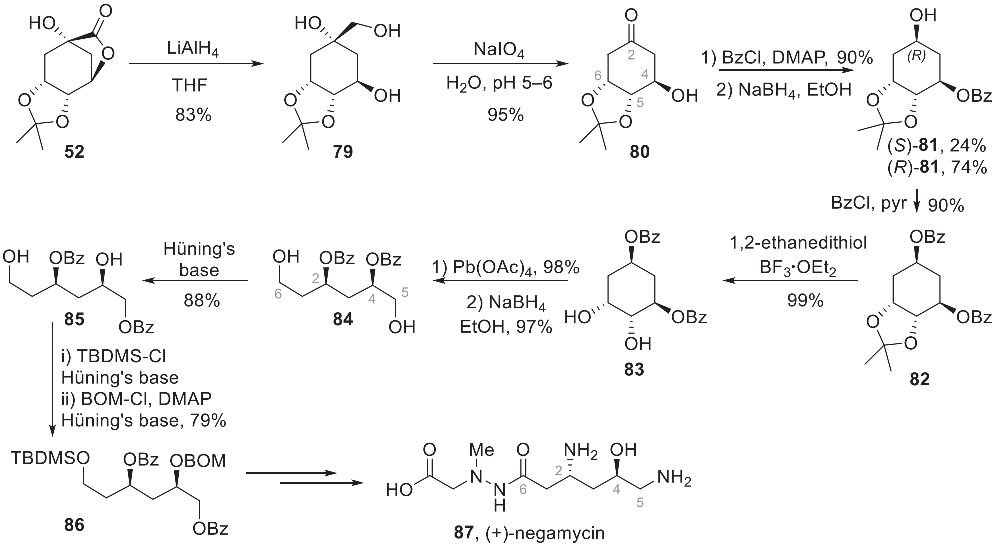
52
LiAlH4
THF
83%
79
NaIO4
H2O, pH 5–6
95%
80
1) BzCl, DMAP, 90%
2) NaBH4, EtOH
(R)
(S)-81, 24%
(R)-81, 74%
BzCl, pyr 90%
82
1,2-ethanedithiol
BF3·OEt2
99%
83
1) Pb(OAc)4, 98%
2) NaBH4
EtOH, 97%
84
Hüning's base
88%
85
i) TBDMS-Cl
Hüning's base
ii) BOM-Cl, DMAP
Hüning's base, 79%
86
87, (+)-negamycin

Scheme 17. Total synthesis of (+)-negamycin. Glycol cleavage was the key reaction to achieve the linear structure.

The vicinal *cis*-diol cleavage of quinic acid derivatives has led to the formation of some interesting chiral building blocks bearing the cyclopentane core, as summarized in Scheme 18. The cyclopentenone **91** and its analog **96** can be seen as an intermediate for prostanoid and pentenomycin syntheses.[101, 102] The C–C cleavage product **92** was utilized in the synthesis of chiral carbocycle nucleosides **94** and **95**.[102]

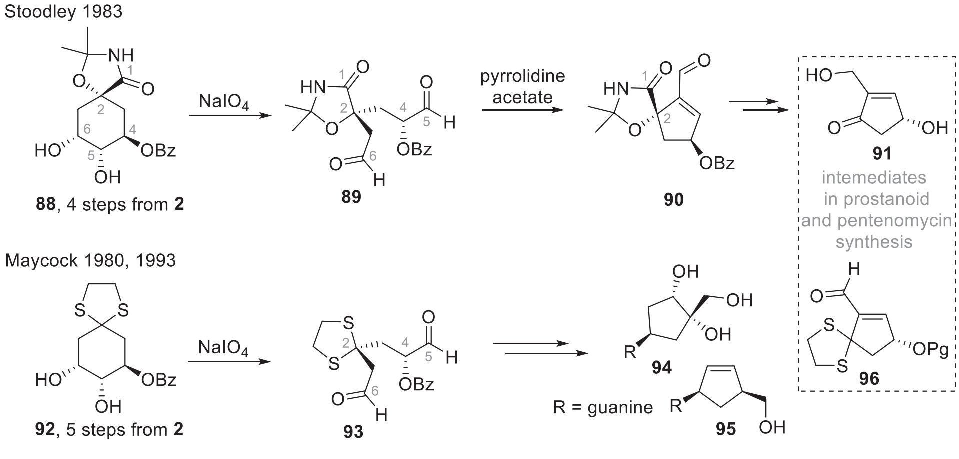
Stoodley 1983
88, 4 steps from 2
NaIO4
89
pyrrolidine
acetate
90
91
intemediates
in prostanoid
and pentenomycin
synthesis
Maycock 1980, 1993
92, 5 steps from 2
NaIO4
93
94
R = guanine
95
96

Scheme 18. Carbacycles synthesized by C1–C2 and C5–C6 glycol cleavage of quinic acid.

Quinic acid can be also transformed into acyclic nitrogenase cofactor homocitric acid **111** (figure 3) by glycol cleavage.[103, 104] The deoxygenation of secondary 4-OH of **97** gave *cis*-diol **89**, which could undergo oxidative cleavage to yield trimethyl homocitrate **99** along with its lactonic form **100** (Scheme 19). Alternative route for intermediate **98** is presented as part of this thesis' experimental work in Chapter 5 along with studies of oxidative glycol cleavage of some new synthetic intermediates.

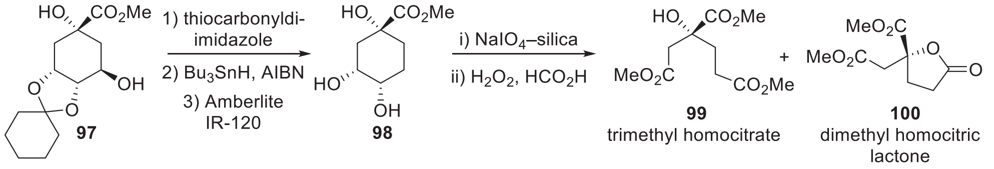

Scheme 19. Synthesis of homocitrates **99** and **100** by glycol cleavage.

The oxidative C–C cleavage of diols is widely used as part of total synthesis routes by trimming the terminal diol moieties and cleaving the cyclic vicinal-diol moieties.[98] Along with examples presented above, the glycol cleavage in quinic acid derivatives has been exploited in the total synthesis of (–)-malyngolide[105] and in the synthesis of chiral furanone building blocks.[106] Further oxidation of quinic acid (e.g. oxidation of C7 position) reveals new possibilities to synthesize acyclic products.[107,108]

3.3 Quinic acid in total syntheses

Like presented in previous chapters, the abundance of available synthetic manipulations of quinic acid makes it an attracting starting material for syntheses of natural products. In 1997 Barco *et al.* summarized quinic acid's applications in total syntheses[37] and the natural product syntheses between 1998 and 2008 was updated by Enev *et al.*[109] The following chapter will focus on the total syntheses after these two excellent reviews to introduce the latest accomplishments. The template created from quinic acid will be highlighted without going into deeper discussion of later-stage modifications.

The recent growing interest on circular bioeconomy and on utilization of biomass-based compounds has given new impetus to the use of chiral pool in total synthesis.[110] After 2008 a dozen of natural products or subunits of natural products has been synthesized from quinic acid and the structures are shown in Figure 3.

These natural products are structurally diverse and quinic acid skeleton spans from the major cores of carbasugars (+)-pericosines A and and C (**109** and **110**)[111] to subunits of complex natural products (**101–108**).

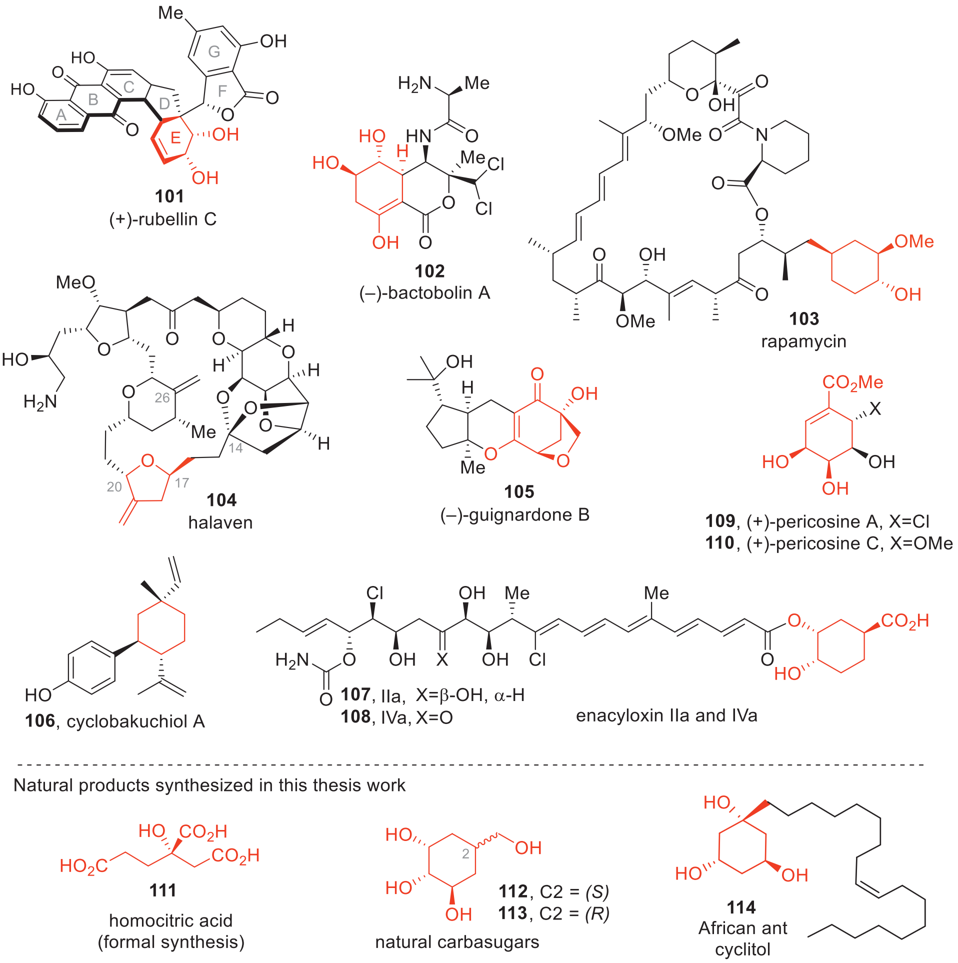
101
(+)-rubellin C
102
(–)-bactobolin A
103
rapamycin
104
halaven
105
(–)-guignardone B
109, (+)-pericosine A, X=Cl
110, (+)-pericosine C, X=OMe
106, cyclobakuchiol A
107, IIa, X=β-OH, α-H
108, IVa, X=O
enacyloxin IIa and IVa
Natural products synthesized in this thesis work
111
homocitric acid
(formal synthesis)
112, C2 = (S)
113, C2 = (R)
natural carbasugars
114
African ant
cyclitol

Figure 3. Natural products where quinic acid has been used to construct complex structures (the quinic acid-derived carbons are highlighted in red). The natural products synthesized in this thesis work are presented in the bottom section.

The E-ring of (+)-rubellin C was built up from enone **115** (Scheme 20).[92, 112] Previously described ketone **80** was synthesized from quinic acid in 3 steps. Enone **115** was later exploited in copper-catalyzed 1,4-addition of benzylic Grignard reagent to yield intermediate **116**. The hydrogenation of enone's **115** double bond delivered the six-membered carbon skeleton as terpene core for synthesis of cyclobacuchiol A **106** (Figure 3).[70]

The synthesis of (–)-bactobolin **102** also encompassed a quinic acid-derived enone intermediate (Scheme 20). The protection of *trans*-diol (4-OH and 5-OH) gives access to the selective manipulation of 6-OH, this permitting the synthesis of enone **118** (diastereomer of **115**) using a similar reduction–Malaprade oxidation–elimination sequence as in the synthesis of (+)-rubellin.[67, 113] In the construction of the bicyclic bactobolin core **121**, enone **118** was converted into silyl enol ether for vinylogous Mukaiyama-reaction to yield **120**.

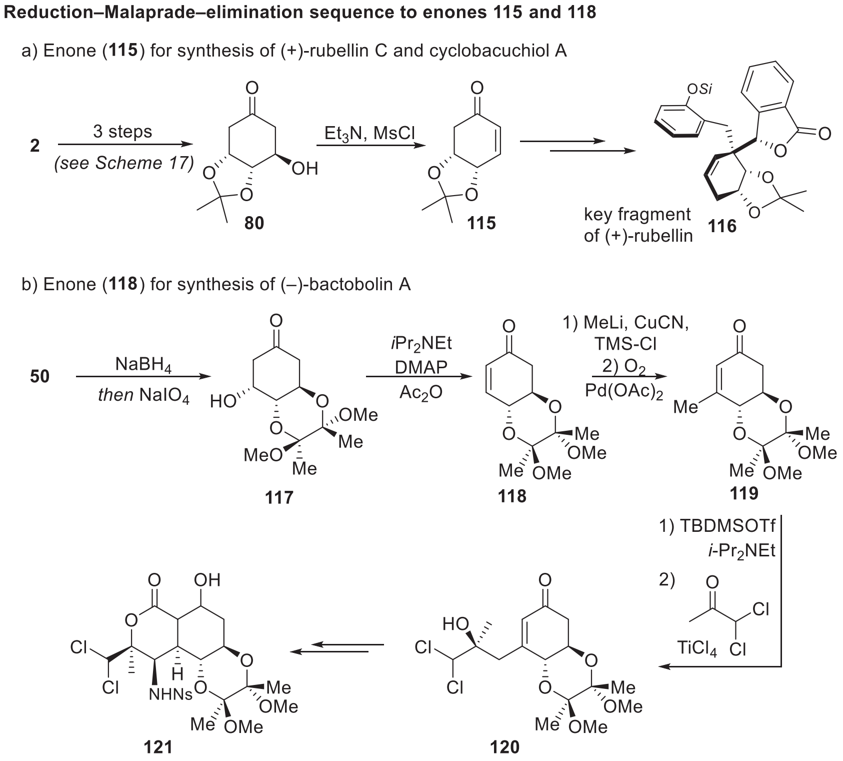
Reduction–Malaprade–elimination sequence to enones 115 and 118
a) Enone (115) for synthesis of (+)-rubellin C and cyclobacuchiol A
2
3 steps
(see Scheme 17)
80
Et$_3$N, MsCl
115
key fragment of (+)-rubellin
116
OSi
b) Enone (118) for synthesis of (–)-bactobolin A
50
NaBH$_4$
then NaIO$_4$
117
iPr$_2$NEt
DMAP
Ac$_2$O
118
1) MeLi, CuCN, TMS-Cl
2) O$_2$
Pd(OAc)$_2$
119
1) TBDMSOTf
i-Pr$_2$NEt
2)
TiCl$_4$
120
121
NHNs

Scheme 20. Diastereomeric enone fragments (**115** and **118**) were the key intermediates of total syntheses of a) (+)-rubellin and cyclobakuchiol and b) (–)-bactobolin.

The total syntheses of (–)-guignardone B (**105**) and of halaven C14–C26 fragment (**131**) utilized diacetates **124** or **125** as intermediates (Scheme 21). The TMS-protected lactone (**122** or **123**) was reduced to hemiacetal with DIBAL-H followed by acetylation to yield the fragments (**124** or **125**) suitable for further manipulation.

Synthesis of 6-oxabicyclo[3.2.1]octane core **128** of (–)-guignardone started by converting diacetate **124** into thiosemiacetal **126**, which treatment with Raney nickel yielded cyclic ether **127**. [114] Acetal deprotection of **127**, elimination and subsequent oxidations led to 6-oxabicyclo[3.2.1]octane core **128**. The equivalent bicyclic oxabicyclo[3.2.1]octane precursor **127** was synthesized in the scope of this thesis (Chapter 5, chiron **180**) in five steps from quinic acid.

In halaven C14–C26 fragment **131** synthesis, diacetate **125** was exposed to Lewis-acid mediated C-glycosidation (**125→129**) (Scheme 21).[115] This reaction followed by treatment with base yielded polycyclic pyran fragment **130**, which served the construction of C20 and C23 stereocenters of halaven. After multiple side-chain manipulations and other chemical transformations, chiral substituted THF-derivative **131** was obtained to be further involved in the synthesis as C14–C26 unit.

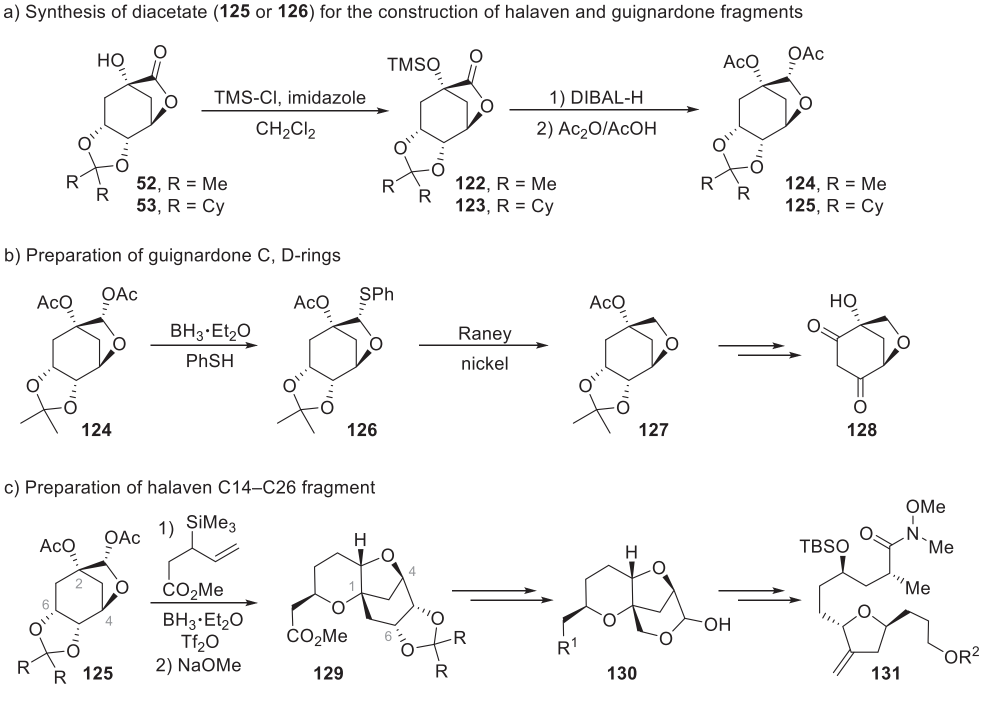
a) Synthesis of diacetate (**125** or **126**) for the construction of halaven and guignardone fragments

b) Preparation of guignardone C, D-rings

c) Preparation of halaven C14–C26 fragment

HO
O
TMS-Cl, imidazole
CH2Cl2
TMSO
1) DIBAL-H
2) Ac2O/AcOH
AcO
OAc
52, R = Me
53, R = Cy
122, R = Me
123, R = Cy
124, R = Me
125, R = Cy
BH3·Et2O
PhSH
SPh
Raney
nickel
124
126
127
128
1) SiMe3
CO2Me
BH3·Et2O
Tf2O
2) NaOMe
125
H
CO2Me
129
R1
OH
130
TBSO
OMe
N
Me
Me
OR2
131

Scheme 21. a) Analogous diacetate fragment's (**124** or **125**) syntheses. b) Preparation of (–)-guignardone B subunit. c) Preparation of halaven subunit.

Esters **134** and **137** can be seen as subunits of rapamycin and enacyloxins (Figure 3). Both synthesis strategies relied on Barton–McCombie deoxygenation. Treatment of benzylidene acetal **54** with NBS followed by tertiary hydroxyl activation with thiocarbonylimidazolide group allowed the double Barton–McCombie deoxygenation (**133**) in the synthesis of rapamycin. In enacyloxin synthesis the Barton–McCombie deoxygenation was performed in two stages (**52→135** and **136→137**) to achieve the desired synthetic intermediate deoxygenated at C2 and C4.

a) Synthesis of ester **134**, a subunit of rapamycin

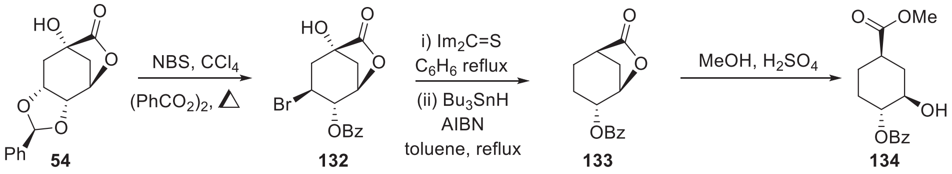
HO
O
O
O
O
Ph
54
NBS, CCl4
(PhCO2)2, Δ
HO
O
O
Br
OBz
132
i) Im2C=S
C6H6 reflux
(ii) Bu3SnH
AIBN
toluene, reflux
O
O
OBz
133
MeOH, H2SO4
O
OMe
OH
OBz
134

b) Synthesis of ester **137**, a subunit of enacyloxins

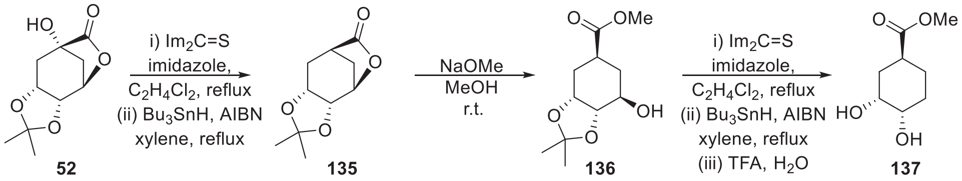
HO
O
O
O
O
52
i) Im2C=S
imidazole,
C2H4Cl2, reflux
(ii) Bu3SnH, AIBN
xylene, reflux
O
O
O
O
135
NaOMe
MeOH
r.t.
O
OMe
OH
O
O
136
i) Im2C=S
imidazole,
C2H4Cl2, reflux
(ii) Bu3SnH, AIBN
xylene, reflux
(iii) TFA, H2O
O
OMe
HO
OH
137

Scheme 22. Formal total syntheses of enacyloxin and rapamycin exploited Barton–McCombie deoxygenation to yield esters **134** and **137**. a) Synthesis of **134**. b) Synthesis of **137**.

The formal total synthesis of (+)-homocitric acid **111**, total syntheses of African ant cyclitol **114** and carbasugars **112** and **113** (Figure 3, bottom) will be discussed in Chapters 5–7 as part of the experimental work of this thesis.

3.4 Use of quinic acid in medicinal chemistry

Quinic acid has been exploited in drug discovery and the examples gathered in this chapter are the synthesis of Tamiflu, vitamin D analogues and a study of C7 substituted quinic acid derivatives as enzyme inhibitors.

Tamiflu is an important anti-influenza drug and industrially synthesized from shikimic acid **3** (available from extraction of star anis). Both shikimic acid and Tamiflu can be synthesized from quinic acid. Because of their structural similarity, multiple syntheses of shikimic acid from quinic acid have been attempted after the first report by Dangschat and Fischer in 1938.[116] Later, the syntheses of **3** or its epimers and methyl esters has been reported by groups of Géro, Grewe and

Hanessian amongst others.[117] The shortest synthesis route for (–)-methyl shikimate **140** by Géro *et al.* is presented in Scheme 23.[118] Selective benzoylation of secondary hydroxyls of methyl quinate **43** gave an intermediate **138**, which was dehydrated with SO_2Cl_2 to afford protected shikimate **139**. Deprotection of **139** gave (–)-methyl shikimate **140**.

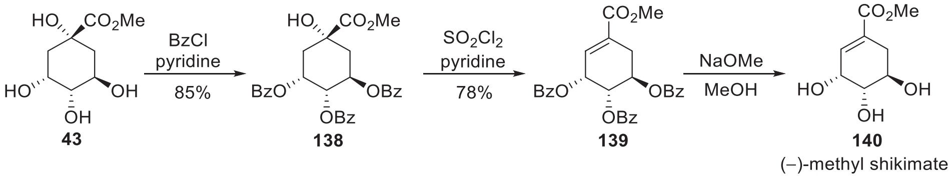

Scheme 23. Synthesis of (–)-methyl shikimate from methyl quinate by Géro *et al.*[118]

Quinic acid was explored as a starting material as an alternative to shikimic acid in the synthesis of Tamiflu (Scheme 24).[119, 120] In Rohloff's Tamiflu **149** (oseltamivir phosphate) synthesis, the vicinal diol moiety of methyl quinate (**43**) was protected with acetonide, followed by secondary 4-OH mesylation and tertiary hydroxyl dehydration to yield intermediate **141**.[120] Perchloric acid-catalyzed transketalization yielded **142** and an elegant reductive regioselective ketal opening exposed secondary hydroxyl 5-OH (**143**) readily for epoxide formation (**144**) upon treatment with base. The correct stereochemistry and amine functions of Tamiflu was achieved *via* epoxide opening with sodium azide (**145**) followed by formation of aziridine **146** and its regioselective opening with sodium azide (**147**). Finally, the acetylation of 5-NH, azide reduction and subsequent phosphorylation yielded **149**.

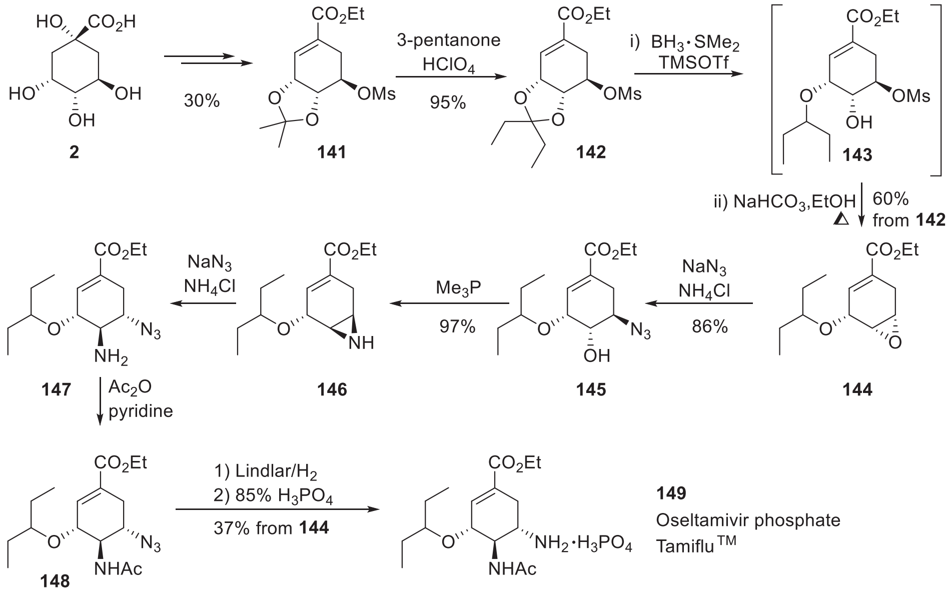

2
30%
141
3-pentanone
HClO4
95%
142
i) BH3·SMe2
TMSOTf
143
ii) NaHCO3,EtOH
Δ
60%
from 142
144
NaN3
NH4Cl
86%
145
Me3P
97%
146
NaN3
NH4Cl
147
Ac2O
pyridine
148
1) Lindlar/H2
2) 85% H3PO4
37% from 144
149
Oseltamivir phosphate
Tamiflu™

Scheme 24. Oseltamivir phosphate (Tamiflu™) synthesis from quinic acid.

Vitamin D derivatives' southern fragments have been synthesized from quinic acid by oxidative C1–C2 cleavage and deoxygenation or oxidation of secondary hydroxyl group at C5 (Scheme 25).[121, 122] The overlapping of the hydroxyls' stereochemistry of quinic acid with the vitamin derivatives provided the facile construction of kidney disease drug VS-105 **150** and proliferation inhibitor 19-nor-vitamin-D3 analogues (**151**). An alternative route for the preparation of the A-ring precursors is presented as part of this thesis work in Chapter 6.

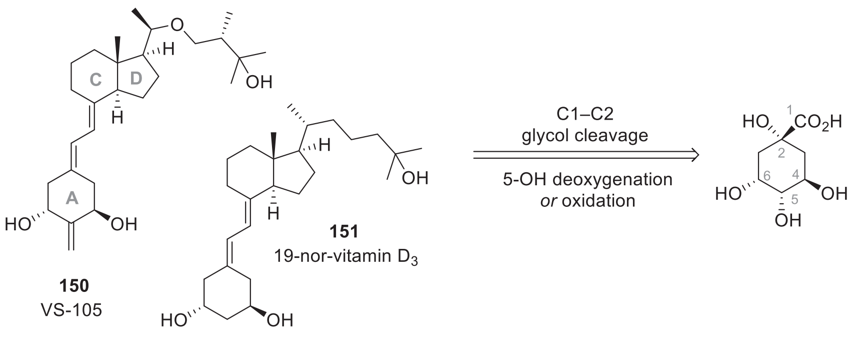

150
VS-105
151
19-nor-vitamin D3
C1–C2
glycol cleavage
5-OH deoxygenation
or oxidation

Scheme 25. Simplified retrosynthetic analysis of VS-105 and 19-nor-vitamin D3.

González-Bello and co-workers studied dehydroquinic acid analogues as potential inhibitors of 3-dehydroquinate dehydratase. The substitution of unnatural position of quinic acid (C7) has been exploited by selective epoxidation yielding valienamine analogues **154–159** (Scheme 26a).[123] The diastereomeric aminosugar-mimetics were shrewdly synthesized taking the advantage of anchimeric assistance and steric bulk: epoxide **153** is selectively formed from **152** while lactone moiety hinders the *Re*-face and hydroxyl group (5-OH) directs the epoxidation. Respectively, in **156** the selectivity of epoxide formation is *anti* to tertiary hydroxyl due to steric bulk by silyl groups. Moreover, the halogenation of C7 position (**164** and **165**) has yielded antimicrobial agents, time-dependent irreversible inhibitors of type I dehydroquinase from *E. coli* (Scheme 26b).[51, 124]

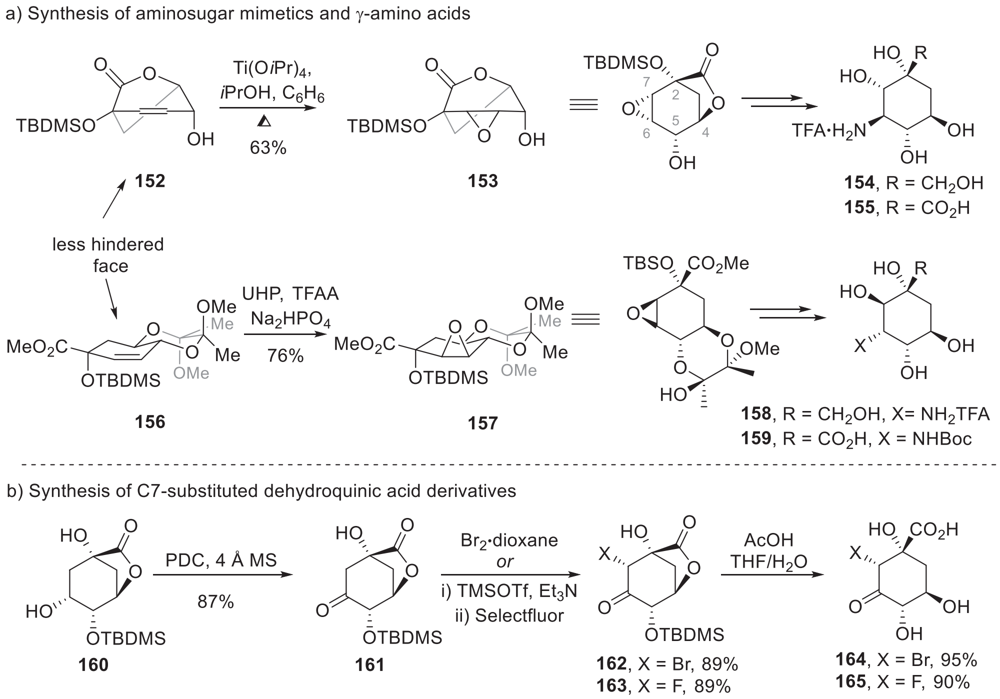
a) Synthesis of aminosugar mimetics and γ-amino acids

b) Synthesis of C7-substituted dehydroquinic acid derivatives

TBDMSO
OH
Ti(O*i*Pr)$_4$, *i*PrOH, C$_6$H$_6$
63%
152
153
TBDMSO
7
2
5
6
4
OH
HO
R
HO
TFA·H$_2$N
OH
154, R = CH$_2$OH
155, R = CO$_2$H
less hindered face
MeO$_2$C
OTBDMS
OMe
Me
UHP, TFAA
Na$_2$HPO$_4$
76%
156
157
TBSO
CO$_2$Me
OMe
HO
X
158, R = CH$_2$OH, X= NH$_2$TFA
159, R = CO$_2$H, X = NHBoc
PDC, 4 Å MS
87%
160
161
Br$_2$·dioxane
or
i) TMSOTf, Et$_3$N
ii) Selectfluor
162, X = Br, 89%
163, X = F, 89%
AcOH
THF/H$_2$O
CO$_2$H
164, X = Br, 95%
165, X = F, 90%

Scheme 26. Synthesis of C7-substituted quinic acid derivatives. a) Synthesis of aminosugar mimetics. b) Synthesis of halogenated quinic acid derivatives.

Natural products and their derivatives play a notable role in medicinal chemistry. From the new drugs discovered between 1981 and 2014, half of them are related to natural products either as such, or more often, as natural product mimetics or variants.[10] For modern biological research purposes, a structural diversification of natural products raises an opportunity for improving their activity.[125] The optimization of the chemical structure and building up large libraries of natural product congeners can increase the efficiency and hopefully lower the toxicity of drug candidates. The facile structural diversification of quinic acid facilitates the construction of libraries in the quest for finding more biological active substances (see also Chapter 8).

4 MATERIALS AND METHODS

All reactions were performed in oven-dried glassware with magnetic stirring under argon atmosphere, unless otherwise stated. The reactions performed in elevated temperatures were heated using a silicon oil bath. Low temperature reactions were performed in a Dewar flask filled with isopropanol and liquid nitrogen or brine/ice or water/ice baths. Dry solvents (THF, Et_2O, CH_2Cl_2) were obtained by passing deoxygenated solvents through activated alumina columns (PureSolv micro solvent purification system). Acetonitrile was left standing over 3 Å molecular sieves (beads) and used without further drying. Reactions were monitored through thin-layer chromatography (TLC) with commercial silica gel plates (Merck silica gel, 60 F254). Visualization of the developed plates was performed under UV light at 254 nm and by staining with cerium ammonium molybdate, phosphomolybdic acid, potassium permanganate or vanillin stains.

4.1 Compound characterization

Flash column chromatography was performed on silica gel 60 (40−63 µm) as stationary phase. ^{1}H NMR spectra were recorded at 300 MHz and ^{13}C NMR spectra were recorded at 75 MHz on a 300 MHz Varian Mercury spectrometer at room temperature, using $CDCl_3$, D_2O, CD_3OD or DMSO-d_6 as solvent. Alternatively, ^{1}H and ^{13}C spectra were recorded at 500 MHz and 125 MHz respectively in a JEOL ECZR 500 instrument at room temperature. Chemical shifts (δ) are reported in ppm referenced to TMS peak (δ 0.00). Alternatively, the residual peak from the deuterated solvent was used as reference: $CDCl_3$ (δ 7.26), D_2O (δ 4.79), DMSO-d_6 (δ 2.50), CD_3OD (δ 4.78) for ^{1}H NMR and $CDCl_3$ (δ 77.16), DMSO-d_6 (δ 39.52), CD_3OD (δ 49.00) for ^{13}C NMR, or acetone in D_2O (δ 2.50 in ^{1}H NMR, and δ 30.89 in ^{13}C NMR). The following abbreviations were used to describe peak splitting patterns: s = singlet, d = doublet, t = triplet, m = multiplet. Coupling constants *J* were reported in Hertz (Hz).

High-resolution mass spectra were recorded on a Waters ESI-TOF MS spectrometer. Specific rotations were obtained on a Polax-2L (Altago) polarimeter equipped with a sodium lamp (λ = 589 nm) utilizing a 100 mm cell. Single crystals suitable for X-ray diffraction analysis were obtained by slow evaporation method. The single crystal x-ray diffraction data was collected at 120(2) K on an Agilent SuperNova dual wavelength diffractometer with micro-focus x-ray source and Atlas detector and using multilayer optics monochromatized Cu-Kα (λ = 1.54184 Å) radiation.

4.2 Computational details

All calculations were performed using the Gaussian 09 software package, without symmetry constraints. The optimized geometries in Publication **I** were obtained employing the M06-2X functional with a standard 6-31G(d,p) basis set and solvent effects (CH_2Cl_2) were considered using the Polarizable Continuum Model (PCM). Single point energy calculations were performed using the M06-2X functional and a standard 6-311++G(d,p) basis set. The optimized geometries in Publication III were obtained using the PBE1PBE functional, keeping the standard 6-31G(d,p) basis set in gas phase. Transition state optimizations were performed with the Synchronous Transit-Guided Quasi-Newton Method (STQN). Frequency calculations were performed to confirm the nature of the stationary points, yielding only real frequency for the minima and one imaginary frequency for the transition states. Each transition state was further confirmed by following its vibrational mode downhill on both sides, and obtaining the minima presented on the energy profile. A Natural Population Analysis (NPA) and the resulting Wiberg indices were used to study the electronic structure and bonding of the optimized species and calculate as implemented on Gaussian 09. The electronic energies (E_{b1}) obtained at the PBE1PBE/6-31G(d,p) level of theory in Publication **I** were converted to free energy at 298.15 K and 1 atm (G_{b1}). The free energy values presented along the text (G_{b2}) were derived from the electronic energy values obtained at the M06-2X/6-311G(d,p)// M06-2X /6-31G(d,p) level, including solvent effects (E_{b2}), according to the following expression:

$G_{b2} = E_{b2} + G_{b1} – E_{b1}$.

Further details for each computational study are presented in Publication **I** and Publication **III**.

4.3 Experimental section

This chapter briefly describes the general synthetic procedures and preparation of key compounds presented in Chapters 5 and 6 (Publications **I** and **II**). Synthetic procedures of compounds described in Chapters 7 and 8 (Publications **III** and **IV**) are shown in the copies of original publications in the end of the thesis. Further details and synthetic procedures for all compounds including spectral characterization can be found from Supporting material of each publication.

4.3.1 General procedure for $B(C_6F_5)_3/R_3SiH$ deoxygenation

Mesylated quinic acid derivative **174** or **179** (0.09–0.14 mmol) was dissolved in dry CH_2Cl_2 (0.05–3 M) under argon. $B(C_6F_5)_3$ (1–10 mol%) was added followed by addition of Et_3SiH (1.05–4 equiv.) at room temperature. The mixture was stirred at room temperature for 1 hour and the reaction was quenched by addition of Et_3N (3 drops). Volatiles were removed under reduced pressure and the residue obtained was purified using flash column chromatography.

Characterization of key compounds:

175: ^{1}H NMR (500 MHz, $CDCl_3$) δ 7.80 (dd, *J* = 8.0, 1.4 Hz, 2H), 7.69 (dd, *J* = 8.0, 1.3 Hz, 2H), 7.63 (dd, *J* = 8.0, 1.3 Hz, 2H), 7.52 (dd, *J* = 8.0, 1.3 Hz, 2H), 7.45 (dd, *J* = 5.6, 4.3 Hz, 2H), 7.40 (ddd, *J* = 8.3, 4.9, 1.5 Hz, 4H), 7.37–7.31 (m, 6H), 7.30–7.18 (m, 8H), 7.06 (t, *J* = 7.7 Hz, 2H), 3.97 (bs, 1H), 3.21 (d, *J* = 10.5 Hz, 1H), 2.96 (ddd, *J* = 12.4, 3.8, 2.4 Hz, 1H), 2.85 (dd, *J* = 10.4, 0.7 Hz, 1H), 2.56 (s, 3H), 2.51 (t, *J* = 12.4 Hz, 1H), 1.97 (td, *J* = 13.8, 3.8 Hz, 1H), 1.68 (d, *J* = 13.8 Hz, 1H), 1.45–1.39 (m, 1H), 1.19 (m, 1H), 1.17 (s, 9H), 0.98 (s, 9H), 0.87 (m, 10H). ^{13}C NMR (125 MHz, $CDCl_3$) δ 136.4, 136.2, 136.2, 136.1, 136.0, 135.9, 135.2, 135.1, 134.4, 134.3, 133.9, 133.0, 129.8, 129.8, 129.7, 129.6, 129.6, 129.5, 127.7, 127.7, 127.7, 127.6, 127.6, 127.5, 75.8, 72.5, 70.5, 70.4, 39.4, 36.9, 27.9, 27.8, 27.3, 27.2, 26.9, 19.7, 19.6, 18.9; HRMS $[M+Cl]^-$ *m/z* calcd for $C_{56}H_{70}O_6SSi_3Cl$ 989.3890, found 989.3878; $[\alpha]_D^{22}$ –19.3 (c = 0.06 g/ml, CH_2Cl_2).

176: ^{1}H NMR (500 MHz, $CDCl_3$) δ 7.84 (dd, *J* = 8.0, 1.3 Hz, 2H), 7.69 (dd, *J* = 8.0, 1.3 Hz, 2H), 7.64–7.60 (m, 6H), 7.47 (dd, *J* = 8.0, 1.3 Hz, 2H), 7.42–7.32 (m, 14 H), 7.29 (t, *J* = 7.5 Hz, 4H), 7.21 (t, *J* = 7.6 Hz, 2H), 4.12 (bs, 1H), 3.48 (ddd, *J* = 11.5, 3.8, 2.2 Hz, 1H), 3.38 (ddd, *J* = 23.4, 9.8, 5.9 Hz, 2H), 1.86 (q, *J* = 11.8 Hz, 1H), 1.53–1.48 (m, 2H), 1.37 (td, *J* = 12.7, 3.4 Hz, 1H), 1.28–1.19 (m, 2H), 1.11 (s, 9H), 1.01 (s, 9H), 1.00 (s, 10 H). ^{13}C NMR (125 MHz, $CDCl_3$) δ 136.5, 136.2, 136.1, 136.0, 135.8, 135.8, 135.1, 134.8, 134.5, 134.4, 134.2, 134.2, 129.6, 129.6, 129.6, 129.4, 129.4, 127.7, 127.7, 127.6, 127.5, 127.5, 127.5, 75.4, 72.2, 68.9, 39.2, 32.3, 31.3, 27.4, 27.3, 27.0, 22.4, 19.6, 19.4, 19.2. HRMS $[M+Na]^+$ *m/z* calcd for $C_{55}H_{68}O_3Si_3Na$ 883.4374, found 883.4448; $[\alpha]_D^{26}$ – 3.9 (c = 0.06 g/ml, CH_2Cl_2).

180: ^{1}H NMR (500 MHz, $CDCl_3$) δ 7.69 (dd, *J* = 8.0, 1.3 Hz, 2H), 7.60–7.54 (m, 6H), 7.50 (dd, *J* = 8.0, 1.3 Hz, 2H), 7.45–7.26 (m, 18H), 7.17 (dd, *J* = 7.9, 7.4 Hz, 1H), 3.99–3.96 (t, *J* = 5.5, 1H), 3.80–3.68 (m, 1H), 3.23 (dd, *J* = 7.4, 2.0 Hz, 1H), 2.81 (d, *J* = 7.4 Hz, 1H), 2.03 (d, *J* = 10.6 Hz, 1H), 1.85 (td, *J* = 11.5, 1.8 Hz, 1H), 1.64 (ddd, *J* = 10.5, 6.1, 2.7 Hz, 1H), 1.42 (ddd, *J* = 11.4, 5.7, 2.5 Hz, 1H), 1.32–1.22 (m, 1 H), 0.99 (s, 9H), 0.91 (s, 9H), 0.88 (s, 9 H). ^{13}C NMR (75 MHz, $CDCl_3$) δ 136.4, 136.2, 136.1, 136.0, 135.9, 135.8, 135.0, 134.8, 134.5, 134.1, 133.9, 133.5, 129.9, 129.8, 129.7, 129.5, 129.5, 127.8, 127.7, 127.7, 127.6, 127.6, 127.5, 78.6, 77.4, 75.1, 71.7, 69.8, 43.4, 37.8, 27.4, 27.1, 27.1, 19.6, 19.2, 19.0. HRMS $[M+Na]^+$ *m/z* calcd for $C_{55}H_{66}O_4Si_3Na$ 897.4167, found 897.4183; $[\alpha]_D^{23}$ –22.2 (c = 0.09 g/ml, CH_2Cl_2).

4.3.2 General procedure for Malaprade reaction

Vicinal diol **180** (obtained by complete cleavage of silyl groups) or **187** (0.07–0.08 mmol) was dissolved in acetonitrile-water mixture (ratio 3:2, 0.2–0.3 M) at room temperature. The solution was cooled down to 0 °C, sodium periodate (1.2 equiv.) was added, and the solution was stirred at room temperature for 1 hour. The reaction was filtrated through a silica pad and rinsed with acetonitrile. Volatiles were removed under reduced pressure to yield corresponding dialdehyde.

Characterization of key compounds:

181 (in equilibrium with corresponding hydrate): ^{1}H NMR (500 MHz, D_2O, MeOH used as reference) δ 9.72 (t, *J* = 2.0 Hz), 5.28 (dd, *J* = 6.1, 5.2 Hz), 4.96 (d, *J* = 5.4 Hz), 4.94 (d, *J* = 5.3 Hz), 4.18–4.08 (m), 3.94 (dd, *J* = 9.7, 1.5 Hz), 3.84–3.80 (m), 3.75 (d, *J* = 9.7 Hz), 3.41 (d, *J* = 1.3 Hz), 2.94 (qd, *J* = 16.9, 2.1 Hz), 2.26 (ddd, *J* = 13.6, 6.5, 1.5 Hz), 2.13 (ddd, *J* = 13.5, 6.4, 1.5 Hz), 2.05 (dd, *J* = 14.5, 5.1 Hz), 2.02–1.99 (m), 1.98–1.96 (m), 1.95–1.85 (m). ^{13}C NMR (125 MHz, D_2O, MeOH used as reference) δ 205.64, 91.68, 91.50, 89.01, 81.04, 80.88, 79.71, 78.91, 78.43, 78.12, 50.55, 44.28, 40.73, 40.15. HRMS $[M+Na]^+$ *m/z* calcd for $C_7H_{10}O_4Na$ 181.0477, found 181.0488.

188: ^1H NMR (500 MHz, $CDCl_3$) δ 9.77 (t, *J* = 1.4 Hz, 2H), 3.60 (dd, *J* = 10.0, 4.6 Hz, 1H), 3.47 (dd, *J* = 10.0, 6.3 Hz, 1H), 2.54–2.48 (m, 3H), 2.35 (ddd, *J* = 16.9, 5.8, 1.6 Hz, 1H), 2.22–2.13 (m, 1H), 1.72 (dq, *J* = 14.8, 7.4 Hz, 1H), 1.63 (qd, *J* = 7.6, 6.6 Hz, 1H), 0.87 (s, 9H), 0.03 (s, 6H). ^{13}C NMR (125 MHz, $CDCl_3$) δ 202.12, 201.99, 65.24, 46.43, 41.62, 35.55, 25.98, 23.50, 18.36, -5.42. HRMS $[M+H]^+$ *m/z* calcd for $C_{13}H_{27}O_3Si$ 259.1729, found 259.1736; $[\alpha]_D^{23}$ –18.9 (c = 8.8 mg/ml, CH_2Cl_2).

4.3.3 General procedure for silyl migration reaction

Diol **171** or **195** (0.11–0.19 mmol) was dissolved in solvent (0.1–0.2 M) and base (1–5 equiv.) was added at room temperature. Reaction mixture was heated to desired temperature, and after stirring, allowed to cool down. The solvent was evaporated under reduced pressure, and the residue obtained was purified using flash chromatography, yielding pure **192–194** or **196–198**.

Characterization of key compounds:

192: ^1H NMR (500 MHz, DMSO-d_6) δ 7.80 (d, *J* = 6.5 Hz, 2H), 7.66 (d, *J* = 7.0 Hz, 2H), 7.59 (ddd, *J* = 7.9, 5.8, 1.3 Hz, 5H), 7.48 – 7.30 (m, 17H), 7.22 – 7.05 (m, 4H), 4.74 (d, *J* = 3.2 Hz, 1H), 4.07 (s, 1H), 4.01 (bs, 1H), 3.84 (d, *J* = 11.7 Hz, 1H), 3.64 (bs, 1H), 3.31 (d, *J* = 9.6 Hz, 1H), 2.73 (d, *J* = 9.6 Hz, 1H), 2.10 (t, *J* = 11.2 Hz, 1H), 1.88 (d, *J* = 13.3 Hz, 1H), 1.66 (dd, *J* = 13.3, 2.6, 1H), 1.23 (d, *J* = 11.2 Hz, 1H), 1.08 (s, 9H), 0.89 (s, 9H), 0.88 (s, 9H). ^{13}C NMR (125 MHz, DMSO-d_6) δ 135.8, 135.5, 135.4, 135.2, 135.1, 134.0, 133.8, 133.5, 133.3, 129.8, 129.6, 129.5, 129.4, 127.7, 127.5, 127.5, 127.4, 74.9, 71.7, 69.6, 68.6, 68.6, 38.4, 34.1, 26.9, 26.8, 26.8, 19.2, 19.0, 18.5. HRMS (ESI) m/z: $[M+Na]^+$ Calcd for $C_{55}H_{68}O_5Si_3Na$ 915.4272; found 915.4302. $[\alpha]_D^{21}$ +0.6 (c = 0.07 g/ml, CH_2Cl_2).

193: ^1H NMR (500 MHz, DMSO-d_6) δ 7.66 (dd, *J* = 8.0, 1.2, 2H), 7.63 (dd, *J* = 8.0, 1.2, 2H), 7.60 (dd, *J* = 8.0, 1.2, 2H), 7.55 (dd, *J* = 8.0, 1.2, 2H), 7.42 – 7.34 (m, 10H), 7.33 – 7.21 (m, 12H), 4.60 (d, *J* = 3.7 Hz, 1H), 4.18 (ddd, *J* = 11.8, 4.3, 2.8, 1H), 4.12 (s, 1H), 3.83 (dd, *J* = 6.1, 3.7 Hz, 1H), 3.74 (d, *J* = 10.2 Hz, 1H), 3.47 (dd, *J* = 6.0, 3.4 Hz, 1H), 3.26 (d, *J* = 10.2 Hz, 1H), 2.16 (d, *J* = 11.8, 2.9 Hz, 1H), 1.84 (t, *J* = 11.8 Hz, 1H), 1.62 (dd, *J* = 13.2, 3.4 Hz, 1H), 1.32 (d, *J* = 13.2 Hz, 1H), 1.00 (s, 9H), 0.94 (s, 9H), 0.69 (s, 9H). ^{13}C NMR (125 MHz, DMSO-d$_6$) δ 135.4, 135.4, 135.3, 135.3, 135.3, 135.2, 133.9, 133.8, 133.7, 133.4, 132.9, 132.9, 129.8, 129.8, 129.6, 129.5, 127.6, 127.6, 127.5, 72.1, 71.8, 71.4, 69.6, 69.1, 37.1, 36.2, 26.9, 27.0, 26.7, 19.1, 19.0, 18.4. HRMS (ESI) m/z: [M+Na]$^+$ Calcd for $C_{55}H_{68}O_5Si_3Na$ 915.4272; found 915.4233. $[\alpha]_D^{22}$ –4.3 (c = 0.12 g/ml, CH_2Cl_2).

194: ^{1}H NMR (500 MHz, DMSO-d$_6$) δ 7.64 (dd, *J* = 13.6, 6.8 Hz, 4H), 7.59 (d, *J* = 7.1 Hz, 2H), 7.44 – 7.34 (m, 10H), 7.31 (dd, *J* = 12.7, 7.3 Hz, 5H), 7.18 (t, *J* = 7.4 Hz, 5H), 7.10 (dd, *J* = 15.7, 7.8 Hz, 4H), 4.65 (d, *J* = 4.5 Hz, 1H), 4.29 (s, 1H), 4.05 (bs, 1H), 3.90 (m, 2H), 3.71 (bs, 1H), 3.26 (d, *J* = 10.3 Hz, 1H), 2.29 (s, 1H), 1.87 (t, *J* = 9.9 Hz 1H), 1.67 (dd, *J* = 14.1, 3.2 Hz, 1H), 1.11 (d, *J* = 13.8 Hz, 1H), 1.02 (s, 9H), 0.91 (s, 9H), 0.61 (s, 9H). ^{13}C NMR (125 MHz, DMSO-d$_6$) δ 135.8, 135.3, 135.3, 135.2, 135.1, 133.7, 133.5, 133.3, 133.2, 132.7, 129.6, 129.4, 129.3, 127.7, 127.7, 127.5, 127.4, 127.3, 127.2, 74.4, 72.1, 71.1, 69.7, 65.4, 37.4, 35.9, 26.8, 26.7, 26.5, 19.0, 19.0, 18.3. HRMS (ESI) m/z: [M+Na]$^+$ Calcd for $C_{55}H_{68}O_5Si_3Na$ 915.4272; found 915.4287. $[\alpha]_D^{22}$ +4.0 (c = 0.07 g/ml, CH_2Cl_2).

4.3.4 Gilman reaction

Oleyl bromide **216’** (156 mg, 0.47 mmol, 6 equiv.) was weighed into a dried round-bottom flask and purged with argon after which Et_2O (2 ml) was added and reaction mixture cooled down to –78 °C. *t*-BuLi (0.55 ml, 1.7 M in pentane, 0.94 mmol, 12 equiv.) was slowly added and the mixture was stirred for 15 minutes. Suspension of CuI (15 mg, 0.08 mmol, 1 equiv.; in 0.5 ml of Et_2O) was added at –78 °C and stirred for additional 15 minutes before a solution of the epoxide **214** (30 mg, 0.08 mmol, 1equiv.) in diethyl ether (1 ml) was added. The reaction mixture was allowed to warm up to –20 °C over 45 minutes, diluted with hexane and quenched with sat. aq. NH_4Cl solution (5 ml). After stirring at room temperature for 30 minutes the layers were separated. The aqueous phase was extracted with EtOAc (3 x 3 ml), the organic phases were combined, dried with $MgSO_4$, filtered, and the solvent was removed under reduced pressure. The residue was purified by flash chromatography (CH_2Cl_2) to yield Gilman product **218** as clear oil (36 mg, 73%). ^{1}H NMR (500 MHz, $CDCl_3$) δ 7.69 (ddd, *J* = 7.9, 3.5, 1.5 Hz, 4H), 7.46 – 7.35 (m, 6H), 5.36 (t, *J* = 4.9 Hz, 2H), 4.35 (tt, *J* = 10.9, 4.4 Hz, 1H), 4.19 – 4.07 (m, 1H), 2.80 (d, *J* = 6.6 Hz, 1H), 2.25 (s, 1H), 2.08 (d, *J* = 14.9 Hz, 1H), 2.02 (dd, *J* = 12.5, 6.8 Hz, 4H), 1.88 – 1.82 (m, 1H), 1.76 (dd, *J* = 14.4, 2.0 Hz, 1H), 1.47 (ddd, *J* = 13.6, 11.1, 2.8 Hz, 1H), 1.42 – 1.38 (m, 2H), 1.38 – 1.22 (m, 27H), 1.07 (s, 9H), 0.93 (s, 1H), 0.89 (t, *J* = 7.0 Hz, 3H). ^{13}C NMR (125 MHz, $CDCl_3$) δ 135.9, 135.9, 134.7, 134.6, 130.1, 130.0, 129.7, 127.7, 75.4, 68.7, 65.4, 65.2, 56.1, 48.3, 46.6, 44.0, 42.5, 42.3, 41.8, 40.1, 32.1, 31.7, 31.5, 30.2, 29.9, 29.9, 29.8, 29.7, 29.7, 29.5, 27.4, 27.1, 23.0, 22.8, 19.3, 14.3. HRMS (ESI) m/z: $[M+Na]^+$ Calcd for $C_{41}H_{66}O_3SiNa$ 657.4679; Found 657.4700. $[\alpha]_D^{20}$ –17.2 (c = 0.10 g/ml, CH_2Cl_2).

Diol **218** (30 mg, 0.05 mmol) was dissolved in THF (0.5 ml) and TBAF (0.5 ml, 0.5 mmol, 10 eq.; 1M in THF) was added and the reaction mixture was refluxed for 3 hours. The reaction mixture was allowed to cool down to room temperature, diluted with EtOAc and quenched with sat. aq. NH_4Cl solution (5 ml). Layers were separated and the aqueous phase was extracted with EtOAc (3 x 3 ml), the organic phases were combined, dried with $MgSO_4$, filtered, and the solvent was removed under reduced pressure. The residue was purified by flash chromatography (EtOAc) to yield African ant cyclitol **114** as white thick oil (17 mg, 90%). ^{1}H NMR (500 MHz, $CDCl_3$) δ 5.34 (t, *J* = 5.1 Hz, 2H), 4.34 (td, *J* = 11.2, 5.5 Hz, 1H), 4.29 (bs, 1H), 3.59 (bs, 1H), 3.18 (bs, 1H), 2.26 (d, *J* = 12.7 Hz, 1H), 2.08 (dd, *J* = 12.7, 1.7 Hz, 1H), 2.01 (dd, *J* = 12.5, 6.7 Hz, 4H), 1.91 – 1.85 (m, 1H), 1.49 – 1.37 (m, 4H), 1.37 – 1.23 (m, 27H), 1.04 (s, 1H), 0.87 (t, *J* = 6.9 Hz, 3H). ^{13}C NMR (125 MHz, $CDCl_3$) δ 130.6, 130.5, 76.0, 69.3, 64.0, 46.8, 44.5, 42.6, 40.5, 32.5, 32.3, 30.7, 30.4, 30.3, 30.2, 30.2, 30.2, 23.0, 27.8, 23.6, 23.3, 14.8. HRMS (ESI) m/z: $[M+Cl]^-$ Calcd for $C_{25}H_{48}O_3Cl$ 431.3292; Found 431.3283. $[\alpha]_D^{22}$ –7.3 (c = 0.03 g/ml, EtOH).

5 $B(C_6F_5)_3$-CATALYZED DEOXYGENATION OF QUINIC ACID DERIVATIVES

5.1 Aim of the study

As discussed in Chapter 2.2, the $B(C_6F_5)_3$-catalyzed selective deoxygenation with hydrosilanes ($B(C_6F_5)_3$/SiH) applied to sugars produces valuable chiral synthons, while Chapter 3 showed the potential of quinic acid for the syntheses of complex structures. While the Barton–McCombie reaction and dehydration–hydrogenation sequence have been the tools commonly used for decreasing the content of hydroxyl groups of quinic acid, it was envisioned that the borane-catalyzed partial deoxygenation could provide new valuable chiral synthons with more user-friendly chemicals. This chapter gives an overview and presents the most significant accomplishments of the complete study presented as Publication **I**.

5.2 Initial studies

The transposition of the $B(C_6F_5)_3$-catalyzed selective deoxygenation with hydrosilanes to quinic acid derivatives should consider the higher reactivity of primary and secondary hydroxyl groups as they are known to be cleaved smoothly while tertiary hydroxyls are somewhat tolerant to this transformation.[29, 31] Additionally, the application of $B(C_6F_5)_3$/SiH to carboxylic acid derivatives have shown to cause full reduction and deoxygenation up to methyl unit.[126, 127] Aware of the substrate and protecting group dependency and aiming at the partial deoxygenation of quinic acid, the study was started with screening of different protecting groups of quinide vicinal diol. Since the available protecting groups that tolerate $B(C_6F_5)_3$/SiH are limited, stable carbamoyl and sulfone/sulfoxide protected lactones were prepared. Protected quinides **57** and **59** (along with unprotected quinide **35**) were treated with multiple silyl hydrides, although the lack of solubility or reactivity hampered the formation of deoxygenated products (Scheme 27). On the other hand, quinides protected with sulfur groups (**166** and **58**) were reduced to silylated diols **167** and **168** (Scheme 27) though this same transformation can be performed with other reducing agents such as $NaBH_4$. Further treatment of the silylated diols **167** and **168** with $B(C_6F_5)_3$/SiH proved futile and no deoxygenation products were observed.

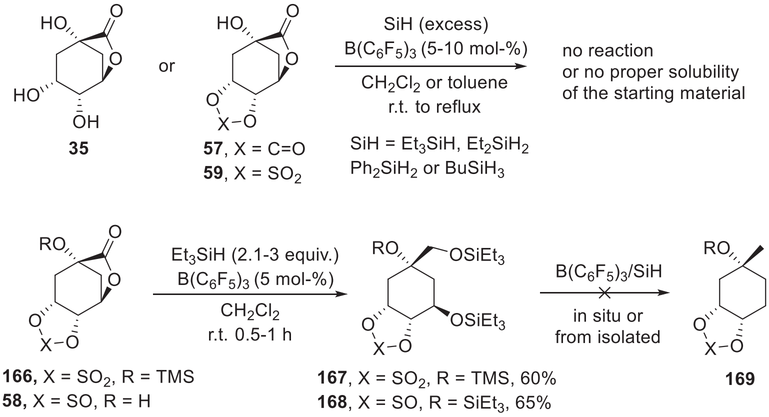
HO
O
O
HO
OH
35
or
HO
O
O
O
X–O
57, X = C=O
59, X = SO2
SiH (excess)
B(C6F5)3 (5-10 mol-%)
CH2Cl2 or toluene
r.t. to reflux
SiH = Et3SiH, Et2SiH2
Ph2SiH2 or BuSiH3
no reaction
or no proper solubility
of the starting material
RO
O
O
O
X–O
166, X = SO2, R = TMS
58, X = SO, R = H
Et3SiH (2.1-3 equiv.)
B(C6F5)3 (5 mol-%)
CH2Cl2
r.t. 0.5-1 h
RO
OSiEt3
OSiEt3
O
X–O
167, X = SO2, R = TMS, 60%
168, X = SO, R = SiEt3, 65%
B(C6F5)3/SiH
in situ or
from isolated
RO
O
X–O
169

Scheme 27. Deoxygenation attempts on quinide and protected lactones with $B(C_6F_5)_3$/SiH.

It was suspected that the lack of reactivity observed was due to the rigidity imposed by the cyclic protecting groups, since only acyclic protecting groups were previously reported for the intended transformation in polyols. Moreover, treatment of cyclic sugar derivatives with $B(C_6F_5)_3$/SiH promote ring opening which greatly increases the flexibility of the molecule and is likely to facilitate C–O bond cleavage. The formation of disilyl oxonium ion is crucial for the deoxygenation. In sugar derivatives the neighboring group participation (silylated hydroxyl groups) supported the formation of the reactive species leading to deoxygenation instead of the direct hydride delivery.[34] It was suspected that the use of acyclic silyl protecting groups in quinic acid would also initiate the formation of similar species due to released ring strain in the molecule leading to cyclic silyloxonium formation (Scheme 28). The presence of large silyl ethers in positions C2, C5 and C6 of quinide combined with small silyl hydrides was hypothesized to provide the desired cyclic silyloxonium (**TS-1**, Scheme 28a) after opening of the lactone. In such an event, the opening of the three-membered rings should be conditioned by stereochemical constrains and the hydride delivery would be expected to occur at C1 and C4. Moreover, large silyl groups are known to deeply effect the conformation of cyclohexanes by the 1,3-*syn*-diaxial repulsion,[58, 128] which could be beneficial for the desired hydride delivery regioselectivity.

To test the stated hypothesis on anchimeric assistance by silyl groups, silylated lactones were prepared (Scheme 28b). Lactones **65** and **66** were exposed to $B(C_6F_5)_3$/SiH conditions but no deoxygenation was observed. TBDMS-protected lactone **65** was reduced to silyl ether **170**, but the substrate with larger silyl groups (TBDPS) showed different reactivity leading to formation of multiple non-isolated products. This observation confirmed the effect of the silane substituents on the reactivity of quinic acid derivatives.

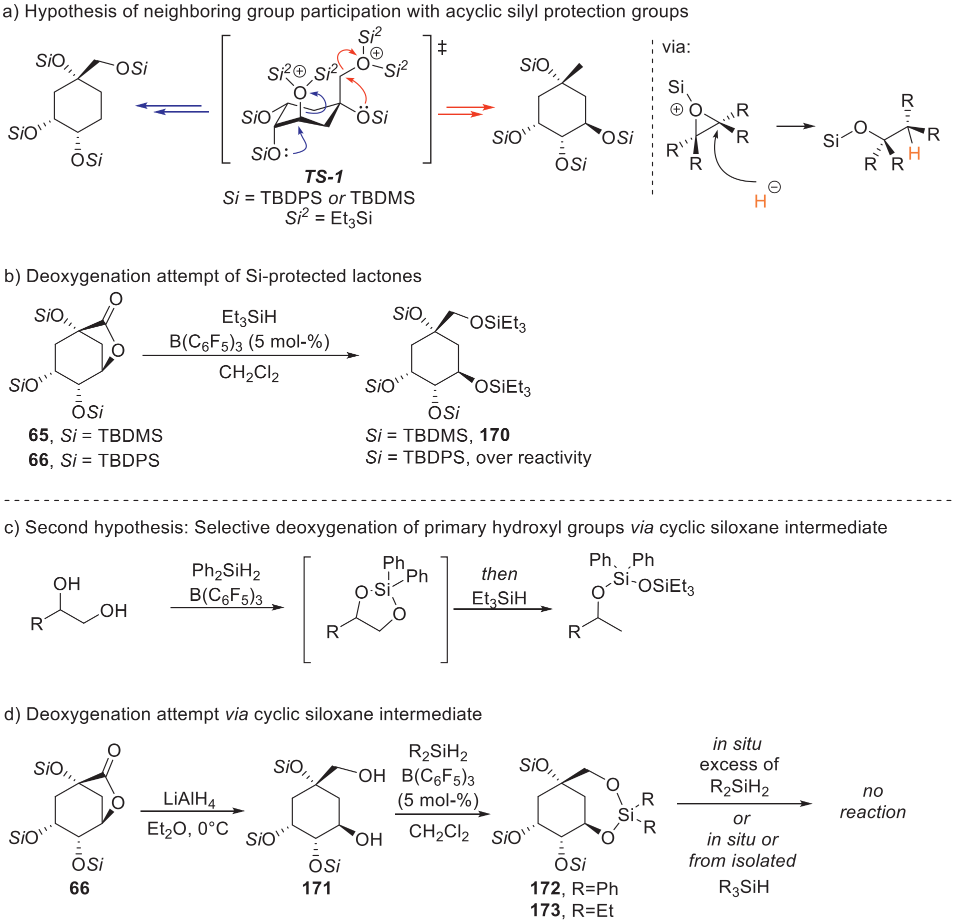
a) Hypothesis of neighboring group participation with acyclic silyl protection groups

b) Deoxygenation attempt of Si-protected lactones

c) Second hypothesis: Selective deoxygenation of primary hydroxyl groups *via* cyclic siloxane intermediate

d) Deoxygenation attempt *via* cyclic siloxane intermediate

SiO
OSi
‡
TS-1
Si = TBDPS or TBDMS
Si² = Et₃Si
via:
H
Et₃SiH
B(C₆F₅)₃ (5 mol-%)
CH₂Cl₂
OSiEt₃
65, Si = TBDMS
66, Si = TBDPS
Si = TBDMS, 170
Si = TBDPS, over reactivity
Ph₂SiH₂
B(C₆F₅)₃
then
Et₃SiH
LiAlH₄
Et₂O, 0°C
R₂SiH₂
B(C₆F₅)₃
(5 mol-%)
CH₂Cl₂
66
171
172, R=Ph
173, R=Et
in situ
excess of
R₂SiH₂
or
in situ or
from isolated
R₃SiH
no
reaction

Scheme 28. Initial studies of deoxygenation with acyclic protecting groups. a) Hypothesis of anchimeric assistance. b) Reduction of silylated lactones. c) Hypothesis of cyclic siloxane intermediate. d) Cyclic siloxanes derived from quinic acid and deoxygenation attempts.

The second hypothesis was based on the study of Morandi *et al.*,[129] where terminal vicinal diols were deoxygenated *via* cyclic siloxane intermediate (Scheme 28c).

Lactone **66** was reduced to diol **171** and treated with secondary silyl hydrides. The formation of cyclic silyl ether was rapid on both secondary silanes tested (Ph_2SiH_2, Et_2SiH_2, **172** and **173**, respectively) but the quinic acid-derived siloxanes proved unreactive (Scheme 28d).

5.3 Deoxygenation studies

The focus of the work was then turned to the anchimeric assistance of sulfonyl groups as previously reported by Oestreich *et al.*, since excellent chemoselectivities on the C–O cleavage of primary alkyl-tosylates were achieved (Scheme 29).[130] However, vicinal terminal diols did not yield similar chemoselectivity due to formation of rearrangement products. A superior chemoselectivity was expected for the herein studied system due to its higher complexity when comparing with simple aliphatic systems.

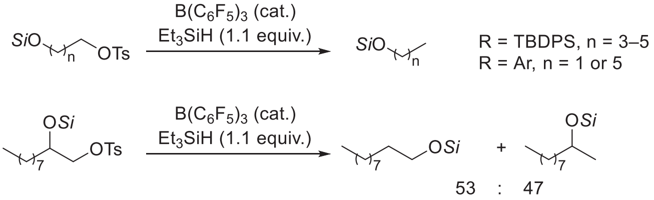

Scheme 29. C(sp^3)-O bond cleavage of primary alkyl tosylates with $B(C_6F_5)_3$/SiH system.

The treatment of mesylate **174** with different amounts of catalyst and Et_3SiH resulted in formation of **175** and/or **176** in different ratios (Table 2). Full deoxygenation of the mesylate moieties and excellent selectivity was achieved with excess of Et_3SiH (93%, entry 11) producing protected triol **176** in 93% yield. Although 3-membered silyloxonium ions are more prone to be opened with hydrides from the less hindered site,[129, 131] the participation of neighboring groups has shown to have a deep impact on the deoxygenation.[34, 130] The stereochemistry of the deoxygenation product **176** was confirmed by crystal X-ray diffraction analysis of derivative **177** (Scheme 30).

Table 2. Screenings of the quinic acid derivative deoxygenation.

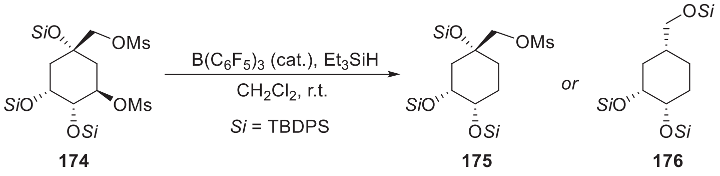
SiO
OMs
SiO
OMs
OSi
174
B(C6F5)3 (cat.), Et3SiH
CH2Cl2, r.t.
Si = TBDPS
SiO
OMs
SiO
OSi
175
or
OSi
SiO
OSi
176

Entry[a]	[**174**] (M)	B(C_6F_5)$_3$ (mol-%)	Et$_3$SiH (equiv.)	Yield (%)	**175:176**[b]
1	0.3	5	1.5	38	7.9:2.1
2	0.05	5	1.5	46	7.8:2.2
3	0.05	1	1.5	44	7.7:2.3
4	0.05	10	1.5	49	8.0:2.0
5[c]	0.05	5	1.5	78	7.8:2.2
6[c]	0.05	5	1.75	74	6.6:3.4
7[c],[d]	0.05	5	1.5	52	8.1:1.9
8[d]	0.05	5	1.05	37	8.1:1.9
9[c], [e]	0.05	5	1.05	18	0:10
10	0.05	5	4.0	82	2.3:7.7
11[f]	0.3	5	4.0	93	0:10

[a]Unless otherwise noted, **174** (0.14 mmol) and B(C_6F_5)$_3$ in CH_2Cl_2, at r.t. followed by dropwise addition of Et$_3$SiH for 1 h. [b]ratio determined from isolated yields [c]fast addition of silane, [d]reaction performed at 10 ˚C, [e]reaction performed in toluene. [f]B(C_6F_5)$_3$ in CH_2Cl_2 at r.t. followed by dropwise addition of Et$_3$SiH for 5 min. Solution of **174** (0.11 mmol in CH_2Cl_2) was added dropwise.

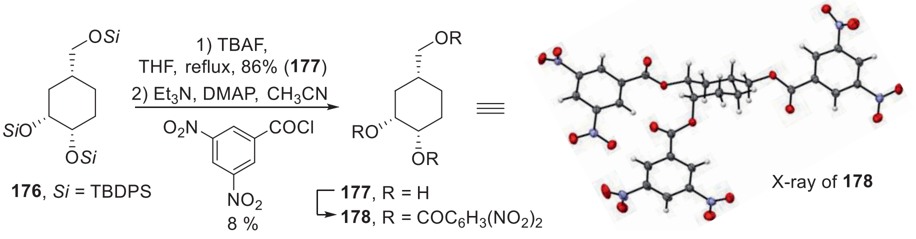
OSi
SiO
OSi
176, Si = TBDPS
1) TBAF,
THF, reflux, 86% (177)
2) Et3N, DMAP, CH3CN
O2N
COCl
NO2
8 %
OR
RO
OR
≡
177, R = H
178, R = COC6H3(NO2)2
X-ray of 178

Scheme 30. Preparation and X-ray crystal structure of protected triol **178**.

The reaction of the secondary mesylate at C4 proved to be faster than the primary mesylate at C1 yielding monomesylate **175**, which was further deoxygenated at C2. The second C–O bond cleavage is likely facilitated by the smaller steric hindrance and ring strain in the monomesylate, when considering a putative formation of a 3-membered silyloxonium at C1–C2. Different reaction conditions were screened aiming at reaching different selectivity. With 1.5 equivalents of silane in presence of 5 mol-% of catalyst, selectivity towards **175** was good but the overall yield remained poor (entries 1 and 2, [**174**]=0.3 or 0.05, respectively). The selectivity was not affected by the catalyst loading (1–10 mol-%, entries 2–4).

Finally, the fast addition of silane improved the yield of **175** while keeping good selectivity (entry 5). Slight increase of silane worsened the selectivity (entry 6) while decreasing temperature or silane equivalents deteriorated the overall yield (entries 7 and 8, respectively). Interestingly, reaction performed in toluene gave full selectivity to **176** with scanty amount of silane (entry 9), although in very low yield.

Aiming at the selective deoxygenation of 2-OH and to overcome the higher propensity of C4 towards deoxygenation, 4-OH was protected with different groups (Scheme 31). Treatment of **179a** with Et_3SiH first led to formation of secondary silyl ether (R-O-$SiEt_3$) followed by intramolecular cyclization to ether **180**. Similar reactivity was observed with TMS-protected **179b**. MOM-protected analog **179c** treated in same conditions yielded methyl ether **179d**, which was further cyclized to cyclic silyl ether **180** upon addition of more silane. Despite the harsh reaction conditions (5.0 equiv. Et_3SiH, 20 mol-% $B(C_6F_5)_3$, refluxing in toluene), carbamoyl protected **179e** was found to be unreactive and only starting material was recovered from the reaction.

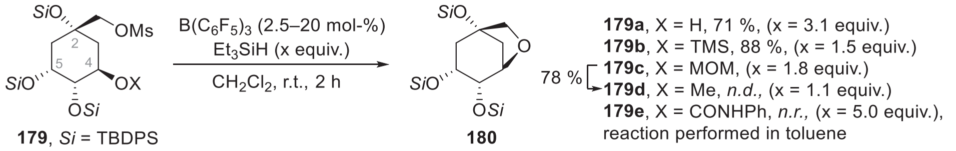

*Si*O
OMs
2
5
4
*Si*O
OX
O*Si*
179, *Si* = TBDPS
$B(C_6F_5)_3$ (2.5–20 mol-%)
Et_3SiH (x equiv.)
CH_2Cl_2, r.t., 2 h
*Si*O
O
*Si*O
O*Si*
180
78 %
179a, X = H, 71 %, (x = 3.1 equiv.)
179b, X = TMS, 88 %, (x = 1.5 equiv.)
179c, X = MOM, (x = 1.8 equiv.)
179d, X = Me, *n.d.,* (x = 1.1 equiv.)
179e, X = CONHPh, *n.r.,* (x = 5.0 equiv.), reaction performed in toluene

Scheme 31. Deoxygenation of mono mesylates yielded cyclic ether **180**. *n.d.* = not determined, *n.r.* = no reaction.

5.4 Valorization of deoxygenation products

Despite the futile attempt on the selective deoxygenation of 2-OH, an intriguing product **180** was formed in excellent yields, whose reactivity was studied further. The oxidative vicinal diol cleavage was envisioned to produce unforeseen chiral THF-derivatives. Deprotection of silyl groups followed by Malaprade reaction yielded dialdehyde **181**, which along with alcohol analog **182**, can be seen as interesting synthetic intermediates due to the presence of two stereogenic centers in the tetrahydrofuran core (Scheme 32).

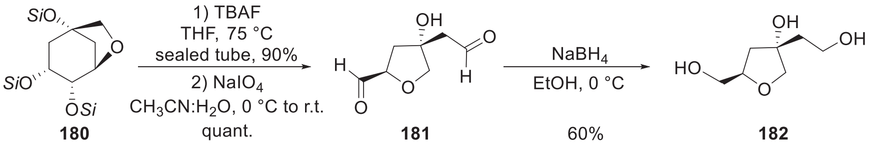

Scheme 32. Modification of cyclic ether **180**.

The recent study by Gagné and co-workers on sugar-derivatives reduction revealed a site-selectivity dependence on the hydride source (R_3SiH or HBCat) and the hydroxyl protecting group (silyl or BCat).[36] The attempts to expose cyclic ether **180** to reductive $B(C_6F_5)_3$/SiH conditions proved ineffective as only starting material was recovered from the reaction. Instead, cyclic ether moiety of **180** was opened with HBCat yielding alcohol **184** in 87% yield (Scheme 33a). In Gagné's protocol, bulkier protecting groups seemed to suppress the reactivity and increase the chemoselectivity of the reduction. A similar effect was detected in the transformation of bicyclic tetrahydrofuran **183**, as the deprotection of tertiary silyl group and treatment with HBCat/$B(C_6F_5)_3$ yielded **185**. Contrastingly, in this system the ether moiety was disentangled from more hindered position while opening from less hindered site was favored for sugar-derivatives.

To reveal the stereochemistry of **185**, the silyl groups were cleaved, and the NMR spectra were compared with previously obtained **177**. After silylation of the primary hydroxyl group of **186**, the vicinal diol moiety was cleaved with Malaprade reaction. The similarity of the chiral dialdehyde obtained with Perlin aldehydes **189** suggest that **188** can be a valuable synthetic fragment (Scheme 33b).[132]

The value of **184** was exemplified by using it in the formal synthesis of nitrogenase cofactor homocitric acid **111**. The known intermediate of synthesis of homocitric acid (**98**)[104] was accomplished by oxidation of primary hydroxyl moiety followed by desilylation (Scheme 33c). Despite the unexecuted experiments, it is noteworthy that the manipulation of **183** with deuterated catechol borane would provide deuterium labelled homocitric acid.[104]

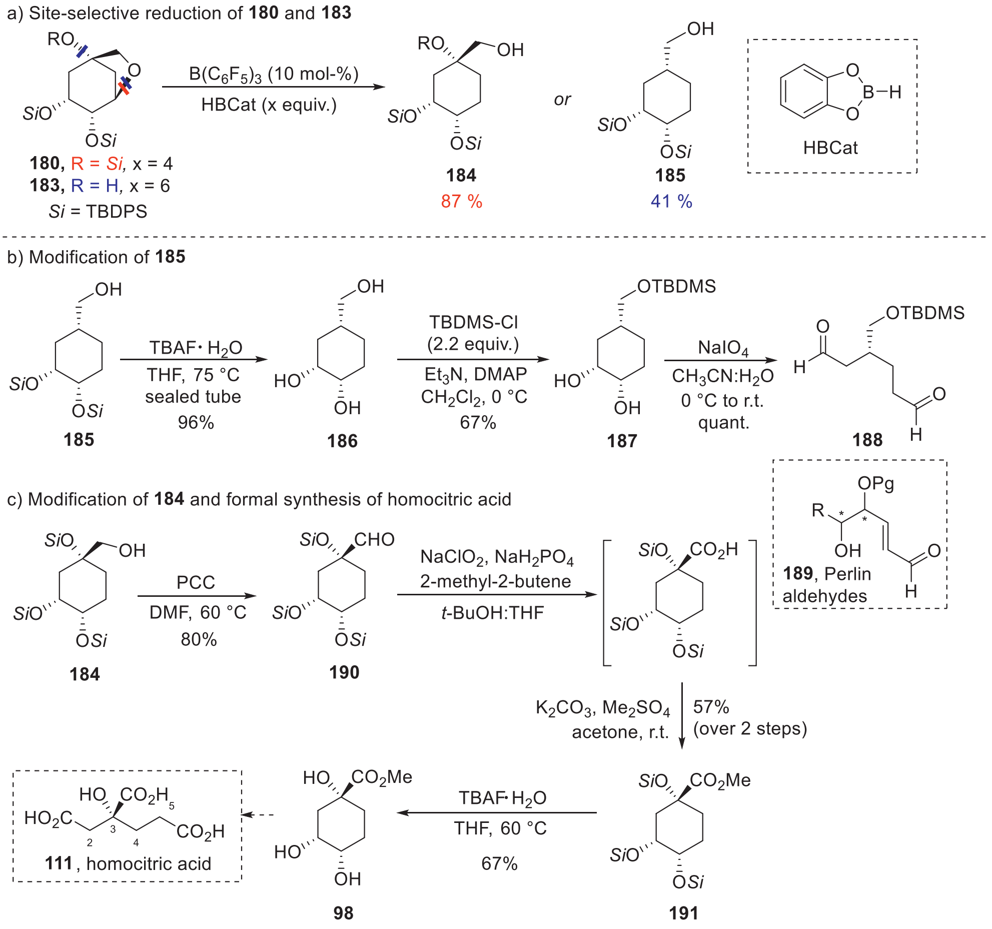
a) Site-selective reduction of 180 and 183
B(C6F5)3 (10 mol-%)
HBCat (x equiv.)
or
180, R = Si, x = 4
183, R = H, x = 6
Si = TBDPS
184
87 %
185
41 %
HBCat
b) Modification of 185
TBAF·H2O
THF, 75 °C
sealed tube
96%
TBDMS-Cl
(2.2 equiv.)
Et3N, DMAP
CH2Cl2, 0 °C
67%
NaIO4
CH3CN:H2O
0 °C to r.t.
quant.
185
186
187
188
c) Modification of 184 and formal synthesis of homocitric acid
PCC
DMF, 60 °C
80%
NaClO2, NaH2PO4
2-methyl-2-butene
t-BuOH:THF
189, Perlin aldehydes
184
190
K2CO3, Me2SO4
acetone, r.t.
57%
(over 2 steps)
TBAF·H2O
THF, 60 °C
67%
111, homocitric acid
98
191

Scheme 33. a) Reduction of **180** and **183** with HBCat. b) Protecting group manipulations and C–C cleavage of **184**. c) Formal synthesis of homocitric acid.

5.5 Mechanistic insight

As previously proposed by Oestreich,[130] a cyclic three-membered silyloxonium is a likely intermediate in the herein presented system. The easier formation of silyloxonium at C4–C5 compared to spiro-silyloxonium in C2, seems to control the extent of the deoxygenation. The spiro-silyloxonium formation after removal of mesylate from the cyclohexane ring should be less energy demanding, as the 1,3-diaxial repulsion between the mesylate and the C1–C2 silyloxonium is diminished. The regioselective hydride delivery to C4 in opening of the C4–C5 silyloxonium can be explained by the steric hindrance in C5 imposed by the silyl group at the vicinal C6 position. The same effect can be seen in C4–C5 epoxide opening selectivities on quinic acid derivatives with different nucleophiles.[133-136]

To justify the silyloxonium formation and study the selectivity, a simpler analog of **174** was prepared (**174’**) and exposed to reduction conditions (Scheme 34). Full selectivity of tertiary hydroxyl deoxygenation and silyl migration was observed and **176’** was obtained. Alkyl migration[131] or rearrangements that would cause a lack of chemoselectivity[130] in the reduction were not observed. When Et_3SiD was used in the deoxygenation of both **174’** and **174**, the deuterium was delivered to C1 and C4. Presence of deuterium in the product and the absolute configuration of C4 position was confirmed by NMR coupling constants, which also proved the direct silyloxonium opening from the less-hindered site. These observations suggest different mechanisms for C–O bond cleavage at C4 and C2 of **174**. While the former seems to have undergone a direct silyloxonium opening, the latter can be rationalized by a 1,2-hydride shift.

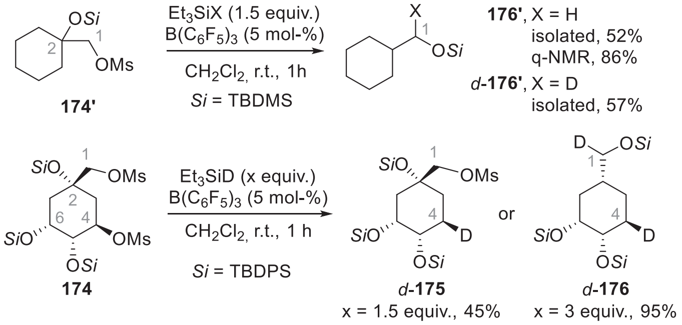
OSi
1
2
OMs
174'
Et3SiX (1.5 equiv.)
B(C6F5)3 (5 mol-%)
CH2Cl2, r.t., 1h
Si = TBDMS
X
1
OSi
176', X = H
isolated, 52%
q-NMR, 86%
d-176', X = D
isolated, 57%
SiO
1
OMs
2
6
4
SiO
OMs
OSi
174
Et3SiD (x equiv.)
B(C6F5)3 (5 mol-%)
CH2Cl2, r.t., 1 h
Si = TBDPS
SiO
1
OMs
4
SiO
D
OSi
d-175
x = 1.5 equiv., 45%
or
D
OSi
1
4
SiO
D
OSi
d-176
x = 3 equiv., 95%

Scheme 34. $B(C_6F_5)_3$-Catalyzed silyloxonium opening with Et_3SiD.

In order to elucidate the reaction mechanism operating in the deoxygenation at C1–C2, a simplified derivative 2-methylpropane-1,2-diol (**sm**) was considered as substrate in a Density Functional Theory (DFT) study (Scheme 35). The interaction of silylium ion with the mesylate group of the substrate **sm** is energetically favored and increases the electrophilic character of the primary carbon, leading to cyclic silyloxonium ion **int2**. The 1,2-hydride shift intermediate **int3** is energetically more stable than **int2** leading to oxocarbenium ion **int4** *via* a low energy barrier (2.5 kcal/mol). The hydride delivery to electrophilic oxocarbenium ion requires only 2.5 kcal/mol leading to very stable primary silyl ether **int5**. The deeper analysis and full computational details are presented in Publication **I** and its supporting material.

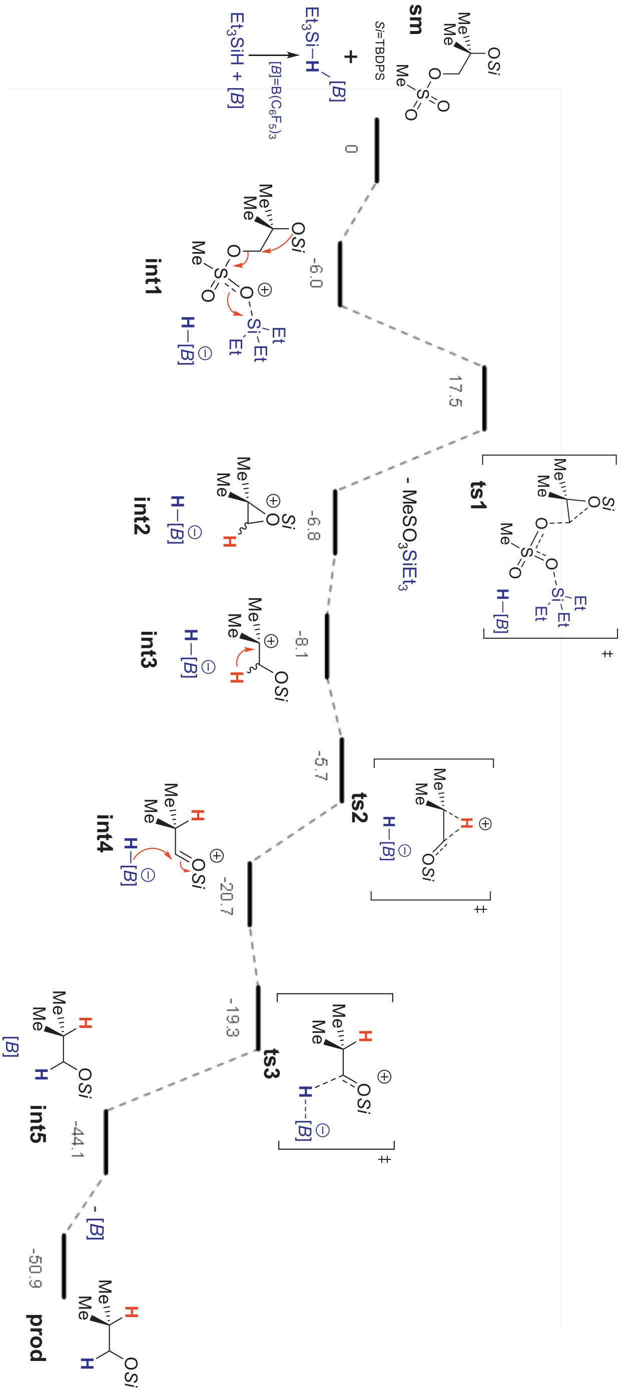
sm
Si=TBDPS
Et$_3$Si–H
[B]=B(C$_6$F$_5$)$_3$
Et$_3$SiH + [B]
0
int1
-6.0
ts1
17.5
- MeSO$_3$SiEt$_3$
int2
-6.8
int3
-8.1
ts2
-5.7
int4
-20.7
ts3
-19.3
int5
-44.1
- [B]
prod
-50.9

Scheme 35. Free energy profile (M06-2X/6-311++G**//M06-2X/6-31G**) and mechanistic representation for deoxygenation of model substrate **sm**, *via* silyloxonium and 1,2-hydride shift.

As a conclusion, the $B(C_6F_5)_3$ -catalyzed defunctionalization of quinic acid was developed by the installation of methanesulfonyl groups in the vicinal positions of silyl ethers. The study utilized a common intermediate which provided several chiral small molecules seen as value-added building blocks for further synthetic modifications. The divergent deoxygenation strategy led to a formal synthesis of homocitric acid. The achieved deoxygenations proved highly stereoselective through hydride delivery to cyclic silyloxonium ions. Computational and experimental studies revealed different mechanisms for the two opening of the two cyclic silyloxoniums involved.

6 *O,O*-SILYL GROUP MIGRATIONS IN QUINIC ACID DERIVATIVES: TOWARDS DIVERGENT SYNTHESIS

6.1 Aim of the study

In previous attempts on the sulfonylation of **171** (Chapter 5) *O,O*-silyl migration reactions across the cyclitol backbone of quinic acid derivative were observed. While protecting group migration is well-studied in the field of carbohydrate chemistry,[137] a thorough research study on protecting group migration for cyclitols such as quinic acid is missing. Therefore, this was taken as an opportunity for developing a divergent synthesis strategy by valorization of new regioisomers that could be achieved by migration of protecting groups, as presented in Publication **II**. As the valorization of biomass becomes more urgent, it is also important to study how the protecting groups can affect hemisynthesis strategies.

6.2 Silyl group migration in quinic acid derivatives and the effect of the protecting groups

The study started with treatment of protected diols **171** and **195** with the same sulfonylation conditions but in the absence of any sulfonyl chloride (Table 3, entry 1). A great selectivity towards **192** and **196** and excellent yields (95%) were observed for both silyl groups. Elongated reaction times yielded secondary→secondary migration only with TBDPS-protected alcohol producing a mixture of all three isomers **192–194** with decent selectivity on **193** (entry 2). Surprisingly, the use of stronger base Et_3N did not activate the migration, and only traces of **192** were detected (entry 3). Even stronger base NaH promoted the formation of **193** and **194** but the overall yield remained low (entry 4). Despite the previously reported excellent overall yields for NaH-promoted migrations on sugar derivatives,[138, 139] lowering the temperature (data not shown) did not return **193** or **194**. Side products detected by TLC in reactions at higher temperatures are believed to be silyl cleavage products.

Table 3. Selected experiments for optimization of silyl migration.

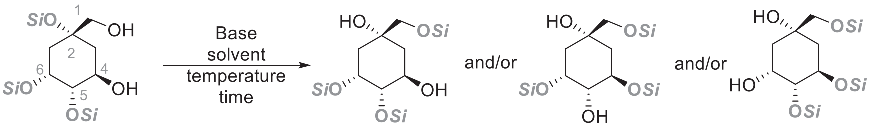

171, *Si* = TBDPS
195, *Si* = TBDMS

192, *Si* = TBDPS
196, *Si* = TBDMS

193, *Si* = TBDPS
197, *Si* = TBDMS

194, *Si* = TBDPS
198, *Si* = TBDMS

Entry[a]	Solvent	Base (equiv.)	Time (h)	*Si* = TBDPS[b]			*Si* = TBDMS[b]		
				192	**193**	**194**	**196**	**197**	**198**
1[c]	THF	Imidazole (2.0)	6	95	n.d.	n.d.	95	n.d.	n.d.
2	THF	Imidazole (3.0)	72	14	63	23	92	n.d.	n.d.
3	THF	Et$_3$N (3.0)	18	traces	n.d.	n.d.	n.d.	n.d.	n.d.
4	THF	NaH (3.0)	18	traces	57	17	-	-	-
5[d]	Toluene	Imidazole (2.0)	6	93	7	traces	99	n.d.	n.d.
6[d]	Toluene	Imidazole (5.0)	56	traces	78	16	66	25	traces
7[e]	DMF	Imidazole (2.0)	18	5	62	33	-	-	-
8[d], [f]	MeOH	Et$_3$N (1.0)	18	98	n.d.	n.d.	99	n.d.	n.d.
9[d]	MeOH	Imidazole (2.0)	18	78	11	traces	-	-	-
10	MeOH	DMAP (2.0)	18	traces	65	28	82	12	traces
11	MeOH	Imidazole (2.0) Et$_3$N (2.0)	18	5	56	29	68	22	8
12[g]	MeOH	Imidazole (2.0) Et$_3$N (2.0)	18	traces	50	35	14	49	27

[a]All reactions were carried out at 0.2 M of **171** or **195** in refluxing temperature, except indicated otherwise. [b]Isolated yield. [c]Substrate was used at 0.4 M; [d]Substrate was used at 0.1 M. [e] Carried out at 120 °C. [f]Carried out at room temperature; [g]Reaction in a sealed tube at 100 °C., n.d. – not detected.

The reaction temperature was raised by changing the solvent from THF to toluene and **193** was detected after only 6 hours (entry 5). Elongated reaction time and increased amount of the base improved the selectivity tremendously and **193** was detected with 78% yield (entry 6). The analogous reaction with TBDMS-protected derivative gave only 25% yield of **197** and traces of **198**. Further increase of the temperature using DMF as solvent (entry 7) resulted in the formation of **194** in higher yield (33%) but still in moderate regioselectivity.

Et$_3$N along with methanol has promoted the secondary→secondary silyl migrations in various substrates.[140, 141] The full selectivity towards **192** or **196** was achieved already at room temperature with one equivalent of Et$_3$N in MeOH (entry 8), which contrasted with the combined use of THF and Et$_3$N (entry 3) where only traces of products were observed. Such difference in reactivity clearly points to the importance of the combination of base and solvent. Next, other bases were screened together with MeOH (entries 9–11), which promoted the formation of **194** or **198** in moderate yields (up to 35% and 27%, **194** and **198**, respectively).

The reactivity difference between the facile tertiary→primary and more challenging secondary→secondary migrations were inferred to originate from the conformation of the molecule. The 2-*O*→1-*O* migratory process should occur regardless the conformation of the silyl ether as the oxygen groups involved in the migration are able to adopt a *syn*-periplanar conformation. Other migrations were not detected in absence of tertiary→primary migration. From a careful NMR-study, the conformations of the regioisomers (**192–194**) were determined (Scheme 36; see also Scheme 2 of Publication **II**, for detailed NMR data). The conformation of **192** was determined to be **192*** by nOe correlations (such as C1-H↔C6-H; C6-H↔C5-H and C5-H↔C4-H) and ^{1}H coupling constants. The peaks of C4-H and C5-H were observed as broad singlets due to the small coupling constants between them, which well agrees with 60° angle between the two vicinal C–H bonds in equatorial positions. The *trans*-relation between 5-OSi and 4-OH in **192*** does not favor the migration process, as suggested by the failed migration observed in experiments done at room temperature. High selectivity towards **193** was only achieved at elevated temperatures, which supports the event of a required ring flip prior to the migration. The *cis* relation between 6-*O* and 5-*O* in **193** should allow the silyl migration (**193→194**) on both conformations but the moderate reactivity towards **193** may be caused by a higher stability of isomer **193** where the secondary silyl ether groups are kept more distant. The conformations of **193** and **194** were determined by nOe correlations (for **193***: C1-H↔C6-H; C6-H↔C5-H and C5-H↔C4-H; for **194***: C2-OH↔C6-OH; C6-OH↔C4-H) and ^{1}H coupling constants (for **193*** e.g. small coupling constants (3.4 Hz and 3.7 Hz) between C4-H and C5-H indicates the 60° angle between the two vicinal C–H bonds in equatorial positions; 11.8 Hz coupling constant between C6-H and C7-H indicates the 180° angle between the vicinal C-H protons).

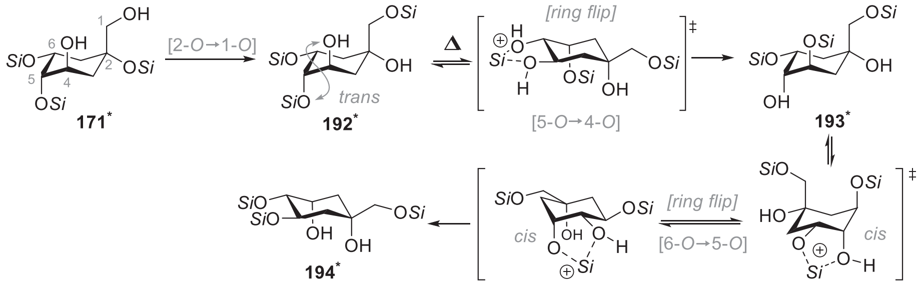

OH
1
6 OH
SiO
2
OSi
5
4
OSi
171*
[2-O→1-O]
OSi
OH
SiO
OH
SiO
trans
192*
Δ
[ring flip]
H
⊕O
Si
O
H
OSi
OH
OSi
[5-O→4-O]
‡
OSi
OSi
SiO
OH
OH
193*
SiO
OSi
HO
O
⊕
Si
O
H
cis
‡
[ring flip]
[6-O→5-O]
SiO
OSi
cis
OH
O
H
O
⊕Si
SiO
SiO
OSi
OH
OH
194*

Scheme 36. Proposed ring flip during secondary→secondary (5-*O*→4-*O*) migration. The most stable conformations determined by NMR-analysis are marked with *.

The different reactivity observed for the two sets of protected derivatives seems to be better explained by electronic factors rather than by stereochemical ones. The different electronic nature of the phenyl groups compared to alkyl ones is envisioned as the cause for the different propensity towards migration in the studied system, considering that the bulkier TBDPS group undergoes migration easier than the smaller TBDMS.[142]

6.3 Total synthesis of African ant cyclitol

Ants of the genus *Crematogaster* are known to produce venom in their Dufour glands.[143] Different species of *Crematogaster* have a distinctive feature to produce venoms which have long alkene chain with either *E*- or *Z*-configurations. In 2002 an African species of *Crematogaster* ants (*C. nigriceps*) were studied by Braekman *et al.* and unforeseen 1-alk(en)yl-1,3,5-trihydroxycyclohexanes (**114**, **200–204**, Figure 4) were found.[143]

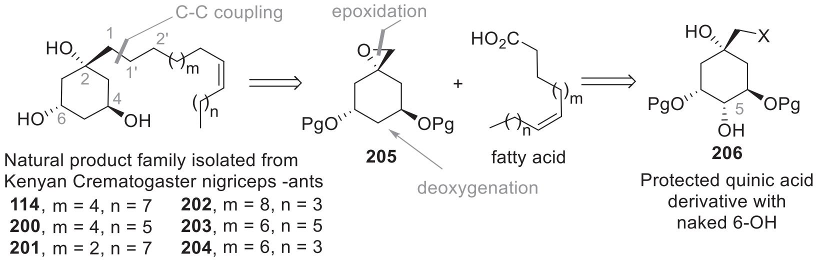

C-C coupling
epoxidation
HO
1
2'
1'
2
4
6
m
n
HO
OH
Natural product family isolated from Kenyan Crematogaster nigriceps -ants
114, m = 4, n = 7
200, m = 4, n = 5
201, m = 2, n = 7
202, m = 8, n = 3
203, m = 6, n = 5
204, m = 6, n = 3
O
PgO
OPg
205
deoxygenation
+
HO2C
m
n
fatty acid
HO
X
PgO
5
OPg
OH
206
Protected quinic acid derivative with naked 6-OH

Figure 4. Retrosynthetic analysis of African ant cyclitols.

The cyclitol backbone of the natural ant venoms has a great functional group overlap with quinic acid and the alkenyl side chains were recognized to be derivatives of common fatty acids. Retrosynthetically, C1–C1' disconnection would result in a fatty acid and epoxide **205** (Figure 4). The epoxide moiety is known to form under basic conditions from quinic acid derivatives (**206**, Figure 4; X=OTs),[88] while the regioselective deoxygenation of C5 hydroxyl group could be achieved from silyl migration product **193**.

With rearrangement product **193** in hands, the deoxygenation of secondary hydroxyl at C5 was targeted. The $B(C_6F_5)_3$-catalyzed deoxygenation was firstly considered (Chapter 5) as a continuation of the previous study. However, concerns about regioselectivity issues on the silyloxonium ring opening (Scheme 37, also see examples of opening C4–C5-epoxide with different nucleophiles[133-136]), moved the focus to the Barton–McCombie deoxygenation as a safer way to reach the desired deoxygenation (Scheme 38).

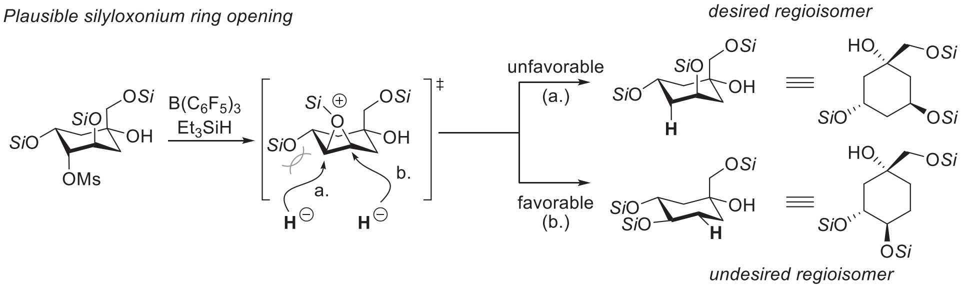

Scheme 37. Proposed silyloxonium ring formation and regioselectivity of $B(C_6F_5)_3$-catalyzed deoxygenation to two possible regioisomers.

In the initial attempts to install the carbonothioyl unit, the hindered secondary hydroxyl group of **193** was unreactive towards thiocarbonyldiimidazole (TCDI) at room temperature, and silyl migration took place at elevated temperatures due to the released imidazole. Similar problems were faced when attempting formation of a methyl xanthate ester **207** (Scheme 38a). Despite the low reaction temperatures, strong basic conditions caused silyl migration and mixtures of difficultly separable xanthates **207** and **208** (~4:1, respectively) were formed. As shown in Table 3 (Chapter 6.2), the migration can be controlled by the choice of the base. Benefitting from this information, pyridine was used along with phenyl chlorothionocarbonate under mild heating (Scheme 38b). The migration was not observed under these conditions and xanthate **209** was formed in 89% yield followed by clean Barton–McCombie deoxygenation to give alcohol **210** in 91% yield.

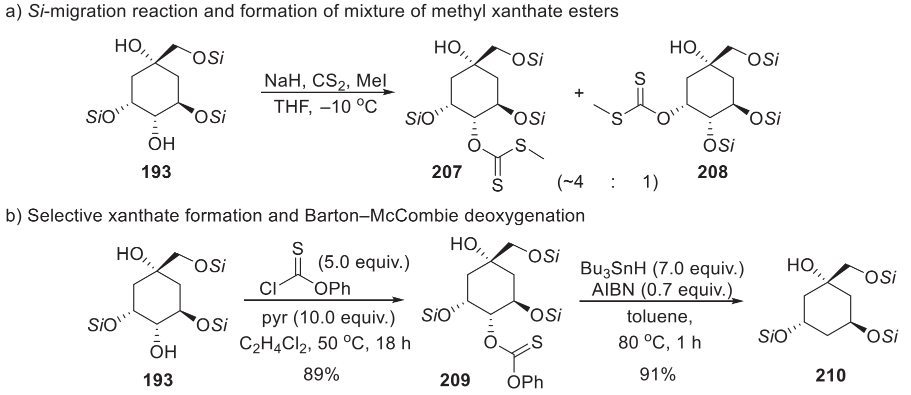
a) *Si*-migration reaction and formation of mixture of methyl xanthate esters
NaH, CS$_2$, MeI
THF, –10 °C
193
207
208
(~4 : 1)
b) Selective xanthate formation and Barton–McCombie deoxygenation
(5.0 equiv.)
pyr (10.0 equiv.)
C$_2$H$_4$Cl$_2$, 50 °C, 18 h
89%
193
209
Bu$_3$SnH (7.0 equiv.)
AIBN (0.7 equiv.)
toluene,
80 °C, 1 h
91%
210

Scheme 38. a) Methyl xanthate ester formation was not selective and yielded mixture of products. b) Successful xanthate formation and Barton–McCombie deoxygenation of alcohol **193**.

After the deoxygenation, a rather distracting and surprising observation was made. The selective deprotection of primary silyl ether of **210**, which was thought to be trivial, proved infeasible. Several different deprotection methods (see Table 4) were tested but cleavage of secondary silyl group was always observed to yield **212**. The regioisomer was identified by nOe-correlation of tertiary and secondary hydroxyl groups. The use of 2 equivalents of TBAF promoted the secondary and primary TBDPS-groups cleavage to yield **211** with excellent yield (92%).

Table 4. Screening the desilylation conditions.

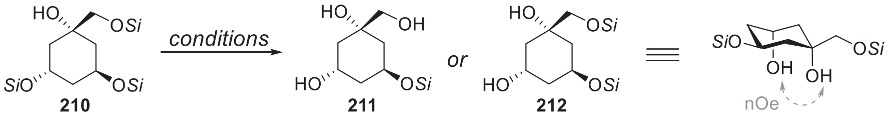
conditions
or
210
211
212
nOe

Entry	Conditions	Results
1	NH$_4$F (10.0 equiv.), MeOH/CH$_2$Cl$_2$, 50 °C	-
2	*p*TsOH·pyr (1.0 equiv.), EtOH, 0 °C→r.t.	-
3	TBAF (1.0 equiv.), THF, 0 °C	n.d.
4	AcCl (3.0 equiv.), MeOH/CH$_2$Cl$_2$, 0 °C	**212**, 61%
5	CSA (0.3 equiv.), MeOH/CH$_2$Cl$_2$, 0 °C	n.d
6	AcOH (1.2 equiv.), TBAF (1.0 equiv.), THF, 0 °C→r.t.	**212**, 38%
7	CsF (1.5 equiv.), 18-crown-6 (2.0 equiv.), THF, r.t.	**211**, 32%
8	TBAF (2.0 equiv.), THF, 0 °C→r.t.	**211**, 91%

n.d. = not determined: complex mixture of products or formation of undesired product judged by TLC; - = no reaction.

Fortunately, despite the presence of the exposed secondary hydroxyl group, treatment of triol **211** with 1.15 equivalents of MsCl resulted in chemoselective mesylation of the more reactive primary hydroxyl in 92% yield (Scheme 39). The mesylated derivative **213** was cyclized into epoxide **214** in quantitative yield. Later, a one-pot mesylation–cyclization sequence was adapted for the synthesis of key intermediate **214** by adding DBU to the mixture after mesylate **213** formation to generate **214** in 68% yield.

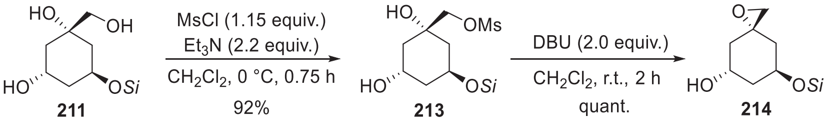
HO
OH
HO
OSi
211
MsCl (1.15 equiv.)
Et3N (2.2 equiv.)
CH2Cl2, 0 °C, 0.75 h
92%
HO
OMs
HO
OSi
213
DBU (2.0 equiv.)
CH2Cl2, r.t., 2 h
quant.
O
HO
OSi
214

Scheme 39. Synthesis of epoxide **214**.

The epoxide opening with a Grignard reagent derived from oleic acid was attempted. Oleic acid **216** was reduced to oleyl alcohol and further transformed into the bromide **216’** by an Appel-reaction (Scheme 40b). After presumed formation of the oleyl magnesium bromide, copper(I)iodide and later the epoxide **214** were added to the reaction mixture to yield halohydrins **215** instead of the desired product.

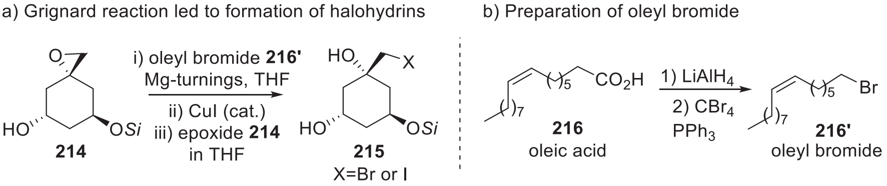
a) Grignard reaction led to formation of halohydrins
O
HO
OSi
214
i) oleyl bromide 216'
Mg-turnings, THF
ii) CuI (cat.)
iii) epoxide 214
in THF
HO
X
HO
OSi
215
X=Br or I
b) Preparation of oleyl bromide
5
CO2H
7
216
oleic acid
1) LiAlH4
2) CBr4
PPh3
5
Br
7
216'
oleyl bromide

Scheme 40. a) The initial studies of epoxide opening with Grignard reaction. b) Synthesis of oleyl bromide.

The formation of the halohydrin was circumvented by reaction of the epoxide with Gilman reagent. A model reaction with *n*-butyllithium gave **217** with 75% yield (Scheme 41a). Then, oleyl bromide-derived Gilman reagent was prepared by treatment of **216’** with *tert*-butyllithium at –78 °C which was then exposed to CuI to provide organocopper reagent (Scheme 41b). The epoxide **214** was then slowly added on top of the freshly prepared Gilman reagent to yield the coupling product **218** in 73% yield. The remaining TBDPS-group was then cleaved with TBAF to finalize the total synthesis of **114**.

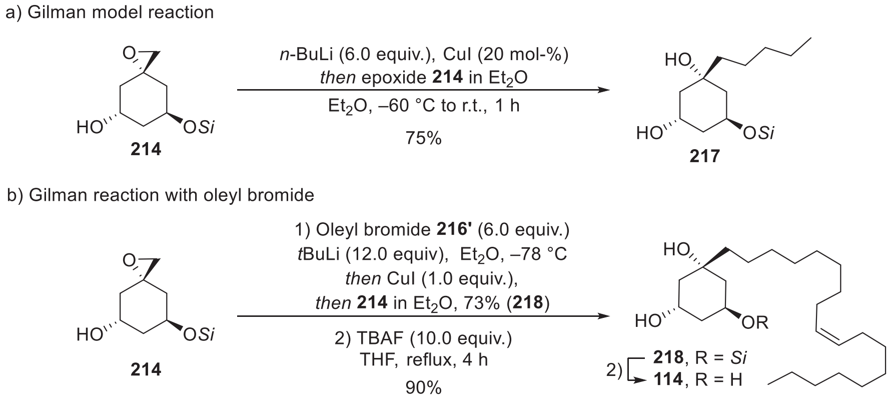
a) Gilman model reaction
n-BuLi (6.0 equiv.), CuI (20 mol-%)
then epoxide 214 in Et2O
Et2O, –60 °C to r.t., 1 h
75%
214
217
b) Gilman reaction with oleyl bromide
1) Oleyl bromide 216' (6.0 equiv.)
tBuLi (12.0 equiv), Et2O, –78 °C
then CuI (1.0 equiv.),
then 214 in Et2O, 73% (218)
2) TBAF (10.0 equiv.)
THF, reflux, 4 h
90%
214
2) 218, R = Si
114, R = H

Scheme 41. a) Gilman model reaction with *n*-BuLi. b) Completion of total synthesis of African ant cyclitol **114**.

6.4 Formal synthesis of VS-105

Along with the first total synthesis of African ant cyclitol **114**, the additional valorization of **193** was further considered. The oxidized form of **193** could serve as a precursor for the synthesis of kidney disease drug VS-105 **150** (Scheme 42), a vitamin D receptor modulator.[121] Similarly, the deoxygenation of **193**, would give southern fragment of 19-nor-vitamin D_3 **151**.[122]

Previously an analogue of **193** has been oxidized successfully with Dess–Martin periodinane (molecule **44**, Scheme 11).[144] Despite the bulkier silyl groups of **193**, the Dess–Martin periodinane oxidation of **193** afforded the corresponding ketone in an excellent 98% yield (Scheme 42). The previous attempts to olefinate the ketonic form of **44** with commonly used Witting and Horner–Wadsworth–Emmons resulted in only traces of the desired olefin due to a lack of reactivity caused by the steric congestion of TBDMS-groups. Such drawback was circumvented using Tebbe reaction to afford the desired olefin in excellent yield, which was successfully employed in the preparation of exocyclic alkene **219** (Scheme 42).

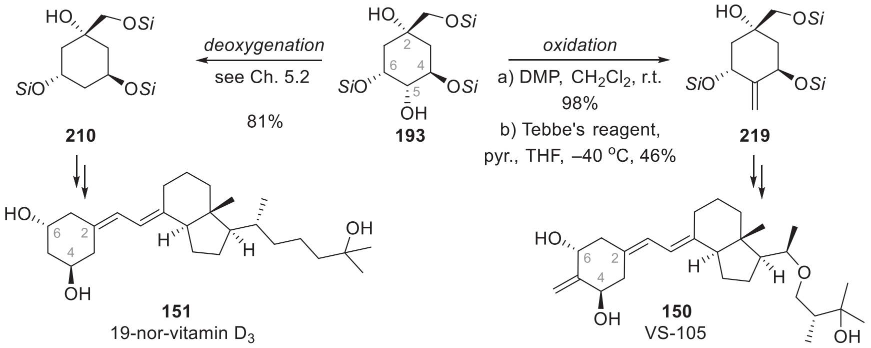

HO
OSi
SiO
OSi
210
deoxygenation
see Ch. 5.2
81%
2
6
4
5
OH
193
oxidation
a) DMP, CH2Cl2, r.t.
98%
b) Tebbe's reagent,
pyr., THF, –40 °C, 46%
219
OH
H
151
19-nor-vitamin D3
O
150
VS-105

Scheme 42. Oxidation and deoxygenation of **193** and formal synthesis of **150** and **151.**

To summarize, the first total synthesis of natural ant cyclitol **114** was reached with 34% overall yield from quinic acid. The route utilized selective silyl group migration across the quinic acid backbone to achieve epoxide intermediate **214**, from which the natural products can be synthesized by Gilman addition. In addition, selective silyl group migration allowed the formal synthesis of VS-105 **150** by selective oxidation of C5 hydroxyl group.

7 CONCISE TOTAL SYNTHESIS OF NATURAL CARBASUGARS

7.1 Aim of the study

Carbasugars are highly oxidized natural products with a carbacycle core. The concise synthesis of two epimeric carbasugars isolated from *Streptomyces lincolnensis* from quinic acid was envisioned. A redesigned total synthesis starting from quinic acid would shorten the previously reported route by several steps owing to chiron approach strategy. The new synthetic route established from quinic acid is presented in this chapter and in Publication **III**.

The atom numbering of quinic acid derivatives used in this chapter differs from the numbering used in the original publication (Publication **III**). In this chapter the numbering presented in Scheme 7 is used.

7.2 Isolation of the carbasugars and previous total synthesis

In 2004 Sedmera *et al.* isolated a group of carbasugars from *Streptomyces lincolnensis* (Figure 5).[145] Three years after the isolation, Nanda *et al.* conducted the first total synthesis of these natural carbasugars **112** and **113** along with some unnatural analogues (Scheme 43).[135] Their synthesis strategy relied on kinetic enzymatic resolution and subsequent oxidations of common intermediate **221** yielded carbasugars **112** and **113** with 12 and 10 steps, respectively. An analog of **112** has been previously synthesized by Trost *et al.*, as a synthetic intermediate of isoquinuclidines.[146]

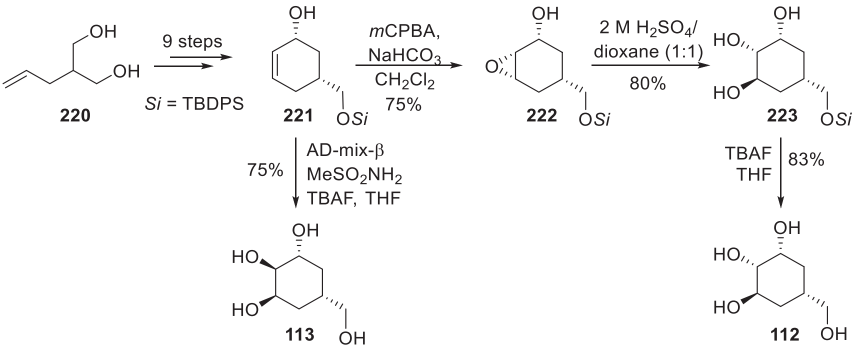
9 steps
Si = TBDPS
220
221
mCPBA, NaHCO3
CH2Cl2
75%
222
2 M H2SO4/ dioxane (1:1)
80%
223
AD-mix-β
75%
MeSO2NH2
TBAF, THF
113
TBAF
THF
83%
112
OSi

Scheme 43. Previous total synthesis of **112** and **113** by Nanda *et al.*

During the isolation of the carbasugars **112** and **113** from S. *lincolnensis* by Sedmera, also previously recognized valienol **224**, gabosine I **225**, quinic acid **2** and shikimic acid **3** were found (Figure 5). As stated before, carbasugars can be subunits of more complex natural products and the structural relation to other highly oxidized natural products is evident. As examples, carbasugar **112** relates to carba-L-rhamnose derivatives **227** and to (–)-dihydroshikimic acid **226** by sharing similar stereochemistry, but having different oxidation states. Similarly, carbasugar **113** is structurally related to natural products (+)-palitantin **229** and (–)-gabosine B **228**. Given such relations, the development of methods for the manipulation of carbasugar cores can broaden the structural diversity of chemical entities by divergent synthesis.

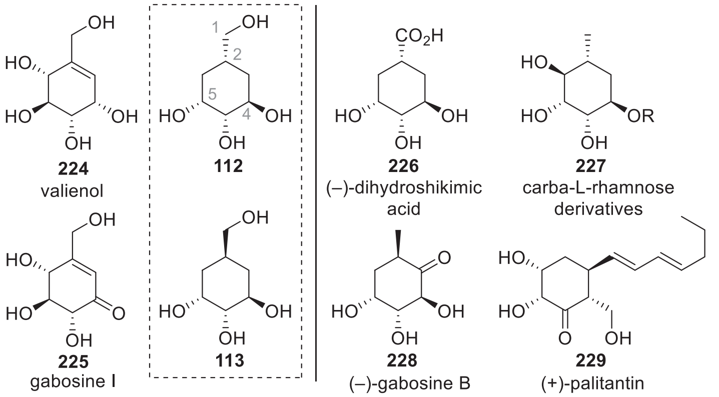
224
valienol
225
gabosine I
112
113
226
(–)-dihydroshikimic acid
227
carba-L-rhamnose derivatives
228
(–)-gabosine B
229
(+)-palitantin

Figure 5. Left-hand column: carbasugars isolated from S. lincolnensis, right-hand column: natural products structurally related to carbasugars **112** and **113**.

7.3 Total synthesis of natural carbasugars isolated from *S. lincolnensis*

The total synthesis route of **112** and **113** was redesigned and envisioned that quinic acid **2** could be used as a starting material due to extensive functional group overlapping of these carbasugars. The reduction of quinide's lactone moiety and *in situ* formation of epoxide followed by its regioselective opening would lead to carbasugar **112** or its epimer **113**. Suitable starting material for screening the reduction conditions was prepared by simultaneous lactonization and acetal protection of quinic acid (**52**) followed by mesylation of tertiary hydroxyl (**230**) (Scheme 44).

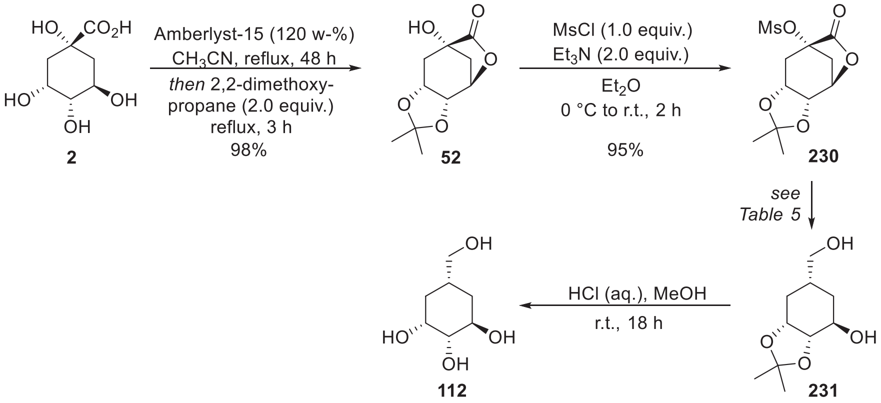
HO
CO2H
HO
OH
OH
2
Amberlyst-15 (120 w-%)
CH3CN, reflux, 48 h
then 2,2-dimethoxy-
propane (2.0 equiv.)
reflux, 3 h
98%
HO
O
O
O
O
52
MsCl (1.0 equiv.)
Et3N (2.0 equiv.)
Et2O
0 °C to r.t., 2 h
95%
MsO
O
O
O
O
230
see
Table 5
OH
O
O
OH
231
HCl (aq.), MeOH
r.t., 18 h
OH
HO
OH
OH
112

Scheme 44. Synthesis of **112**.

The previous use of lithium aluminum hydride in the smooth reduction of lactone moiety (Chapter 5) motivated testing the conditions with substrate **230**. Unfortunately, along with multiple products, only traces of the desired diol **231** was observed supposedly because of $LiAlH_4$'s high reactivity (Table 5, entry 1). Instead, no product was observed with less reactive DIBAL-H (entry 2).

The previously reported conditions for sodium borohydride mediated cleavage of primary, secondary and tertiary tosylates in DMSO[147] were also tested, but the desired diol **231** was isolated with only 3% yield from a complex mixture of products (entry 3). Given the know sodium borohydride's reactivity dependence on the solvent,[148] other solvents were considered. By changing from DMSO to protic solvent ethanol, a great improvement on the formation of **231** was observed (39%, entry 4). To achieve a complete consumption of starting material, 10 equivalents of hydride source was used, though the yield remained moderate (entry 5).

The addition of methanol to THF has been previously recognized to improve the selectivity in the reductions of lactone and ester moieties with $NaBH_4$.[149] Initial studies with this solvent system (data not shown) showed a somewhat violent reaction even at low temperatures. Adding the lactone in solution to a cooled suspension of $NaBH_4$, tamed the reactivity of the hydride and improved the yield of **231** (55%, entry 6). Finally, **231** was obtained as the clear major product in 84% yield upon decreasing the amount of $NaBH_4$ to 3 equivalents (entry 7).

Table 5. Selected optimization conditions of **230→231**.

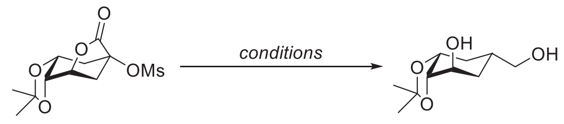

230 **231**

Entry[a]	Hydride (equiv.)	Conditions	Yield %
1	$LiAlH_4$ (2)	THF, 0 °C	traces[c]
2	DIBAL-H (2)	THF, 0 °C to reflux	n.d. [c]
3	$NaBH_4$ (2)	DMSO, 0 °C to 80 °C	3
4	$NaBH_4$ (2)	EtOH, 0 °C to RT	39
5	$NaBH_4$ (10)	MeOH, 0 °C to RT	42
6[b]	$NaBH_4$ (10)	THF/MeOH 9:1, 0 °C	55
7[d]	$NaBH_4$ (3)	THF/MeOH 9:1, –5 °C	84

[a]Lactone **230** was dissolved in the specified solvent and the mixture cooled to 0 °C or maintained at room temperature. The reducing agent was added, and the mixture allowed to stir 3–18 h. The starting temperature was raised if no reaction was observed. [b]Lactone **231** in THF was added to a stirred suspension of $NaBH_4$ in THF/MeOH. [c]Complex mixture of multiple products, no product isolation.

Removal of the acetal protecting group (**231→112**; HCl, MeOH, Scheme 44) and NMR-data comparison with previously reported spectra revealed that stereoinversion of C2 center occurred during the reduction. The selectivity of the reaction could be rationalized by either mesyl group migration or the direct displacement of OMs with hydride (Scheme 45a). Both pathways go through one inversion of the C2 center, which leads to diol **231**. The epoxide formation straight from the reduced lactone moiety would invert the stereocenter, after which the hydride delivery would reinvert it yielding the product **232** (Scheme 45b). However, diol **232** was not detected from the reaction mixtures.

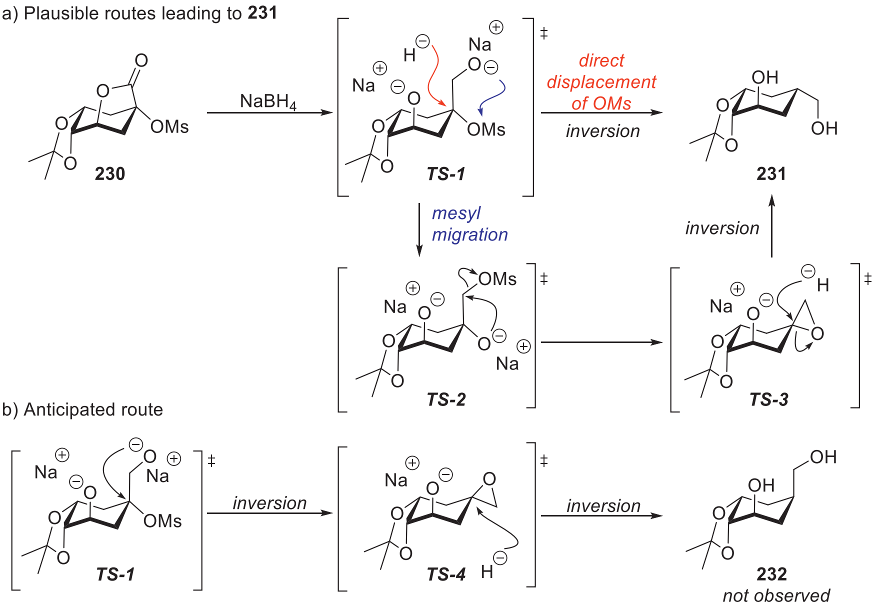
a) Plausible routes leading to **231**
230
NaBH$_4$
TS-1
direct displacement of OMs
inversion
231
mesyl migration
inversion
TS-2
TS-3
b) Anticipated route
TS-1
inversion
TS-4
inversion
232
not observed
Na
OMs
OH

Scheme 45. a) Reasoning of the observed stereoinversion. b) Anticipated epoxide intermediate.

The epimeric natural carbasugar **113** was envisioned to be achieved by oxidation of primary hydroxyl moiety followed by epimerization of α-carbonyl position of **112**. The *syn*-arrangement of secondary alcohol (4-OH) and aldehyde moiety of **113** would allow intramolecular hydrogen bonding thus pushing the epimerization equilibrium towards the desired product.

Chemoselectivity issues were found during the first attempts to oxidize the primary alcohol **231** with DMP and PCC, despite the equimolar use of oxidizing agent (Scheme 46). As oxidative radical processes are known to be milder and more chemoselective, TEMPO-oxidation was adapted.[150] Catalytic amount of TEMPO in combination with (diacetoxyiodo)benzene improved the yield (34%), though the formation of side products was still remarkable. Changing the (diacetoxyiodo)benzene to *N*-chlorosuccinimide resulted in the increased formation of **233** with 77% yield. Control of the reaction times was determined extremely important as shorter reaction times did not allow the full consumption of the starting material, but elongated reaction times led to the undesired formation of side products.

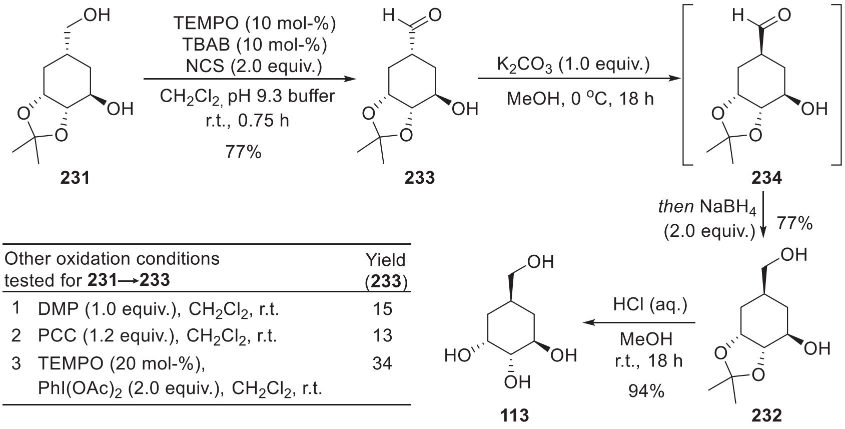

	Other oxidation conditions tested for **231**→**233**	Yield (**233**)
1	DMP (1.0 equiv.), CH_2Cl_2, r.t.	15
2	PCC (1.2 equiv.), CH_2Cl_2, r.t.	13
3	TEMPO (20 mol-%), $PhI(OAc)_2$ (2.0 equiv.), CH_2Cl_2, r.t.	34

Scheme 46. Screening the oxidation conditions of **231** and synthesis of carbasugar **113**.

Since aldehydes **233** and **234** had different R_f-values, the epimerization process was followed by TLC (**233** →**234**, Scheme 46). Different bases and reaction conditions were screened for the reaction and most of the conditions initially tested led to the promising formation of aldehyde **234**. However, the isolated yields of **234** remained poor and epimerization to original material **233** was detected. Because of the labile character of **234**, the aldehyde was intercepted by *in situ* reduction with $NaBH_4$ allowing the isolation of diol **232** in 77% yield, which corresponded to the observed amount of **234** on TLC. The acetal deprotection with HCl in MeOH revealed natural carbasugar **113** (Scheme 46).

The epimerization reaction was studied by DFT to verify the assumption of higher stability of epimer **234** by hydrogen bonding (Scheme 47). The plausible conformations of **233** (**233$_A$** and **233$_B$**) showed only slight energy difference in both chair conformations. The epimeric aldehyde **234** can adapt a chair conformation with formyl and 4-OH groups in both equatorial position (**234'$_B$**), which was found to be energetically more stable by 2.1 kcal/mol than for the other epimer. The epimer's **234** twisted boat conformation by intramolecular hydrogen bonding was 0.8 kcal/mol more stable than the **234'$_B$** chair conformation.

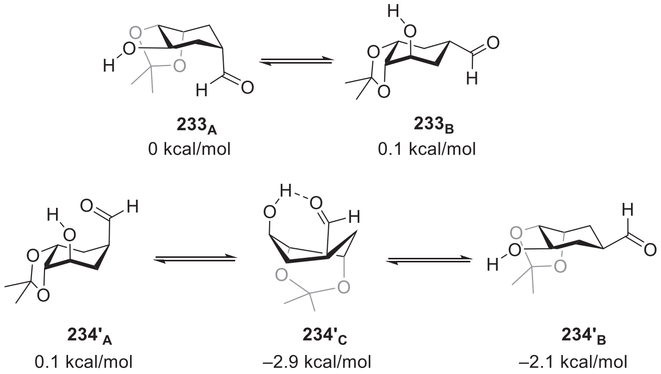

Scheme 47. Simplified conformational analysis of epimers **233** and **234**. Energy values relate to **233$_A$** as the zero value and are given as electronic energies, optimized at PBE1PBE/6-31G** level of theory.

To summarize, the shortest and high-yielding synthesis of carbasugars **112** and **113** was reached in this work by exploiting quinic acid as starting material. Carbasugar **112** was achieved in only 4 steps from quinic acid in 76% overall yield. The epimeric carbasugar **113** was achieved in 3 steps from **112** (44% overall yield from quinic acid). When considering highly functionalized small molecules such as carbasugars, quinic acid is a superior starting material for cases of evident functional group overlap.

8 QUINIC ACID DERIVATIVES: ANTICANCER EFFECT ON GLIOBLASTOMA

8.1 Aim of the study

Glioblastoma is the most common and aggressive brain cancer type in adults, usually treated with chemotherapy and surgery.[151] The current drugs for treatment of glioblastoma are insufficient and generally the problems of anticancer agents are the lack of *in vivo* effectivity, malignant side effects and weak intervention. Therefore, the development of new effective but safe drugs for the treatment of glioblastoma is required. Since quinic acid derivatives have demonstrated potential activity in various biological assays showing anticancer and anti-inflammatory properties,[152-154] a small library of quinic acid derivatives was built and tested against glioblastoma multiforme.

The first set of compounds comprised quinic acid derivatives prepared for the synthetic works described in Chapter 5 and was tested in an attempt to identify a possible structure–activity relationship. A second set was later synthesized, guided by the observations from the initial screening. According to author's expertise on synthetic organic chemistry, this chapter focuses on the synthesis of the molecules and deeper discussion on the biological methods used in the assay is presented in Publication **IV**.

The atom numbering of quinic acid derivatives used in this chapter also differs from the numbering used in the original publication (Publication **IV**). As before, in this chapter the numbering presented in Scheme 7 is used.

8.2 Preliminary biological screening

To screen the effect of quinic acid functional groups and the impact of free hydroxyl moieties as well as protecting group effect on anticancer properties, derivatives in Figure 6 were studied. Derivatives **59**, **65**, **66**, **171** and **174** were synthesized previously to study the deoxygenation of quinic acid (Chapter 5). Triol **263** was obtained either by direct TBDPS-protection and reduction of quinide **35** or by selective deprotection of tertiary silyl group of **66** and reduction of lactone moiety with $NaBH_4$. Triols **235** and **195** were obtained by reduction of lactone moiety with $NaBH_4$ of **59** and **65**, respectively.

All the selected lactone derivatives (**59**, **65** and **66**) showed minor activity on the cell viability assay in human glioblastoma cell lines LN229 (0–6% cell growth inhibition (Figure 7). For their reduced analogues, only TBDPS-protected derivative **171** seemed to have a notable cytotoxicity effect (31%) while sulfoxide- (**235**) and TBDMS-protected (**195**) derivatives remained ineffective. The methanesulfonate derivatization of the hydroxyl groups of **171** (compound **174**) seemed not to have a deep influence on the activity (38%), but exposure of the tertiary hydroxyl group (**236**) raised the cytotoxicity level dramatically (90%). The impact of 5,6-OH protection was also notable; in contrast to insufficient activity of sulfone derivative **235**, the bis-silyl ether **236** showed superior cytotoxicity. TBDPS-derivatives showed the most promising activity and comparison of the active analogues (**171**, 174 and **236**) the free tertiary hydroxyl group combined with the 5,6-OSi-groups seemed to be pivotal for the desired activity.

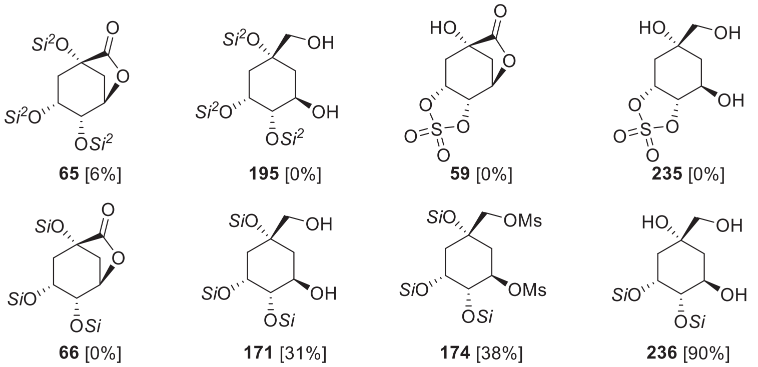

65 [6%] **195** [0%] **59** [0%] **235** [0%]

66 [0%] **171** [31%] **174** [38%] **236** [90%]

Figure 6. First-generation structures tested on anticancer effect on glioblastoma. *Si* = TBDPS; *Si*^{2} = TBDMS. The cell growth inhibition percentage for LN229 is presented in brackets.

8.3 Quinic acid amides

Quinic acid amides (quinamides) have been reported to have anti-inflammatory, antimicrobial and anticancer effects.[154-157] Impelled by the abovementioned observation on the cytotoxicity, quinic acid amide derivatives bearing TBDPS-groups on 5-OH and 6-OH were considered, while 2-OH and 4-OH were kept unmodified (Scheme 48a and c). Amides were prepared by opening of the lactone moiety with primary or secondary amines (**238–242**). In addition to amides, ethyl ester derivative **245** was prepared to compare the C1 functional group effect on the cell growth inhibition (Scheme 48d).

Attempts to expand the library by mimicking the structure of **236** were aimed by the reduction of amide functions to amines. Unfortunately, neither the direct reductive amination[158] of **56** nor other reducing agents screened provided the desired amines, despite the harsh reaction conditions (Scheme 48a, Table 1). Aiming at the preparation of aldehyde **244** in order to perform reductive amination on more reactive species, Weinreb amide **243** was prepared. The route proved to be infeasible and Weinreb amide unreactive towards reducing agents.

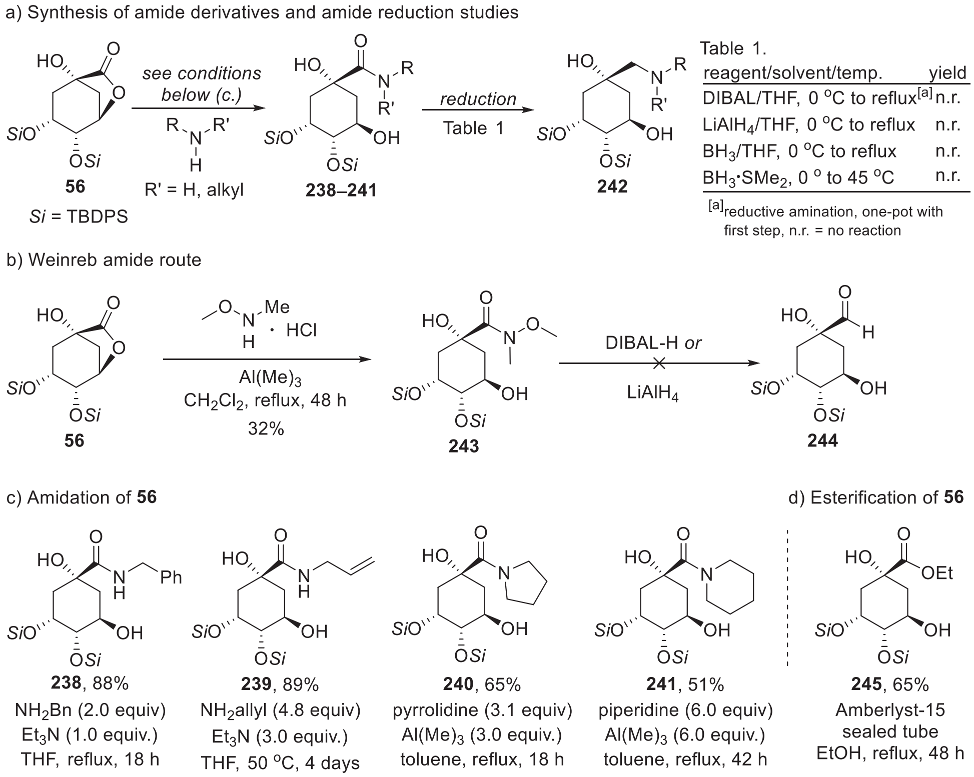
a) Synthesis of amide derivatives and amide reduction studies
56
Si = TBDPS
see conditions below (c.)
R' = H, alkyl
238–241
reduction
Table 1
242
b) Weinreb amide route
56
Al(Me)3
CH2Cl2, reflux, 48 h
32%
243
DIBAL-H or
LiAlH4
244
c) Amidation of 56
238, 88%
NH2Bn (2.0 equiv)
Et3N (1.0 equiv.)
THF, reflux, 18 h
239, 89%
NH2allyl (4.8 equiv)
Et3N (3.0 equiv.)
THF, 50 °C, 4 days
240, 65%
pyrrolidine (3.1 equiv)
Al(Me)3 (3.0 equiv.)
toluene, reflux, 18 h
241, 51%
piperidine (6.0 equiv)
Al(Me)3 (6.0 equiv.)
toluene, reflux, 42 h
d) Esterification of 56
245, 65%
Amberlyst-15
sealed tube
EtOH, reflux, 48 h

Table 1.

reagent/solvent/temp.	yield
DIBAL/THF, 0 °C to reflux[a]	n.r.
$LiAlH_4$/THF, 0 °C to reflux	n.r.
BH_3/THF, 0 °C to reflux	n.r.
$BH_3{\cdot}SMe_2$, 0 ° to 45 °C	n.r.

[a] reductive amination, one-pot with first step, n.r. = no reaction

Scheme 48. a) Synthesis of amide derivatives and attempts on amide reductions yielding corresponding amines. b) Weinreb amide route. c) Amide products. d) Esterification of **56**.

8.4 Cytotoxicity results

The detailed description of cell and molecular biology methods in testing the molecules presented in Figure 6 and Scheme 48 is described in Publication **IV**. Summarily, above described quinic acid derivatives and encapsulated poly (lactic-co-glycolic acid) nanoparticle NP-**236** were screened for their anti-glioblastoma effects. Some of the derivatives were identified as potential antitumor agents, with **236** showing the highest inhibition of cancer cell growth at 100 μM (90 %), and IC_{50} of 10.66 μM and 28.22 μM for human glioblastoma cell lines LN229 and SNB19, respectively. The Figure 7 shows the percentage of growth inhibition for series of compounds **55**, **65–66**, **171**, **174**, **195**, **235–236**, **234–241**, **242** and **245**. The structures and synthesis of the tested molecules are presented in Chapters 8.2 and 8.3.

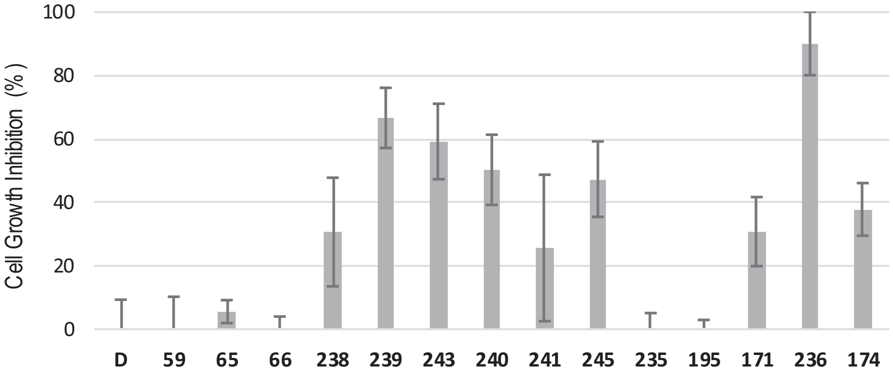

Figure 7. Percentage of growth inhibition (100 μM) for series of compounds. D = DMSO.

As a summary, quinic acid-derived libraries can be easily prepared. The functional group abundance enables a facile diversification of quinic acid by protecting group variation or by changing the oxidation states of C1 or hydroxyl groups. The structural relation of quinic acid to sugars and pseudo-sugars is evident and new active compounds can be prepared for medicinal chemistry purposes by its synthetic modification.

9 CONCLUSIONS

The discovery of new drugs is emphatically leaning on natural products – between 1981 and 2014 around 50% of new drugs were based on natural products.[10] Our ability to design and carry out the total synthesis of natural products determines our possibilities to exploit the full potential of these wonderful structures created by Nature. The complexity and abundance of stereogenic centers in many natural products are their most challenging feature when designing their syntheses. Use of synthetic routes that start from chiral pool molecules help to circumvent some of the laborious synthetic steps and challenging transformations, while being an urgently required action in moving along from fossils towards sustainable bioeconomy.

In this thesis work, a method for divergent deoxygenation strategy for quinic acid derivatives was developed. $B(C_6F_5)_3$-catalyzed deoxygenation with silyl hydrides was found to be dependent on protecting groups and of the nature of silyloxonium intermediate. The achieved deoxygenations were highly stereoselective and the divergent strategy led to formation of unforeseen chiral alcohols, aldehydes and tetrahydrofuran derivatives. However, the dependence on the anchimeric assistance and silyloxonium intermediate precluded the opportunity of primary C–O bond cleavage. This chemoselective transition metal-free C–O bond cleavage of quinic acid innovatively expanded the deoxygenation protocol to cyclitols. This method was further utilized in the formal synthesis of homocitric acid and the other achieved chirons can been seen as chiral building blocks of natural products (e.g. guignardone[114]). The reaction mechanism was studied by isotopically labeling with deuterium and DFT calculations, suggesting different mechanisms of cleavage of secondary silyl ether/secondary mesylate versus tertiary silyl ether/primary mesylate moieties.

The three-dimensional arrangement of quinic acid allowed a regioselective *O,O*-silyl group migration across the highly oxygenated backbone. The migration reaction was studied with two substrates bearing different silyl groups (TBDPS and TBDMS) and by changing the reaction conditions. On both substrates the tertiary→primary migration was found to be highly selective while the secondary→secondary migration occurred more selectively on TBDPS-derivative. The migration allowed the diversification of a common intermediate selectively into new regioisomers and the utility of the newly formed migration products were demonstrated by their use in the first total synthesis of an African ant cyclitol and the formal synthesis of kidney disease drug VS-105.

A shorter total synthesis of natural epimeric carbasugars isolated from *S. lincolnensis* was developed leaning on the functional group overlap with quinic acid. The key steps of the synthesis were the regioselective reduction of quinic acid and the epimerization of the synthetic intermediate into new epimeric natural product. The reduction step was carefully optimized, and the hydride delivery was found to be highly stereoselective.

Lastly, the versatility of quinic acid allowed to build a small library of derivatives to study the anticancer effect on glioblastoma multiforme. Facile diversification of quinic acid by changing the hydroxyl protecting groups, C1 functional groups, or the oxidation state, makes quinic acid an eminent cyclitol for medicinal chemistry purposes.

The valorization of biomass-based molecules is still a developing area of organic chemistry. The current methods for deoxygenation are efficient but do not yet serve all the needs of ideal synthesis, such as scalability and broad substrate scope. Despite these limitations in the current deoxygenation methods, we have made enormous progress in the last decade in taming the reactivity and modifying the diverse functionalities of biomass-based molecules. While many challenges in the modification of biomass-derived molecules for added-value compounds remain unsolved, the transposition of modern synthetic methods to specific abundant chiral pool elements is likely to flourish into new valuable chemical entities.

REFERENCES

1. Casiraghi, G.; Zanardi, F.; Rassu, G.; Spanu, P., Stereoselective Approaches to Bioactive Carbohydrates and Alkaloids-With a Focus on Recent Syntheses Drawing from the Chiral Pool. *Chem. Rev.* **1995**, *95*, 1677-1716.

2. Baran, P. S., Natural Product Total Synthesis: As Exciting as Ever and Here To Stay. *J. Am. Chem. Soc.* **2018**, *140*, 4751-4755.

3. Brill, Z. G.; Condakes, M. L.; Ting, C. P.; Maimone, T. J., Navigating the Chiral Pool in the Total Synthesis of Complex Terpene Natural Products. *Chem. Rev.* **2017**, *117*, 11753-11795.

4. Li, L.; Chen, Z.; Zhang, X.; Jia, Y., Divergent Strategy in Natural Product Total Synthesis. *Chem. Rev.* **2018**, *118*, 3752-3832.

5. Bartok, M., Unexpected inversions in asymmetric reactions: reactions with chiral metal complexes, chiral organocatalysts, and heterogeneous chiral catalysts. *Chem. Rev.* **2010**, *110*, 1663-705.

6. Koskinen, A. M. P., Chirospecific synthesis: Catalysis and chiral pool hand in hand. *Pure Appl. Chem.* **2011**, *83*, 435-443.

7. Atanasov, A. G.; Zotchev, S. B.; Dirsch, V. M.; International Natural Product Sciences, T.; Supuran, C. T., Natural products in drug discovery: advances and opportunities. *Nat. Rev. Drug Discov.* **2021**, *20*, 200-216.

8. Cragg, G. M.; Newman, D. J., Natural products: a continuing source of novel drug leads. *Biochim. Biophys. Acta* **2013**, *1830*, 3670-95.

9. Mishra, B. B.; Tiwari, V. K., Natural products: an evolving role in future drug discovery. *Eur. J. Med. Chem.* **2011**, *46*, 4769-807.

10. Newman, D. J.; Cragg, G. M., Natural Products as Sources of New Drugs from 1981 to 2014. *J. Nat. Prod.* **2016**, *79*, 629-61.

11. Wender, P. A., Toward the Ideal Synthesis and Transformative Therapies: The Roles of Step Economy and Function Oriented Synthesis. *Tetrahedron* **2013**, *69*, 7529-7550.

12. Schlaf, M., Selective deoxygenation of sugar polyols to alpha,omega-diols and other oxygen content reduced materials--a new challenge to homogeneous ionic hydrogenation and hydrogenolysis catalysis. *Dalton Trans.* **2006**, 4645-4653.

13. Sheldon, R. A., The Road to Biorenewables: Carbohydrates to Commodity Chemicals. *ACS Sustain. Chem. Eng.* **2018**, *6*, 4464-4480.

14. Arjona, O.; Gomez, A. M.; Lopez, J. C.; Plumet, J., Synthesis and conformational and biological aspects of carbasugars. *Chem. Rev.* **2007**, *107*, 1919-2036.

15. Soengas, R. G.; Otero, J. M.; Estévez, A. M.; Rauter, A. P.; Cachatra, V.; Estévez, J. C.; Estévez, R. J., An overview of key routes for the transformation of sugars into carbasugars and related compounds. In *Carbohydrate Chemistry*,2012; pp 263-302.

16. Clifford, M. N.; Jaganath, I. B.; Ludwig, I. A.; Crozier, A., Chlorogenic acids and the acyl-quinic acids: discovery, biosynthesis, bioavailability and bioactivity. *Nat. Prod. Rep.* **2017**, *34*, 1391-1421.

17. Tuck, C. O.; Perez, E.; Horvath, I. T.; Sheldon, R. A.; Poliakoff, M., Valorization of biomass: deriving more value from waste. *Science* **2012**, *337*, 695-699.

18. Corma, A.; Iborra, S.; Velty, A., Chemical routes for the transformation of biomass into chemicals. *Chem. Rev.* **2007**, *107*, 2411-2502.

19. Bender, T. A.; Dabrowski, J. A.; Gagné, M. R., Homogeneous catalysis for the production of low-volume, high-value chemicals from biomass. *Nat. Rev. Chem.* **2018**, *2*, 35-46.

20. Besson, M.; Gallezot, P.; Pinel, C., Conversion of biomass into chemicals over metal catalysts. *Chem. Rev.* **2014**, *114*, 1827-1870.

21. Petersen, A. R.; Fristrup, P., New Motifs in Deoxydehydration: Beyond the Realms of Rhenium. *Chem. Eur. J.* **2017**, *23*, 10235-10243.

22. Ahmed, M. J.; Hameed, B. H., Hydrogenation of glucose and fructose into hexitols over heterogeneous catalysts: A review. *J. Taiwan Inst. Chem. Eng.* **2019**, *96*, 341-352.

23. Sun, D.; Yamada, Y.; Sato, S.; Ueda, W., Glycerol as a potential renewable raw material for acrylic acid production. *Green Chem.* **2017**, *19*, 3186-3213.

24. Gallezot, P., Conversion of biomass to selected chemical products. *Chem. Soc. Rev.* **2012**, *41*, 1538-1558.

25. Shiramizu, M.; Toste, F. D., Deoxygenation of biomass-derived feedstocks: oxorhenium-catalyzed deoxydehydration of sugars and sugar alcohols. *Angew. Chem. Int. Ed.* **2012**, *51*, 8082-6.

26. Wan, W.; Ammal, S. C.; Lin, Z.; You, K. E.; Heyden, A.; Chen, J. G., Controlling reaction pathways of selective C-O bond cleavage of glycerol. *Nat. Commun.* **2018**, *9*, 4612.

27. Nakagawa, Y.; Liu, S.; Tamura, M.; Tomishige, K., Catalytic total hydrodeoxygenation of biomass-derived polyfunctionalized substrates to alkanes. *Chem. Sus. Chem.* **2015**, *8*, 1114-1132.

28. Gevorgyan, V.; Liu, J.-X.; Rubin, M.; Benson, S.; Yamamoto, Y., A novel reduction of alcohols and ethers with a HSiEt3catalytic B(C6F5)3 system. *Tetrahedron Lett.* **1999**, *40*, 8919-8922.

29. Gevorgyan, V. V.; Rubin, M.; Benson, S.; Liu, J. X.; Yamamoto, Y., A novel B(C(6)F(5))(3)-catalyzed reduction of alcohols and cleavage of aryl and alkyl ethers with hydrosilanes. *J. Org. Chem.* **2000**, *65*, 6179-6186.

30. Blackwell, J. M.; Foster, K. L.; Beck, V. H.; Piers, W. E., B(C(6)F(5))(3)-Catalyzed Silation of Alcohols: A Mild, General Method for Synthesis of Silyl Ethers. *J. Org. Chem.* **1999**, *64*, 4887-4892.

31. Nimmagadda, R. D.; McRae, C., A novel reduction reaction for the conversion of aldehydes, ketones and primary, secondary and tertiary alcohols into their corresponding alkanes. *Tetrahedron Lett.* **2006**, *47*, 5755-5758.

32. McLaughlin, M. P.; Adduci, L. L.; Becker, J. J.; Gagne, M. R., Iridium-catalyzed hydrosilylative reduction of glucose to hexane(s). *J. Am. Chem. Soc.* **2013**, *135*, 1225-1227.

33. Adduci, L. L.; McLaughlin, M. P.; Bender, T. A.; Becker, J. J.; Gagne, M. R., Metal-free deoxygenation of carbohydrates. *Angew. Chem. Int. Ed.* **2014**, *53*, 1646-1649.

34. Adduci, L. L.; Bender, T. A.; Dabrowski, J. A.; Gagne, M. R., Chemoselective conversion of biologically sourced polyols into chiral synthons. *Nat. Chem.* **2015**, *7*, 576-581.

35. Seo, Y.; Lowe, J. M.; Gagné, M. R., Controlling Sugar Deoxygenation Products from Biomass by Choice of Fluoroarylborane Catalyst. *ACS Cat.* **2019**, *9*, 6648-6652.

36. Lowe, J. M.; Seo, Y.; Gagné, M. R., Boron-Catalyzed Site-Selective Reduction of Carbohydrate Derivatives with Catecholborane. *ACS Cat.* **2018**, *8*, 8192-8198.

37. Barco, A.; Benetti, S.; Risi, C. D.; Marchetti, P.; Pollini, G. P.; Zanirato, V., D-(−)-Quinic acid: a chiron store for natural product synthesis. *Tetrahedron: Asymmetry* **1997**, *8*, 3515-3545.

38. Fischer, H. O. L.; Dangschat, G., Konstitution der Chlorogensäure (3. Mitteil. über Chinasäure Derivate). *Ber. Dtsch. Chem. Ges.* **1932**, *65*, 1037-1040.

39. Abell, C.; Allen, F. H.; Bugg, T. D. H.; Doyle, M. J.; Raithby, P. R., Structure of (–)-quinic acid. *Acta Cryst.* **1988**, *44*, 1287-1290.

40. Herrmann, K. M.; Weaver, L. M., The Shikimate Pathway. *Annu. Rev. Plant Physiol. Plant Mol. Biol.* **1999**, *50*, 473-503.

41. Bianco, A.; Brufani, M.; Manna, F.; Melchioni, C., Synthesis of a carbocyclic sialic acid analogue for the inhibition of influenza virus neuraminidase. *Carbohydrate Research* **2001**, *332*, 23-31.

42. Perlman, K. L.; Swenson, R. E.; Paaren, H. E.; Schnoes, H. K.; DeLuca, H. F., Novel synthesis of 19-nor-vitamin D compounds. *Tetrahedron Lett.* **1991**, *32*, 7663-7666.

43. Box, J. M.; Harwood, L. M.; Humphreys, J. L.; Morris, G. A.; Redon, P. M.; Whitehead, R. C., Dehydration of Quinate Derivatives: Synthesis of a Difluoromethylene Homologue of Shikimic Acid. *Synlett.* **2002**, *2002*, 0358-0360.

44. Philippe, M.; Sepulchre, A. M.; Gero, S. D.; Loibner, H.; Streicher, W.; Stutz, P., 1-N-acylation of gentamicin C1a by a cyclic, chiral gamma-amino-alpha-hydroxy acid related to the (S)-4-amino-2-hydroxybutyric acid. *J. Antibiot.* **1982**, *35*, 1507-1512.

45. Huang, P.-q.; Sabbe, K.; Pottie, M.; Vandewalle, M., A Novel Synthesis of 19-Nor 1α,25-dihydroxyvitamin D3 and Related Analogues. *Tetrahedron Lett.* **1995**, *36*, 8299-8302.

46. Abreu, P.; Relva, A., Carbohydrates from Detarium microcarpum bark extract. *Carbohydr. Res.* **2002**, *337*, 1663-1666.

47. Clifford, M. N.; Knight, S.; Surucu, B.; Kuhnert, N., Characterization by LC-MS(n) of four new classes of chlorogenic acids in green coffee beans: dimethoxycinnamoylquinic acids, diferuloylquinic acids, caffeoyl-dimethoxycinnamoylquinic acids, and feruloyl-dimethoxycinnamoylquinic acids. *J. Agric. Food Chem.* **2006**, *54*, 1957-1969.

48. Armesto, N.; Ferrero, M.; Fernandez, S.; Gotor, V., Novel enzymatic synthesis of 4-O-cinnamoyl quinic and shikimic acid derivatives. *J. Org. Chem.* **2003**, *68*, 5784-5787.

49. Sun, X.; Lee, H.; Lee, S.; Tan, K. L., Catalyst recognition of cis-1,2-diols enables site-selective functionalization of complex molecules. *Nat. Chem.* **2013**, *5*, 790-795.

50. Wang, L.; Akhani, R. K.; Wiskur, S. L., Diastereoselective and enantioselective silylation of 2-arylcyclohexanols. *Org. Lett.* **2015**, *17*, 2408-2411.

51. Manthey, M. K.; González-Bello, C.; Abell, C., Synthesis of (2R)-2-bromodehydroquinic acid and (2R)-2-fluorodehydroquinic acid *J. Chem. Soc. Perkin Trans. 1* **1997**, 625-628.

52. Kuwano, S.; Hosaka, Y.; Arai, T., Chiral Benzazaborole-Catalyzed Regioselective Sulfonylation of Unprotected Carbohydrate Derivatives. *Chem. Eur. J.* **2019**, *25*, 12920-12923.

53. Hanessian, S.; Pan, J.; Carnell, A.; Bouchard, H.; Lesage, L., Total Synthesis of (-)-Reserpine Using the Chiron Approach. *J. Org. Chem.* **1997**, *62*, 465-473.

54. Li, R.-Z.; Tang, H.; Wan, L.; Zhang, X.; Fu, Z.; Liu, J.; Yang, S.; Jia, D.; Niu, D., Site-Divergent Delivery of Terminal Propargyls to Carbohydrates by Synergistic Catalysis. *Chem.* **2017**, *3*, 834-845.

55. Yagami, N.; Imamura, A., Stereodirecting Effect of Cyclic Silyl Protecting Groups in Chemical Glycosylation. *Agric. Sci. Rev.* **2018**, *6*, 1-20.

56. Guo, J.; Ye, X. S., Protecting groups in carbohydrate chemistry: influence on stereoselectivity of glycosylations. *Molecules* **2010**, *15*, 7235-7265.

57. Bols, M.; Pedersen, C. M., Silyl-protective groups influencing the reactivity and selectivity in glycosylations. *Beilstein J. Org. Chem.* **2017**, *13*, 93-105.

58. Painter, G. F.; Falshaw, A.; Wong, H., Conformation inversion of an inositol derivative by use of silyl ethers: a modified route to 3,6-di-O-substituted-L-ido-tetrahydroxyazepane derivatives. *Org. Biomol. Chem.* **2004**, *2*, 1007-1012.

59. Diaz, M.; Ferrero, M.; Fernandez, S.; Gotor, V., 6-s-cis locked analogues of the steroid hormone 1alpha, 25-dihydroxyvitamin D(3). Synthesis Of novel A-ring stereoisomeric 1, 25-dihydroxy-3-epi-19-nor-previtamin D(3) derivatives. *J. Org. Chem.* **2000**, *65*, 5647-5652.

60. Panza, L.; Valsecchi, E.; Tacchi, A.; Prosperi, D.; Compostella, F., An Efficient Transformation of (-)-Quinic Acid into Carba-l-rhamnose. *Synlett*. **2004**, *2004*, 2529-2532.

61. Delfourne, E. D., Pierre; Gorrichon, Liliane; Veronique, Jacqueline, Synthese de derives des acides quinique et shikimique. *J. Chem. Res.* **1991**, *3*, 532-544.

62. Hanessian, S.; Reddy, G. V.; Huynh, H. K.; Pan, J.; Pedatella, S.; Ernst, B.; Kolb, H. C., Design and synthesis of sialyl Lex mimetics based on carbocyclic scaffolds derived from (−) quinic acid. *Bioorg. Med. Chem. Lett.* **1997**, *7*, 2729-2734.

63. Montchamp, J. L.; Frost, J. W., Irreversible inhibition of 3-dehydroquinate synthase. *J. Am. Chem. Soc.* **1991**, *113*, 6296-6298.

64. Bianco, A.; Romagnoli, P., Germanium (IV) chloride as catalyst for the protection of diols as cyclic orthoesters. *Synth. Commun.* **2006**, *28*, 3179-3182.

65. Arthurs, C. L.; Morris, G. A.; Piacenti, M.; Pritchard, R. G.; Stratford, I. J.; Tatic, T.; Whitehead, R. C.; Williams, K. F.; Wind, N. S., The synthesis of 2-oxyalkyl-cyclohex-2-enones, related to the bioactive natural products COTC and antheminone A, which possess anti-tumour properties. *Tetrahedron* **2010**, *66*, 9049-9060.

66. Murray, L. M.; O'Brien, P.; Taylor, R. J., Stereoselective reactions of a (-)-quinic acid-derived enone: application to the synthesis of the core of scyphostatin. *Org. Lett.* **2003**, *5*, 1943-1946.

67. Vojackova, P.; Michalska, L.; Necas, M.; Shcherbakov, D.; Bottger, E. C.; Sponer, J.; Sponer, J. E.; Svenda, J., Stereocontrolled Synthesis of (-)-Bactobolin A. *J. Am. Chem. Soc.* **2020**, *142*, 7306-7311.

68. Schuster, H.; Martinez, R.; Bruss, H.; Antonchick, A. P.; Kaiser, M.; Schurmann, M.; Waldmann, H., Synthesis of the B-seco limonoid scaffold. *Chem. Commun.* **2011**, *47*, 6545-6547.

69. Begum, L.; Box, J. M.; Drew, M. G. B.; Harwood, L. M.; Humphreys, J. L.; Lowes, D. J.; Morris, G. A.; Redon, P. M.; Walker, F. M.; Whitehead, R. C., Difluorinated analogues of shikimic acid. *Tetrahedron* **2003**, *59*, 4827-4841.

70. Kawashima, H.; Sakai, M.; Kaneko, Y.; Kobayashi, Y., Further study on synthesis of the cyclobakuchiols. *Tetrahedron* **2015**, *71*, 2387-2392.

71. Ulibarri, G.; Nadler, W.; Skrydstrup, T.; Audrain, H.; Chiaroni, A.; Riche, C.; Grierson, D. S., Construction of the Bicyclic Core Structure of the Enediyne Antibiotic

Esperamicin-A1 in Either Enantiomeric Form from (-)-Quinic Acid. *J. Org. Chem.* **2002**, *60*, 2753-2761.

72. White, J. D.; Cammack, J. H.; Sakuma, K., The synthesis and absolute configuration of mycosporins. A novel application of the Staudinger reaction. *J. Am. Chem. Soc.* **1989**, *111*, 8970-8972.

73. Kok, S. H.; Lee, C. C.; Shing, T. K., A new synthesis of valienamine. *J. Org. Chem.* **2001**, *66*, 7184-7190.

74. White, J. D.; Cammack, J. H.; Sakuma, K.; Rewcastle, G. W.; Widener, R. K., Transformations of Quinic Acid. Asymmetric Synthesis and Absolute Configuration of Mycosporin I and Mycosporin-gly. *J. Org. Chem.* **2002**, *60*, 3600-3611.

75. Kaila, N.; Somers, W. S.; Thomas, B. E.; Thakker, P.; Janz, K.; DeBernardo, S.; Tam, S.; Moore, W. J.; Yang, R.; Wrona, W.; Bedard, P. W.; Crommie, D.; Keith, J. C., Jr.; Tsao, D. H.; Alvarez, J. C.; Ni, H.; Marchese, E.; Patton, J. T.; Magnani, J. L.; Camphausen, R. T., Quinic acid derivatives as sialyl Lewis(x)-mimicking selectin inhibitors: design, synthesis, and crystal structure in complex with E-selectin. *J. Med. Chem.* **2005**, *48*, 4346-4357.

76. Holmstedt, S.; George, L.; Koivuporras, A.; Valkonen, A.; Candeias, N. R., Deoxygenative Divergent Synthesis: En Route to Quinic Acid Chirons. *Org. Lett.* **2020**, *22*, 8370-8375.

77. Sefkow, M., First Efficient Synthesis of Chlorogenic Acid. *Eur. J. Org. Chem.* **2001**, *2001*, 1137-1141.

78. Herzig, J.; Ortony, H., Ueber die vollkommen methylierte Chinasäure. *Arch. Pharm.* **1920**, *258*, 91-96.

79. Snyder, C. D.; Rapoport, H., Stereochemistry of quinate-shikimate conversions. Synthesis of (-)-4-epi-shikimic acid. *J. Am. Chem. Soc.* **1973**, *95*, 7821-7828.

80. McCombie, S. W.; Motherwell, W. B.; Tozer, M. J., The Barton-McCombie Reaction. In *Org. React.*,2012; pp 161-432.

81. Hanessian, S.; Sakito, Y.; Dhanoa, D.; Baptistella, L., Synthesis of (+)-palitantin. *Tetrahedron* **1989**, *45*, 6623-6630.

82. Haller, B.-U.; Kruber, S.; Maier, M. E., A Practical Synthesis of the Cyclohexyl Part of the Immunosuppressant FK506. *J. Prakt. Chem.* **1998**, *340*, 656-661.

83. Saito, A.; Igarashi, W.; Furukawa, H.; Yamada, T.; Kuwahara, S.; Kiyota, H., Facile synthesis of the cyclohexane fragment of enacloxins, a series of antibiotics isolated from Frateuria sp. W-315. *Biosci. Biotechnol. Biochem.* **2014**, *78*, 766-769.

84. Chapelon, A.-S.; Moraléda, D.; Rodriguez, R.; Ollivier, C.; Santelli, M., Enantioselective synthesis of steroids. *Tetrahedron* **2007**, *63*, 11511-11616.

85. Sibilska, I.; Barycka, K. M.; Sicinski, R. R.; Plum, L. A.; Deluca, H. F., 1-desoxy analog of 2MD: synthesis and biological activity of (20S)-25-hydroxy-2-methylene-19-norvitamin D3. *J. Steroid. Biochem. Mol. Biol.* **2010**, *121*, 51-55.

86. Barros, M. T.; Maycock, C. D.; Ventura, M. R., The First Synthesis of (−)-Asperpentyn and Efficient Syntheses of (+)-Harveynone, (+)-Epiepoformin and (−)-Theobroxide. *Chem. Eur. J.* **2000**, *6*, 3991-3996.

87. Herrera, L.; Feist, H.; Michalik, M.; Quincoces, J.; Peseke, K., Synthesis of anellated carbasugars from (−)-quinic acid. *Carbohydr. Res.* **2003**, *338*, 293-298.

88. Kusumi, S.; Nakayama, H.; Kobayashi, T.; Kuriki, H.; Matsumoto, Y.; Takahashi, D.; Toshima, K., Total Synthesis of Aquayamycin. *Chem. Eur. J.* **2016**, *22*, 18733-18736.

89. Arceo, E.; Ellman, J. A.; Bergman, R. G., A direct, biomass-based synthesis of benzoic acid: formic acid-mediated deoxygenation of the glucose-derived materials quinic acid and shikimic acid. *Chem. Sus. Chem.* **2010**, *3*, 811-813.

90. Assoah, B.; Veiros, L. F.; Afonso, C. A. M.; Candeias, N. R., Biomass-Based and Oxidant-Free Preparation of Hydroquinone from Quinic Acid. *Eur. J. Org. Chem.* **2016**, *2016*, 3856-3861.

91. Harris, J. M.; Watkins, W. J.; Hawkins, A. R.; Coggins, J. R.; Abell, C., Comparison of the substrate specificity of type I and type II dehydroquinases with 5-deoxy- and 4,5-dideoxy-dehydroquinic acid. *J. Chem. Soc., Perkin Trans. 1* **1996**, 2371-2377.

92. Gartman, J. A.; Tambar, U. K., Total Synthesis of (+)-Rubellin C. *Org. Lett.* **2020**, *22*, 9145-9150.

93. Spino, C.; Hill, B.; Dubé, P.; Gingras, S., A diene-transmissive approach to the quassinoid skeleton. *Can. J. Chem.* **2003**, *81*, 81-108.

94. Colas, C.; Quiclet-Sire, B.; Cleophax, J.; Delaumeny, J. M.; Sepulchre, A. M.; Gero, S. D., Synthesis of 2,5,6-trideoxystreptamine and its transformation into bioactive

pseudodisaccharides by microbial and chemical methods. *J. Am. Chem. Soc.* **2002**, *102*, 857-858.

95. de Sousa, S. E.; O'Brien, P.; Pilgram, C. D., Chiral base route to cyclic polyols: asymmetric synthesis of aminodeoxyconduritols and conduritol F. *Tetrahedron Lett.* **2001**, *42*, 8081-8083.

96. Paquette, L. A.; Kuo, L. H.; Doyon, J., Enhanced Channeling of the Squarate Cascade through the Dianionic Oxy-Cope Option. Oxy Substitution Markedly Augments Syn Delivery of the Second Alkenyllithium. *J. Am. Chem. Soc.* **1997**, *119*, 3038-3047.

97. Jeroncic, L. O.; Cabal, M. P.; Danishefsky, S. J.; Shulte, G. M., On the diastereofacial selectivity of Lewis acid-catalyzed carbon-carbon bond forming reactions of conjugated cyclic enones bearing electron-withdrawing substituents at the .gamma.-position. *J. Org. Chem.* **1991**, *56*, 387-395.

98. Stark, C.; Schmidt, A.-K., The Glycol Cleavage in Natural Product Synthesis: Reagent Classics and Recent Advances. *Synthesis* **2014**, *46*, 3283-3308.

99. Gonzalez, C.; Carballido, M.; Castedo, L., Synthesis of polyhydroxycyclohexanes and relatives from (-)-quinic acid. *J Org Chem* **2003**, *68*, 2248-55.

100. Maycock, C. D.; Barros, M. T.; Santos, A. G.; Godinho, L. S., An application of quinic acid to the synthesis of linear homochiral molecules: A synthesis of (+)-negamycin. *Tetrahedron Lett.* **1992**, *33*, 4633-4636.

101. Barton, D. H. R.; Géro, S. D.; Maycock, C. D., Studies related to maytansinoids. *J. Chem. Soc. Perkin Trans. 1* **1980**, 1089-1091.

102. Maycock, C. D.; Barros, M. T.; Santos, A. G.; Godinho, L. S., An application of quinic acid to the synthesis of cyclic homochiral molecules: A common route to some interesting carbocyclic nucleoside precursors. *Tetrahedron Lett.* **1993**, *34*, 7985-7988.

103. Thomas, U.; Kalyanpur, M. G.; Stevens, C. M., The absolute configuration of homocitric acid (2-hydroxy-1,2,4-butanetricarboxylic acid), an intermediate in lysine biosynthesis. *Biochemistry* **1966**, *5*, 2513-2516.

104. Tavassoli, A.; Duffy, J. E.; Young, D. W., Synthesis of trimethyl (2S,3R)- and (2R,3R)-[2-2H1]-homocitrates and dimethyl (2S,3R)- and (2R,3R)-[2-2H1]-homocitrate lactones-an assay for the stereochemical outcome of the reaction catalysed both by homocitrate synthase and by the Nif-V protein. *Org. Biomol. Chem.* **2006**, *4*, 569-580.

105. Matsuo, K.; Matsumoto, T.; Nishiwaki, K., Alternative Synthesis of (-)-Malyngolide Utilizing (-)-Quinic Acid. *Heterocycles* **1998**, *48*, 1213-1220.

106. Baptistella, L.; Jorge, A. d. C., Efficient Access to Novel Furanofurone Compounds from Quinic Acid: Studies of Inter-and Intramolecular Wittig Reactions on Lactones. *Synlett.* **2007**, *2007*, 3045-3049.

107. Belosludtsev, Y. Y.; Kollah, R. O.; Falck, J. R.; Capdevila, J. H., Hepoxilins B3: Synthesis of all four stereoisomers and a glutathione adduct. *Tetrahedron Lett.* **1994**, *35*, 5327-5330.

108. Shih, T.-L.; Gao, W.-L., The first synthesis of 7-(hydroxymethyl)thiepane-3,4,5-triols from d-(−)-quinic acid. *Tetrahedron* **2013**, *69*, 1897-1903.

109. Mulzer, J.; Drescher, M.; Enev, V., Quinic Acid as Versatile Chiral Scaffold in Organic Synthesis. *Curr. Org. Chem.* **2008**, *12*, 1613-1630.

110. Kuhlborn, J.; Gross, J.; Opatz, T., Making natural products from renewable feedstocks: back to the roots? *Nat. Prod. Rep.* **2020**, *37*, 380-424.

111. Usami, Y.; Ohsugi, M.; Mizuki, K.; Ichikawa, H.; Arimoto, M., Facile and efficient synthesis of naturally occurring carbasugars (+)-pericosines A and C. *Org. Lett.* **2009**, *11*, 2699-2701.

112. Li, M.; Li, Y.; Ludwik, K. A.; Sandusky, Z. M.; Lannigan, D. A.; O'Doherty, G. A., Stereoselective Synthesis and Evaluation of C6''-Substituted 5a-Carbasugar Analogues of SL0101 as Inhibitors of RSK1/2. *Org. Lett.* **2017**, *19*, 2410-2413.

113. Murray, L. M.; O'Brien, P.; Taylor, R. J. K.; Wünnemann, S., Lithium enolates from a (−)-quinic acid-derived cyclohexanone with a β-alkoxy leaving group: regioselective preparation and evaluation of enolate stability towards β-elimination. *Tetrahedron Lett.* **2004**, *45*, 2597-2601.

114. Yan, Z.; Zhao, C.; Gong, J.; Yang, Z., Asymmetric Total Synthesis of (-)-Guignardones A and B. *Org. Lett.* **2020**, *22*, 1644-1647.

115. Belanger, F.; Chase, C. E.; Endo, A.; Fang, F. G.; Li, J.; Mathieu, S. R.; Wilcoxen, A. Z.; Zhang, H., Stereoselective synthesis of the Halaven C14-C26 fragment from D-quinic acid: crystallization-induced diastereoselective transformation of an alpha-methyl nitrile. *Angew. Chem. Int. Ed.* **2015**, *54*, 5108-5111.

116. Dangschat, G.; Fischer, H. O. L., Übergang der Chinasäure in Shikimisäure. *Sci. Nat.* **1938**, *26*, 562-563.

117. Candeias, N. R.; Assoah, B.; Simeonov, S. P., Production and Synthetic Modifications of Shikimic Acid. *Chem. Rev.* **2018**, *118*, 10458-10550.

118. Cleophax, J.; Mercier, D.; Géro, S. D., A Stereospecific Conversion of (−)-Methyl Tri-O-benzoylquinate to the Corresponding (−)-Methyl Shikimate. *Angew. Chem. Int. Edi.* **1971**, *10*, 652-653.

119. Kim, C. U.; Lew, W.; Williams, M. A.; Liu, H.; Zhang, L.; Swaminathan, S.; Bischofberger, N.; Chen, M. S.; Mendel, D. B.; Tai, C. Y.; Laver, W. G.; Stevens, R. C., Influenza neuraminidase inhibitors possessing a novel hydrophobic interaction in the enzyme active site: design, synthesis, and structural analysis of carbocyclic sialic acid analogues with potent anti-influenza activity. *J. Am. Chem. Soc.* **1997**, *119*, 681-690.

120. Rohloff, J. C.; Kent, K. M.; Postich, M. J.; Becker, M. W.; Chapman, H. H.; Kelly, D. E.; Lew, W.; Louie, M. S.; McGee, L. R.; Prisbe, E. J.; Schultze, L. M.; Yu, R. H.; Zhang, L., Practical Total Synthesis of the Anti-Influenza Drug GS-4104. *J. Org. Chem.* **1998**, *63*, 4545-4550.

121. Chen, B.; Kawai, M.; Wu-Wong, J. R., Synthesis of VS-105: A novel and potent vitamin D receptor agonist with reduced hypercalcemic effects. *Bioorg. Med. Chem. Lett.* **2013**, *23*, 5949-5952.

122. Fernandez, S.; Ferrero, M., Strategies for the Synthesis of 19-nor-Vitamin D Analogs. *Pharmaceuticals* **2020**, *13*, 159.

123. Carballido, M.; Castedo, L.; González-Bello, C., Synthesis of Amino Carba Sugars and Conformationally Restricted Polyhydroxyγ-Amino Acids from (−)-Quinic Acid. *Eur. J. Org. Chem.* **2004**, *2004*, 3663-3668.

124. González-Bello, C.; Manthey, M. K.; Harris, J. H.; Hawkins, A. R.; Coggins, J. R.; Abell, C., Synthesis of 2-Bromo- and 2-Fluoro-3-dehydroshikimic Acids and 2-Bromo- and 2-Fluoroshikimic Acids Using Synthetic and Enzymatic Approaches. *J. Org. Chem.* **1998**, *63*, 1591-1597.

125. Li, G.; Lou, H. X., Strategies to diversify natural products for drug discovery. *Med. Res. Rev.* **2018**, *38*, 1255-1294.

126. Gevorgyan, V.; Rubin, M.; Liu, J. X.; Yamamoto, Y., A direct reduction of aliphatic aldehyde, acyl chloride, ester, and carboxylic functions into a methyl group. *J. Org. Chem.* **2001**, *66*, 1672-1675.

127. Yamamoto, Y.; Bajracharya, G. B.; Nogami, T.; Jin, T.; Matsuda, K.; Gevorgyan, V., Reduction of Carbonyl Function to a Methyl Group. *Synthesis* **2004**, 308-311.

128. Marzabadi, C. H.; Anderson, J. E.; Gonzalez-Outeirino, J.; Gaffney, P. R.; White, C. G.; Tocher, D. A.; Todaro, L. J., Why are silyl ethers conformationally different from alkyl ethers? Chair-chair conformational equilibria in silyloxycyclohexanes and their dependence on the substituents on silicon. The wider roles of eclipsing, of 1,3-repulsive steric interactions, and of attractive steric interactions. *J. Am. Chem. Soc.* **2003**, *125*, 15163-15173.

129. Drosos, N.; Morandi, B., Boron-Catalyzed Regioselective Deoxygenation of Terminal 1,2-Diols to 2-Alkanols Enabled by the Strategic Formation of a Cyclic Siloxane Intermediate. *Angew. Chem. Int. Ed.* **2015**, *54*, 8814-8818.

130. Chatterjee, I.; Porwal, D.; Oestreich, M., B(C6 F5)3 -Catalyzed Chemoselective Defunctionalization of Ether-Containing Primary Alkyl Tosylates with Hydrosilanes. *Angew. Chem. Int. Ed.* **2017**, *56*, 3389-3391.

131. Zhang, J.; Park, S.; Chang, S., Piers' borane-mediated hydrosilylation of epoxides and cyclic ethers. *Chem. Commun.* **2018**, *54*, 7243-7246.

132. Reddy, L. V.; Kumar, V.; Sagar, R.; Shaw, A. K., Glycal-derived delta-hydroxy alpha,beta-unsaturated aldehydes (Perlin aldehydes): versatile building blocks in organic synthesis. *Chem. Rev.* **2013**, *113*, 3605-3631.

133. Montchamp, J. L.; Piehler, L. T.; Frost, J. W., Diastereoselection and in vivo inhibition of 3-dehydroquinate synthase. *J. Am. Chem. Soc.* **2002**, *114*, 4453-4459.

134. Schwizer, D.; Patton, J. T.; Cutting, B.; Smiesko, M.; Wagner, B.; Kato, A.; Weckerle, C.; Binder, F. P.; Rabbani, S.; Schwardt, O.; Magnani, J. L.; Ernst, B., Pre-organization of the core structure of E-selectin antagonists. *Chem. Eur. J.* **2012**, *18*, 1342-1351.

135. Rej, R.; Jana, N.; Kar, S.; Nanda, S., Stereoselective synthesis of a novel natural carbasugar and analogues from hydroxymethylated cycloalkenone scaffolds. *Tetrahedron: Asymmetry* **2012**, *23*, 364-372.

136. Corey, E. J.; Venkateswarlu, A., Protection of hydroxyl groups as tert-butyldimethylsilyl derivatives. *J. Am. Chem. Soc.* **1972**, *94*, 6190-6191.

137. Govindarajan, M., Protecting group migrations in carbohydrate chemistry. *Carbohydr. Res.* **2020**, *497*, 108151.

138. Phanumartwiwath, A.; Hornsby, T. W.; Jamalis, J.; Bailey, C. D.; Willis, C. L., Silyl migrations in D-xylose derivatives: total synthesis of a marine quinoline alkaloid. *Org. Lett.* **2013**, *15*, 5734-5737.

139. Lassaletta, J. M.; Meichle, M.; Weiler, S.; Schmidt, R. R., Silyl Group Migration in 1-O-Silyl Protected Sugars-Convenient Synthesis of 2-O-Unprotected Sugars. *J. Carbohydr. Chem.* **1996**, *15*, 241-254.

140. Bogdan, F. M.; Chow, C. S., The synthesis of allyl- and allyloxycarbonyl-protected RNA phosphoramidites. Useful reagents for solid-phase synthesis of RNAs with base-labile modifications. *Tetrahedron Lett.* **1998**, *39*, 1897-1900.

141. Neuner, S.; Santner, T.; Kreutz, C.; Micura, R., The "Speedy" Synthesis of Atom-Specific (15)N Imino/Amido-Labeled RNA. *Chem. Eur. J.* **2015**, *21*, 11634-11643.

142. Brook, A. G., Molecular rearrangements of organosilicon compounds. *Acc. Chem. Res.* **1974**, *7*, 77-84.

143. Laurent, P.; Hamdani, A.; Braekman, J.-C.; Daloze, D.; Isbell, L. A.; de Biseau, J.-C.; Pasteels, J. M., New 1-alk(en)yl-1,3,5-trihydroxycyclohexanes from the Dufour gland of the African ant Crematogaster nigriceps. *Tetrahedron Lett.* **2003**, *44*, 1383-1386.

144. Laplace, D. R.; Van Overschelde, M.; De Clercq, P. J.; Verstuyf, A.; Winne, J. M., Synthesis of 2-Ethyl-19-norAnalogs of 1α,25-Dihydroxyvitamin D3. *European Journal of Organic Chemistry* **2013**, *2013*, 728-735.

145. Sedmera, P.; Halada, P.; Pospisil, S., New carbasugars from Streptomyces lincolnensis. *Magn. Reson. Chem.* **2009**, *47*, 519-522.

146. Trost, B. M.; Romero, A. G., Synthesis of optically active isoquinuclidines utilizing a diastereoselectivity control element. *J. Org. Chem.* **1986**, *51*, 2332-2342.

147. Hutchins, R. O.; Hoke, D.; Keogh, J.; Koharski, D., Sodium borohydride in dimethyl sulfoxide or sulfolane. Convenient systems for selective reductions of primary, secondary and certain tertiary halides and tosylates. *Tetrahedron Lett.* **1969**, *10*, 3495-3498.

148. Brown, H. C.; Krishnamurthy, S., Forty years of hydride reductions. *Tetrahedron* **1979**, *35*, 567-607.

149. Soai, K.; Oyamada, H.; Takase, M.; Ookawa, A., Practical Procedure for the Chemoselective Reduction of Esters by Sodium Borohydride. Effect of the Slow Addition of Methanol. *Bull. Chem. Soc. Jpn.* **1984**, *57*, 1948-1953.

150. Einhorn, J.; Einhorn, C.; Ratajczak, F.; Pierre, J. L., Efficient and Highly Selective Oxidation of Primary Alcohols to Aldehydes by N-Chlorosuccinimide Mediated by Oxoammonium Salts. *J. Org. Chem.* **1996**, *61*, 7452-7454.

151. Murugesan, A.; Holmstedt, S.; Brown, K. C.; Koivuporras, A.; Macedo, A. S.; Nguyen, N.; Fonte, P.; Rijo, P.; Yli-Harja, O.; Candeias, N. R.; Kandhavelu, M., Design and synthesis of novel quinic acid derivatives: in vitro cytotoxicity and anticancer effect on glioblastoma. *Future Med. Chem.* **2020**, *12*, 1891-1910.

152. Tripathi, V.; Singh, A.; Chauhan, S., Quinic acid attenuates oral cancer cell proliferation by downregulating cyclin D1 Expression and Akt signaling. *Pharmacogn. Mag.* **2018**, *14*, 14-19.

153. L. Inbathamizh, E. P., Quinic acid as a potent drug candidate for prostate cancer - A comparative pharmacokinetic approach. *Asian J Pharm. Clin. Res.* **2013**, *6*, 106-112.

154. Zanello, P. R.; Koishi, A. C.; Rezende Junior Cde, O.; Oliveira, L. A.; Pereira, A. A.; de Almeida, M. V.; Duarte dos Santos, C. N.; Bordignon, J., Quinic acid derivatives inhibit dengue virus replication in vitro. *Virol. J.* **2015**, *12*, 223.

155. He, H.; Weir, R. L.; Toutounchian, J. J.; Pagadala, J.; Steinle, J. J.; Baudry, J.; Miller, D. D.; Yates, C. R., The quinic acid derivative KZ-41 prevents glucose-induced caspase-3 activation in retinal endothelial cells through an IGF-1 receptor dependent mechanism. *Plos One* **2017**, *12*, e0180808.

156. Zeng, K.; Thompson, K. E.; Yates, C. R.; Miller, D. D., Synthesis and biological evaluation of quinic acid derivatives as anti-inflammatory agents. *Bioorg. Med. Chem. Lett.* **2009**, *19*, 5458-5460.

157. Metaferia, B. B.; Chen, L.; Baker, H. L.; Huang, X. Y.; Bewley, C. A., Synthetic macrolides that inhibit breast cancer cell migration in vitro. *J. Am. Chem. Soc.* **2007**, *129*, 2434-2435.

158. Wang, Y. H.; Ye, J. L.; Wang, A. E.; Huang, P. Q., Reductive hydroxyalkylation/alkylation of amines with lactones/esters. *Org. Biomol. Chem.* **2012**, *10*, 6504-6511.

PUBLICATIONS

Publication **I**	Suvi Holmstedt, Lijo George, Alisa Koivuporras, Arto Valkonen, and Nuno R. Candeias. Deoxygenative Divergent Synthesis: En Route to Quinic Acid Chirons. *Org. Lett.* **2020**, 22, 8370−8375.
Publication **II**	Suvi Holmstedt, Alexander Efimov, and Nuno R. Candeias. *O,O*-Silyl Group Migrations in Quinic acid derivatives: An Opportunity for Divergent Synthesis. *Org. Lett.* **2021**, *23*, 3083−3087.
Publication **III**	Suvi Holmstedt and Nuno R. Candeias. A Concise Synthesis of Carbasugars Isolated from *Streptomyces Lincolnensis. Tetrahedron*, **2020**, *76*, 131346.
Publication **IV**	Akshaya Murugesan*, Suvi Holmstedt*, Kenna C. Brown*, Alisa Koivuporras, Ana S. Macedo, Nga Nguyen, Pedro Fonte, Patricia Rijo, Olli Yli-Harja, Nuno R. Candeias, and Meenakshisundaram Kandhavelu. Design and synthesis of novel quinic acid derivatives: in vitro cytotoxicity and anticancer effect on glioblastoma. Future Med. Chem., **2020**, *12*, 1891-1910. *Equal contribution.

PUBLICATION
I

Deoxygenative Divergent Synthesis: En Route to Quinic Acid Chirons

Suvi Holmstedt, Lijo George, Alisa Koivuporras, Arto Valkonen, and Nuno R. Candeias

Organic Letters, **2020**, *22*, 8370–8375.
DOI: 10.1021/acs.orglett.0c02995

Publication reprinted with the permission of ACS Publications.

OL Organic Letters

pubs.acs.org/OrgLett

Letter

Deoxygenative Divergent Synthesis: En Route to Quinic Acid Chirons

Suvi Holmstedt,* Lijo George, Alisa Koivuporras, Arto Valkonen, and Nuno R. Candeias*

Cite This: *Org. Lett.* 2020, 22, 8370−8375

Read Online

ACCESS | Metrics & More | Article Recommendations | Supporting Information

Downloaded via TAMPERE UNIV on May 3, 2021 at 05:47:10 (UTC).
See https://pubs.acs.org/sharingguidelines for options on how to legitimately share published articles.

ABSTRACT: The installation of vicinal mesylate and silyl ether groups in a quinic acid derivative generates a system prone for stereoselective borane-catalyzed hydrosilylation through a siloxonium intermediate. The diversification of the reaction conditions allowed the construction of different defunctionalized fragments foreseen as useful synthetic fragments. The selectivity of the hydrosilylation was rationalized on the basis of deuteration experiments and computational studies.

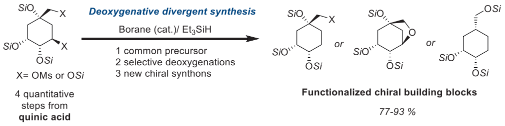
X= OMs or OSi
4 quantitative steps from quinic acid
Deoxygenative divergent synthesis
Borane (cat.)/ Et3SiH
1 common precursor
2 selective deoxygenations
3 new chiral synthons
or
or
Functionalized chiral building blocks
77-93 %

Synthetic strategies remain critically dependent on hemisynthesis or chiral pool synthesis despite the plethora of currently available catalytic asymmetric transformations.[1] The contemporary mandatory transition from fossil to biobased carbon resources calls for the development of synthetic transformations that maximize the full potential of chemical entities or fragments created by nature. Saccharides are the main components of biomass, and the efforts done for their integration in biorefineries have augmented the development of methods for removal of their oxygen functionalities.[2] Dehydration[3] and selective cleavage of C−O bonds[4] of saccharides have been explored in the expansion of the biomass-derived chemical space.[5] Yamamoto's seminal B(C_6F_5)$_3$-catalyzed hydrosilylation of C−O bonds[6] has been used in the extensive deoxygenation of saccharides[7] and recently in the regioselective deoxygenation of saccharides[8] and polyols[8c] to provide new chiral entities (Scheme 1a). Alternative boron catalysts such as Piers' borane (HB(C_6F_5)$_2$)[9] and more recently B((3,5-CF_3)$_2C_6H_3$)$_3$[10] have been demonstrated to catalyze the silylative deoxygenation of biomass-derived sugars.[11] The outcome of this deoxygenation method depends on several stereochemical and electronic parameters: first and foremost is the structure of the oxygenated substrate,[8a] as vicinal groups can assist the C−O bond cleavage.[8c] The second parameter is the hydrosilane employed,[8b,c] and the third is the fluoroarylborane catalyst.[12] Gagné and co-workers have recently progressed the field by replacing hydrosilanes by hydroboranes as precursors of H−B(C_6F_5)$_3^-$ hydride in the C−O bond cleavage with different selectivities than the ones observed in the hydrosilylation.[13]

Morandi[14] and Oestreich[15] have expanded the B(C_6F_5)$_3$-catalyzed hydrosilylation of C(sp^3)−O bonds to 1,2-diols and primary tosylates, respectively. Both methods are effective in cleaving the terminal C−O bond, the former due to the formation of a cyclic siloxane intermediate and the latter due to the higher reactivity of the tosylate compared with the silyl

Scheme 1. B(C_6F_5)$_3$-Catalyzed Selective Deoxygenation of 1,2-Diols and Primary Alkyl Tosylates

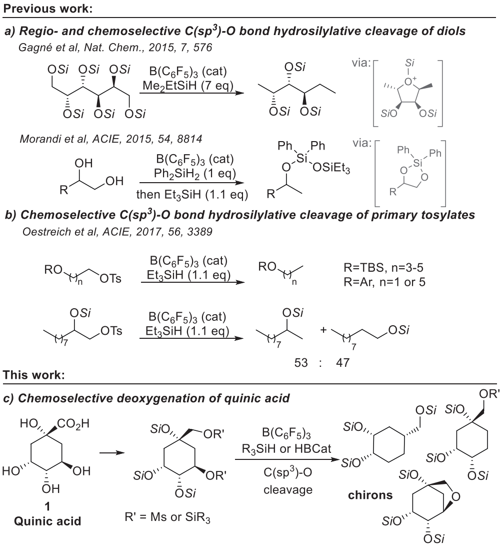
Previous work:
a) Regio- and chemoselective C(sp3)-O bond hydrosilylative cleavage of diols
Gagné et al, Nat. Chem., 2015, 7, 576
B(C6F5)3 (cat)
Me2EtSiH (7 eq)
via:
Morandi et al, ACIE, 2015, 54, 8814
B(C6F5)3 (cat)
Ph2SiH2 (1 eq)
then Et3SiH (1.1 eq)
via:
b) Chemoselective C(sp3)-O bond hydrosilylative cleavage of primary tosylates
Oestreich et al, ACIE, 2017, 56, 3389
B(C6F5)3 (cat)
Et3SiH (1.1 eq)
R=TBS, n=3-5
R=Ar, n=1 or 5
B(C6F5)3 (cat)
Et3SiH (1.1 eq)
53 : 47
This work:
c) Chemoselective deoxygenation of quinic acid
1
Quinic acid
R' = Ms or SiR3
B(C6F5)3
R3SiH or HBCat
C(sp3)-O cleavage
chirons

Received: September 8, 2020
Published: October 1, 2020

© 2020 American Chemical Society

ether. Although suitable for the cleavage of primary tosylates containing a primary silyl ether (Scheme 1b, R = TBDMS, *n* = 3−5), or an aryl ether (Scheme 1b, R = Ar, *n* = 1 or 5), rearranged products from anchimeric assistance were observed for 1,2-diols (Scheme 1b, bottom). Indeed, the nonselective opening of a three-membered silyloxonium ion leads to the indiscriminate formation of a primary and secondary silyl ether. Substituents' migration competing with direct deoxygenation processes was further explored by Morandi, providing a reductive pinacol-type rearrangement of vicinal diols.[16] On a related note, the $B(C_6F_5)_3$-catalyzed hydrosilylation of tetrasubstituted epoxides leads to a migratory ring-opening process after the formation of a silyloxonium ion intermediate.[17] While the $B(C_6F_5)_3$-catalyzed hydrosilylation of C−O bonds has been rapidly expanding the accessibility to saccharides-derived chiral fragments for synthesis,[8c,10,11,13,18] we envisioned that different chiral synthons[19] could be reached by focusing on natural cyclitols.

Quinic acid **1** was provisionally considered as one suitable feedstock for the biobased benzoic acid production[20] or other aromatics.[21] However, high cost associated with the use of glucose as feedstock for bacterial production of quinic acid[22] has again relegated this cyclitol to the chiral pool.[23] Nevertheless, quinic acid and its acyl-derivatives are widespread secondary metabolites of the shikimic acid pathway[24] in plants and can be obtained for instance from coffee beans, plants, fruits, and even food wastes.[25] Herein we present our efforts toward the selective cleavage of $C(sp^3)$−O bonds of a common quinic acid-derived precursor with judiciously selected *O*-substituents, into diverse chiral fragments (Scheme 1c).

Aware of putative effects imposed by the diverse conformations of cyclitols on the regioselectivity of deoxygenation using the $B(C_6F_5)_3$/SiH system, the vicinal *cis* diol moiety of quinide **2** was derivatized to several functional groups. Besides conferring the desired conformational effect, further deprotection after deoxygenation would provide substrates prone to typical C−C oxidative cleavage and subsequently give chiral linear C_7 fragments. Attempts on the hydrosilylation of cyclitol derivatives **3**−**13** (Scheme 2) failed in providing any deoxygenated products (see Supporting Information section 1 for complete rationale).

The discouraging lack of reactivity of the silylated quinic acid derivatives prompted us to explore the anchimeric assistance by silyl ethers in the C−O bond cleavage of tosylates, as previously reported by Oestreich and coworkers.[15] Excellent chemoselectivity was reported for the deoxygenation of primary alkyl tosylates from nonvicinal diol derivatives. However, the formation of a three-membered silyloxonium ion intermediate resulted in rearranged products, and a lack of regioselectivity was observed when considering aliphatic 1,2-vicinal diol systems. Gratifyingly, treatment of **15** with different catalyst loadings and amounts of triethylsilane resulted in formation of **16** and/or **17** in different ratios (Scheme 3 and Table S1 in SI for further experiments). Silyl ethers derived from primary and secondary alcohols have been reported to be more reactive toward $B(C_6F_5)_3$-catalyzed reduction with hydrosilanes than the ones derived from tertiary homologues.[6c,d] On the other hand, the neighboring group assistance can deeply impact the regioselectivity. Notably, cleavage of the primary mesylate in **15** was accompanied by stereospecific migration of the silyloxy group from the vicinal tertiary carbon to provide **17** (Scheme 3). The absolute configuration of the deoxygenated product was determined through X-ray diffraction analysis of the 3,5-dinitrobenzoyl derivative **18**, obtained after desilylation of **17** and benzoylation of the triol **17′**.

Scheme 2. Quinic Acid Derivatives Explored in $B(C_6F_5)_3$-Catalyzed Hydrosilylation

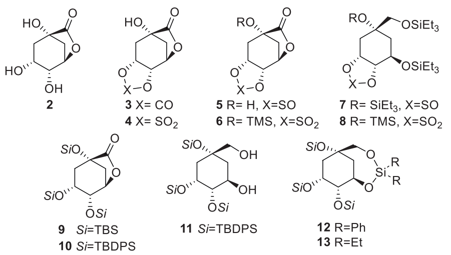

Scheme 3. Deoxygenation of Quinic Acid Derivative 15

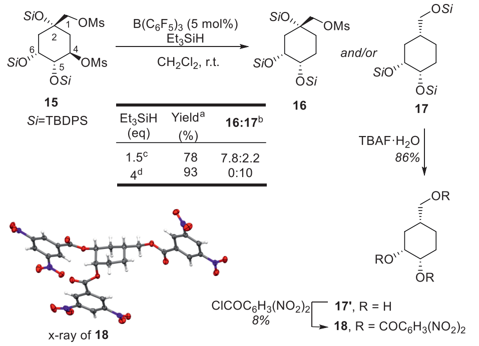

Et_3SiH (eq)	Yield[a] (%)	**16**:**17**[b]
1.5[c]	78	7.8:2.2
4[d]	93	0:10

[a]**15** (0.14 mmol) and $B(C_6F_5)_3$ in CH_2Cl_2, at r.t. followed by addition of Et_3SiH. [b]Ratio determined from isolated yields. [c][**15**] = 0.05 M. [d][**15**] = 0.3 M.

Attempts to overcome the higher propensity of C4 toward deoxygenation by replacing the mesylate with protecting groups proved futile. Instead, $B(C_6F_5)_3$/SiH treatment of **20** having the secondary hydroxyl protected as silyl ether (**20b**) resulted in fast intramolecular cyclization to bicyclic compound **21** in up to 88% yield (Scheme 4). Exposure of MOM-ether **20c** to the same conditions resulted in the formation of compound **20d** in 78% yield (Scheme 5). Treatment of methyl ether **20d** with additional triethylsilane (1.1 equiv) in the presence of $B(C_6F_5)_3$ led to formation of cyclic ether **21**, as deduced from crude NMR. Carbamoyl protected **20e** was unreactive toward $B(C_6F_5)_3$-catalyzed hydrosilylation, and only starting material was recovered, despite the harsh reaction conditions used (20 mol % catalyst, excess of silane and refluxing toluene). The structural complexity of compound **21**[26] was broken down through oxidative cleavage of the C−C bond upon desilylation and oxidation of the *cis* glycol moiety via Malaprade oxidation to provide dialdehyde **22** in excellent yield. The cyclic ethers **22** and **23** are envisioned as interesting synthetic intermediates due to the presence of oxygen functionality-containing substituents at C1 and C3 positions of the tetrahydrofuran core.[27] The selective deprotection of the

Scheme 4. Formation and Controlled Cleavage of Bicyclic Tetrahydrofuran 21[a]

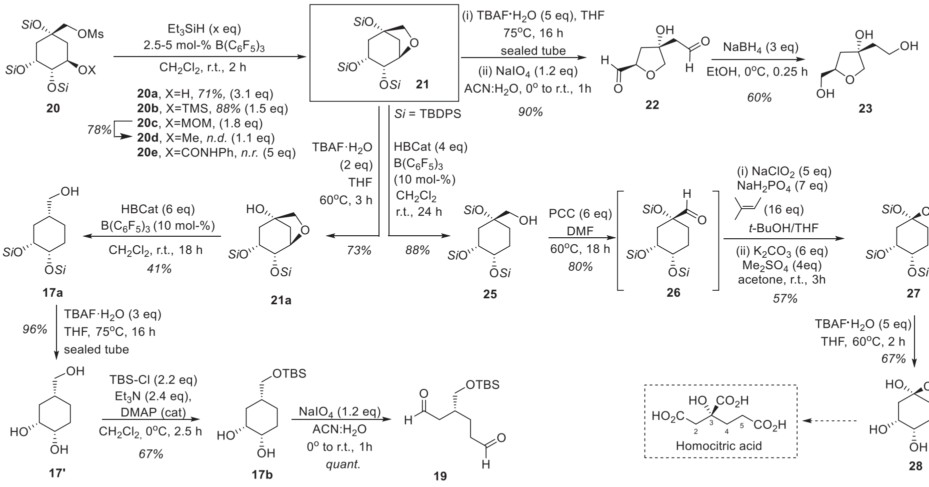
SiO OMs SiO OX OSi
20
Et3SiH (x eq)
2.5-5 mol-% B(C6F5)3
CH2Cl2, r.t., 2 h
20a, X=H, 71%, (3.1 eq)
20b, X=TMS, 88% (1.5 eq)
78%
20c, X=MOM, (1.8 eq)
20d, X=Me, n.d. (1.1 eq)
20e, X=CONHPh, n.r. (5 eq)
21
Si = TBDPS
(i) TBAF·H2O (5 eq), THF
75°C, 16 h
sealed tube
(ii) NaIO4 (1.2 eq)
ACN:H2O, 0° to r.t., 1h
90%
22
NaBH4 (3 eq)
EtOH, 0°C, 0.25 h
60%
23
TBAF·H2O (2 eq) THF 60°C, 3 h
73%
HBCat (4 eq) B(C6F5)3 (10 mol-%) CH2Cl2 r.t., 24 h
88%
21a
HBCat (6 eq)
B(C6F5)3 (10 mol-%)
CH2Cl2, r.t., 18 h
41%
17a
25
PCC (6 eq)
DMF
60°C, 18 h
80%
26
(i) NaClO2 (5 eq)
NaH2PO4 (7 eq)
(16 eq)
t-BuOH/THF
(ii) K2CO3 (6 eq)
Me2SO4 (4eq)
acetone, r.t., 3h
57%
27
96%
TBAF·H2O (3 eq)
THF, 75°C, 16 h
sealed tube
17'
TBS-Cl (2.2 eq)
Et3N (2.4 eq),
DMAP (cat)
CH2Cl2, 0°C, 2.5 h
67%
17b
NaIO4 (1.2 eq)
ACN:H2O
0° to r.t., 1h
quant.
19
TBAF·H2O (5 eq)
THF, 60°C, 2 h
67%
28
Homocitric acid

[a]n.d. = yield not deternined; n.r. = no reaction.

Scheme 5. $B(C_6F_5)_3$-Catalyzed Siloxonium Opening with Et_3SiD

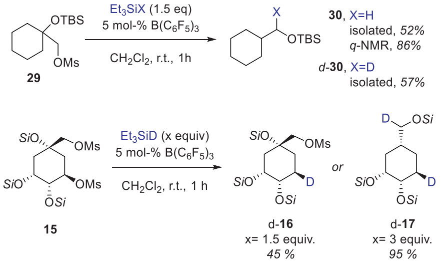
29
Et3SiX (1.5 eq)
5 mol-% B(C6F5)3
CH2Cl2, r.t., 1h
30, X=H
isolated, 52%
q-NMR, 86%
d-30, X=D
isolated, 57%
15
Et3SiD (x equiv)
5 mol-% B(C6F5)3
CH2Cl2, r.t., 1 h
or
d-16
x= 1.5 equiv.
45 %
d-17
x= 3 equiv.
95 %

tertiary silyl ether of **21** followed by similar cleavage with catechol borane and desilylation also provided compound **17a**. A sequence of silyl ethers' cleavage and primary alcohol protection resulted in **17b** that was submitted to Malaprade oxidation providing dialdehyde **19**, envisioned as a rich fragment for stereoselective synthesis due to the three functionalities and structural similarities with Perlin aldehydes.[28] Impelled by the bicyclic skeleton of **21**, the controlled modification of its stereogenic carbons was attempted. The lack of reactivity of **21** toward cleavage of the O−Si bond by $B(C_6F_5)_3$-catalyzed hydrosilylation was overcome by reduction with catechol borane, as recently developed by Gagné,[13] resulting in the selective cleavage of the C−O bond from the secondary carbon to provide **25** in 88% yield.

Selective oxidation of primary alcohol moiety of **25** followed by one-pot esterification and desilylation led to **28**, a known intermediate in the synthesis of homocitric acid.[29] Even though not attempted, it is worth noticing that the use of deuteriocatecholborane in the manipulation of **21** would provide an entry for the preparation of labeled homocitrate. Although of potential interest for biological studies, deuterium labeling at position 5 remains unveiled.[29a,30]

The observed preferred chemoselectivity for C−O bond cleavage of the secondary carbon over the primary mesylate in **15** suggests the formation of the three-membered silyloxonium ion as proposed previously by Oestreich. The higher propensity of C4 for deoxygenation compared to C1 is justified by the easier formation of the strained three-membered silyloxonium ion in C4−C5 than in C1−C2, as the later will turn C2 into a spiro carbon. Such events should become less energy demanding after removal of one of the carbocycle substituents. Additionally, the easier access of the hydride to C4 over C5 renders this process highly regioselective in the opening of the siloxonium. Motivated by the excellent regioselectivity in opening of the putative three-membered silyloxonium ion with hydrosilanes, compound **29**, an analogue of **15**, was submitted to similar deoxygenation protocol. The treatment of cyclohexanol derivative **29** with $B(C_6F_5)_3$ and silyl hydrides resulted in cleavage of the C−O bond and migration of the silyl ether moiety to the primary carbon (Scheme 5), contrasting with the previously reported lack of selectivity for deoxygenation of primary tosylates vicinal to a secondary silyl ether.[15] While no alkyl migration was observed in the deoxygenations of quinic acid derivatives, which was expected given the precedents on the hydrosilylation of epoxides in acyclic systems[17] the migration of hydride from the primary to tertiary carbon was considered.[31] When using Et_3SiD as a reducing agent, the deuteration occurred selectively at the primary carbon, affording *d*-**30** in 57% after isolation. Similar behavior was observed in the hydrosilylation of **15** with Et_3SiD. The delivery of the deuteride to the opposite face of the silyl ethers of the cyclohexane derivative (absolute configuration determined from inspection of vicinal coupling constants) seems to indicate a different mechanism when comparing with the tertiary silyl ether/primary mesylate counterpart.

In order to get further insight on the formation of the silyloxonium intermediate and its regioselective opening, a simplified system was studied by means of Density Functional Theory[32] (Scheme 6), and geometries of the transition states

Scheme 6. Free Energy Profile (M06-2X/6-311++G**//M06-2X/6-31G**) and Mechanistic Representation for Deoxygenation of Model Substrate sm, via Siloxonium and 1,2-Hydride Shift[a]

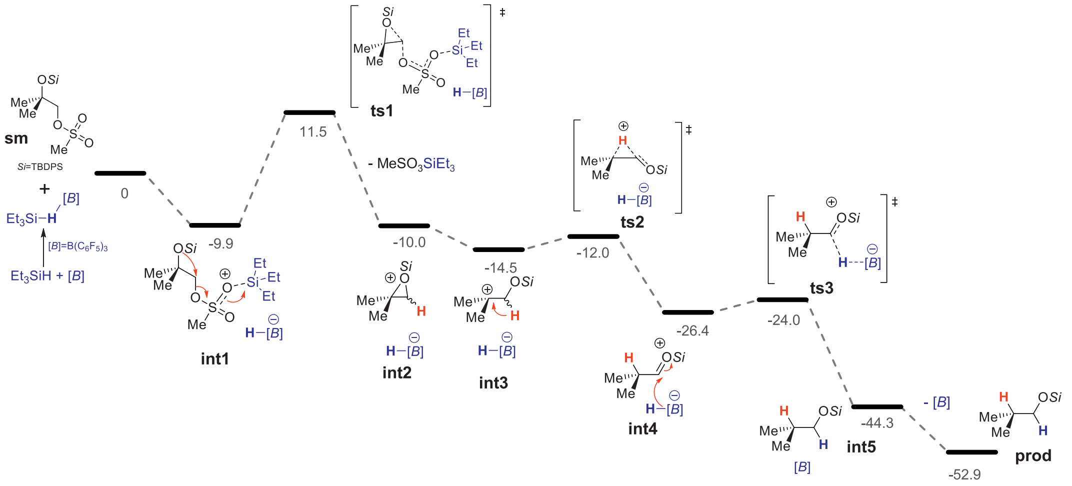

[a]Values are presented in kcal/mol, referring to the initial pair of **sm** and Et$_3$Si–H–B(C$_6$F$_5$)$_3$.

were calculated (please consult Figure S1 and full computational account in the SI). The energetically favorable interaction of the mesylate group of **sm** with silylium ion in **int1** increases the electrophilic character of the primary carbon, triggering the formation of the silyloxonium ion **int2** through a 21.4 kcal/mol energy barrier. C–O bond lengths in the siloxonium **int2** differ by 0.05 Å, with the most substituted bond being elongated. The equilibration of the siloxonium to **int3**, where the above-mentioned C–O bond is clearly broken (d_{C-O} = 2.385 Å), is energetically more favorable by 4.5 kcal/mol. The 1,2-hydride shift for neutralization of the positive charge on the tertiary carbon is a favorable process with **int4** being 11.9 kcal/mol more stable than **int3**. Additionally, the energy barrier for the 1,2-hydride migration through **ts2** is only 2.5 kcal/mol. The hydride delivery from the hydridoborate anion to the electrophilic carbon of the oxocarbenium is almost spontaneous and **int4** can simply overcome the barely existent energy barrier of 2.4 kcal/mol for **ts3** to ultimately form the very stable silyl ether **int5**. The overall process is energetically favored as demonstrated by the ΔG_f of **prod** (52.9 kcal/mol) with the rate limiting step being the formation of the siloxonium **int2**.

In conclusion, we have described the B(C$_6$F$_5$)$_3$-catalyzed defunctionalization of a cyclitol through hydride delivery to three-membered silyloxonium ions. The success of the deoxygenation of quinide and derivatives using this hydrosilylation depends on the protecting groups. Nevertheless, the achieved deoxygenations proved highly stereoselective and allowed the diversification of chiral fragments that can be obtained from quinic acid. The expansion of this transition-metal-free deoxygenation protocol to cyclitols has diversified the array of molecules and fragments that can be obtained from biorenewables.

■ ASSOCIATED CONTENT

Supporting Information

The Supporting Information is available free of charge at https://pubs.acs.org/doi/10.1021/acs.orglett.0c02995.

> Experimental details, preliminary studies on hydrosilylation and characterization data of all synthetic intermediates, full accounts on computational calculations, and ^{1}H and ^{13}C NMR copies of spectra for all reported compounds (PDF)

Accession Codes

CCDC 2005907 contains the supplementary crystallographic data for this paper. These data can be obtained free of charge via www.ccdc.cam.ac.uk/data_request/cif, or by emailing data_request@ccdc.cam.ac.uk, or by contacting The Cambridge Crystallographic Data Centre, 12 Union Road, Cambridge CB2 1EZ, UK; fax: +44 1223 336033.

■ AUTHOR INFORMATION

Corresponding Authors

Suvi Holmstedt – *Faculty of Engineering and Natural Sciences, Tampere University, 33101 Tampere, Finland;*
Email: suvi.holmstedt@tuni.fi
Nuno R. Candeias – *Faculty of Engineering and Natural Sciences, Tampere University, 33101 Tampere, Finland; LAQV-REQUIMTE, Department of Chemistry, University of Aveiro, 3810-193 Aveiro, Portugal;* orcid.org/0000-0003-2414-9064; Email: ncandeias@ua.pt

Authors

Lijo George – *Faculty of Engineering and Natural Sciences, Tampere University, 33101 Tampere, Finland*
Alisa Koivuporras – *Faculty of Engineering and Natural Sciences, Tampere University, 33101 Tampere, Finland*

Arto Valkonen − *Department of Chemistry, University of Jyväskylä, 40014 Jyväskylä, Finland;* orcid.org/0000-0003-2806-3807

Complete contact information is available at:
https://pubs.acs.org/10.1021/acs.orglett.0c02995

Notes

The authors declare no competing financial interest.

■ ACKNOWLEDGMENTS

The Academy of Finland is duly acknowledged for financial support to N.R.C. (Decisions No. 326487 and 326486) and to A. V. (No. 314343). Finnish Cultural Foundation is acknowledged for financial support to S.H. (00190336). CSC−IT Center for Science Ltd., Finland is acknowledged for the allocation of computational resources. Professor Luis F. Veiros (Centro de Química Estrutural, Instituto Superior Técnico, Universidade de Lisboa, Portugal) is acknowledged for fruitful discussions on the computational section.

■ REFERENCES

(1) (a) Brill, Z. G.; Condakes, M. L.; Ting, C. P.; Maimone, T. J. Navigating the Chiral Pool in the Total Synthesis of Complex Terpene Natural Products. *Chem. Rev.* **2017**, *117*, 11753−11795. (b) Pfaffenbach, M.; Bakanas, I.; O'Connor, N. R.; Herrick, J. L.; Sarpong, R. Total Syntheses of Xiamycins A, C, F, H and Oridamycin A and Preliminary Evaluation of their Anti-Fungal Properties. *Angew. Chem., Int. Ed.* **2019**, *58*, 15304. (c) Hu, N.; Dong, C.; Zhang, C.; Liang, G. Total Synthesis of (−)-Indoxamycins A and B. *Angew. Chem., Int. Ed.* **2019**, *58*, 6659−6662. (d) Hung, K.; Condakes, M. L.; Novaes, L. F. T.; Harwood, S. J.; Morikawa, T.; Yang, Z.; Maimone, T. J. Development of a Terpene Feedstock-Based Oxidative Synthetic Approach to the Illicium Sesquiterpenes. *J. Am. Chem. Soc.* **2019**, *141*, 3083−3099.

(2) (a) Sheldon, R. A. The Road to Biorenewables: Carbohydrates to Commodity Chemicals. *ACS Sustainable Chem. Eng.* **2018**, *6*, 4464−4480. (b) Mika, L. T.; Csefalvay, E.; Nemeth, A. Catalytic Conversion of Carbohydrates to Initial Platform Chemicals: Chemistry and Sustainability. *Chem. Rev.* **2018**, *118*, 505−613.

(3) (a) Zhang, X.; Wilson, K.; Lee, A. F. Heterogeneously Catalyzed Hydrothermal Processing of C_5-C_6 Sugars. *Chem. Rev.* **2016**, *116*, 12328−12368. (b) Gómez Millán, G.; Hellsten, S.; Llorca, J.; Luque, R.; Sixta, H.; Balu, A. M. Recent Advances in the Catalytic Production of Platform Chemicals from Holocellulosic Biomass. *ChemCatChem* **2019**, *11*, 2022−2042.

(4) Kühne, B.; Vogel, H.; Meusinger, R.; Kunz, S.; Kunz, M. Mechanistic study on − C−O− and − C−C− hydrogenolysis over Cu catalysts: identification of reaction pathways and key intermediates. *Catal. Sci. Technol.* **2018**, *8*, 755−767.

(5) (a) Brun, N.; Hesemann, P.; Esposito, D. Expanding the biomass derived chemical space. *Chem. Sci.* **2017**, *8*, 4724−4738. (b) Bender, T. A.; Dabrowski, J. A.; Gagné, M. R. Homogeneous Catalysis for the Production of Low-volume, High-value Chemicals from Biomass. *Nat. Rev. Chem.* **2018**, *2*, 35−46.

(6) (a) Yamamoto, Y.; Bajracharya, G. B.; Nogami, T.; Jin, T.; Matsuda, K.; Gevorgyan, V. Reduction of Carbonyl Function to a Methyl Group. *Synthesis* **2004**, 308−311. (b) Gevorgyan, V.; Liu, J.-X.; Rubin, M.; Benson, S.; Yamamoto, Y. A novel reduction of alcohols and ethers with a $HSiEt_3$ catalytic $B(C_6F_5)_3$ system. *Tetrahedron Lett.* **1999**, *40*, 8919−8922. (c) Gevorgyan, V. V.; Rubin, M.; Benson, S.; Liu, J. X.; Yamamoto, Y. A novel $B(C_6F_5)_3$-catalyzed reduction of alcohols and cleavage of aryl and alkyl ethers with hydrosilanes. *J. Org. Chem.* **2000** *65*, 6179−6186. (d) Gevorgyan, V.; Rubin, M.; Liu, J.-X.; Yamamoto, Y. A Direct Reduction of Aliphatic Aldehyde, Acyl Chloride, Ester, and Carboxylic Functions into a Methyl Group. *J. Org. Chem.* **2001**, *66*, 1672−1675.

(7) Adduci, L. L.; McLaughlin, M. P.; Bender, T. A.; Becker, J. J.; Gagné, M. R. Metal-Free Deoxygenation of Carbohydrates. *Angew. Chem., Int. Ed.* **2014**, *53*, 1646−1649.

(8) (a) Seo, Y.; Gagné, M. R. Positional Selectivity in the Hydrosilylative Partial Deoxygenation of Disaccharides by Boron Catalysts. *ACS Catal.* **2018**, *8*, 81−85. (b) Hein, N. M.; Seo, Y.; Lee, S. J.; Gagné, M. R. Harnessing the reactivity of poly-(methylhydrosiloxane) for the reduction and cyclization of biomass to high-value products. *Green Chem.* **2019**, *21*, 2662−2669. (c) Adduci, L. L.; Bender, T. A.; Dabrowski, J. A.; Gagné, M. R. Chemoselective Conversion of Biologically Sourced Polyols into Chiral Synthons. *Nat. Chem.* **2015**, *7*, 576−581.

(9) (a) Parks, D. J.; Piers, W. E.; Yap, G. P. A. Synthesis, Properties, and Hydroboration Activity of the Highly Electrophilic Borane Bis(pentafluorophenyl)borane, $HB(C_6F_5)_2$. *Organometallics* **1998**, *17*, 5492−5503. (b) Parks, D. J.; von H. Spence, R. E.; Piers, W. E. Bis(pentafluorophenyl)borane: Synthesis, Properties, and Hydroboration Chemistry of a Highly Electrophilic Borane Reagent. *Angew. Chem., Int. Ed. Engl.* **1995**, *34*, 809−811. (c) Zhang, J.; Park, S.; Chang, S. Selective C-O Bond Cleavage of Sugars with Hydrosilanes Catalyzed by Piers' Borane Generated In Situ. *Angew. Chem., Int. Ed.* **2017**, *56*, 13757−13761.

(10) Seo, Y.; Lowe, J. M.; Gagné, M. R. Controlling Sugar Deoxygenation Products from Biomass by Choice of Fluoroarylborane Catalyst. *ACS Catal.* **2019**, *9*, 6648−6652.

(11) Seo, Y.; Gagné, M. R. Silylium (R_3Si^+) Catalyzed Condensative Cyclization for Anhydrosugar Synthesis. *ACS Catal.* **2018**, *8*, 6993−6999.

(12) Patrick, E. A.; Piers, W. E. Twenty-five years of bis-pentafluorophenyl borane: a versatile reagent for catalyst and materials synthesis. *Chem. Commun.* **2020**, *56*, 841−853.

(13) Lowe, J. M.; Seo, Y.; Gagné, M. R. Boron-Catalyzed Site-Selective Reduction of Carbohydrate Derivatives with Catecholborane. *ACS Catal.* **2018**, *8*, 8192−8198.

(14) Drosos, N.; Morandi, B. Boron-Catalyzed Regioselective Deoxygenation of Terminal 1,2-Diols to 2-Alkanols Enabled by the Strategic Formation of a Cyclic Siloxane Intermediate. *Angew. Chem., Int. Ed.* **2015**, *54*, 8814−8818.

(15) Chatterjee, I.; Porwal, D.; Oestreich, M. $B(C_6F_5)_3$-Catalyzed Chemoselective Defunctionalization of Ether-Containing Primary Alkyl Tosylates with Hydrosilanes. *Angew. Chem., Int. Ed.* **2017**, *56*, 3389−3391.

(16) Drosos, N.; Cheng, G. J.; Ozkal, E.; Cacherat, B.; Thiel, W.; Morandi, B. Catalytic Reductive Pinacol-Type Rearrangement of Unactivated 1,2-Diols through a Concerted, Stereoinvertive Mechanism. *Angew. Chem., Int. Ed.* **2017**, *56*, 13377−13381.

(17) The regioselective silyloxonium opening was reported to occur when using Piers borane: Zhang, J.; Park, S.; Chang, S. Piers' Borane-Mediated Hydrosilylation of Epoxides and Cyclic Ethers. *Chem. Commun.* **2018**, *54*, 7243−7246.

(18) Bender, T. A.; Dabrowski, J. A.; Zhong, H.; Gagné, M. R. Diastereoselective $B(C_6F_5)_3$-Catalyzed Reductive Carbocyclization of Unsaturated Carbohydrates. *Org. Lett.* **2016**, *18*, 4120−4123.

(19) For selected examples on the use of chiral synthons, from carbohydrates: (a) Lin, S.; Guo, X.; Qin, K.; Feng, L.; Zhang, Y.; Tang, Y. Efficient Production of Biomass-Derived C4 Chiral Synthons in Aqueous Solution. *ChemCatChem* **2017**, *9*, 4179−4184. (b) Hollingsworth, R. I.; Wang, G. Toward a Carbohydrate-Based Chemistry: Progress in the Development of General-Purpose Chiral Synthons from Carbohydrates. *Chem. Rev.* **2000**, *100*, 4267−4282. (c) Ramesh, N. G.; Balasubramanian, K. K. 2-C-Formyl Glycals: Emerging Chiral Synthons in Organic Synthesis. *Eur. J. Org. Chem.* **2003**, *2003*, 4477−4487. (d) Cairns, R.; Gomm, A.; Ryan, J.; Clarke, T.; Kulcinskaja, E.; Butler, K.; O'Reilly, E. Conversion of Aldoses to Valuable ω-Amino Alcohols Using Amine Transaminase Biocatalysts. *ACS Catal.* **2019**, *9*, 1220−1223. From noncarbohydrates: (e) Hoffmann, R. W. meso Compounds: stepchildren or favored children of stereoselective synthesis? *Angew. Chem., Int. Ed.* **2003**, *42*, 1096−1109. (f) Guo, C.; Saifuddin, M.; Saravanan, T.; Sharifi, M.; Poelarends, G. J.

Biocatalytic Asymmetric Michael Additions of Nitromethane to α,β-Unsaturated Aldehydes via Enzyme-bound Iminium Ion Intermediates. *ACS Catal.* **2019**, *9*, 4369−4373. (g) Brenna, E.; Crotti, M.; Gatti, F. G.; Monti, D.; Parmeggiani, F.; Santangelo, S. Asymmetric Bioreduction of β-Acylaminonitroalkenes: Easy Access to Chiral Building Blocks with Two Vicinal Nitrogen-Containing Functional Groups. *ChemCatChem* **2017**, *9*, 2480−2487. (h) Chen, Y. H.; McDonald, F. E. New chiral synthons for efficient introduction of bispropionates via stereospecific oxonia-cope rearrangements. *J. Am. Chem. Soc.* **2006**, *128*, 4568−4569. (i) Hudlicky, T.; Thorpe, A. J. Current status and future perspectives of cyclohexadiene-*cis*-diols in organic synthesis: versatile intermediates in the concise design of natural products. *Chem. Commun.* **1996**, 1993−2000. (j) Padarti, A.; Han, H. Rationally Designed Chiral Synthons Enabling Asymmetric Z- and E-Selective Vinylogous Aldol Reactions of Aldehydes. *Org. Lett.* **2018**, *20*, 1448−1452.

(20) Arceo, E.; Ellman, J. A.; Bergman, R. G. A direct, biomass-based synthesis of benzoic acid: formic acid-mediated deoxygenation of the glucose-derived materials quinic acid and shikimic acid. *ChemSusChem* **2010**, *3*, 811−813.

(21) (a) Assoah, B.; Veiros, L. F.; Afonso, C. A. M.; Candeias, N. R. Biomass-Based and Oxidant-Free Preparation of Hydroquinone from Quinic Acid. *Eur. J. Org. Chem.* **2016**, *2016*, 3856−3861. (b) Ran, N.; Knop, D. R.; Draths, K. M.; Frost, J. W. Benzene-Free Synthesis of Hydroquinone. *J. Am. Chem. Soc.* **2001**, *123*, 10927−10934.

(22) Pfennig, T.; Carraher, J. M.; Chemburkar, A.; Johnson, R. L.; Anderson, A. T.; Tessonnier, J.-P.; Neurock, M.; Shanks, B. H. A new selective route towards benzoic acid and derivatives from biomass-derived coumalic acid. *Green Chem.* **2017**, *19*, 4879−4888.

(23) (a) Enev, V. *2.11 Chiral Pool Synthesis: Chiral Pool Synthesis from Quinic Acid In Comprehensive Chirality*; Carreira, E. M., Yamamoto, H., Eds.; Elsevier: Amsterdam, 2012; pp 325−345. (b) Barco, A.; Benetti, S.; Risi, C. D.; Marchetti, P.; Pollini, G. P.; Zanirato, V. D-(−)-Quinic acid: a chiron store for natural product synthesis. *Tetrahedron: Asymmetry* **1997**, *8*, 3515−3545. (c) Mulzer, J.; Drescher, M.; Enev, V. S. Quinic Acid as Versatile Chiral Scaffold in Organic Synthesis. *Curr. Org. Chem.* **2008**, *12*, 1613−1630.

(24) Candeias, N. R.; Assoah, B.; Simeonov, S. P. Production and Synthetic Modifications of Shikimic Acid. *Chem. Rev.* **2018**, *118*, 10458−10550.

(25) (a) Wianowska, D.; Gil, M. Recent advances in extraction and analysis procedures of natural chlorogenic acids. *Phytochem. Rev.* **2019**, *18*, 273−302. (b) Clifford, M. N.; Jaganath, I. B.; Ludwig, I. A.; Crozier, A. Chlorogenic acids and the acyl-quinic acids: discovery, biosynthesis, bioavailability and bioactivity. *Nat. Prod. Rep.* **2017**, *34*, 1391−1421. (c) Yuda, N.; Tanaka, M.; Suzuki, M.; Asano, Y.; Ochi, H.; Iwatsuki, K. Polyphenols extracted from black tea (*Camellia sinensis*) residue by hot-compressed water and their inhibitory effect on pancreatic lipase in vitro. *J. Food Sci.* **2012**, *77*, H254−261. (d) Grunovaitė, L.; Pukalskienė, M.; Pukalskas, A.; Venskutonis, P. R. Fractionation of black chokeberry pomace into functional ingredients using high pressure extraction methods and evaluation of their antioxidant capacity and chemical composition. *J. Funct. Foods* **2016**, *24*, 85−96. (e) Wang, J.; Lu, D.; Sun, Q.; Zhao, H.; Ling, X.; Ouyang, P. Reactive extraction and recovery of mono-caffeoylquinic acids from tobacco wastes by trialkylphosphine oxide. *Chem. Eng. Sci.* **2012**, *78*, 53−62. (f) Santana-Méridas, O.; González-Coloma, A.; Sánchez-Vioque, R. Agricultural residues as a source of bioactive natural products. *Phytochem. Rev.* **2012**, *11*, 447−466.

(26) For the synthesis of unprotected derivative, see: Gorin, P. A. J. Replacement Reactions in the Quinic Acid Series. *Can. J. Chem.* **1963**, *41*, 2417−2423.

(27) (a) Benhamou, L.; Foster, R. W.; Ward, D. P.; Wheelhouse, K.; Sloan, L.; Tame, C. J.; Bučar, D.-K.; Lye, G. J.; Hailes, H. C.; Sheppard, T. D. Functionalised tetrahydrofuran fragments from carbohydrates or sugar beet pulp biomass. *Green Chem.* **2019**, *21*, 2035−2042. (b) Foster, R. W.; Tame, C. J.; Bucar, D. K.; Hailes, H. C.; Sheppard, T. D. Sustainable Synthesis of Chiral Tetrahydrofurans through the Selective Dehydration of Pentoses. *Chem. - Eur. J.* **2015**, *21*, 15947−15950. (c) Monasterolo, C.; Muller-Bunz, H.; Gilheany, D. G. Very short highly enantioselective Grignard synthesis of 2,2-disubstituted tetrahydrofurans and tetrahydropyrans. *Chem. Sci.* **2019**, *10*, 6531−6538.

(28) Reddy, L. V.; Kumar, V.; Sagar, R.; Shaw, A. K. Glycal-derived D-hydroxy a,b-unsaturated aldehydes (Perlin aldehydes): versatile building blocks in organic synthesis. *Chem. Rev.* **2013**, *113*, 3605−3631.

(29) (a) Tavassoli, A.; Duffy, J. E.; Young, D. W. Synthesis of trimethyl (2*S*,3*R*)- and (2*R*,3*R*)-[2-$^2H_1$]-homocitrates and dimethyl (2*S*,3*R*)- and (2*R*,3*R*)-[2-$^2H_1$]-homocitrate lactones-an assay for the stereochemical outcome of the reaction catalysed both by homocitrate synthase and by the Nif-V protein. *Org. Biomol. Chem.* **2006**, *4*, 569−580. (b) Tavassoli, A.; Duffy, J. E. S.; Young, D. W. Synthesis of trimethyl (2*S*,3*R*)- and (2*R*,3*R*)-[2-$^2H_1$]-homocitrates and the corresponding dimethyl ester lactones—towards elucidating the stereochemistry of the reaction catalysed by homocitrate synthase and by the Nif-V protein. *Tetrahedron Lett.* **2005**, *46*, 2093−2096.

(30) Pansare, S. V.; Adsool, V. A. Enantioselective synthesis of (*R*)-homocitric acid lactone. *Tetrahedron Lett.* **2007**, *48*, 7099−7101.

(31) 1,2-Hydride shifts triggered by boron Lewis acids have been explored in 1,1-carboborations: (a) Chen, C.; Voss, T.; Frohlich, R.; Kehr, G.; Erker, G. 1,1-carboboration of 1-alkynes: a conceptual alternative to the hydroboration reaction. *Org. Lett.* **2011**, *13*, 62−65. (b) Kehr, G.; Erker, G. 1,1-Carboboration. *Chem. Commun.* **2012**, *48*, 1839−1850. (c) Hansmann, M. M.; Melen, R. L.; Rudolph, M.; Rominger, F.; Wadepohl, H.; Stephan, D. W.; Hashmi, A. S. Cyclopropanation/Carboboration Reactions of Enynes with B-$(C_6F_5)_3$. *J. Am. Chem. Soc.* **2015**, *137*, 15469−15477.

(32) Parr, R. G.; Yang, W. *Density Functional Theory of Atoms and Molecules*; Oxford University Press: New York, 1989.

PUBLICATION
II

O,O-Silyl Group Migrations in Quinic Acid Derivatives: An Opportunity for Divergent Synthesis

Suvi Holmstedt, Alexander Efimov, Nuno R. Candeias

Organic Letters, **2021**, *23*, 3083–3087.
DOI: 10.1021/acs.orglett.1c00755

Publication reprinted with the permission of ACS Publications.

Organic Letters

pubs.acs.org/OrgLett

Letter

O,O-Silyl Group Migrations in Quinic Acid Derivatives: An Opportunity for Divergent Synthesis

Suvi Holmstedt,* Alexander Efimov, and Nuno R. Candeias*

Cite This: *Org. Lett.* 2021, 23, 3083−3087

Read Online

ACCESS | Metrics & More | Article Recommendations | Supporting Information

Downloaded via TAMPERE UNIV on May 3, 2021 at 05:49:01 (UTC).
See https://pubs.acs.org/sharingguidelines for options on how to legitimately share published articles.

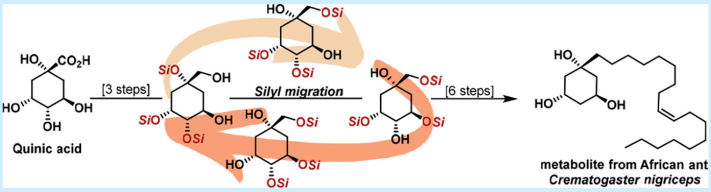

ABSTRACT: The *O*,*O*-silyl group migrations on a quinic acid-derived cyclitol have been studied, and the ease of migration was observed to be dependent on the silicon substituents and reaction conditions. Conditions were found to improve the formation of a main isomer during the *O*,*O*-silyl group migrations that could be integrated into the formal synthesis of vitamin D receptor modulator VS-105 and in the first total synthesis of a metabolite from the African ant *Crematogaster nigriceps*.

The chiron approach in organic synthesis enables the planning of concise and efficient routes toward stereoselective total syntheses of natural products by recognition of the chiral substructures as fragments of the target molecule.[1] The advantages of using chiral building blocks from nature are numerous, particularly because of the diversity of carbon frameworks containing specific stereochemistries as well as the global need of decreasing the use of carbon from nonrenewable fossil resources.[2] Notwithstanding the high synthetic value of chiral carbohydrates and derived polyols, their usage is often disadvantageous because the use of protecting groups is required to allow differentiation in the reactivity of hydroxy groups.[3] While strategies for segregating the reactivity of similar functionalities are limited, such a problem is often obviated by exploring the selective protection of functional groups and functional group rearrangement (i.e., migration).[3d,4]

Silyl ethers are commonly used as protecting groups of alcohols to suppress their reactivity.[5] Moreover, the steric and electronic properties of the silyl ether molecule, and subsequently their reactivity, are dependent on the silyl group employed.[5a,6] Thus, despite the emerging trend of protecting group-free syntheses,[7] the use of such a tool can occasionally warrant structural diversification, especially when considering the vast knowledge gathered about the selective formation[4b,8] and cleavage[9] of silyl ethers. Although relatively stable in basic media, silyl ethers vicinal to a hydroxy group can undergo 1,4-*O*,*O*-silyl migration in good yields. This can proceed via a putative pentacoordinate intermediate formed upon alkoxide attack to silicon,[10] which seems to be hampered under Luche reduction conditions.[11] Such a type of migration in carbohydrates and derivatives is widely acknowledged.[12]

Despite its common occurrence in carbohydrates, only a few of the reported 1,4-*O*,*O*-silyl migrations have been methodically studied.[13] The regioselectivity of reactions of α-D-pyranosides with *tert*-butyldimethylsilyl (TBDMS) and *tert*-butyldiphenylsilyl (TBDPS) chlorides was observed to be dependent on the reaction conditions. The combination of imidazole in DMF promotes *O*,*O*-silyl migrations under kinetic control and does not result in the formation of the most stable regioisomer, while harder bases change the isomer distribution profile (Scheme 1a).[13b] Similar intramolecular silyl migrations under basic conditions have also been observed for polyols (Scheme 1b),[14] although in acyclic systems the 1,5-*O*,*O*-silyl migration competes with the 1,4-migratory process.[15] Besides carbohydrates and their derivatives, the *O*,*O*-silyl group migration in cyclic systems has been somewhat overlooked. Ferrero and coworkers reported the occasionally competitive 1,4-*O*,*O*-silyl migration during a Colvin rearrangement step in the synthesis of a pre-vitamin D_3 analogue from shikimic acid (Scheme 1c).[16] The fluctuating regioselectivities were attributed to the different batches of *n*-BuLi, containing different amounts of lithium hydroxide.

During our previous studies of the modification of quinic acid,[17] when attempting to convert a primary hydroxyl function of trisilylated quinic alcohol **1** into a sulfonate moiety, we

Received: March 4, 2021
Published: April 7, 2021

© 2021 American Chemical Society

Scheme 1. *O*,*O*-Silyl Migrations in Polyols

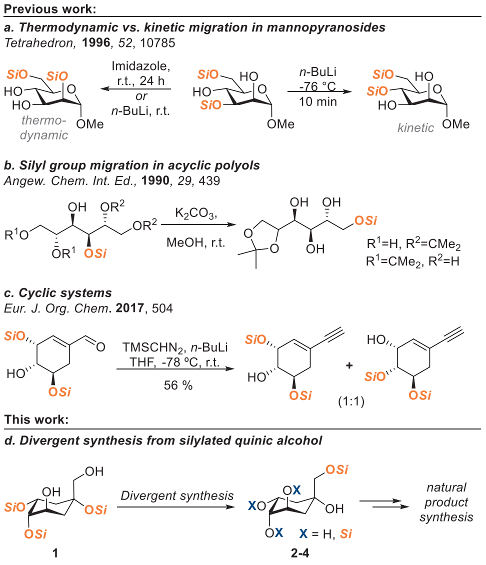
Previous work:
a. Thermodynamic vs. kinetic migration in mannopyranosides
Tetrahedron, 1996, 52, 10785
Imidazole, r.t., 24 h
or
n-BuLi, r.t.
n-BuLi
-76 °C
10 min
thermo-dynamic
kinetic
OMe
b. Silyl group migration in acyclic polyols
Angew. Chem. Int. Ed., 1990, 29, 439
K2CO3,
MeOH, r.t.
R1=H, R2=CMe2
R1=CMe2, R2=H
c. Cyclic systems
Eur. J. Org. Chem. 2017, 504
TMSCHN2, n-BuLi
THF, -78 °C, r.t.
56 %
(1:1)
This work:
d. Divergent synthesis from silylated quinic alcohol
Divergent synthesis
X = H, Si
natural product synthesis
1
2-4

observed multiple silyl migrations as an untraceable mixture of products. Considering that the diversification of a common precursor into several synthetic intermediates is a powerful tool for synthesizing molecules otherwise difficult or impossible to reach, and the limited number of studies on the *O*-silyl migration in carbacyles, we set out to improve the selectivity of the migration process (Scheme 1d). This approach would provide us synthetically rich intermediates in a divergent synthesis strategy.[18]

To study the silyl group migration reaction in quinic acid derivatives, trisilylated diols **1a** and **1b** were synthesized and subjected to different bases and solvents (Table 1). We were pleased to notice the exclusive formation of **2**, regardless of the different silyl ethers, upon treatment with imidazole as a base for 6 h (Table 1, entry 1). Intriguingly, when attempting to push the secondary → secondary *O*,*O*-silyl migration (5-*O* → 4-*O*) by increasing the reaction time and increasing the amount of imidazole, we found the migration took place with a TBPDS-protected derivative while no **3b** or **4b** was detected with the less bulky TBDMS group (entry 2). While targeting a better selectivity toward **3** or **4**, we screened other bases (entries 3−6). DMAP was also able to provide isomer **2a** from TBDPS-protected derivative **1a**, but TBDMS congener **1b** underwent migration in only 20% to the corresponding isomer **2b** (entry 3). Surprisingly, the use of stronger base Et_3N proved futile with the exclusive isolation of recovered starting material (entry 4). Treatment of **1a** with even stronger bases KHMDS and NaH promoted the formation of both 4-*O*-TBDPS-protected isomers **3a** and **4a** (entries 5 and 6, respectively), although in lower overall yield compared to that with prolonged use of imidazole (entry 2). Sodium hydride has been previously used in silyl migrations of sugar derivatives with great overall yields, though full selectivity has not been reached.[12b,19] Decreasing the temperature when using NaH, to minimize the formation of other unknown side products, did not return the desired isomers (data not shown). Replacement of THF with toluene (entry 7) allowed some formation of **3a** together with **4a**, and the selectivity toward the former was greatly improved by elongating the reaction time and increasing the amount of base (entry 8). Although **3a** could be obtained in 78% yield, the analogous reaction from the TBDMS derivative returned only 25% of **3b** and traces of **4b**, clearly indicating the importance of the silane substituents on the migratory process. A further increase in the temperature using DMF as a solvent (entry 9) resulted in the formation of **4a** in higher yield but still in moderate

Table 1. Optimization of Silyl Migration

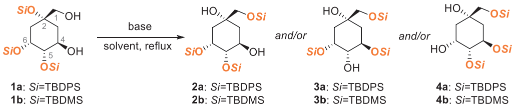
base
solvent, reflux
and/or
and/or
1a: Si=TBDPS
1b: Si=TBDMS
2a: Si=TBDPS
2b: Si=TBDMS
3a: Si=TBDPS
3b: Si=TBDMS
4a: Si=TBDPS
4b: Si=TBDMS

				Si=TBDPS[b]			Si=TBDMS[b]		
entry[a]	solvent	base (equiv)	time (h)	2a	3a	4a	2b	3b	4b
1[c]	THF	imidazole (2.0)	6	95	nd[h]	nd[h]	95	nd[h]	nd[h]
2	THF	imidazole (3.0)	72	14	63	23	92	nd[h]	nd[h]
3	THF	DMAP (2.0)	18	81	trace	nd[h]	20	nd[h]	nd[h]
4	THF	Et_3N (2.0)	18	trace	nd[h]	nd[h]	nd[h]	nd[h]	nd[h]
5	THF	KHMDS (2.0)	18	trace	51	15	–	–	–
6	THF	NaH (3.0)	18	trace	57	17	–	–	–
7[d]	toluene	imidazole (2.0)	6	93	7	trace	99	nd[h]	nd[h]
8[d]	toluene	imidazole (5.0)	56	trace	78	16	66	25	trace
9[e]	DMF	imidazole (2.0)	18	5	62	33	–	–	–
10[d,f]	MeOH	Et_3N (1.0)	18	98	nd[h]	nd[h]	>99	nd[h]	nd[h]
11[d]	MeOH	imidazole (2.0)	18	78	11	trace	–	–	–
12	MeOH	DMAP (2.0)	18	trace	65	28	82	12	trace
13[g]	MeOH	imidazole (2.0) and Et_3N (2.0)	18	5 (trace)	56 (50)	29 (35)	68 (14)	22 (49)	8 (27)

[a] All reactions were carried out at 0.2 M **1** at refluxing temperature, except indicated otherwise. [b] Isolated yield. [c] With 0.4 M substrate. [d] With 0.1 M substrate. [e] Carried out at 120 °C. [f] Carried out at room temperature. [g] The results from a reaction in a sealed tube at 100 °C are shown in parentheses. [h] Not detected.

regioselectivity. Using methanol as a solvent together with Et_3N resulted in room-temperature selective 2-*O*- → 1-*O*-silyl group migration to primary silyl ethers **2a** and **2b** (entry 10), in contrast with the lack of reactivity observed in refluxing THF (entry 4). Notably, **3** and **4** were not observed under these conditions, although secondary → secondary silyl migration was reported for nucleosides.[20] Invigorated by this, we tested other bases with MeOH (entries 11−13), allowing the formation of **4** in moderate yields (**4a**, 35%; **4b**, 27%) using a combination of bases in a sealed tube (entry 13).

In contrast to the facile 2-*O* → 1-*O* silyl group migration to form **2a**, the migrations within the six-membered ring required harsher reaction conditions and were never observed in the absence of tertiary → primary migration. A more difficult 5-*O*- → 4-*O*-silyl group migration would be expected given the relative *trans* position of the oxygen atoms. This aspect was confirmed by a careful NMR analysis of NOESY and other multidimensional experiments of TBDPS-containing compounds **1a**−**4a** in DMSO-d_6 (Scheme 2; also see the Supporting Information). The spectra of **2a** and **3a** point to a preferable conformation in which the primary silyl ether occupies axial positions, thus requiring interconversion to a more suitable conformation for the migration to take place (Scheme 2b).

Scheme 2. Selected ^{1}H NMR Data of TBDPS Derivatives

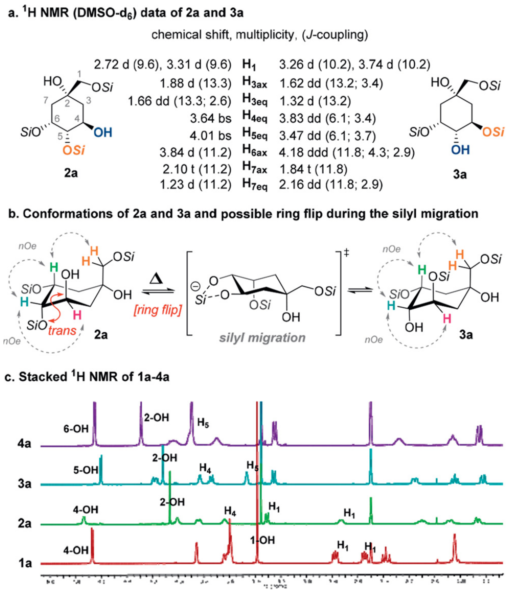
a. ¹H NMR (DMSO-d₆) data of 2a and 3a
chemical shift, multiplicity, (J-coupling)
2.72 d (9.6), 3.31 d (9.6) H₁ 3.26 d (10.2), 3.74 d (10.2)
1.88 d (13.3) H₃ₐₓ 1.62 dd (13.2; 3.4)
1.66 dd (13.3; 2.6) H₃ₑq 1.32 d (13.2)
3.64 bs H₄ₑq 3.83 dd (6.1; 3.4)
4.01 bs H₅ₑq 3.47 dd (6.1; 3.7)
3.84 d (11.2) H₆ₐₓ 4.18 ddd (11.8; 4.3; 2.9)
2.10 t (11.2) H₇ₐₓ 1.84 t (11.8)
1.23 d (11.2) H₇ₑq 2.16 dd (11.8; 2.9)
HO
OSi
SiO
OH
OSi
1
2
3
4
5
6
7
2a
3a
b. Conformations of 2a and 3a and possible ring flip during the silyl migration
nOe
H
OH
trans
Δ
[ring flip]
Si
silyl migration
‡
c. Stacked ¹H NMR of 1a-4a
4a
3a
2a
1a
6-OH
2-OH
H₅
5-OH
H₄
H₁
4-OH
1-OH

Having in hand suitable conditions for the formation of regioisomers **2**−**4**, we envisioned their suitability for divergent synthesis approaches. The structural similarities between **2** and **4** and biologically relevant compounds are evident. For instance, their oxidized forms could be useful in the preparation of carbasugars,[21] the ketonic form of **2** could become a synthetic intermediate in the recent synthesis of (−)-pseudohygrophorones,[22] while the deoxygenation of **4** could provide the unusual hydroxylated ring of hydroisoflavone B.[23] Despite such possibilities, we decided to explore regioisomer **3a** in divergent synthesis by changing the oxidation state of C-5 (Scheme 3).

Scheme 3. Divergent Modification of 3a and Preparation of the VS-105 Precursor

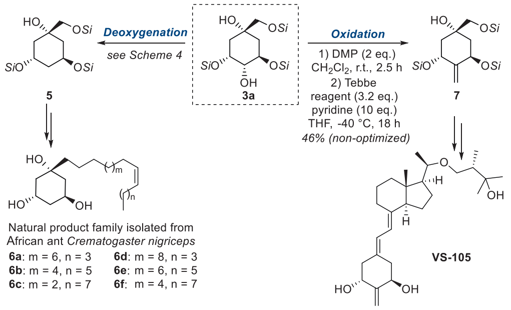
HO
OSi
SiO
Deoxygenation
see Scheme 4
OH
5
3a
Oxidation
1) DMP (2 eq.)
CH₂Cl₂, r.t., 2.5 h
2) Tebbe reagent (3.2 eq.)
pyridine (10 eq.)
THF, -40 °C, 18 h
46% (non-optimized)
7
m
n
Natural product family isolated from African ant Crematogaster nigriceps
6a: m = 6, n = 3
6b: m = 4, n = 5
6c: m = 2, n = 7
6d: m = 8, n = 3
6e: m = 6, n = 5
6f: m = 4, n = 7
O
H
VS-105

Such a strategy would provide us the possibility of preparing compound **7**, a synthetic intermediate of the vitamin D receptor agonist VS-105 (a kidney disease drug that completed phase 1 clinical trials),[24] and performing the first total synthesis of a metabolite isolated from the African ant *Crematogaster nigriceps*. These ants were found to produce a family of 1-alk(en)yl-1,3,5-trihydroxycyclohexanes (**6a**−**6f**), isolated and characterized by Braekman et al.[25] The long carbon chains of natural products **6a**−**6f** are derived from common fatty acids and have a mutual cyclitol backbone that could be built from **3a** after deoxygenation into **5** and further synthetic manipulation.

Gladly, the Dess−Martin periodinane oxidation of **3a** gave ketone in an excellent 98% yield, which was further transformed into exocyclic alkene **7** using Tebbe's reagent (Scheme 3). The olefination took place despite the congestion around the secondary alcohol caused by the TBDPS groups, similar to the reported olefination of the TBDMS-protected quinic acid ester derivative.[26]

We envisioned that the syntheses of the family of natural products **6** could be easily achieved by selective epoxide opening of key intermediate **10** with an organometallic reagent derived from the corresponding fatty acid, after deoxygenation of **3a** (Scheme 4a). To avoid regio- and diastereoselective issues in the opening of a cyclic siloxonium ion, we decided to proceed with the Barton−McCombie deoxygenation of **3a** instead of using the previously explored borane-catalyzed deoxygenation with hydrosilanes.[17]

The introduction of the *O*-thiocarbonyl group proved to be challenging due to the required use of a base and subsequent *O*,*O*-silyl group migrations. After failed attempts in preparing the thiocarbonylimidazolide or methyl xanthate from **3a**, phenyl thionocarbonate **8** could be prepared in 89% yield (Scheme 4b) due to the high electrophilicity of phenyl chlorothionocarbonate.

Alcohol **5** was cleanly obtained in 91% yield after Barton−McCombie deoxygenation. Despite the myriad of conditions tested for the selective deprotection of the primary TBDPS group in **5**, cleavage of the secondary silyl ether was always observed. Treatment of **5** with excess acetyl chloride provided alcohol **9a**; its structure was elucidated from NOE contacts between the secondary and tertiary hydroxy groups. The use of 2 equiv of TBAF promoted the secondary and primary TBDPS group cleavage to **9b** in 92% yield. Chemoselective mesylation of the primary alcohol over secondary and tertiary hydroxy groups of triol **9b** followed by treatment with DBU for intramolecular S_N reaction resulted in the formation of epoxide **10**, a key

Scheme 4. Synthesis of the Oleyl Derivative of a Trihydroxycyclohexane Metabolite from the African Ant *C. nigriceps*

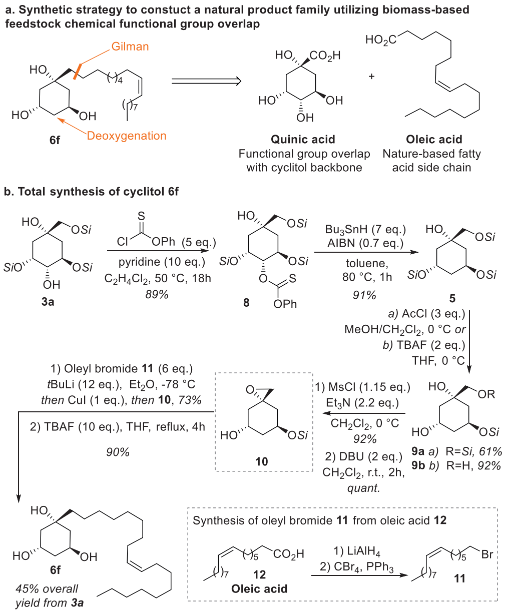
a. Synthetic strategy to constuct a natural product family utilizing biomass-based feedstock chemical functional group overlap
Gilman
HO
HO
OH
6f
Deoxygenation
Quinic acid
Functional group overlap with cyclitol backbone
Oleic acid
Nature-based fatty acid side chain
b. Total synthesis of cyclitol 6f
3a
Cl OPh (5 eq.)
pyridine (10 eq.)
C2H4Cl2, 50 °C, 18h
89%
8
Bu3SnH (7 eq.)
AIBN (0.7 eq.)
toluene, 80 °C, 1h
91%
5
a) AcCl (3 eq.) MeOH/CH2Cl2, 0 °C or
b) TBAF (2 eq.) THF, 0 °C
9a a) R=Si, 61%
9b b) R=H, 92%
1) MsCl (1.15 eq.) Et3N (2.2 eq.) CH2Cl2, 0 °C 92%
2) DBU (2 eq.) CH2Cl2, r.t., 2h, quant.
10
1) Oleyl bromide 11 (6 eq.) tBuLi (12 eq.), Et2O, -78 °C then CuI (1 eq.), then 10, 73%
2) TBAF (10 eq.), THF, reflux, 4h
90%
6f
45% overall yield from 3a
Synthesis of oleyl bromide 11 from oleic acid 12
12
Oleic acid
1) LiAlH4
2) CBr4, PPh3
11

intermediate in the synthesis of the 1-alk(en)yl-1,3,5-trihydroxycyclohexane **6** metabolite family. This synthetic approach was showcased for the preparation of oleic acid derivative **6f**. Hence, oleic acid was reduced to the corresponding alcohol with $LiAlH_4$ followed by conversion of alkyl bromide **11** through Appel reaction, as previously reported.[27] After unsuccessful attempts to open the epoxide with the organomagnesium compound, the *in situ* generation of a Gilman reagent by treatment of **11** with *t*-BuLi followed by addition of CuI promoted the desired formation of the tertiary alcohol in 73% yield. Cleaving the secondary TBDPS group led to the formation of African ant cyclitol **6f** in 90% yield, and its structure was verified by comparison with previously reported data of the isolated natural product.

In summary, we herein present the protecting group migrations across a quinic acid-derived cyclitol backbone, as an opportunity for the diverse syntheses of high-value-added molecules. The ease of *O,O*-silyl group migration was observed to depend on the silicon substituents in the cyclitol system, with the TBDPS more easily migrating than the less bulky TBDMS. The diol obtained after 2-*O*- → 1-*O*- and 5-*O*- → 4-*O*-silyl group migration from easily accessible **1a** was incorporated in the first total synthesis of a metabolite from the African ant *C. nigriceps* in 45% overall yield (10 steps, 34% overall yield from quinic acid).

■ ASSOCIATED CONTENT

Supporting Information

The Supporting Information is available free of charge at https://pubs.acs.org/doi/10.1021/acs.orglett.1c00755.

Experimental details and characterization data of all synthetic intermediates and ^1H and ^{13}C NMR copies of spectra for all reported compounds (PDF)

■ AUTHOR INFORMATION

Corresponding Authors

Suvi Holmstedt − *Faculty of Engineering and Natural Sciences, Tampere University, 33101 Tampere, Finland;* orcid.org/0000-0003-0479-3629; Email: suvi.holmstedt@tuni.fi

Nuno R. Candeias − *Faculty of Engineering and Natural Sciences, Tampere University, 33101 Tampere, Finland; LAQV-REQUIMTE, Department of Chemistry, University of Aveiro, 3810-193 Aveiro, Portugal;* orcid.org/0000-0003-2414-9064; Email: ncandeias@ua.pt

Author

Alexander Efimov − *Faculty of Engineering and Natural Sciences, Tampere University, 33101 Tampere, Finland;* orcid.org/0000-0003-4671-3009

Complete contact information is available at: https://pubs.acs.org/10.1021/acs.orglett.1c00755

Notes

The authors declare no competing financial interest.

■ ACKNOWLEDGMENTS

The Academy of Finland (Decisions 326487, 326486, and 326416) and Fundação para a Ciência e Tecnologia (PTDC/QUI-QOR/1131/2020 and CEE-CINST/2018) are acknowledged for financial support. The Finnish Cultural Foundation (00190336) is acknowledged for a grant to S.H.

■ REFERENCES

(1) (a) Hanessian, S. *Total synthesis of natural products, the "Chiron" approach*, 1st ed.; Pergamon Press: Oxford, U.K., 1983; p xvii, 291. (b) Hanessian, S.; Giroux, S.; Merner, B. L. *Design and Strategy in Organic Synthesis: From the Chiron Approach to Catalysis*; Wiley-VCH, 2013; p 822.

(2) (a) Zimmerman, J. B.; Anastas, P. T.; Erythropel, H. C.; Leitner, W. Designing for a green chemistry future. *Science* **2020**, *367*, 397−400. (b) Mika, L. T.; Csefalvay, E.; Nemeth, A. Catalytic Conversion of Carbohydrates to Initial Platform Chemicals: Chemistry and Sustainability. *Chem. Rev.* **2018**, *118*, 505−613. (c) Luterbacher, J. S.; Martin Alonso, D.; Dumesic, J. A. Targeted chemical upgrading of lignocellulosic biomass to platform molecules. *Green Chem.* **2014**, *16*, 4816−4838. (d) Sheldon, R. A. Green and sustainable manufacture of chemicals from biomass: state of the art. *Green Chem.* **2014**, *16*, 950−963. (e) Tuck, C. O.; Perez, E.; Horvath, I. T.; Sheldon, R. A.; Poliakoff, M. Valorization of biomass: deriving more value from waste. *Science* **2012**, *337*, 695−699.

(3) (a) Báti, G.; He, J. X.; Pal, K. B.; Liu, X. W. Stereo- and regioselective glycosylation with protection-less sugar derivatives: An alluring strategy to access glycans and natural products. *Chem. Soc. Rev.* **2019**, *48*, 4006−4018. (b) Kulkarni, S. S.; Wang, C. C.; Sabbavarapu, N. M.; Podilapu, A. R.; Liao, P. H.; Hung, S. C. "One-Pot" Protection, Glycosylation, and Protection-Glycosylation Strategies of Carbohydrates. *Chem. Rev.* **2018**, *118*, 8025−8104. (c) Hung, S.-C.; Wang, C.-C. Protecting Group Strategies in Carbohydrate Synthesis. *Glycochemical Synthesis* **2016**, 35−68. (d) Ren, B.; Rahm, M.; Zhang, X. L.; Zhou, Y. X.; Dong, H. Regioselective Acetylation of Diols and Polyols by Acetate Catalysis: Mechanism and Application. *J. Org. Chem.* **2014**, *79*, 8134−8142.

(4) (a) Lv, J.; Liu, Y.; Zhu, J. J.; Zou, D. P.; Dong, H. Regio/site-selective alkylation of substrates containing a cis-, 1,2-or 1,3-diol with ferric chloride and dipivaloylmethane as the catalytic system. *Green Chem.* **2020**, *22*, 1139−1144. (b) Lv, J.; Luo, T.; Zou, D.; Dong, H. Using DMF as Both a Catalyst and Cosolvent for the Regioselective Silylation of Polyols and Diols. *Eur. J. Org. Chem.* **2019**, *2019*, 6383−6395. (c) Ren, B.; Zhang, L.; Zhang, M. Progress on Selective Acylation

of Carbohydrate Hydroxyl Groups. *Asian J. Org. Chem.* **2019**, *8*, 1813−1823. (d) Xu, H. F.; Lu, Y. C.; Zhou, Y. X.; Ren, B.; Pei, Y. X.; Dong, H.; Pei, Z. C. Regioselective Benzylation of Diols and Polyols by Catalytic Amounts of an Organotin Reagent. *Adv. Synth. Catal.* **2014**, *356*, 1735−1740. (e) Menger, F. M.; Lu, H. Addressing the regioselectivity problem in organic synthesis. *Chem. Commun.* **2006**, 3235−3237. (f) Griswold, K. S.; Miller, S. J. A peptide-based catalyst approach to regioselective functionalization of carbohydrates. *Tetrahedron* **2003**, *59*, 8869−8875.

(5) (a) Crouch, R. D. Recent Advances in Silyl Protection of Alcohols. *Synth. Commun.* **2013**, *43*, 2265−2279. (b) Wuts, P. G. M.; Greene, T. W. *Greene's Protective Groups in Organic Synthesis*; 2006. (c) Lalonde, M.; Chan, T. H. Use of Organosilicon Reagents as Protective Groups in Organic Synthesis. *Synthesis* **1985**, *1985*, 817−845.

(6) (a) Painter, G. F.; Falshaw, A.; Wong, H. Conformation inversion of an inositol derivative by use of silyl ethers: a modified route to 3,6-di-O-substituted-L-ido-tetrahydroxyazepane derivatives. *Org. Biomol. Chem.* **2004**, *2*, 1007−1012. (b) Bols, M.; Pedersen, C. M. Silyl-protective groups influencing the reactivity and selectivity in glycosylations. *Beilstein J. Org. Chem.* **2017**, *13*, 93−105. (c) Ruecker, C. The Triisopropylsilyl Group in Organic Chemistry: Just a Protective Group, or More? *Chem. Rev.* **1995**, *95*, 1009−1064.

(7) (a) Fernandes, R. A.; Kumar, P.; Choudhary, P. Evolution of Strategies in Protecting-Group-Free Synthesis of Natural Products: A Recent Update. *Eur. J. Org. Chem.* **2021**, *2021*, 711−740. (b) Hui, C.; Chen, F.; Pu, F.; Xu, J. Innovation in protecting-group-free natural product synthesis. *Nat. Rev. Chem.* **2019**, *3*, 85−107.

(8) (a) Marin-Luna, M.; Patschinski, P.; Zipse, H. Substituent Effects in the Silylation of Secondary Alcohols: A Mechanistic Study. *Chem. - Eur. J.* **2018**, *24*, 15052−15058. (b) Patschinski, P.; Zhang, C.; Zipse, H. The Lewis base-catalyzed silylation of alcohols - a mechanistic analysis. *J. Org. Chem.* **2014**, *79*, 8348−8357. (c) Corey, E. J.; Venkateswarlu, A. Protection of hydroxyl groups as tert-butyldimethylsilyl derivatives. *J. Am. Chem. Soc.* **1972**, *94*, 6190−6191. (d) Patschinski, P.; Zipse, H. Leaving Group Effects on the Selectivity of the Silylation of Alcohols: The Reactivity-Selectivity Principle Revisited. *Org. Lett.* **2015**, *17*, 3318−3321.

(9) (a) Crouch, R. D. Selective deprotection of silyl ethers. *Tetrahedron* **2013**, *69*, 2383−2417. (b) Ankala, S. V.; Fenteany, G. Selective deprotection of either alkyl or aryl silyl ethers from aryl, alkyl bis-silyl ethers. *Tetrahedron Lett.* **2002**, *43*, 4729−4732. (c) Chen, M. Y.; Lu, K. C.; Shih-Yuan Lee, A.; Lin, C. C. Chemoselective deprotection of primary tert-butyldimethylsilyl ethers on carbohydrate molecules in the presence of secondary silyl ethers. *Tetrahedron Lett.* **2002**, *43*, 2777−2780. (d) Higashibayashi, S.; Shinko, K.; Ishizu, T.; Hashimoto, K.; Shirahama, H.; Nakata, M. Selective deprotection of t-butyldiphenylsilyl ethers in the presence of t-butyldimethylsilyl ethers by tetrabutylammonium fluoride, acetic acid, and water. *Synlett* **2000**, *2000*, 1306−1308.

(10) (a) Miller, A. D.; Furegati, S.; White, A. J. Observation of a 1,5-Silyl-Migration on Fructose. *Synlett* **2005**, 2385−2387. (b) Jones, S. S.; Reese, C. B. Migration of t-butyldimethylsilyl protecting groups. *J. Chem. Soc., Perkin Trans. 1* **1979**, 2762−2764.

(11) Masaguer, C. F.; Blériot, Y.; Charlwood, J.; Winchester, B. G.; Fleet, G. W. J. 6C-Butylglucoses from glucuronolactone: Suppression of silyl migration during borohydride reduction of lactols by cerium (III) chloride: Inhibition of phosphoglucomutase. *Tetrahedron* **1997**, *53*, 15147−15156.

(12) (a) Govindarajan, M. Protecting group migrations in carbohydrate chemistry. *Carbohydr. Res.* **2020**, *497*, 108151. (b) Phanumartwiwath, A.; Hornsby, T. W.; Jamalis, J.; Bailey, C. D.; Willis, C. L. Silyl migrations in D-xylose derivatives: total synthesis of a marine quinoline alkaloid. *Org. Lett.* **2013**, *15*, 5734−5737.

(13) (a) Arias-Pérez, M. S.; López, M. S.; Santos, M. J. Imidazole-promoted 1,4-migration of the tert-butyldiphenylsilyl group: influence on the selectivity control of the silylation reactions of carbohydrate OH groups. *J. Chem. Soc., Perkin Trans. 2* **2002**, 1549−1552. (b) Arias-Pérez, M.; Santos, M. An efficient approach to partially O-methylated α-D-mannopyranosides using bis-tert-butyldiphenylsilyl ethers as intermediates. *Tetrahedron* **1996**, *52*, 10785−10798. (c) Halmos, T.; Montserret, R.; Filippi, J.; Antonakis, K. Studies of the selective silylation of methyl α- and β-d-aldohexopyranosides: stability of the partially protected derivatives in polar solvents. *Carbohydr. Res.* **1987**, *170*, 57−69.

(14) Mulzer, J.; Schöllhorn, B. Multiple 1,2-O,O-Shift oftert-Butyldiphenylsilyl Groups in Polyols. *Angew. Chem., Int. Ed. Engl.* **1990**, *29*, 431−432.

(15) Yamazaki, T.; Oniki, T.; Kitazume, T. 1,2- and 1,3-O,O-Silyl migration reactions of fluorine-containing monosilylated diols. *Tetrahedron* **1996**, *52*, 11753−11762.

(16) Hernández-Martín, A.; Fernández, S.; Verstuyf, A.; Verlinden, L.; Ferrero, M. A-Ring-Modified 2-Hydroxyethylidene Previtamin D3Analogues: Synthesis and Biological Evaluation. *Eur. J. Org. Chem.* **2017**, *2017*, 504−513.

(17) Holmstedt, S.; George, L.; Koivuporras, A.; Valkonen, A.; Candeias, N. R. Deoxygenative Divergent Synthesis: En Route to Quinic Acid Chirons. *Org. Lett.* **2020**, *22*, 8370−8375.

(18) (a) Li, L.; Chen, Z.; Zhang, X.; Jia, Y. Divergent Strategy in Natural Product Total Synthesis. *Chem. Rev.* **2018**, *118*, 3752−3832. (b) Hernandez, L. W.; Sarlah, D. Empowering Synthesis of Complex Natural Products. *Chem. - Eur. J.* **2019**, *25*, 13248−13270.

(19) Lassaletta, J. M.; Meichle, M.; Weiler, S.; Schmidt, R. R. Silyl Group Migration in 1-O-Silyl Protected Sugars-Convenient Synthesis of 2-O-Unprotected Sugars. *J. Carbohydr. Chem.* **1996**, *15*, 241−254.

(20) (a) Bogdan, F. M.; Chow, C. S. The synthesis of allyl- and allyloxycarbonyl-protected RNA phosphoramidites. Useful reagents for solid-phase synthesis of RNAs with base-labile modifications. *Tetrahedron Lett.* **1998**, *39*, 1897−1900. (b) Neuner, S.; Santner, T.; Kreutz, C.; Micura, R. The "Speedy" Synthesis of Atom-Specific (15)N Imino/Amido-Labeled RNA. *Chem. - Eur. J.* **2015**, *21*, 11634−11643.

(21) Gonzalez, C.; Carballido, M.; Castedo, L. Synthesis of polyhydroxycyclohexanes and relatives from (−)-quinic acid. *J. Org. Chem.* **2003**, *68*, 2248−2255.

(22) Das, S.; Dalal, A.; Gholap, S. L. Stereoselective total syntheses of (−)-pseudohygrophorone A12 and (−)-pseudohygrophorone B12. *Synth. Commun.* **2020**, *50*, 580−586.

(23) Tchize Ndejouong, B. L. S.; Sattler, I.; Dahse, H. M.; Kothe, E.; Hertweck, C. Isoflavones with unusually modified B-rings and their evaluation as antiproliferative agents. *Bioorg. Med. Chem. Lett.* **2009**, *19*, 6473−6476.

(24) (a) Chen, B.; Kawai, M.; Wu-Wong, J. R. Synthesis of VS-105: A novel and potent vitamin D receptor agonist with reduced hypercalcemic effects. *Bioorg. Med. Chem. Lett.* **2013**, *23*, 5949−5952. (b) A Study to Investigate the Safety, Tolerability, and Pharmacokinetics of VS 105. https://ClinicalTrials.gov/show/NCT03043482.

(25) Laurent, P.; Hamdani, A.; Braekman, J.-C.; Daloze, D.; Isbell, L. A.; de Biseau, J.-C.; Pasteels, J. M. New 1-alk(en)yl-1,3,5-trihydroxycyclohexanes from the Dufour gland of the African ant Crematogaster nigriceps. *Tetrahedron Lett.* **2003**, *44*, 1383−1386.

(26) Laplace, D. R.; Van Overschelde, M.; De Clercq, P. J.; Verstuyf, A.; Winne, J. M. Synthesis of 2-Ethyl-19-nor Analogs of 1α,25-Dihydroxyvitamin D3. *Eur. J. Org. Chem.* **2013**, *2013*, 728−735.

(27) Aiba, T.; Sato, M.; Umegaki, D.; Iwasaki, T.; Kambe, N.; Fukase, K.; Fujimoto, Y. Regioselective phosphorylation of myo-inositol with BINOL-derived phosphoramidites and its application for protozoan lysophosphatidylinositol. *Org. Biomol. Chem.* **2016**, *14*, 6672−6675.

PUBLICATION
III

A Concise Synthesis of Carbasugars Isolated from *Streptomyces Lincolnensis*

Suvi Holmstedt, Nuno R. Candeias

Tetrahedron, **2020**, *76*, 131346.
DOI: 10.1016/j.tet.2020.131346

Publication reprinted with the permission of Elsevier.

Tetrahedron 76 (2020) 131346

Contents lists available at ScienceDirect

Tetrahedron

journal homepage: www.elsevier.com/locate/tet

A concise synthesis of carbasugars isolated from *Streptomyces lincolnensis*

Suvi Holmstedt [a, **], Nuno R. Candeias [a, b, *]

[a] *Faculty of Engineering and Natural Sciences, Tampere University, 33101, Tampere, Finland*
[b] *LAQV-REQUIMTE, Department of Chemistry, University of Aveiro, 3810-193, Aveiro, Portugal*

ARTICLE INFO

Article history:
Received 10 April 2020
Received in revised form
12 June 2020
Accepted 13 June 2020
Available online 22 June 2020

ABSTRACT

(−)-Quinic acid was used as a starting material in the hemisynthesis of two epimeric carbasugars isolated from *Streptomyces lincolnensis*. Previous 10–12 steps syntheses for the carbasugars have been herein shortened to 4–6 steps by using quinic acid as a chiron, based on a regioselective reduction step, with stereoinversion of a tertiary center. Both C-5 epimers of (1*R*, 2*R*, 3*R*)-5-(hydroxymethyl)cyclohexane-1,2,3-triol were obtained in up to 76% overall yield.

© 2020 Elsevier Ltd. All rights reserved.

Keywords:
Carbasugar
Chiron
Cyclitol
Hemisynthesis
Quinic acid

1. Introduction

Natural product-driven drug discovery combined with hemisynthesis brings together nature's maximum potential to create new biologically active molecules and the development of their structural analogs. Carbasugars are a group of organic small molecules that are abundant in nature and have wide biological potency due to the ability to mimic carbohydrates in biological processes [1,2]. It is noteworthy that the first synthesis of a natural carbasugar by McCasland [3] preceded its isolation in 7 years [4], followed by extensive studies and raising the interest of many research groups. Simpler cyclitols often are side chains and subunits of larger natural products owning versatile biological activity (e.g. massonianoside B [5], nicotiflorin [6], and verbascoside [7] are carba-L-rhamnose derivatives).

In 2004 Sedmera et al. isolated two structurally new carbasugars **1** and **2** from *Streptomyces lincolnensis*, which is known to produce many antibiotics such as antibacterial lincomycin as well as C7 cyclitols like valienol and gabosine I [8]. The first total synthesis of these carbasugars has been reported by Nanda et al. three years after their isolation from natural sources [9]. Such de novo synthesis relied on the kinetic enzymatic resolution and the use of (hydroxymethyl)cycloalkenone scaffold as a key intermediate. Subsequent oxidations into several epimers provided natural and unnatural carbasugars. Overall, final carbasugars **1** and **2** were obtained in 10–12 steps, through formation of the above-mentioned key intermediate in 8 steps. In 1986, before the isolation and the first total synthesis of carbasugars **1** and **2**, a protected analog of **1** has been prepared and used as a synthetic intermediate by Trost et al. in the stereoselective synthesis of isoquinuclidines from quinic acid [10].

In the present work, we redesigned the hemisynthesis strategy aiming at a more concise and simple synthesis for these natural carbasugars from a common synthetic intermediate. Quinic acid, a secondary metabolite of the shikimate pathway [11], has been explored in many natural product syntheses as chiral pool element [12,13] and the quest for new compounds with biological activity [14–16]. The three-dimensional arrangement of the secondary hydroxy groups and methylene unit serves as a great overlap of the functional groups to be adapted for the chiron strategy in total synthesis [17–19]. Indeed this plain strategy is a powerful tool to synthesize natural products with similar scaffolds such as the ones shown in Fig. 1. Structurally, carbasugar **1** corresponds to

---

* Corresponding author. LAQV-REQUIMTE, Department of Chemistry, University of Aveiro, 3810-193, Aveiro, Portugal.
** Corresponding author. Faculty of Engineering and Natural Sciences, Tampere University, 33101, Tampere, Finland.
E-mail addresses: suvi.holmstedt@tuni.fi (S. Holmstedt), ncandeias@ua.pt (N.R. Candeias).

https://doi.org/10.1016/j.tet.2020.131346
0040-4020/© 2020 Elsevier Ltd. All rights reserved.

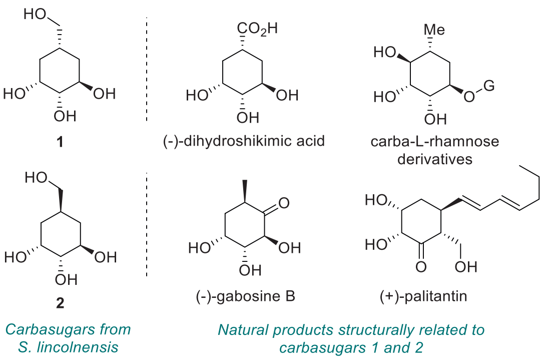
1
(-)-dihydroshikimic acid
carba-L-rhamnose derivatives
2
(-)-gabosine B
(+)-palitantin
Carbasugars from S. lincolnensis
Natural products structurally related to carbasugars 1 and 2

Fig. 1. Selected natural products structurally related to carbasugars **1** and **2**.

Table 1
Optimization of reduction conditions.

Entry[a]	Hydride (equiv.)	Conditions	**5** Yield %
1	$LiAlH_4$ (2)	THF, 0 °C	*traces*[c]
2	DIBAL-H (2)	THF, 0 °C to reflux	n.d.[c]
3	$NaBH_4$ (2)	DMSO, 0 °C–80 °C	3
4	$NaBH_4$ (2)	EtOH, 0 °C to RT	39
5	$NaBH_4$ (10)	MeOH, 0 °C to RT	42
6[b]	$NaBH_4$ (10)	THF/MeOH 16:1, 0 °C	55
7[b]	$NaBH_4$ (3)	THF/MeOH 16:1, −5 °C	84

[a] Lactone **4** was dissolved in the specified solvent and the mixture cooled to 0 °C or maintained at room temperature. The reducing agent was added, and the mixture was allowed to stir 3–18 h. The starting temperature was raised if no reaction was observed.
[b] Lactone **4** in THF was added to a stirred suspension of $NaBH_4$ in THF/MeOH.
[c] Complex mixture of multiple products, no product isolation.

(−)-dihydroshikimic acid with only one oxidation state difference and is an analog to many carba-L-rhamnose side chains derivatives. Additionally, carbasugar **2** is a structural analog to (−)-gabosine B [20] and (+)-palitantin [21]. We herein present an efficient total synthesis of natural carbasugars **1** and further modification to its epimer **2**, both isolated from *S. lincolnensis*.

2. Results and discussion

*2.1. Synthesis of (1R,2R,3R,5S)-5-(hydroxymethyl)cyclohexane-1,2,3-triol (**1**)*

The synthesis of **1** started with the simultaneous protection of quinic acid's (**3**) carboxyl and secondary hydroxy functionalities yielding acetal protected lactone **4** as previously described (Scheme 1) [22]. We envisioned that preparation of diol **5** (or its C-5 epimer), previously prepared by Trost [10], could be shortened by *in situ* formation of an epoxide during the reduction of the lactone, followed by its regioselective reduction [23–25]. While not certain about the stereo- and regioselectivity of the epoxide opening, the reduction of mesylated **4** was carefully optimized with common hydride sources (Table 1).

Despite the complete consumption of lactone **4,** reduction attempts with lithium aluminum hydride provided only traces of the desired product **5**, while no product was observed with less reactive DIBAL-H (Table 1, entries 1 and 2). When changing the reducing agent to $NaBH_4$ in DMSO, **5** was isolated in 3% yield (Table 1, entry 3) from a complex mixture of non-characterized products (as judged by TLC). Motivated by the previous use of this reductant in the cleavage of primary, secondary, and tertiary alkyl halides and tosylates [26], we set to increase the selectivity towards formation of **5**. As sodium borohydride reductions are known to be solvent dependent [27,28], we decided to test different solvents. Replacing DMSO by protic ethanol resulted in the formation of **5** in a moderate 39% yield (Table 1, entry 4). The complete consumption of starting material was achieved by increasing the amount of hydride to 10 equivalents in methanol (Table 1, entry 5). Ketal **5** was obtained in similar 42% yield as when using 2 equivalents of hydride source (entry 4), together with plenty of uncharacterized side products. The addition of methanol to THF has been demonstrated to improve selectivity in the reduction of esters and lactones with $NaBH_4$ [29]. Upon testing similar conditions and inverting the addition order, we were glad to obtain **5** in improved 55% yield (Table 1, entry 6). Generally, the portion-wise addition of the dissolved lactone to a suspension of $NaBH_4$ provided better yields than the standard portion-wise addition of powder reducing agent to the solution of the lactone. We believe this can be due to the high reactivity of the product towards the reducing agent. Ultimately, the best conditions obtained for the reduction of the lactone and removal of the tertiary hydroxy group derivative relied on using low temperatures to slow down the reactivity during the exothermic addition of the lactone to an excess of $NaBH_4$ (3 equivalents). The desired synthetic intermediate **5** was obtained in 84% yield (Table 1, entry 7).

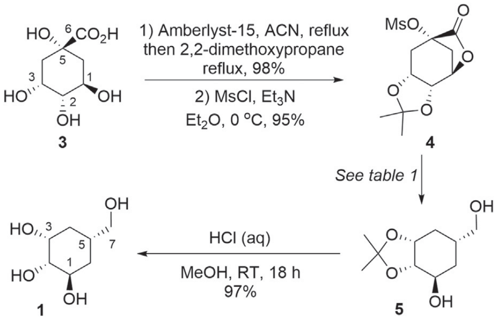

Scheme 1. Synthesis of carbasugar **1** from (−)-quinic acid.

Regioselectivities on epoxide opening have been reported to depend on the electrophilicity of hydride reagents [30]. Namely, BH_3 allows the opening of epoxides from the most substituted carbon [31]. With this in mind, different possibilities to justify the unexpected stereochemistry of the product obtained have been considered (Scheme 2a). After the reduction of the lactone moiety and putative formation of unidentified borane hydride species, the reactive primary alkoxide **4a** can undergo two different paths. The direct displacement of the methanesulfonate group by the hydride may provide the observed compound **5** if, a somewhat concerted hydride delivery on the stereochemically hindered tertiary carbon occurs. Alternatively, **4a** may undergo *O, O*-methanesulfonyl migration to form primary mesylate **4b** [32–34]. The obtained stereocenter inversion may occur upon hydride delivery on the more substituted carbon of the epoxide intermediate **4c**, formed by the attack of tertiary alkoxide. Notably, the more immediate formation of epoxide **4d** (Scheme 2b), upon the attack of the primary alkoxide to the tertiary vicinal carbon in **4a,** could lead to epimer **7**, which we have not been able to identify in our mixtures.

After deoxygenation, the acetal deprotection with HCl/MeOH yielded natural carbasugar **1** (Scheme 1) with a 76% overall yield from (−)-quinic acid. The spectral comparison with the original reports on the isolation of this natural product [8] confirmed the

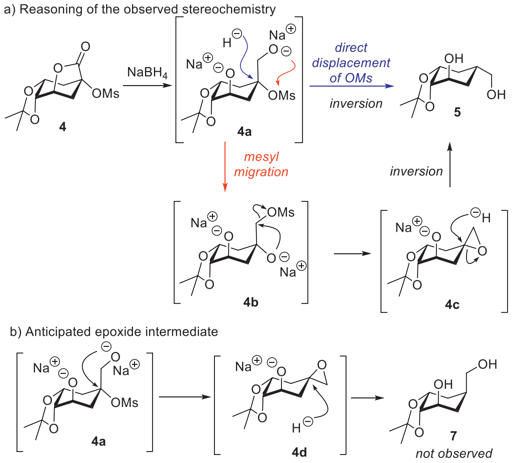
a) Reasoning of the observed stereochemistry
NaBH4
4
4a
direct displacement of OMs
inversion
5
mesyl migration
inversion
4b
4c
b) Anticipated epoxide intermediate
4a
4d
7
not observed

Scheme 2. Proposed reaction mechanism for the formation of **5**.

removal of the tertiary hydroxy group and the stereo-inversion of the C-5 carbon.

The unexpected stereoinversion at C-5 upon hydride delivery in **4** → **5** was further confirmed by a careful comparison of the reported [8] chemical shifts and *J*-couplings of natural product **1**. The two hydroxymethyl protons show very similar chemicals shifts (3.301 and 3.265 ppm) in the form of a multiplet that deconvolves to two sets of doublet of doublets with 11.3 and 6.6 Hz coupling constants (*vs* 11.0 and 6.3 Hz) [8]. The hydrogen at C-5 has a chemical shift of 1.715 ppm appearing as a multiplet due to the multiple couplings with the vicinal protons (at C-4, C-6 and C-7), also matching closely with the original report (1.714 ppm). Notably, all ^{13}C NMR chemical shifts of the final product differ from the paper on isolation of **1** in less than 0.06 ppm. Secondary C-7 and tertiary C-5 resonate at 66.55 and 32.71 ppm, respectively, in close agreement with Sedmera's report (66.55 and 32.71 ppm) [8].

2.2. Synthesis of (1R,2R,3R,5R)-5-(hydroxymethyl)cyclohexane-1,2,3-triol (2)

Considering the synthesis of the epimer **2**, we envisioned that this second natural product could be achieved by epimerization of the α-carbonyl position of the corresponding aldehyde (Scheme 3). The putative establishment of an intramolecular hydrogen bond between the hydroxy and the carbonyl groups on the same face of the six-membered ring should drive the epimerization towards the desired product. Bearing this in mind, conditions to target the selective oxidation of the primary alcohol were investigated and the results are presented in Table 2. The reaction suffered a lack of regioselectivity and the yields were poor for the exclusive oxidation of primary alcohol despite the use of parsimonious oxidizing agents (Table 2, entries 1 and 2). Better regioselectivity was observed when oxidizing with catalytic TEMPO in combination with (diacetoxyiodo)benzene, although the isolated yield remained poor (Table 2, entry 3). Changing the oxidizing agent from iodobenzene based oxidizing agents to *N*-chlorosuccinimide, resulted in an increased formation of **6** in 77% yield after 45 min (Table 2, entry 4). Precise control of the reaction time was required, as extended reaction times resulted in increased amounts of side products whilst shorter reaction times were not sufficient for complete consumption of the starting material.

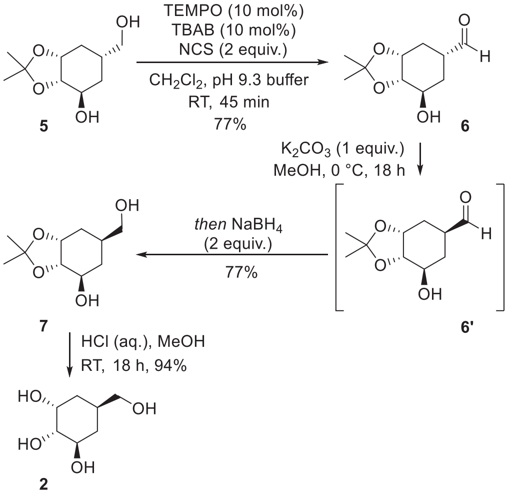

Scheme 3. Synthesis of carbasugar **2** from protected carbasugar **5**.

Table 2
Optimization of oxidation conditions.

Entry	Oxidation conditions	Yield %
1[a]	DMP (1 equiv.), CH_2Cl_2, RT, 1 h	15
2[a]	PCC (1.2 equiv.), CH_2Cl_2, RT, 20 h	13
3[a]	TEMPO (20 mol%), $PhI(OAc)_2$, (2 equiv.), CH_2Cl_2, RT, 4 h	34
4[b]	TEMPO (10 mol%), TBAB (10 mol%), NCS (2 equiv.), CH_2Cl_2/buffer, RT, 45 min	77

[a] Alcohol **5** was dissolved in CH_2Cl_2 (0.1 M) and the specified oxidizing agent was added at RT. Mixture was stirred at for specified time, quenched and purified using flash column chromatography.

[b] Procedure described in experimental section.

The α-carbonyl position of the aldehyde **6** was epimerized using 1 equivalent of K_2CO_3 as base (Scheme 3) in methanol. While testing epimerization conditions, the TLC analysis from reaction mixtures showed the aldehyde **6** being a minor product and the equilibrium largely favoring epimer **6'**. The simple evaporation of the reaction solvent or quenching by adjusting to pH 7 (using aqueous HCl) followed by column chromatography purification resulted in equilibration to starting material **6**. The difficult isolation of **6'** was circumvented by *in situ* reduction to alcohol **7** with sodium borohydride, thus allowing the isolation of the diol in 77% yield. Finally, the acetal deprotection gave the natural carbasugar **2**, also with NMR spectral characterization in close agreement with the values reported by Sedmera [8]. Comparison of chemical shifts of **1** and **2** show little changes in positions 1, 3 and 7, contrarily to the remaining cyclohexyl positions. A significant change in the chemical shift of C-2 between **1** (71.71 ppm) and **2** (76.30 ppm) could be explained by the establishment of an intramolecular hydrogen bond with C-1 in **1**.

2.3. Computational study

In order to verify our assumption on the stabilization of epimer **6**′ due to the establishment of an intramolecular hydrogen bond, we have performed the conformational analysis of both C-5 epimers using DFT [35] (Scheme 4). The conformational analysis of **6** resulted in the identification of the two chair conformers $\mathbf{6_A}$ and $\mathbf{6_B}$ as the most stable conformations. A somewhat distorted chair

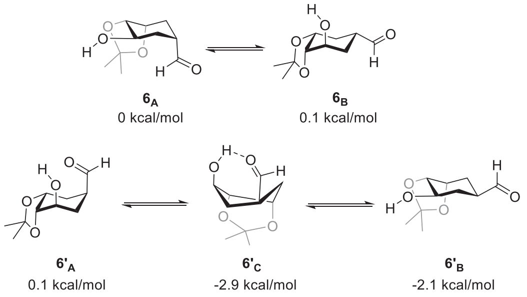

Scheme 4. Simplified conformational analysis of epimers **6** and **6'**. Energy values relate to $\mathbf{6_A}$ as the zero value and are given as electronic energies, optimized at PBE1PBE/6-31G** level of theory.

conformation can be detected in the case of $\mathbf{6_A}$, due to an intramolecular hydrogen bond between the secondary hydroxy group and the vicinal oxygen from the acetonide. Notwithstanding a similar effect observed for the most stable chair conformation of epimer **6′**, i.e. $\mathbf{6'_A}$, the placement of the carbonyl group in the more favorable equatorial position has a clear stabilizing effect (−2.1 kcal/mol) when compared with epimer **6**. As envisioned, a more stable conformation for epimer **6′** could be found, namely twist-boat conformation $\mathbf{6'_C}$ (−2.9 kcal/mol) where an intramolecular hydrogen bond is established between the aldehyde oxygen and the hydroxy group (2.027 Å).

3. Conclusion

In summary, we herein report the shortest and the highest yielding synthesis of the two natural 3,4,5-trihydroxycyclohexyl cyclitols isolated from *Streptomyces lincolnensis*. Both C-5 epimers of (1*R*, 2*R*, 3*R*)-5-(hydroxymethyl)cyclohexane-1,2,3-triol were obtained in 4–6 steps in 76% or 44% overall yields from (−)-quinic acid. The regioselective reduction of a quinic acid-derived lactone was used as a key step in the installation of the hydroxymethyl substituent, upon stereoselective hydride delivery to a tertiary carbon. The unprecedented conversion of the less stable epimer of the corresponding aldehyde into the more stable C-5 epimer allowed the preparation of both natural carbasugars by the insertion of an oxidation-epimerization-reduction sequence.

4. Experimental section

4.1. General remarks

All syntheses were carried out in oven-dried glassware under inert atmosphere. Anhydrous diethyl ether and triethylamine were obtained using PureSolv Micro multi-unit purification system. Acetonitrile was left standing over 3 Å molecular sieves and used without further purification. All other reagents were purchased from Sigma Aldrich or TCI and used without purification. Reactions were monitored through thin-layer chromatography (TLC) with commercial silica gel plates (Merck silica gel, 60 F254). Plates were visualized by staining upon heating with vanillin stain. Flash column chromatography was performed on silica gel 60 (40–63 μm) as stationary phase. The ^{1}H and ^{13}C spectra were recorded at 500 MHz and 125 MHz respectively in a JEOL ECZR 500 instrument. $CDCl_3$ or D_2O (in D_2O samples 4 μl of acetone was used as internal reference) were used as solvents for NMR analysis. Chemical shifts (δ) are reported in ppm and are referenced to the residual chloroform signal (δ ^{1}H 7.26 ppm, δ ^{13}C 77.16 ppm) or to the internal acetone (δ ^{1}H 2.03 ppm, δ ^{13}C 30.50 ppm). The following abbreviations were used to describe peak splitting patterns: s = singlet, d = doublet, t = triplet, m = multiplet. Coupling constants J were reported in Hertz (Hz). High-resolution mass spectra were recorded on a Waters ESI-TOF MS spectrometer.

4.2. (3a*R*,4*R*,7*S*,8a*R*)-2,2-dimethyl-6-oxotetrahydro-4,7-methano[1,3]dioxolo[4,5-c]oxepin-7(6*H*)-yl methanesulfonate (***4***)

i) Quinic acid **3** (3.0 g, 15.6 mmol) was weighed into round bottomed flask equipped with stirring bar. Acetonitrile (200 mL) was added, followed by addition of Amberlyst 15 (3.5 g), and the mixture was refluxed for 2 days. The mixture was cooled to room temperature and 2,2-dimethoxypropane (3.8 mL, 3.25 g, 31.2 mmol, 2 equiv.) was added and refluxed for 3 h. The reaction mixture was filtrated through Celite plug and the solvent was evaporated to give pure (3a*R*,4*R*,7*S*,8a*R*)-7-hydroxy-2,2-dimethyltetrahydro-4,7-methano[1,3]dioxolo[4,5-c]oxepin-6(4*H*)-one as a beige solid (3.28 g, 98%). ^{1}H NMR (500 MHz, $CDCl_3$): δ 4.71 (dd, J = 6.1, 2.5 Hz, 1H-1), 4.51–4.47 (m, 1H-3), 4.29 (ddd, J = 6.7, 2.4, 1.5 Hz, 1H-2), 3.16 (s, 1H–OH), 2.63 (d, J = 11.7 Hz, 1H-6), 2.36 (ddd, J = 14.7, 7.6, 2.3 Hz, 1H-4), 2.33–2.27 (m, 1H-6), 2.17 (dd, J = 14.6, 2.9 Hz, 1H-4), 1.51 (s, 3H–CH_3), 1.31 (s, 3H–CH_3); ^{13}C NMR (125 MHz, $CDCl_3$): δ 179.08 (C=O), 109.90 ($C_{isop.}$), 75.97 (C1), 72.19 (C5), 71.66 (C2), 71.60 (C3), 38.23 (C4), 34.37 (C6), 27.08 (CH_3), 24.41 (CH_3); HRMS calculated for $[M]^+$ 214.0841, found 214.0913. The spectral data of the compound is consistent with the literature data [10].

ii) Lactone ((3a*R*,4*R*,7*S*,8a*R*)-7-hydroxy-2,2-dimethyltetrahydro-4,7-methano[1,3]dioxolo[4,5-c]oxepin-6(4*H*)-one) synthesized in section 4.2 *i)* (3.28 g, 15.3 mmol) was dissolved in Et_2O (100 mL) at 0 °C. Et_3N (4.3 mL, 3.1 g, 30.6 mmol, 2 equiv.) was added followed by slow addition of MsCl (1.8 mL, 2.6 g, 23 mmol, 1 equiv.). The ice bath was removed after 5 min and the mixture was left stirring for 2 h at room temperature forming a thick solution. The mixture was diluted with EtOAc (100 mL) and quenched with H_2O (100 mL). Layers were separated and the aqueous phase was extracted with CH_2Cl_2 (3 × 50 mL). The organic phases were combined, dried with anhydrous $MgSO_4$, filtered through silica pad (3 cm) and the solvents were evaporated to give pure **4** as a beige solid (4.24 g, 95%). ^{1}H NMR (500 MHz, $CDCl_3$): δ 4.80 (dd, J = 6.4, 2.5 Hz, 1H-1), 4.57–4.45 (m, 1H-3), 4.31 (ddd, J = 6.2, 2.1, 0.9 Hz, 1H-2), 3.28 (s, 3H -OMs-CH_3), 3.12–3.05 (m, 1H-6), 2.83 (d, J = 11.8 Hz, 1H-4), 2.54 (ddd, J = 14.4, 7.7, 2.4 Hz, 1H-6), 2.39 (dd, J = 14.5, 3.0 Hz, 1H-4), 1.52 (s, 3H–CH_3), 1.32 (s, 3H–CH_3). ^{13}C NMR (125 MHz, $CDCl_3$): δ 172.91 (C=O), 110.41 ($C_{isop.}$), 82.27 (C5), 75.82 (C1), 72.01 (C2), 71.17 (C3), 41.34 (OMs-CH_3), 36.60 (C4), 33.24 (C6), 27.06 (CH_3), 24.45 (CH_3); HRMS calculated for $[M+Na]^+$ 315.0515, found 315.0479. The spectral data of the compound is consistent with the literature data [36].

4.3. (3a*S*,4*R*,6*R*,7a*R*)-6-(hydroxymethyl)-2,2-dimethylhexahydrobenzo[d][1,3]dioxol-4-ol (***5***)

Methanol (0.2 mL) was added to a −5 °C suspension of $NaBH_4$ (78 mg, 2.1 mmol, 3 equiv.) in THF (1 mL) and the mixture was stirred until little bubbling was visible. A solution of lactone **4** (200 mg, 0.68 mmol) in THF (2.2 mL) was added dropwise and the reaction mixture was allowed to warm up to room temperature and was left stirring overnight. The reaction was quenched with H_2O (3 mL) and after 30 min stirring, solvents were evaporated under reduced pressure. The residue was purified by flash column chromatography (dry loading) using EtOAc as eluent to yield product **5** as a clear oil (116 mg, 84%). ^{1}H NMR (500 MHz, $CDCl_3$): δ 4.35 (dd, J = 11.5, 6.1 Hz, 1H-1), 4.09 (td, J = 7.5, 3.8 Hz, 1H-3), 3.96 (t, J = 5.6 Hz, 1H-2), 3.64–3.55 (m, 2H-7), 2.07–1.98 (m, 2H-5 and 6), 1.91 (t, J = 5.3 Hz, 1H–OH), 1.79 (d, J = 4.6 Hz, 1H–OH), 1.76 (dd, J = 7.5, 3.9 Hz, 1H-4), 1.65–1.58 (m, 2H-6 and 4), 1.50 (s, 3H–CH_3), 1.36 (s, 3H–CH_3); ^{13}C NMR (125 MHz, $CDCl_3$): δ 108.77 ($C_{isop.}$), 78.71 (C2), 73.37 (C1), 68.64 (C3), 67.06 (C7), 31.87 (C5), 30.26 (C4), 29.25 (C6), 27.99 (CH_3), 25.80 (CH_3); HRMS calculated for $[M+H]^+$ 203.1283, found 203.1296. The spectral data of the compound is consistent with the literature data [10].

4.4. (1R,2S,3R,5S)-5-(hydroxymethyl)cyclohexane-1,2,3-triol (**1**)

Protected alcohol **5** (115 mg, 0.57 mmol) was dissolved in MeOH (4 mL) and aqueous 4M HCl (0.4 mL) was added. The mixture was stirred for 18 h at room temperature and then diluted with MeOH and neutralized with NaOH (4 M aq. soln.). Solvents were evaporated and crude compound was purified using flash column chromatography (EtOAc/MeOH 9:1) to yield product **1** as white solid (89 mg, 97%).^{1}H NMR (500 MHz, D_2O): δ 3.86 (q, J = 3.3 Hz, 1H-3), 3.75 (ddd, J = 11.7, 4.4, 3.1 Hz, 1H-1), 3.63 (t, J = 3.4 Hz, 1H-2), 3.30 (dd, J = 11.3, 6.6 Hz, 1H-7), 3.26 (dd, J = 11.3, 6.6 Hz, 1H-7), 1.76–1.66 (m, 1H-5), 1.54 (dt, J = 12.2, 3.9 Hz, 1H-6), 1.43 (d, J = 14.4 Hz, 1H-4), 1.27–1.19 (m, 1H-4), 1.12 (q, J = 11.9 Hz, 1H-6); ^{13}C NMR (125 MHz, D_2O): δ 71.71 (C2), 70.04 (C3), 67.85 (C1), 66.55 (C7), 32.71 (C5), 30.36 (C6), 29.18 (C4). HRMS calculated for $[M+Cl]^-$ 197.0581, found 197.0591. The spectral data of the compound is consistent with the literature data [8].

4.5. (3aR,5R,7R,7aS)-7-hydroxy-2,2-dimethylhexahydrobenzo[d][1,3]dioxole-5-carbaldehyde (**6**)

Alcohol **5** (430 mg, 2.1 mmol) was dissolved in CH_2Cl_2 (20 mL) followed by addition of TEMPO (33 mg, 0.2 mmol, 0.1 equiv.) and TBAB (68 mg, 0.2 mmol, 0.1 equiv.). Then 20 mL of aqueous buffer solution (0.5M $NaHCO_3$, 0.05M K_2CO_3) was added followed by addition of *N*-chlorosuccinimide (560 mg, 4.3 mmol, 2 equiv.) and the mixture was allowed to stir at room temperature for 45 min after which layers were separated, aqueous phase was saturated with NaCl and extracted with CH_2Cl_2 (5 × 10 mL). Combined organic phases were dried with anhydrous $MgSO_4$, filtered and concentrated under reduced pressure. The residue was purified using flash column chromatography (CH_2Cl_2/EtOAc, 1:1) to yield product **6** as a pale yellow oil (330 mg, 77%). ^{1}H NMR (500 MHz, $CDCl_3$): δ 9.68 (s, 1H-7), 4.39–4.33 (m, 1H-1), 4.02–3.96 (m, 1H-3), 3.93 (t, J = 5.5 Hz, 1H-2), 2.61–2.54 (m, 1H-5), 2.25 (ddd, J = 10.3, 8.2, 4.4 Hz, 2H-4,6), 2.15 (ddd, J = 14.9, 6.7, 4.4 Hz, 1H-6), 1.62 (ddd, J = 14.1, 8.5, 5.7 Hz, 1H-4), 1.41 (s, 3H–CH_3), 1.34 (s, 3H–CH_3); ^{13}C NMR (125 MHz, $CDCl_3$): δ 203.19 (C7), 109.24 (C_{isop}), 79.00 (C2), 72.92 (C1), 68.08 (C3), 42.45 (C5), 27.69 (C4), 27.27 (CH_3), 25.98 (C6), 25.93 (CH_3); HRMS calculated for $[M+Na]^+$ 223.0946, found 223.0918.

4.6. (3aS,4R,6S,7aR)-6-(hydroxymethyl)-2,2-dimethylhexahydrobenzo[d][1,3]dioxol-4-ol (**7**)

Aldehyde **6** (70 mg, 0.34 mmol) was dissolved in MeOH (4 mL), K_2CO_3 (48 mg, 0.34 mmol, 1.0 equiv.) was added and the mixture was stirred 18 h at room temperature. The mixture was cooled down to 0 °C, stirred at 0 °C for 2 h, $NaBH_4$ (26 mg, 0.7 mmol, 2 equiv.) was added, and the reaction mixture was allowed to warm up to room temperature over 2 h while stirring. Reaction mixture was diluted with EtOAc and quenched with H_2O (0.2 mL). The solvents were evaporated and the residue was purified using flash column chromatography (dry loading) using EtOAc as eluent to yield product **7** as a clear oil (54 mg, 77%).^{1}H NMR (500 MHz, $CDCl_3$): δ 4.37 (bs, 1H-1), 3.81 (t, J = 5.8 Hz, 1H-2), 3.77–3.67 (m, 1H-3), 3.6–3.46 (m, 2H-7), 2.79 (s, 1H–OH), 2.13 (d, J = 14.9 Hz, 1H-6), 2.07–1.85 (m, 3H-4, 5, OH), 1.49 (s, 4H, overlapped peaks 6, CH_3), 1.36 (s, 3H–CH_3), 1.16–1.03 (m, 1H-4); ^{13}C NMR (125 MHz, $CDCl_3$): δ 108.81 ($C_{isop.}$), 81.27 (C2), 74.20 (C1), 72.25 (C3), 66.95 (C7), 33.17 (C5), 33.15 (C4), 29.21 (C6), 28.42 (CH_3), 26.23 (CH_3); HRMS calculated for $[M+H]^+$ 203.1283, found 203.1290.

4.7. (1R,2R,3R,5R)-5-(hydroxymethyl)cyclohexane-1,2,3-triol (**2**)

Protected alcohol **7** (20 mg, 0.1 mmol) was dissolved in MeOH (1 mL) and aqueous 4M HCl (0.1 mL) was added. The mixture was stirred for 18 h at room temperature after which MeOH was added and the mixture neutralized with NaOH (4 M aq. soln.). Solvents were evaporated and the mixture was purified using flash column chromatography (EtOAc/MeOH 9:1) to yield product **2** as a white solid (15 mg, 94%). ^{1}H NMR (500 MHz, D_2O): δ 3.93 (bs, 1H-3), 3.59 (td, J = 10.1, 4.2 Hz, 1H-1), 3.32–3.25 (m, 2H-7), 3.19 (dd, J = 9.6, 2.9 Hz, 1H-2), 1.82–1.79 (m, 1H-5), 1.76–1.74 (m, 1H-4), 1.64 (d, J = 14.2 Hz, 1H-4), 1.10 (t, J = 13.4 Hz, 1H-4), 0.87 (q, J = 11.8 Hz, 1H-6); ^{13}C NMR (125 MHz, D_2O): δ 76.30 (C2), 70.04 (C3), 69.45 (C1), 66.25 (C7), 35.49 (C6), 33.50 (C4), 32.43 (C5).; HRMS calculated for $[M+Cl]^-$ 197.0581, found 197.0612. The spectral data of the compound is consistent with the literature data [8].

4.8. Computational details

All calculations were performed using the Gaussian 09 software package [37], without symmetry constraints. The optimized geometries were obtained employing the PBE1PBE functional with a standard 6-31G(d,p) [38–42] basis set. That functional uses a hybrid generalized gradient approximation (GGA), including 25% mixture of Hartree-Fock [43] exchange with DFT [35] exchange-correlation, given by Perdew, Burke and Ernzerhof functional (PBE) [44,45]. Frequency calculations were performed to confirm the nature of the stationary points, yielding no imaginary frequency for the minima.

Declaration of competing interest

The authors declare that they have no known competing financial interests or personal relationships that could have appeared to influence the work reported in this paper.

Acknowledgments

The Academy of Finland is duly acknowledged for financial support to N. R. C. (Decisions No. 326487 and 326486), Finnish Cultural Foundation is acknowledged for financial support to S. H. (00190336). CSC–IT Center for Science Ltd, Finland is acknowledged for the allocation of computational resources.

Supplementary Material

Spectral characterization of the compounds prepared and coordinates of the computational optimized structures are available as supplementary material.

Appendix A. Supplementary data

Supplementary data to this article can be found online at https://doi.org/10.1016/j.tet.2020.131346.

References

[1] O. Arjona, A.M. Gomez, J.C. Lopez, J. Plumet, Chem. Rev. 107 (2007) 1919–2036.
[2] R.G. Soengas, J.M. Otero, A.M. Estévez, A.P. Rauter, V. Cachatra, J.C. Estévez, R.J. Estévez, An Overview of Key Routes for the Transformation of Sugars into Carbasugars and Related Compounds in Carbohydrate Chemistry, vol. 38, The Royal Society of Chemistry, 2012, pp. 263–302, 38.
[3] G.E. McCasland, S. Furuta, L.J. Durham, J. Org. Chem. 31 (1966) 1516–1521.
[4] T.W. Miller, B.H. Arison, G. Albers-Schonberg, Biotechnol. Bioeng. 15 (1973) 1075–1080.
[5] W.Q. Chen, Z.J. Song, H.H. Xu, Bioorg. Med. Chem. Lett 22 (2012) 5819–5822.
[6] Y.H. Jo, S.B. Kim, Q. Liu, S.G. Do, B.Y. Hwang, M.K. Lee, PloS One 12 (2017), e0172069.
[7] T.G. Kim, J.H. Lee, M.Y. Lee, K.U. Kim, J.H. Lee, C.H. Park, B.H. Lee, K.S. Oh, Biol. Pharm. Bull. 40 (2017) 1454–1462.
[8] P. Sedmera, P. Halada, S. Pospisil, Magn. Reson. Chem. 47 (2009) 519–522.
[9] R. Rej, N. Jana, S. Kar, S. Nanda, Tetrahedron: Asymmetry 23 (2012) 364–372.
[10] B.M. Trost, A.G. Romero, J. Org. Chem. 51 (1986) 2332–2342.
[11] N.R. Candeias, B. Assoah, S.P. Simeonov, Chem. Rev. 118 (2018) 10458–10550.
[12] S. Kobayashi, M. Sugiura, C. Ogawa, Adv. Synth. Catal. 346 (2004) 1023–1034.
[13] S.W. McCombie, W.B. Motherwell, M.J. Tozer, The Barton-McCombie Reaction in Organic Reactions, vol. 77, John Wiley & Sons, Inc., 2012, pp. 161–432.
[14] C. Ogawa, H. Konishi, M. Sugiura, S. Kobayashi, Org. Biomol. Chem. 2 (2004) 446–448.
[15] M. Yasuda, S. Yamasaki, Y. Onishi, A. Baba, J. Am. Chem. Soc. 126 (2004) 7186–7187.
[16] S. Rendler, M. Oestreich, Synthesis (2005) 1727–1747.
[17] S. Hanessian, Total Synthesis of Natural Products, the "Chiron" Approach, first ed., Pergamon Press, Oxford Oxfordshire ; New York, 1983.
[18] S. Hanessian, J. Pan, A. Carnell, H. Bouchard, L. Lesage, J. Org. Chem. 62 (1997) 465–473.
[19] A. Barco, S. Benetti, C.D. Risi, P. Marchetti, G.P. Pollini, V. Zanirato, Tetrahedron: Asymmetry 8 (1997) 3515–3545.
[20] T. Shinada, T. Fuji, Y. Ohtani, Y. Yoshida, Y. Ohfune, Synlett (2002) 1341–1343.
[21] S. Hanessian, Y. Sakito, D. Dhanoa, L. Baptistella, Tetrahedron 45 (1989) 6623–6630.
[22] H. Kawashima, M. Sakai, Y. Kaneko, Y. Kobayashi, Tetrahedron 71 (2015) 2387–2392.
[23] L. Rodrigues, M.S. Majik, S.G. Tilve, S. Wahidulla, Tetrahedron Lett. 59 (2018) 3413–3415.
[24] T.M. Flaherty, J. Gervay, Tetrahedron Lett. 37 (1996) 961–964.
[25] S. Florio, F.M. Perna, A. Salomone, P. Vitale, in: P. Knochel (Ed.), 8.29 Reduction of Epoxides in Comprehensive Organic Synthesis II, second ed., Elsevier, Amsterdam, 2014, pp. 1086–1122.
[26] R.O. Hutchins, D. Hoke, J. Keogh, D. Koharski, Tetrahedron Lett. 10 (1969) 3495–3498.
[27] L. Banfi, E. Narisano, R. Riva, N. Stiasni, M. Hiersemann, T. Yamada, T. Tsubo, Sodium Borohydride in Encyclopedia of Reagents for Organic Synthesis, John Wiley & Sons, Ltd., 2014.
[28] H.C. Brown, S. Krishnamurthy, Tetrahedron 35 (1979) 567–607.
[29] K. Soai, H. Oyamada, M. Takase, A. Ookawa, Bull. Chem. Soc. Jpn. 57 (1984) 1948–1953.
[30] R.O. Hutchins, I.M. Taffer, W.J. Burgoyne, Org. Chem. 46 (1981) 5214–5215.
[31] H.C. Brown, N.M. Yoon, J. Am. Chem. Soc. 90 (1968) 2686–2688.
[32] V.A. Zagorevskii, Z.D. Kirsanova, Chem. Heterocycl. Compd. 6 (1970) 288–289.
[33] W. Zhang, J. Chu, A.M. Cyr, H. Yueh, L.E. Brown, T.T. Wang, J. Pelletier, J.A. Porco Jr., J. Am. Chem. Soc. 141 (2019) 12891–12900.
[34] A.J. Flynn, A. Ford, A.R. Maguire, Org. Biomol. Chem. 18 (2020) 2549–2610.
[35] R.G. Parr, W. Yang, Density Functional Theory of Atoms and Molecules, Oxford University Press, New York, 1989.
[36] J.C. Rohloff, K.M. Kent, M.J. Postich, M.W. Becker, H.H. Chapman, D.E. Kelly, W. Lew, M.S. Louie, L.R. McGee, E.J. Prisbe, L.M. Schultze, R.H. Yu, L. Zhang, J. Org. Chem. 63 (1998) 4545–4550.
[37] M.J.T. Frisch, G W, H.B. Schlegel, G.E. Scuseria, M.A. Robb, J.R. Cheeseman, G. Scalman, V. Barone, B. Mennucci, G.A. Petersson, H. Nakatsuji, M. Caricato, X. Li, H.P. Hratchian, A.F. Izmaylov, J. Bloino, G. Zheng, J.L. Sonnenberg, M. Hada, M. Ehara, K. Toyota, R. Fukuda, J. Hasegawa, M. Ishida, T. Nakajima, Y. Honda, O. Kitao, H. Nakai, T. Vreven, J.A. Montgomery, J, J.E. Peralta, F. Ogliaro, M. Bearpark, J.J. Heyd, E. Brothers, K.N. Kudin, V.N. Staroverov, R. Kobayashi, J. Normand, K. Raghavachari, A. Rendell, J.C. Burant, S.S. Iyengar, J. Tomasi, M. Cossi, N. Rega, J.M. Millam, M. Klene, J.E. Knox, J.B. Cross, V. Bakken, C. Adamo, J. Jaramillo, R. Gomperts, R.E. Stratmann, O. Yazyev, A.J. Austin, R. Cammi, C. Pomelli, J.W. Ochterski, R.L. Martin, K. Morokuma, V.G. Zakrzewski, G.A. Voth, P. Salvador, J.J. Dannenberg, S. Dapprich, A.D. Daniels, Ö. Farkas, J.B. Foresman, J.V. Ortiz, J. Cioslowski, D.J. Fox, Gaussian 09, Revision D.01, Gaussian, Inc, Wallingford CT, 2009.
[38] R. Ditchfield, W.J. Hehre, J.A. Pople, J. Chem. Phys. 54 (1971) 724–728.
[39] W.J. Hehre, R. Ditchfield, J.A. Pople, J. Chem. Phys. 56 (1972) 2257–2261.
[40] P.C. Hariharan, J. Pople, A. Mol. Phys. 27 (1974) 209–214.
[41] M.S. Gordon, Chem. Phys. Lett. 76 (1980) 163–168.
[42] P.C. Hariharan, J.A. Pople, Theor. Chim. Acta 28 (1973) 213–222.
[43] W.J. Hehre, L. Radom, P.v.R. Schleyer, J. Pople, Ab Initio Molecular Orbital Theory, John Wiley & Sons, New York, 1986.
[44] J.P. Perdew, Phys. Rev. B 33 (1986) 8822–8824.
[45] J.P. Perdew, K. Burke, M. Ernzerhof, Phys. Rev. Lett. 78 (1997), 1396-1396.

PUBLICATION
IV

Design and synthesis of novel quinic acid derivatives: in vitro cytotoxicity and anticancer effect on glioblastoma

Akshaya Murugesan*, Suvi Holmstedt*, Kenna C. Brown*, Alisa Koivuporras, Ana S. Macedo, Nga Nguyen, Pedro Fonte, Patricia Rijo, Olli Yli-Harja, Nuno R. Candeias, and Meenakshisundaram Kandhavelu

Future Medicinal Chemistry, **2020**, *12*, 1891–1910.
DOI: 10.4155/fmc-2020-0194

Publication reprinted with the permission of Future Science.

Research Article

For reprint orders, please contact: reprints@future-science.com

Future Medicinal Chemistry

Design and synthesis of novel quinic acid derivatives: *in vitro* cytotoxicity and anticancer effect on glioblastoma

Akshaya Murugesan[‡,1,2,3], Suvi Holmstedt[‡,4], Kenna C Brown[‡,1], Alisa Koivuporras[4], Ana S Macedo[5], Nga Nguyen[1], Pedro Fonte[6,7,8], Patrícia Rijo[9,10], Olli Yli-Harja[11,12], Nuno R Candeias*[,4,13] & Meenakshisundaram Kandhavelu**[,1,2,3]

[1]Molecular Signaling Lab, Faculty of Medicine & Health Technology, Tampere University, Finland
[2]BioMeditech & Tays Cancer Center, Tampere University Hospital, P.O. Box 553, 33101, Tampere, Finland
[3]Department of Biotechnology, Lady Doak College, Thallakulam, Madurai, 625002, India
[4]Faculty of Engineering & Natural Sciences, Tampere University, 33101, Tampere, Finland
[5]LAQV-REQUIMTE, Department of Chemistry, University of Aveiro, 3810-193, Aveiro, Portugal
[6]Center for Marine Sciences (CCMAR), University of Algarve, Gambelas Campus, 8005-139, Faro, Portugal
[7]Department of Chemistry & Pharmacy, Faculty of Sciences & Technology, University of Algarve, Gambelas Campus, 8005-139, Faro, Portugal
[8]iBB – Institute for Bioengineering & Biosciences, Department of Bioengineering, Instituto Superior Técnico, Universidade de Lisboa, 1049-001, Lisboa, Portugal
[9]Research Center for Biosciences & Health Technologies (CBIOS), Universidade Lusófona de Humanidades e Tecnologias, 1749-024, Lisboa, Portugal
[10]Instituto de Investigação do Medicamento (iMed.ULisboa), Faculdade de Farmácia, Universidade de Lisboa, 1649-003, Lisboa, Portugal
[11]Computational Systems Biology Group, Faculty of Medicine & Health Technology, Tampere University, P.O. Box 553, 33101, Tampere, Finland
[12]Institute for Systems Biology, 1441N 34th Street, Seattle, WA 98103-8904, USA
[13]Escola de Ciências e Tecnologias da Saúde Universidade Lusófona Lisboa, 1749-024, Portugal
*Author for correspondence: ncandeias@ua.pt
**Author for correspondence: meenakshisundaram.kandhavelu@tuni.fi
‡Authors contributed equally

Aim: Quinic acid (QA) is a cyclic polyol exhibiting anticancer properties on several cancers. However, potential role of QA-derivatives against glioblastoma is not well established. **Methodology & results:** Sixteen novel QA-derivatives and QA-**16** encapsulated poly (lactic-co-glycolic acid) nanoparticles (QA-**16**-NPs) were screened for their anti-glioblastoma effect using standard cell and molecular biology methods. Presence of a tertiary hydroxy and silylether groups in the lead compound were identified for the antitumor activity. QA-**16** have 90% inhibition with the IC_{50} of 10.66 μM and 28.22 μM for LN229 and SNB19, respectively. The induction of apoptosis is faster with the increased fold change of caspase 3/7 and reactive oxygen species. **Conclusion:** QA-**16** and QA-**16**-NPs shows similar cytotoxicity effect, providing opportunity to use QA-**16** as a potential chemotherapeutic agent.

First draft submitted: 12 June 2020; Accepted for publication: 5 August 2020; Published online: 30 October 2020

Keywords: chemotherapeutic drugs • cytotoxicity • glioblastoma • nanoparticle • PLGA • quinic acid

Glioblastoma (GS) is the most common and aggressive intracranial tumor in adults with unique macrophage infiltration. It is grade IV astrocytoma and a high grade glial tumor with extreme invasive characteristic features. Astrocytomas are graded based on their growth rate such as low-grade (slow growth), mid-grade (moderate) and high-grade (rapid) [1]. The malignant astrocytoma is usually treated with chemotherapy and surgery, despite the advanced treatment modalities the long-term survival rate is poor [2]. Current anticancer drugs are limited by their deleterious side effects, resistance to the drug interventions and the inefficient activity *in vivo*. Even targeted drug therapies have poor therapeutic outcomes in GS patients. Hence, novel broad-spectrum drugs with less side effects are necessary to improve the GS treatment [3–7].

newlands press

Quinic acid (QA) is a cyclic polyol, that have exhibited broad-spectrum antioxidant, anti-inflammatory, hepatoprotective [8] and anticancer properties on several cancer lines, including oral [4], cervical [9] and prostate cancers [8]. QA is a biochemical intermediate in the shikimate biosynthetic pathway that produces aromatic compounds in plants and microorganisms, whereas in mammals QA cannot be synthesized and must be introduced into their systems [10]. Once it is absorbed by mammals, QA will be used to synthesize nicotinamide [11]. Nicotinamide is an important molecule for inducing DNA repair and NF-κB inhibition [8] which is a major regulator transcription for cell survival, and therefore, its inhibition can induce cell death [12]. Thus, QA derivatives could be a promising chemotherapeutic agent for developing anticancer drugs.

QA-derived amides were reported as anti-inflammatory agents through the inhibition of pro-inflammatory transcription factor NF-κB. Structure–activity relationship studies revealed the importance of the exposed (non-protected) hydroxyl groups for such inhibitory activities. Low or absent anti-proliferative or cytotoxic activities (<100 μM) were observed for QA-derived amides against adenocarcinomic human alveolar basal epithelial cells (A549) [13]. A derivative, KZ-41 derived from propyl amine, has been shown to counteract p38MAPK-dependent pro-apoptotic and inflammatory signaling in primary human retinal endothelial cells. It provides an opportunity for the development of therapy for inflammatory retinal disorders, such as ischemic optic neuropathy or inflammatory retinal vasculopathy [14,15]. Other amide derivatives are inhibitors of dengue virus replication *in vitro* and safe for use in Huh7.5, human hepatoma cell lines [16].

Selectins are carbohydrate-binding molecule, that helps in cancer cell interaction due to the increased selectin ligands in the cell surface [17]. The expression of selectin is correlated with the cancer metastasis and cancer patients' prognosis condition. Likewise, co-crystal structure of QA with E-selectin was developed [18,19] as selectin inhibitors. Recently, polymer conjugates derived from QA ligands were found to target E- and P-selectin expressing cells through endocytosis. These markers are frequently overexpressed in the blood vessels of human cancers and thus present a suitable target for directed chemotherapy [20]. Notwithstanding the many studies on the research of antitumor and therapeutic properties of chlorogenic acids [21], antitumor properties of simpler carbocycles derived from QA but devoid of the phenol counterpart have been overlooked. QA conjugated nanoparticles (NPs) acts as a promising chemotherapeutic drugs for solid tumors [22] but its effect against GS has not been explored.

Poly(lactide-*co*-glycolide) (PLGA) nanoparticle is a specific type of nanosystem that has been extensively used for drug-delivery in a controlled, sustained or targeted manner. PLGA is biodegradable, biocompatible and approved by US FDA for the clinical application in humans [23]. PLGA microspheres, ranging from 100 nm to 50 μm in diameter are used to deliver the siRNA, proteins, drugs, cytokines, hormones, enzymes, vaccines, etc. [24]. The encapsulation of known chemotherapeutic agent, temozolomide (TMZ) in PLGA NPs increased the drug efficacy with lower toxicity in healthy tissues by targeting the tumor-specific cells *in vitro* and *in vivo* [25]. In addition, PLGA also has the ability to deliver the active drug to the localized tumor environment [26]. Yet, the anticancer activity is only effective depending on the drug to be delivered in the target cells [5–7,27]. In the present study, we intended to synthesize a panel of novel QA derivatives and develop PLGA NPs to encapsulate the lead-QA derivative and assess its efficiency in GS tumor cells including patients' samples. Specifically, the ability to reduce metastatic activity of the GS cells was investigated via migration assay, the reactive oxygen species (ROS) signaling of treated GS cells and the activation of caspases 3/7 were measured.

Experimental section

Synthesis of quinic acid derivatives

Sulfate 3

Thionyl chloride (3.5 ml, 42 mmol) was added dropwise to a -10°C solution of 1,5-quinide (**2**) (5 g, 28 mmol) and Et_3N (16 ml, 112 mmol) in CH_3CN (350 ml). After reacting for 1 h at that temperature, the reaction mixture was quenched by addition of water (5 ml) until clearing of the reaction mixture. After CH_3CN removal under vacuum, the reaction mixture was extracted with EtOAc (3× 10 ml). The combined EtOAc extracts were washed with brine, dried over Na_2SO_4, filtered and concentrated under reduced pressure. The residue obtained was purified by flash chromatography using a mixture of hexane/EtOAc (7:3), yielding **3** in 50% yield (3.3 g, 14.0 mmol) as a white solid. ^{1}H NMR (300 MHz, DMSO-d_6): δ 6.51 (br. s, 1H), 5.61 (td, J = 6.2, 8.2 Hz, 1H), 5.42 (dd, J = 3.5, 5.9 Hz, 1H), 5.17 (dd, J = 3.2, 6.2 Hz, 1H), 2.65–2.57 (m, 1H), 2.54–2.48 (m, 1H, overlapped with DMSO), 2.26 (d, J = 12.9 Hz, 1H), 2.14 (dd, J = 6.2, 14.4 Hz, 1H); ^{13}C NMR (75 MHz, DMSO-d_6): δ 175.59, 79.04, 75.99, 71.82, 69.41, 36.15, 34.70. High-resolution mass spectrometry (HRMS) [M]$^-$ m/z calcd for $C_7H_8O_7S$ 235.9991, found 234.9936.

(1R,3R,4S,5R)-1,3,4-Tris((tert-butyldimethylsilyl)oxy)cyclohexane-1,3-carbolactone (4)

Imidazole (3.1 g, 30.8 mmol) was added to a solution of **2** (1.0 g, 5.7 mmol) in CH_3CN (25 ml) at 0°C, followed by TBDMSCl (3.7 g, 24.5 mmol). The reaction was heated at reflux and left stirring overnight. Water (5 ml) was added, the mixture concentrated under reduced pressure and the concentrate was extracted with EtOAc (3× 10 ml). The combined organic extracts were washed with Brine, dried over Na_2SO_4, filtered and concentrated under reduced pressure. The residue obtained was purified by flash chromatography using a mixture of hexane/EtOAc (98:2) as eluent, yielding **4** in 71% (2.1 g, 4.0 mmol) as an oil. ^{1}H NMR (500 MHz, $CDCl_3$): δ 4.52 (t, J = 5.4 Hz, 1H), 4.01 (t, J = 4.3 Hz, 1H), 3.81 (ddd, J = 4.0, 6.4, 10.7 Hz, 1H), 2.55 (d, J = 11.5 Hz, 1H), 2.21 (ddd, J = 2.6, 6.0, 10.9 Hz, 1H), 2.00–1.91 (m, 2H), 0.92–0.89 (m, 27H), 0.18 (s, 3H), 0.15 (s, 3H), 0.13 (s, 3H), 0.08–0.05 (m, 9H); ^{13}C NMR (125 MHz, $CDCl_3$): δ 176.40, 77.26, 77.00, 76.76, 76.13, 74.15, 67.98, 67.82, 40.60, 38.11, 26.03, 25.77, 25.64, 18.23, 18.11, 18.00, -2.81, -4.23, -4.40, -4.83, -4.85. HRMS [M + Cl]$^-$ m/z calcd for $C_{25}H_{52}O_5Si_3Cl$ 551.2811, found 551.2807.

(1R,3R,4S,5R)-1,3,4-Tris((tert-butyldiphenylsilyl)oxy)cyclohexane-1,3-carbolactone (5)

TBDPSCl (65.5 g, 0.24 mol) was added to a solution of quinide **2** (10.4 g, 0.06 mol) and imidazole (22 g, 0.33 mol) in acetonitrile (120 ml) and the mixture heated to reflux for 60 h. Water (50 ml) was added after cooling to room temperature, the residue concentrated under reduced pressure and extracted with CH_2Cl_2 (3× 50 ml). The combined organic layers were dried over anhydrous $MgSO_4$, filtered and concentrated under reduced pressure. The residue obtained was recrystallized in MeOH upon stirring overnight at room temperature, yielding **5** in 82% yield (43.4 g, 0.05 mol) as a white solid; ^{1}H NMR (500 MHz, $CDCl_3$): δ 7.60–7.54 (m, 6H), 7.43 (t, J = 7.7 Hz, 4H), 7.37–7.28 (m, 10H), 7.24–7.18 (m, 8H), 7.15–7.11 (m, 2H), 4.08 (t, J = 4.3 Hz, 1H), 3.84 (t, J = 5.4 Hz, 1H), 3.65–3.61 (m, 1H), 2.08 (d, J = 10.9 Hz, 1H), 1.75 (ddd, J = 2.6, 5.9, 11.0 Hz, 1H), 1.63 (t, J = 11.5 Hz, 1H), 1.35 (ddd, J = 2.3, 5.9, 11.3 Hz, 1H), 0.88 (s, 9H), 0.86 (s, 9H), 0.84 (s, 9H); ^{13}C NMR (125 MHz, $CDCl_3$): δ 175.01, 136.12, 135.82, 135.78, 135.73, 135.70, 135.44, 134.76, 133.97, 133.82, 133.44, 133.26, 133.09, 132.33, 130.13, 129.95, 129.93, 129.87, 129.68, 129.63, 127.88, 127.72, 127.57, 127.54, 75.06, 74.49, 68.87, 68.09, 39.49, 37.52, 27.11, 26.94, 26.68, 19.25, 19.14, 18.81; HRMS [M + Na]$^+$ m/z calcd for $C_{55}H_{64}O_5Si_3Na$ 911.3952, found 911.4066.

(1S,3S,4S,5R)-3,4-Bis[(tert-butyldiphenylsilyl)oxy]-1hydroxy-6-oxabicyclo[3.2.1]octan-7-one (6)

TBAF•3H_2O (7.7 g, 24.5 mmol) was added to a solution of **5** (21.8 g, 24.5 mmol) in THF (120 ml) and the mixture left stirring overnight. Reaction was quenched by addition of aqueous saturated NH_4Cl solution (50 ml), followed by concentration under reduced pressure to remove THF. The resulting mixture was extracted with CH_2Cl_2 (3 × 50 ml), and the combined organic layers dried with Na_2SO_4, filtered and concentrated under reduced pressure. The residue obtained was purified by flash column chromatography on silica gel with hexane/EtOAc (9:1) as eluent, to provide **6** as a white solid in 87% yield (13.9 g, 21.3 mmol). ^{1}H NMR (500 MHz, DMSO-d_6): δ 7.79–7.77 (m, 2H), 7.65–7.64 (m, 2H), 7.52–7.34 (m, 12H), 7.29–7.24 (m, 4H), 5.93 (s, 1H), 4.27 (t, J = 5.5, 1H), 4.22 (t, J = 4.2, 1H), 3.66 (ddd, J = 3.7, 5.9, 11.6 Hz, 1H), 2.44 (d, J = 11.5 Hz, 1H), 2.05 (ddd, J = 2.3, 6.0, 11.2 Hz, 1H), 1.96 (t, J = 11.5 Hz, 1H), 1.47–1.44 (m, 1H), 1.04 (s, 9H), 0.85 (s, 9H); ^{13}C NMR (125 MHz, DMSO-d_6): δ 176.13, 135.68, 135.63, 135.31, 135.05, 132.97, 132.41, 132.36, 130.43, 130.12, 129.93, 129.87, 128.12, 127.86, 127.77, 127.69, 74.70, 71.20, 68.79, 68.23, 26.91, 26.64, 22.10, 19.08, 18.50; HRMS [M + Cl]$^-$ m/z calcd for $C_{39}H_{46}O_5Si_2Cl$ 685.7414, found 685.2542.

(1R,3R,4S,5R)-N-benzyl-3,4-bis((tert-butyldiphenylsilyl)oxy)-1,5-dihydroxycyclohexane-1-carboxamide (7)

Benzylamine (34 μl, 0.31 mmol) was added to a solution of **6** (0.103 g, 0.16 mmol) and Et_3N (22 μl, 0.158 mmol) in THF (0.8 ml), and the mixture refluxed overnight under argon. The reaction was quenched with aqueous 1 M HCl solution, followed by extraction with CH_2Cl_2 (3× 5 ml). The combined organic layers were dried over Na_2SO_4, filtered and the solvent removed under reduced pressure. The residue was purified by flash column chromatography on silica gel using hexane/EtOAc (4:1) as eluent, providing **7** in 88% yield (0.106 g, 0.14 mmol) as a white solid. ^{1}H NMR (500 MHz, DMSO-d_6): δ 8.47 (t, J = 6.0 Hz, 1H), 7.75 (d, J = 7.4 Hz, 2H), 7.64 (d, J = 6.9 Hz, 2H), 7.51–7.46 (m, 3H), 7.45–7.38 (m, 5H), 7.34–7.24 (m, 10H), 7.21 (d, J = 6.9 Hz, 1H), 7.17–7.15 (m, 2H), 6.39 (d, *J* = 8.6 Hz, 1H), 5.87 (br. s, 1H), 4.21–4.14 (m, 2H), 3.93–3.89 (m, 2H), 3.43 (br. s, 1H), 2.31 (t, *J* = 12.0 Hz, 1H), 1.95 (dd, *J* = 4.3, 14.6 Hz, 1H), 1.61 (d, *J* = 14.3 Hz, 1H), 1.57–1.54 (m, 1H), 1.06 (s, 9H), 0.88 (s, 9H); ^{13}C NMR (125 MHz, DMSO-d_6): δ 177.56, 138.92, 135.75, 135.55, 135.36, 135.16, 133.49, 133.46, 133.31, 133.17, 129.98, 129.74, 129.63, 129.60, 128.18, 127.80, 127.60, 127.55, 127.48, 127.20, 126.73, 75.11, 74.17, 68.53, 67.56, 42.24, 26.98, 26.81, 19.12, 18.63; HRMS [M + Cl]$^-$ *m/z* calcd for $C_{46}H_{55}NO_5Si_2Cl$ 792.8149, found 792.3293.

(1R,3R,4S,5R)-N-allyl-3,4-bis((tert-butyldiphenylsilyl)oxy)-1,5-dihydroxycyclohexane-1-carboxamide (8)

Allylamine (56 μl, 0.75 mmol) was added to a solution of **6** (0.201 g, 0.31 mmol) and Et_3N (43 μl, 0.309 mmol) in THF (1.6 ml) and the mixture refluxed overnight under argon. After addition of further allylamine (56 μl, 0.75 mmol) and Et_3N (86 μl, 0.618 mmol), the mixture was left at 50°C for 3 days. The reaction was quenched with aqueous 1 M HCl solution, followed by extraction with EtOAc (3× 5 ml). The combined organic layers were dried over Na_2SO_4, filtered and the solvent removed under reduced pressure. The residue purified by flash column chromatography on silica gel using hexane/EtOAc (4:1) as eluent, providing **8** in 89% yield (0.195 g, 0.28 mmol) as a white solid. ^{1}H NMR (500 MHz, DMSO-d_6): δ 8.08 (t, *J* = 6.0 Hz, 1H), 7.74 (d, *J* = 7.4 Hz, 2H), 7.64 (d, *J* = 6.9 Hz, 2H), 7.50–7.46 (m, 3H), 7.44–7.38 (m, 5H), 7.34–7.25 (m, 8H), 6.43 (d, *J* = 8.6 Hz, 1H), 5.83 (s, 1H), 5.63 (tdd, *J* = 5.4, 10.5, 17.2 Hz, 1H), 5.02–4.96 (m, 2H), 4.14–4.10 (m, 1H), 3.88 (br. s, 1H), 3.58–3.53 (m, 1H), 3.41–3.37 (m, 2H), 2.29 (t, *J* = 12.3 Hz, 1H), 1.93 (dd, *J* = 4.6, 14.3 Hz, 1H), 1.59 (d, *J* = 14.3 Hz, 1H), 1.51 (dd, *J* = 3.2, 11.7 Hz, 1H), 1.06 (s, 9H), 0.88 (s, 9H); ^{13}C NMR (125 MHz, DMSO-d_6): δ 177.36, 135.75, 135.55, 135.35, 135.15, 134.63, 133.48, 133.29, 133.17, 130.00, 129.72, 129.63, 129.61, 127.82, 127.59, 127.55, 127.49, 115.30, 75.11, 74.15, 68.50, 67.55, 54.95, 41.12, 36.18, 26.99, 26.82, 19.12, 18.65; HRMS [M + Cl]$^-$ *m/z* calcd for $C_{41}H_{51}NO_5Si_2Cl$ 742.7992, found 742.3148.

(1R,3R,4S,5R)-3,4-bis((tert-butyldiphenylsilyl)oxy)-1,5-dihydroxy-N-methoxy-N-methylcyclohexane-1-carboxamide (9)

$AlMe_3$ (0.65 ml, 6.16 mmol) was added at 0°C to a solution of *N,O*-dimethylhydroxylamine hydrochloride (0.45 g, 4.61 mmol) in CH_2Cl_2 (4.6 ml) cooled and let stirring at room temperature for 1 h. The mixture was cooled at 0°C, a solution of **6** (1.00 g, 1.55 mmol) in CH_2Cl_2 (1.5 ml) was added dropwise and the mixture let refluxing overnight. Upon further addition of *N,O*-dimethylhydroxylamine hydrochloride (0.45 g, 4.61 mmol) and $AlMe_3$ (0.51 ml, 4.61 mmol) the mixture was left at reflux for another 24 h. The reaction was quenched with saturated NH_4Cl, acidified with HCl (1 M) to pH 4 and extracted with CH_2Cl_2. The combined organic layers were dried over Na_2SO_4, filtered and the solvent removed under reduced pressure. The obtained residue was purified by flash column chromatography on silica gel, using hexane/EtOAc (4:1) as eluent to deliver **9** in 32% yield (0.348 g, 0.49 mmol) as a white solid. ^{1}H NMR (500 MHz, DMSO-d_6): δ 7.70 (d, *J* = 6.9 Hz, 2H), 7.60 (d, *J* = 6.9 Hz, 2H), 7.51 (d, *J* = 6.9 Hz, 2H), 7.47–7.44 (m, 1H), 7.41–7.35 (m, 7H), 7.32 (t, *J* = 7.6 Hz, 2H), 7.27–7.22 (m, 4H), 5.66 (br. s, 1H), 5.36 (br. s, 1H), 4.07 (dd, *J* = 1.7, 15.5 Hz, 1H), 3.86 (br. s, 1H), 3.48 (br. s, 4H), 2.96 (br. s, 3H), 2.27–2.22 (m, 2H), 2.06 (d, *J* = 14.3 Hz, 1H), 1.87 (dd, *J* = 3.7, 14.0 Hz, 1H), 1.04 (s, 9H), 0.90 (s, 9H); ^{13}C NMR (125 MHz, DMSO-d_6): δ 135.71, 135.52, 135.37, 135.22, 133.68, 133.49, 133.18, 129.94, 129.63, 129.52, 129.50, 127.77, 127.58, 127.41, 75.04, 74.60, 70.24, 68.23, 68.01, 60.18, 37.82, 36.81, 26.93, 26.86, 19.12, 18.82; HRMS [M + Cl]$^-$ *m/z* calcd for $C_{41}H_{53}NO_6Si_2Cl$ 746.7941, found 746.3113.

((1R,3R,4S,5R)-3,4-bis((tert-butyldiphenylsilyl)oxy)-1,5-dihydroxycyclohexyl)(pyrrolidin-1-yl)methanone (10)

$AlMe_3$ (0.15 ml, 1.42 mmol) was added to a solution of pyrrolidine (0.12 ml, 1.44 mmol) in toluene (0.6 ml) and stirred for 30 min. A solution of **6** (0.30 g, 0.46 mmol) in toluene (0.6 ml) was further added and the mixture heated to reflux overnight. The reaction was quenched with MeOH and HCl (1 M), followed by extraction with EtOAc. The combined organic layers were washed with water, dried over Na_2SO_4, filtered and the solvent evaporated under reduced pressure. The obtained residue was purified by flash column chromatography on silica gel, using hexane/EtOAc (9:1) as eluent to deliver **10** in 65% yield (0.216 g, 0.30 mmol) as a white solid. ^{1}H NMR (500 MHz, DMSO-d_6): δ = 7.75 (d, *J* = 6.9 Hz, 2H), 7.65 (d, *J* = 6.9 Hz, 2H), 7.53 (d, *J* = 6.9 Hz, 2H), 7.50–7.39 (m, 6H), 7.37–7.26 (m, 8H), 6.58 (d, *J* = 7.4 Hz, 1H), 5.71 (s, 1H), 3.90–3.88 (m, 2H), 3.73–3.68 (m, 1H), 3.43 (dd, *J* = 2.9, 6.9 Hz, 1H), 3.16–3.12 (m, 1H), 2.97–2.92 (m, 1H), 2.87–2.82 (m, 1H), 2.30 (t, *J* = 12.6 Hz, 1H), 1.85 (d, *J* = 2.9 Hz, 2H), 1.71–1.63 (m, 3H), 1.59–1.64 (m, 2H), 1.06 (s, 9H), 0.87 (s, 9H); ^{13}C NMR (125 MHz, DMSO-d_6): δ 174.05, 135.72, 135.51, 135.37, 135.13, 133.55, 133.47, 133.24, 133.14, 130.01, 129.79, 129.68, 129.63, 127.83, 127.62, 127.60, 127.53, 75.84, 75.25, 68.14, 67.36, 47.35, 46.89, 37.84, 36.64, 26.95, 26.76, 26.00, 22.16, 19.13, 18.65; HRMS [M + Cl]$^-$ *m/z* calcd for $C_{43}H_{55}NO_5Si_2Cl$ 756.8149, found 756.2870.

((1R,3R,4S,5R)-3,4-bis((tert-butyldiphenylsilyl)oxy)-1,5-dihydroxycyclohexyl)(piperidin-1-yl)methanone (11)

$AlMe_3$ (0.10 ml, 0.95 mmol) was added to a solution of piperidine (0.09 ml, 0.91 mmol) in toluene (0.5 ml) and stirred for 30 min. A solution of **6** (0.20 g, 0.31 mmol) in toluene (0.5 ml) was further added and the mixture heated to reflux overnight. Upon further addition of piperidine (0.09 ml, 0.91 mmol) and $AlMe_3$ (0.10 ml, 0.95 mmol) the mixture was left at reflux for another 24 h. The reaction was quenched with MeOH and HCl (1 M), followed by extraction with EtOAc. The combined organic layers were washed with water, dried over Na_2SO_4, filtered and the solvent evaporated under reduced pressure. The obtained residue was purified by flash column chromatography on silica gel, using hexane/EtOAc (9:1) as eluent to deliver **11** in 51% yield (0.116 g, 0.16 mmol) as a white solid. ^1H NMR (500 MHz, DMSO-d_6): δ 7.73 (d, *J* = 6.9 Hz, 2H), 7.64–7.62 (m, 2H), 7.53–7.52 (m, 2H), 7.49–7.44 (m, 3H), 7.41–7.35 (m, 10H), 7.31–7.27 (m, 5H), 6.29 (d, *J* = 6.3 Hz, 1H), 5.88 (s, 1H), 4.10 (d, *J* = 6.3 Hz, 1H), 3.89–3.87 (m, 2H), 3.70 (d, *J* = 8.6 Hz, 1H), 3.45 (d, *J* = 2.9 Hz, 1H), 2.68 (br. s, 1H), 2.56 (br. s, 1H), 1.85–1.81 (m, 2H), 1.56 (br. s, 1H), 1.43–1.18 (m, 7H), 1.06 (s, 9H), 0.86 (s, 9H); ^{13}C NMR (125 MHz, DMSO-d_6): δ 173.68, 135.70, 135.51, 135.38, 135.16, 133.54, 133.49, 133.21, 133.17, 130.00, 129.81, 129.71, 129.62, 127.82, 127.67, 127.63, 127.51, 76.25, 75.10, 68.19, 67.52, 38.17, 37.58, 31.00, 26.94, 26.77, 25.33, 25.31, 23.91, 22.10, 19.14, 18.68; HRMS [M + Cl]$^-$ *m/z* calcd for $C_{44}H_{57}NO_5Si_2Cl$ 770.8305, found 770.3446.

Ethyl (1R,3R,4S,5R)-3,4-bis((tert-butyldiphenylsilyl)oxy)-1,5-dihydroxycyclohexane-1-carboxylate (12)

A mixture of lactone **6** (50 mg, 0.07 mmol) and amberlyst-15 (20 mg) in EtOH (1 ml) in a sealed tube was refluxed for 48 h. Reaction mixture was filtered, concentrated under reduced pressure and the residue obtained purified by flash chromatography on silica gel, using Hexane/EtOAc (90:10) as eluent to deliver **12** in 65 % yield (35 mg, 0.05 mmol). ^1H NMR (500 MHz, DMSO-d_6): δ 7.69 (d, *J* = 6.9 Hz, 2H), 7.58 (d, *J* = 6.9 Hz, 2H), 7.54 (d, *J* = 6.9 Hz, 2H), 7.44 (d, *J* = 6.9 Hz, 3H), 7.40–7.30 (m, 7H), 7.27–7.21 (m, 4H), 5.45 (s, 1H), 4.59 (d, *J* = 3.4 Hz, 1H), 4.34–4.30 (m, 1H), 3.95 (br. s, 1H), 3.79–3.70 (m, 2H), 3.52 (br. s, 1H), 2.18–2.16 (m, 1H), 2.08–1.99 (m, 2H), 1.81 (dd, *J* = 2.3, 13.2 Hz, 1H), 1.03 (s, 9H), 0.92 (s, 9H), 0.90–0.83 (m, 3H); ^{13}C NMR (125 MHz, DMSO-d_6): δ 173.31, 135.76, 135.57, 135.51, 135.31, 134.06, 134.00, 133.55, 133.22, 129.92, 129.55, 129.50, 129.39, 127.75, 127.46, 127.38, 73.81, 72.17, 68.52, 68.00, 59.50, 37.80, 36.62, 26.94, 19.13, 18.88, 13.66; HRMS [M + Cl]$^-$ *m/z* calcd for $C_{41}H_{52}O_6Si_2Cl$ 731.2991, found 731.2992.

(3aS,4R,6R,7aR)-4,6-dihydroxy-6-(hydroxymethyl)hexahydrobenzo[d][1,3,2]dioxathiole 2,2-dioxide (13)

$NaBH_4$ (400 mg, 10.6 mmol) was added to a 0°C solution of sulfate 3 (500 mg, 2.12 mmol) in EtOH (8 ml) and the mixture left stirring at that temperature for 1 h. After addition of few drops of brine, the solid was filtered out and solvent removed under reduced pressure. The residue obtained was purified by flash column chromatography on silica gel, using MeOH/EtOAc (2:8) as eluent to deliver **13** in 77% yield (393 mg, 1.64 mmol). ^1H NMR (300 MHz, DMSO-d_6): δ 5.00 (s, 1H), 4.64 (d, *J* = 4.1 Hz, 1H), 4.23 (t, *J* = 4.7 Hz, 1H), 4.00 (d, *J* = 4.7 Hz, 1H), 3.90 (t, *J* = 4.1 Hz, 1H), 3.80 (d, *J* = 6.4 Hz, 1H), 3.26 (dd, *J* = 2.3, 6.4 Hz, 1H), 3.16 (d, *J* = 4.7 Hz, 1H), 1.94–1.87 (m, 1H), 1.78–1.65 (m, 3H); ^{13}C NMR (75 MHz, DMSO-d_6): δ 77.64, 76.08, 74.42, 74.08, 69.27, 43.93, 38.77; HRMS [M-H]$^-$ *m/z* calcd for $C_7H_{11}O_7S$ 239.0226, found 239.0127.

(1R,2S,3R,5R)-2,3,5-tris((tert-butyldimethylsilyl)oxy)-5-(hydroxymethyl)cyclohexan-1-ol (14)

$LiAlH_4$ (0.01 g, 0.29 mmol) was added in portions to a 0°C cooled solution of **4** (0.10 g, 0.19 mmol) in Et_2O (10 ml). The reaction was let stirring at this temperature for 30 min, water (1 ml) was added and the residue concentrated under reduced pressure. The aqueous layer was extracted with EtOAc (3× 10 ml), the combined organic layers washed with brine, dried over Na_2SO_4, filtered and concentrated under reduced pressure. The obtained residue was purified by flash column chromatography on silica gel, using hexane/EtOAc (85:15) as eluent to deliver **14** in 74% yield (0.07 g, 0.14 mmol) as a white solid. ^1H NMR (500 MHz, DMSO-d_6): δ 5.00 (br. s, 1H), 4.24 (br. s, 1H), 3.87 (td, *J* = 2.1, 11.7 Hz, 1H), 3.65–3.54 (m, 2H), 3.56 (dd, *J* = 4.3, 10.6 Hz, 1H), 3.27–3.25 (m, 1H), 1.85–1.82 (m, 1H), 1.78–1.70 (m, 2H), 1.56 (d, *J* = 13.7 Hz, 1H), 0.87 (s, 9H), 0.86 (s, 9H), 0.80 (s, 9H), 0.04–0.06 (m, 18H); ^{13}C NMR (125 MHz, DMSO-d_6): δ 76.36, 73.80, 69.53, 68.28, 67.28, 37.35, 36.64, 25.96, 25.85, 25.64, 18.03, 17.88, 17.84, -2.22, -4.42, -4.57, -4.65, -5.10. HRMS [M + Na]$^+$ *m/z* calcd for $C_{25}H_{56}O_5Si_3Na$ 543.3326, found 543.3289.

(1R,2S,3R,5R)-2,3,5-tris((tert-butyldiphenylsilyl)oxy)-5-(hydroxymethyl)cyclohexan-1-ol (15)

$LiAlH_4$ (0.25 g, 6.60 mmol) was added in portions to a 0°C cooled solution of **5** (3.93 g, 4.40 mmol) in Et_2O (22 ml). The reaction was let stirring at this temperature for 1 h followed by slow addition of EtOAc (2 ml) for dilution. Water (2 ml) was added dropwise and the white precipitate formed was filtered out through celite and dried over Na_2SO_4. After concentration under reduced pressure, the residue was purified by flash column chromatography on silica gel, using hexane/EtOAc (8:2) as eluent to deliver **15** in quantitative yield (3.93 g, 4.40 mmol) as a white solid ^{1}H NMR (300 MHz, $CDCl_3$): δ 7.73 (d, *J* = 8.2 Hz, 2H), 7.62 (d, *J* = 7.6 Hz, 2H), 7.55 (d, *J* = 8.2 Hz, 2H), 7.43 (dd, *J* = 8.2, 9.4 Hz, 4H), 7.33–7.14 (m, 18H), 7.01–6.96 (m, 2H), 3.82 (br. s, 1H), 3.59 (d, *J* = 2.9 Hz, 1H), 3.50 (d, *J* = 12.3 Hz, 1H), 2.69 (dd, *J* = 11.2, 15.3 Hz, 2H), 2.42 (t, *J* = 12.3 Hz, 1H), 2.10 (dd, *J* = 3.8, 14.4 Hz, 1H), 1.73 (d, *J* = 14.6 Hz, 1H), 1.57 (br. s, 1H), 1.23–1.19 (m, 2H), 1.09 (s, 9H), 0.91 (s, 9H), 0.80 (s, 9H); ^{13}C NMR (75 MHz, $CDCl_3$): δ 136.29, 136.06, 135.95, 135.92, 135.21, 135.11, 134.47, 134.08, 133.57, 133.46, 129.72, 129.46, 127.65, 127.57, 127.45, 127.39, 127.34, 77.63, 74.18, 70.07, 69.99, 68.68, 39.84, 37.10, 27.23, 27.12, 26.92, 19.56, 19.34, 18.86; HRMS [M + Cl]$^-$ *m/z* calcd for $C_{55}H_{68}O_5Si_3Cl$ 927.8905, found 927.4029.

(1R,3R,4S,5R)-4,5-bis((tert-butyldiphenylsilyl)oxy)-1-(hydroxymethyl)cyclohexane-1,3-diol (16)

$NaBH_4$ (0.25 g, 6.75 mmol) was added in portions to a 0°C cooled solution of **6** (0.88 g, 1.35 mmol) in ethanol (10 ml). The reaction was let to reach room temperature and let stirring overnight. The reaction was cooled at 0°C, quenched with brine (10 ml) and let stirring for 30 min at room temperature. The residue was concentrated under reduced pressure, and extracted with EtOAc (3× 10 ml). The combined organic layers were washed with brine, dried over Na_2SO_4, filtered and the volatiles removed under reduced pressure. The residue obtained was purified by flash column chromatography on silica gel, using hexane/EtOAc (6:4) as eluent to deliver **16** in 92% yield (0.81 g, 1.24 mmol) as a white solid. ^{1}H NMR (500 MHz, DMSO-d_6): δ 7.77 (d, *J* = 6.9 Hz, 2H), 7.63 (dd, *J* = 1.0, 9.7 Hz, 2H), 7.56 (dd, *J* = 1.7, 7.4 Hz, 2H), 7.46–7.35 (m, 10H), 7.32 (t, *J* = 7.4 Hz, 2H), 7.27 (t, *J* = 7.4 Hz, 2H), 4.67 (d, *J* = 4.0 Hz, 1H), 4.15 (s, 1H), 3.99–3.89 (m, 3H), 3.57 (br. s, 1H), 2.98 (dd, *J* = 6.0, 11.2 Hz, 1H), 2.70 (dd, *J* = 5.7, 10.9 Hz, 1H), 2.06 (t, *J* = 12.1 Hz, 1H), 1.65 (dd, *J* = 3.5, 15.5 Hz, 1H), 1.55 (d, *J* = 14.9 Hz, 1H), 1.42 (dd, *J* = 2.5, 11.9 Hz, 1H), 1.06 (s, 9H), 0.91 (s, 9H); ^{13}C NMR (125 MHz, DMSO-d_6): δ 135.80, 135.55, 135.51, 135.32, 133.91, 133.81, 133.50, 133.31, 129.86, 129.72, 129.60, 129.56, 127.73, 127.59, 127.56, 127.48, 74.69, 71.73, 68.71, 68.63, 67.75, 38.19, 35.00, 26.93, 26.83, 19.17, 18.60. HRMS [2M + Na]$^+$ *m/z* calcd for $C_{78}H_{100}O_{10}Si_4Na$ 1332.6318, found 1332.6217.

(1R,2R,3R,5S)-2,3,5-tris((tert-butyldiphenylsilyl)oxy)-5-(((methylsulfonyl)oxy)methyl)cyclohexyl methanesulfonate (17)

Mesyl chloride (0.28 g; 2.46 mmol) was added dropwise at 0°C to a cooled mixture of diol **15** (1.00 g, 1.11 mmol) and Et_3N (0.30 g, 2.89 mmol) in Et_2O (6 ml) and the mixture left stirring at that temperature for 2 h. Et_3N (0.23 g, 2.23 mmol) was further added, followed by TMSCl (0.25 g, 2.23 mmol) to trap the unreacted diol in the form of correspondent silyl ether. The mixture was then allowed to reach room temperature and quenched with H_2O (5 ml). The aqueous layer was extracted with CH_2Cl_2 and the organic layers combined dried over $MgSO_4$, filtered and concentrated under reduced pressure. The residue obtained was purified by flash column chromatography on silica gel, using hexane/EtOAc (4:1) as eluent to deliver **17** in 86% yield (1.00 g, 0.95 mmol) as a white foam. ^{1}H NMR (500 MHz, $CDCl_3$): δ 7.81 (dd, *J* = 1.0, 8.0 Hz, 2H), 7.72 (dd, *J* = 1.0, 8.0 Hz, 2H), 7.62 (dd, *J* = 1.1, 8.0 Hz, 2H), 7.53–7.50 (m, 2H), 7.50–7.31 (m, 13H), 7.29–7.26 (m, 1H), 7.23–7.17 (m, 6H), 7.04 (t, *J* = 8.0 Hz, 2H), 4.55 (q, *J* = 3.1 Hz, 1H), 4.06–4.05 (m, 1H), 3.28–3.24 (m, 1H), 2.99 (d, *J* = 10.3 Hz, 1H), 2.90 (dd, *J* = 1.1, 9.7 Hz, 1H), 2.61 (s, 3H), 2.56 (s, 3H), 2.26 (d, *J* = 14.9, 1H), 2.15 (dd, *J* = 2.3, 15.0 Hz, 1H), 1.25–1.22 (m, 1H), 1.19 (s, 10H), 0.99 (s, 9H), 0.84 (s, 9H); ^{13}C NMR (125 MHz, $CDCl_3$): δ 136.18, 136.07, 135.88, 135.71, 135.65, 134.57, 134.19, 133.71, 132.50, 132.17, 130.14, 129.87, 129.72, 129.64, 129.58, 127.96, 127.68, 127.60, 127.51, 76.89, 74.51, 72.04, 71.22, 68.11, 38.19, 37.78, 36.78, 32.72, 27.09, 26.91, 26.66, 19.48, 19.32, 18.76. HRMS [M + Na]$^+$ *m/z* calcd for $C_{57}H_{72}O_9S_2Si_3Na$ 1071.3816, found 1071.3826.

Characterization of compounds

All synthesis was carried out in oven-dried glassware under inert atmosphere. Anhydrous dichloromethane and triethylamine were obtained using PureSolv Micro multi-unit purification system. Acetonitrile was left standing over 3 Å molecular sieves and used without further drying. All other reagents were purchased from Sigma Aldrich (MO, USA) or TCI and used without purification. Reactions were monitored through thin-layer chromatography (TLC) with commercial silica gel plates (Merck silica gel, 60 F254, Darmstadt, Germany). Plates were stained with cerium ammonium molybdate and subsequently developed for visualization under UV lights at 254 nm. Flash column chromatography was performed on silica gel 60 (40–63 μm) as stationary phase. ^{1}H NMR spectra were recorded at 300 MHz and ^{13}C NMR spectra at 75 MHz in a 300 MHz Varian Mercury spectrometer (Varian, CA, USA) or alternatively, ^{1}H and ^{13}C spectra were recorded at 500 MHz and 125 MHz respectively in a JEOL ECZR 500 instrument (JEOL, Tokyo, Japan) (Supplementary data). $CDCl_3$ or DMSO-d_6 were used as solvents for NMR analysis. Chemical shifts (δ) are reported in ppm referenced to the residual peak of the deuterated solvent (δ2.50 for DMSO-d_6, δ7.26 for $CDCl_3$) or TMS peak (δ 0.00) for ^{1}H NMR and to DMSO-d_6 (δ 39.52) or $CDCl_3$ (δ 77.16) for ^{13}C NMR. The following abbreviations were used to describe peak splitting patterns: s = singlet, d = doublet, t = triplet and m = multiplet. Coupling constants J were reported in Hertz (Hz). High-resolution mass spectra were recorded on a Waters ESI-TOF MS spectrometer (Waters, MA, USA).

Cell culture

The human glioblastoma cell lines SNB19, LN229 and a noncancerous cell line, mouse embryonal fibroblast (MEF) cells were used to test the anticancer effect of QA derivatives. Both LN229 and SNB19 exhibit mutated p53 proteins. LN229 was established from a patient with right frontal parieto-occipital glioblastoma with mutated p53 (TP53) and homozygous deletions in the p16 and p14ARF tumor suppressor genes. SNB19 was derived from a patient with the left parietooccipital glioblastoma tumor. MEF cells exhibit an E10.5 genotype with Vin +/+ (vinculin), and has p53 function, providing a preliminary model for comparing p53 activity, and was obtained from Wolfgang H. Ziegler (Hannover Medical School, Hannover, Germany) [28,29]. The Dulbecco's Modified Eagle Medium-high glucose (DMEM) (Biowest, #L0102-500; Biowest, Nuaillé, France) supplemented with 10% fetal bovine serum (FBS) (Biowest, #S181H-500), 100 U/ml Penicillin, 0.1 mg/ml Streptomycin (Sigma-Aldrich, #P4333), 0.025 mg/ml Ampicillin B (Sigma-Aldrich, #A9528), 0.05% 1× trypsin/EDTA (ThermoFisher Scientific, #25300, MO USA), was used to grow these cell lines. Cell cultures were incubated at 37°C supplemented with 5% CO^2 in a humidified incubator. Cultures were passaged at 70% confluence, following standard cell passaging protocol.

QA Derivatives preparation & preliminary cytotoxicity screening

Newly synthesized QA derivatives were dissolved in dimethyl sulfoxide (DMSO) (Sigma Aldrich, #D2650) [30] to obtain an initial concentration of 100 mM. Intermediate dilutions (2 and 4 mM) were prepared from the stock concentration, 100 mM solution. The compounds were screened for cell growth inhibition potential in glioblastoma to measure their chemotherapeutic potential. LN229 were seeded on 12-well plates with a cell density of 1×10^5 cell/well. After 48 h, the cells were treated with 100 μM concentration of each quinic acid derivatives. Untreated, negative control (DMSO) were also maintained. Cell viability was quantified following the trypan blue exclusion method. The live and dead cell populations were counted using a Countess II FL Hemocytometer (ThermoFisher Scientific, #A25750) and the percentage of cell growth inhibition was calculated using the Formula (1):

$$\text{Cell growth inhibitaion (\%)} = \frac{\textit{Mean Nr. of untreated cells (DMSO control)} - \textit{Mean Nr. of treated cells} \times 100}{\textit{Mean Nr. of untreated cells (DMSO control)}} \qquad \text{(Eq. 1)}$$

Three biological and two technical repeats were maintained to obtain the statistical data. The compound that expresses higher cytotoxic effect was selected for further *in-vitro* analysis.

Dose- & time-dependent inhibition assay

Dose- and time-dependent inhibition assay is the next level of screening in which the potency of the top lead compound, QA-16, was measured where the correlation between the dosage of the compound and the growth inhibition was measured [31]. LN229 and SNB19 cells were seeded on 12-well plates with a density of 1×10^5 cell/well. After 48 h, the cells were treated with 100, 75, 50, 25 and 10 μM concentrations of QA-16, TMZ (positive control) and DMSO (0.1%, negative control). Cell viability was quantified after 48 h using the Trypan Blue Exclusion method as outlined above. Semi-log dose-response curves were plotted to calculate the IC_{50} of the compounds specific for each cell line. The cytotoxicity of the QA-16 at a concentration of 28 μM was evaluated in non-cancerous cell line, MEF. Also, time-dependent effect of lead compound was tested against the growth of LN229 and SNB19 cells with the IC_{50} concentration for 24, 48 and 72 h.

The percentage of cell growth inhibition was calculated using the Equation 1. Three biological and technical repeats were used to obtain the statistically significant results.

Ex-vivo cell growth inhibition assay in patient-derived cells

The low-passage primary patient cell lines, MMK1 and RN1 (gifted by Dr. Brett Stringer QIMR Berghofer, Medical Research Institute, Australia) were used for testing the efficacy of the QA-16. Both MMK1 and RN1 cells were seeded with the density of 1×10^5 cells/well and maintained in an incubator at 37°C in humidified air with 5% CO_2. Cells at 70% confluent growth were treated with IC_{50} concentration (28 μM) of the QA-16. Treated cultures were incubated for 48 h and the percentage of cell growth inhibition was quantified by trypan blue assay as described above. All the experiments were conducted with three biological and technical repeats to test the significance.

Wound healing scratch assay

An effective anticancer drug against GS should be able to slow down or halt the cell proliferation and migration, thus the scratch assay is a simple method employed to test the potential of QA-16 affecting the migration of the cells. A cell density of 2×10^5 cells/well of LN229 and SNB19 were seeded in 12-well plates and grown overnight at 37°C with 5% CO_2 to obtain a monolayer of cells which was scratched using a pipette tip for further experimentation. The debris was removed, edges of the scratch were smoothened by washing the cells with 1 ml of the complete medium. This is followed by addition of 1 ml of the culture medium containing 1% FBS and the IC_{50} concentration of the compound. Cells without the compound and with only medium containing 1% FBS was used as an untreated control. The scratch area was imaged under light microscope at 2 h interval for a period of 8 h to measure the distance between the edges of the scratch at each point and the percent of area covered at 0-h distance.

Preparation of QA-16 loaded PLGA nanoparticle (QA-16-NPs)

Poly (lactic-*co*-glycolic acid) (PLGA) 75:25 Purasorb® PDLG 7502A (MW 17,000 Da) was donated by Corbion Purac (Amsterdam, The Netherlands). Dichloromethane and polyvinyl alcohol (PVA) were obtained from Sigma–Aldrich (Steinheim, Germany). MilliQ-water and other reagents used in the experiments were of analytical grade. PLGA nanoparticles were produced by the oil-in-water simple emulsion technique, following the modified solvent emulsification-evaporation protocol [32]. Briefly, 15 mg of PLGA was dissolved in 2 ml of dichloromethane along with 5 mg of top lead compound (QA-16) and the solution was sonicated for 30 s at 70% of amplitude using a Q125 Sonicator (QSonica Sonicators, CT, USA). This phase of solution was poured into 8 ml of a 2% PVA (w/v) and later the dichloromethane was removed after constant stirring in magnetic stirrer for 4 h. Unloaded nanoparticles were also produced.

Particle size, polydispersity index & morphology of QA-16-NP

The particle size and polidispersity index (PDI) were analyzed by dynamic light scattering using a Delsa™ Nano C (Beckman Coulter, Inc., CA, USA) after a proper dilution of the nanoparticle suspensions. All the samples were analyzed in triplicate. The morphology of the QA-16-NP was observed by scanning electron microscopy (SEM) on a JSM-7001F microscope from JEOL (Tokyo, Japan). The nanoparticle suspensions were placed onto metal stubs, dried overnight and vacuum-coated with a layer of gold/palladium during 20 s with a current of 25 mA.

Cytotoxicity effect of QA-16-NPs on glioblastoma cell lines

The glioblastoma cell lines SNB19 and LN229, were seeded on 12-well plates with a cell density of 1×10^5 cell/well. 70% confluent cells were treated with IC_{50} concentration of QA-16, QA-16-NPs s and PGLA alone (NPs). Cell death was quantified at 48 h and 72 h by trypan blue as described above. All the experiments were conducted with three biological and technical repeats to test the significance.

Apoptosis assay by annexin V-FITC/PI staining

To determine whether the GS cells were sensitized to apoptosis by the action of QA-16, Annexin V-FITC and PI staining was performed. In brief, glioblastoma cell lines, SNB19 and LN229, were cultured in 6-well plates with an initial density of 0.8 × 10^6 cells/well using the complete medium. After 24 h, the medium was replaced with serum-free medium and incubated at 37°C overnight. Cells were treated with IC_{50} concentration of the QA-16, QA-16-NPS s conjugate. In addition, untreated and DMSO (0.1%) treated conditions were also maintained. After 24 h of treatment, cells were trypsinized, centrifugation at 3000 rpm for 10 min and the cell pellets were resuspended in ice-cold 1× annexin-binding buffer. Annexin V-FITC and PI working solutions were added to the cell suspension as suggested by the manufacturer protocol. The cells were transferred to a clear-bottom, black 96-well plate and incubated in dark conditions at room temperature for 15 min prior to the fluorescence measurement. The fluorescence images were analyzed for the quantification of necrotic, apoptotic and non-apoptotic cell percentages [3,33] using an Invitrogen Evos XL™ Digital Inverted Brightfield and Phase Contrast Microscope (ThermoFisher Scientific, #Invitrogen™ AME3300).

Caspases 3/7 activity assay

The Caspases 3/7 Activity Assay was performed in SNB19 and LN229 cells. The cells were seeded on 96-well plates in complete medium at an initial density of 1 × 10^4 cells/well and incubated overnight at 37°C with 5% CO_2. The cells were treated with IC_{50} concentration of the QA-16, QA-16-NPs conjugate and NPs along with DMSO (0.1%) and untreated cells and incubated for 5 h. The cells were allowed to equilibrate to room temperature for 30 min and 100 μl of Caspase-Glo reagent (Glo® 3/7 Assay kit, Promega, WI, USA) was added to the treated, untreated and blank wells. The plates were placed on an agitator for 30 s at 300 to 500 rpm and incubated for 1 h in dark conditions. After incubation, the luminescence signal was measured using a plate-reading luminometer (Tecan, Spark, Männedorf, Switzerland). The fold change in caspase 3/7 was calculated using Formula (2).

$$\%\ Change\ of\ Activity = \frac{(F_{test} - F_{blank})}{(F_{control} - F_{blank})} \times 100\% \qquad \text{(Eq. 2)}$$

Where F_{test} is the luminescence from the treated wells, $F_{control}$ is the luminescence from the untreated wells, and F_{blank} is the luminescence from the unstained wells.

Reactive oxygen species assay

Cell lines, SNB19 and LN229, were seeded in 12-well plates with an initial density of 1 × 10^5 cells/well in complete medium and incubated overnight at 37°C with 5% CO_2. After incubation, the medium was replaced with serum-free medium upon treatment. The treatment conditions were maintained as same as the apoptotic assay mentioned above. In addition, 30% H_2O_2 was used as a positive control. After the treatment, the plate was incubated for 5 h at 37°C with 5% CO_2. Cells were trypsinized and centrifuged at 3000 rpm for 10 min. The supernatant was discarded, and the cells were resuspended in 2 μM 2′,7′-dichlorodihydrofluoresceindiacetate (H2DCFDA) [34]. Further, the cells were incubated for 10 min in dark condition, washed with 500 μl of pre-warmed PBS and finally centrifuged at 3000 rpm for 10 min. Cells were recovered in a 100 μl serum free medium and incubated in a 96 black well plate for 20 min at 37°C with 5% CO_2. Fluorescent intensity was measured using a Plate-reading Luminometer (Tecan, Spark) at 485 and 538 nm. The fold change of intracellular ROS was calculated using the Formula (2).

Statistical analysis

The data were shown as means ± standard deviation of all biological and technical replicates. Statistical significance was evaluated by equal variance *t*-tests, and results were considered statistically significant if the $p < 0.05$.

Results

Synthesis of quinic acid derivatives

The compounds to be tested were prepared as described in Figure 1. 1,5-Quinide **2** was first prepared by acid-promoted lactonization of quinic acid **1** as previously described [35]. The hydroxyl groups were converted into sulfate **3** and silyl ethers **4** and **5**, thus the first library of compounds was created. Conventional protective group procedures, namely treatment with thionyl chloride or excess chlorosilanes in the presence of imidazole allowed the installation of sulfate and silyl ethers respectively. Selective desilylation of the tertiary silyl ether **5** was accomplished by treatment with a stoichiometric amount of TBAF hydrate. The second library of compounds, corresponding to amides **7–11** or the ester **12** was obtained from lactone ring-opening of **6** upon treatment with primary and secondary amines, requiring the use of superstoichiometric amounts of trimethylaluminum for the later. Despite

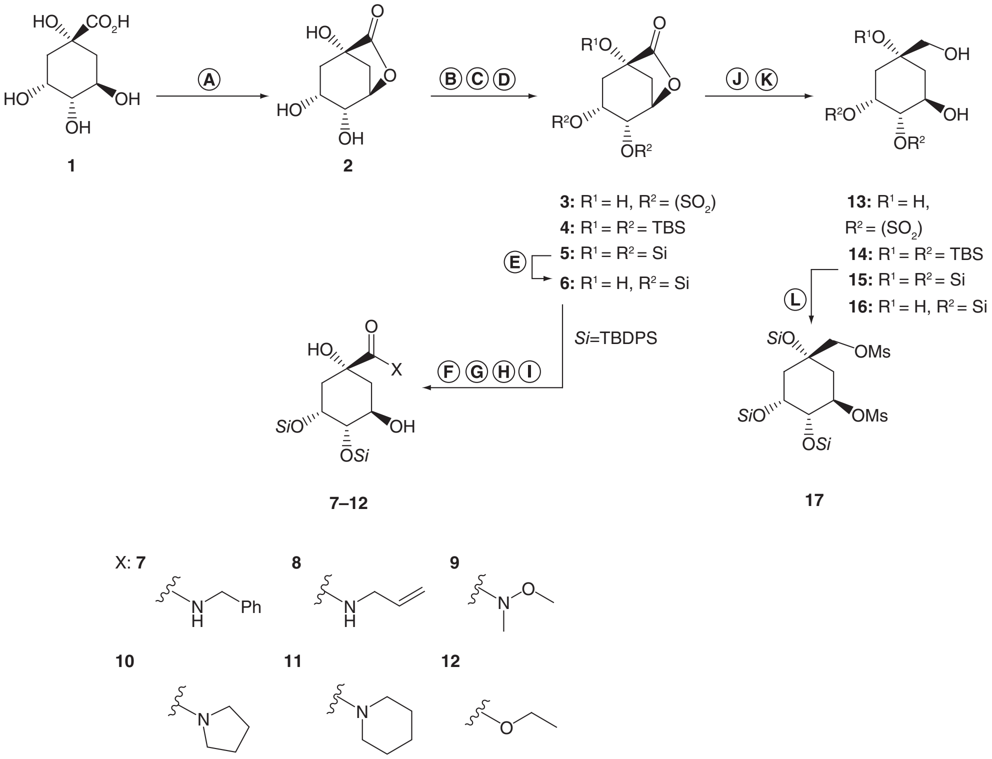

Figure 1. Reagents and conditions. **(A)** Amberlyst, CH_3CN, reflux; **(B)** $SOCl_2$ (1.5 eq.), Et_3N (4 eq.), CH_3CN, -10°C, 50% of **3**; **(C)** TBDMSCl (4.3 eq.), imidazole (5.4 eq.), CH_3CN, reflux, 71% of **4**; **(D)** TBDPSCl (4.0 eq.), imidazole (5.5 eq.), CH_3CN, reflux, overnight, 82% of **5**; **(E)** TBAF•$3H_2O$ (1 eq.), THF, r.t., 5 h, 87%; **(F)** NH_2R (2–4 eq.), Et_3N (1–2 eq.), THF, reflux, 1–3 days, 88–89% of **7–8**; **(G)** $MeONH_2$•HCl (6 eq.), $AlMe_3$ (6 eq.), CH_2Cl_2, r.t. to reflux, overnight, 32% of **9**; **(H)** NHR_2 (3–6 eq.), $AlMe_3$ (3–6 eq.), toluene, reflux, 51–65% of **10–11**; **(I)** amberlyst-15, EtOH, reflux in sealed tube, 65% of **12**; **(J)** $NaBH_4$ (5 eq.), EtOH, r. t., 77–92% of **13** or **16**; **(K)** $LiAlH_4$ (1.5 eq.), Et_2O or THF/Et_2O, 0°C, 30 min, 74% to quantitative of **14–15**; **(l)** MsCl (2.2 eq.), Et_3N (2.6 eq.), Et_2O, 0°C, 86%.
QA: Quinic acid; r.t.: Room temperature.

the good yields (51–88%) of amides **7**, **8**, **10** and **11**, Weinreb amide **9** was found to be only 32%. Ethyl ester **12** was prepared by ethanolysis of lactone **6**. Reduction of lactones **3**–**6** with $NaBH_4$ or $LiAlH_4$ resulted in opening of the ring and subsequent reduction of the terminal carbonyl group to the corresponding primary alcohols, providing the last library of compounds including, **13**–**16**. Diol **15** was further transformed into mesylated derivative **17** by treatment with mesyl chloride.

Cytotoxicity effect of quinic acid derivatives

Cytotoxicity effects for series of quinic acid derivatives **3**–**5** and **7**–**17** at the concentration of 100 μM, against glioblastoma cell line, LN229 was assessed by Trypan Blue exclusion assay. It was found that the lactone moiety of 1,5-quinide derivatives **3**–**5** did not confer any inhibitory effect. However, all tested quinic acid-derived amides containing the TBDPS moiety at C-3 and C-4 were found to induce 25–66% cell growth inhibition. The related ethyl ester derivative **12** did not provide any additional inhibitory effect on comparison with amides **7**–**11**. Contrary to the lack of cytotoxicity in the reduced forms of quinides **3** and **4**, diol **15** showed considerable inhibitory effect when compared with the corresponding quinide form **5**. Notwithstanding the increase in cell growth inhibition by mesylation of the alcohol moieties in **17**, exposure of the tertiary hydroxyl moiety in compound **16** was recognized as more effective. Thus, from the series of compounds tested, bis-TBDPS containing derivative **16**, designated

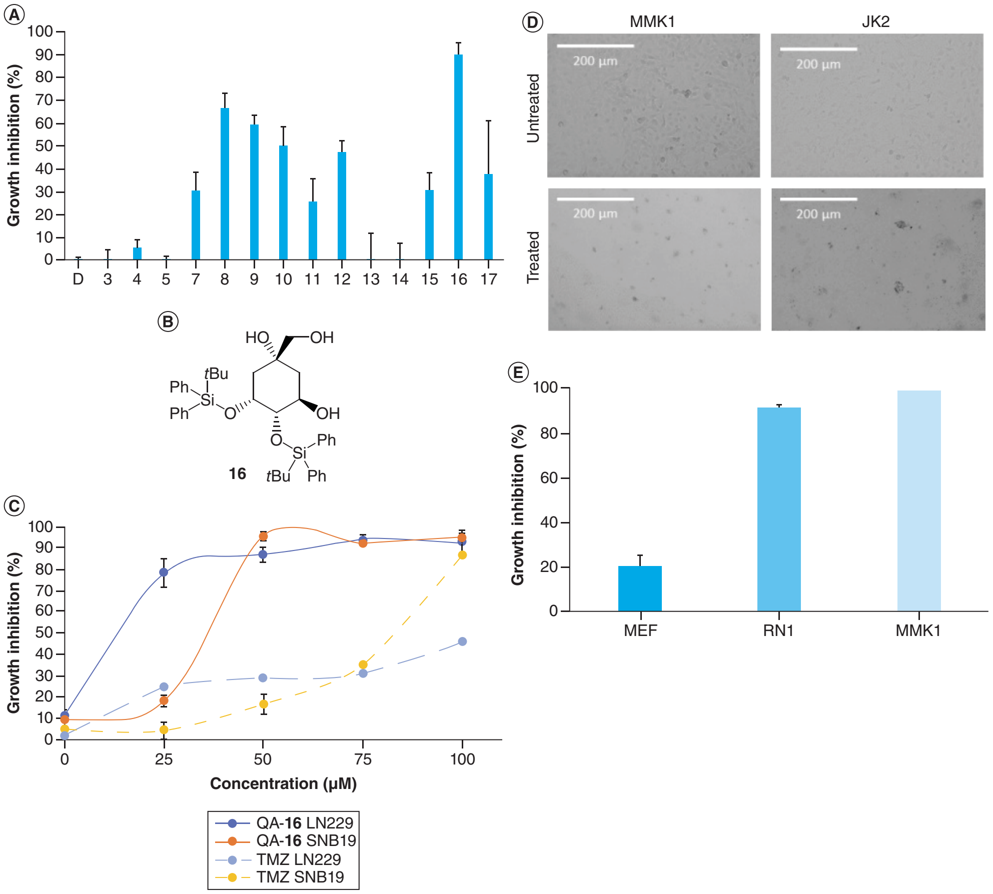

Figure 2. Cell viability assay. (A) Percentage of growth inhibition for series of compounds **3–17**; **(B)** Structure of top lead compound QA-**16**. **(C)** Dose-dependent analysis of QA-**16** and TMZ (positive control). **(D)** Microscopic observation of patients' derived cell lines (RN1 and MMK1) in QA-**16** treated and control. **(E)** Percentage of growth inhibition in MEF (control) and RN1 and MMK1 at a concentration of 28 μM. The significant differences between treated and controls groups are shown as $^*p < 0.05$.
QA: Quinic acid; MEF: Mouse embryonal fibroblast.

as **QA-16**, was identified to have the best inhibitory effect against LN229 with the inhibition percentage of 90.12 ± 5.10 % and hence it was selected and used for further assays (Figure 2A).

The IC_{50} value of QA-**16** (Figure 2B) against LN229 and SNB19 was found to be 10.66 ± 4.71 μM and 28.22 ± 9.87 μM, respectively, whereas TMZ (positive control) was found to have higher IC_{50} of 87.76 ± 6.92 μM and 84.39 ± 2.60 μM for the respective cell lines (Figure 2C). Also, the cytotoxicity of QA-**16** was concurrently tested against patient-derived cell line RN1, MMK1 and mouse embryonic fibroblast (MEF) as described in the method section. QA-**16** exhibited a higher percentage of inhibition in patient-derived cell line RN1 (91.33%) and MMK1 (99.03%) when compared with DMSO which showed around 5%. The phase-contrast microscopic observation revealed the appearance of monolayer of cells in the untreated condition with the disrupted cell growth in the treated conditions (Figure 2D & E). The growth inhibition (%) was found to be lower in the noncancerous cell, MEF, (19.19%) when compared with patients' cell line. These data confirmed the better cytotoxicity effect of QA-**16** on glioma cell lines and in patients' derived cell line with the least effect on noncancerous cells. Although all established chemotherapeutic or biological anti-cancer drugs have shown varied anti-tumor effects, QA-**16** exhibited similar percentage of cell growth inhibition of ∼100% at 100 μM concentration in two GBM cell lines,

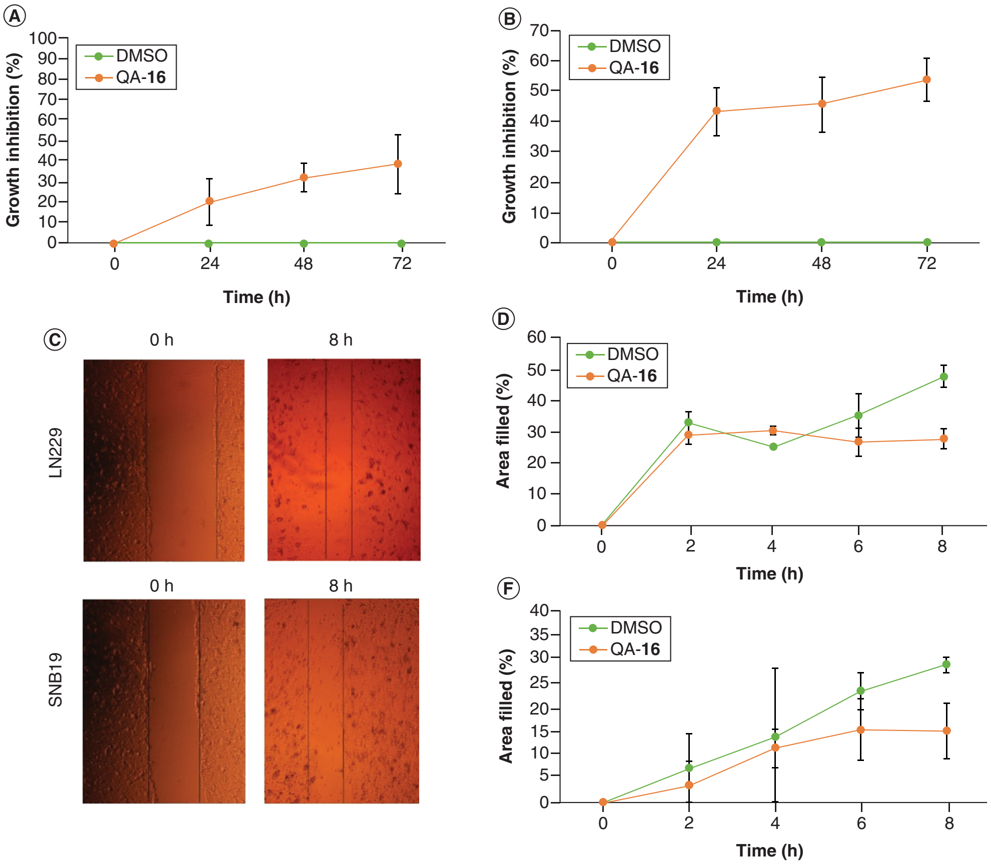

Figure 3. QA-16 affects glioblastoma cell growth. Cell viability of **(A)** LN229 and **(B)** SNB19 treated with IC$_{50}$ concentration, DMSO (positive control) and QA16 (test compound) at 0, 24, 48 and 72 h. **(C)** Microscope images of *in vitro* scratch assay at 0 h and 8 h for LN229 **(E)** and in SNB19. The dark lines outlines the areas lacking cells. **(D)** Percentage of area field at different time points of treatment with QA16 and DMSO in LN229 **(F)** and in SNB19. The significant differences between treated and controls groups are shown as *$p < 0.05$.
DMSO: Dimethyl sulfoxide; QA: Quinic acid.

LN229 & SNB19 and two patients' derived cell lines, RN1 & MMK1, which shows its potential anti-cytotoxicity effect.

QA-16 affects glioblastoma cell migration in a time lapse manner

To further evaluate the effect of QA-**16** in a time-dependent series, IC$_{50}$ concentration on the respective cell lines, LN229 and SNB19 was used. Figure 3A & B compares the time-dependent responses at 0, 24, 48 and 72 h on QA-**16** exposure. As time increases, QA-**16** caused a gradual increase in the cell growth inhibition in LN229 (38%) and in SNB19 (53%) at 72 h from the initial time of treatment. DMSO, negative control showed a negligible percentage of growth inhibition. Thus, our results suggest that QA-16 was able to increase the cytotoxicity in a time-dependent manner.

The *in-vitro* scratch assay was also performed to assess the effect of QA-**16** on the migration rate of both glioblastoma cell lines. The images were captured at 0, 2, 4, 6 and 8 h and the wound closure distance was calculated using Image J software. The calculated values were based on the scratch coverage rate up to 8 h. The migration analysis showed that for both QA-**16** treated cell lines, there is not much significant difference in the rate of migration when compared with DMSO until 4 h. Yet, when the treatment time is increased to 8 h, it showed significant decrease in the percentage of migration rate of about 27.6% for LN229 and 15% for SNB19, when compared with DMSO treated cells with the rate of 47.5 and 28.6%, respectively (Figure 3C–3F). Consequently, the ability of QA-**16** in inhibiting the migration of the glioblastoma cells was confirmed.

Characterization of QA-16 encapsulated PGLA

The QA-**16** was loaded into PLGA nanoparticles (QA-**16**-NP) by a solvent evaporation emulsion technique (Figure 4A). Number based distribution of size were measured by dynamic light scattering and the intensity distribution analysis for the characterization of the diameter of the nanoparticles are shown in Figure 4B. The nanoparticles were also observed by scanning electron microscopy (SEM), and they have shown a characteristic spherical shape, smooth surface and the size was in accordance with the DLS results (Figure 4C). The PLGA nanoparticles produced without the QA-**16** compound showed a particle size of 247 ± 7 nm and a narrow PDI value of 0.19 ± 0.01. Upon encapsulation of QA-**16**, a slight increase in particle size (322 ± 26 nm) and PDI (0.25 ± 0.02) were observed, which shows the association of the drug into the nanoparticles (Figure 4D).

Cytotoxic effect of QA-16-NPs

Time-dependent cytotoxicity study was performed by exposing glioblastoma cell lines with the IC_{50} concentration of QA-**16**, QA-**16**-NPs and NPs as described in the methods. The microscope images of cells treated with QA-**16**, and QA-**16**-NPs, showed the changes in the cellular morphology with least number of cells in both the cell lines upon treatment (Figure 5A). The untreated cells were found to have efficient cell growth with uniform monolayer. For LN229, there was no significant difference in the cell growth inhibition in QA-**16** and QA-**16**-NPs treated condition.

Specifically, it was found to have 26 and 43% for QA-**16** and 23 and 52% for QA-16-NPs at 48 and 72 h, respectively (Figure 5B). In case of SNB19, the cytotoxic effect of QA-**16** was significantly higher, which showed up to 72 and 81% and 54.53 and 54.16% for QA-16-NPs at 48 and 72 h, respectively (Figure 5C). However, the inhibition percentage for NPs alone was less which is below 10% up to 72 h. Thus, the above results show that the cytotoxicity of the QA-**16**-NPs was effective against LN229 than SNB19 at 72 h, thus performed differently in a cell specific and time-dependent manner. The cytotoxicity effect of NPs is highly dependent on the type of the cells they encounter, which might be due to the difference in the cell physiology, proliferation ability and various other characteristic features of the cell membrane [36]. Especially cancer cells are very strong toward the nanoparticle effect than the normal cell due to their increased proliferation rate, metastatic ability and higher metabolic rate [37,38]. It is also noted that the QA-**16**-NPs was highly cytotoxic than NPs alone in both the cell lines.

Induction of apoptosis by QA-16-NPs

To study the effect of NPs on the induction of apoptosis, the glioblastoma cells were treated with the IC_{50} concentration of QA-**16**, QA-**16**-NPs and NPs which were stained with annexin V/PI as described in methods. Annexin V, a phospholipid binding protein functions as a biomarker to identify the cells undergoing apoptosis and propidium iodide is a DNA binding stain that helps to differentiate necrotic cells from apoptotic cells. The changes in the cellular morphology such as reduction in nuclear size, chromatin condensation, and DNA fragmentation was observed under fluorescence microscope. Figure 6A correspond to the DMSO treated cells appearing as nonfluorescent and the treated cell lines as fluorescent bright orange-green-red stain of Annexin V/PI, that demonstrates the process of apoptosis. Figure 6B & C shows the necrosis and different stages of apoptosis in LN229 and SNB19 treated cells, respectively. Percentage of apoptosis on DMSO treated cells were <10% than the QA-**16** and QA-**16**-NPs in both the cell lines. In QA-**16** treated LN229 and SNB19 cells, around 5% and 0.1% of cells were in necrotic, 52 and 94% in early apoptotic and 33 and 5.39% in late apoptotic stage, respectively. Similarly, in QA-**16**-NPs treated LN229 and SNB19 cells, around 15 and 12% were in necrotic, 23 and 19% in early apoptosis and 45 and 26% in late apoptosis, respectively. These results confirm that, QA-**16**-NPs induced the cell death at a faster rate and henceforth higher percentage of late apoptotic cells were observed. Notably, QA-**16** treated cells show the presence of higher percentage of cells in early apoptosis, suggesting the rate of apoptosis is slower than QA-**16**-NPs.

Effect of QA-16-NPs on caspase & ROS production

Caspase, a family of cysteine proteases, plays key role in mediating many biochemical and morphological changes associated with apoptotic cells. Caspase activation is used as a biomarker for the detection of apoptosis process and

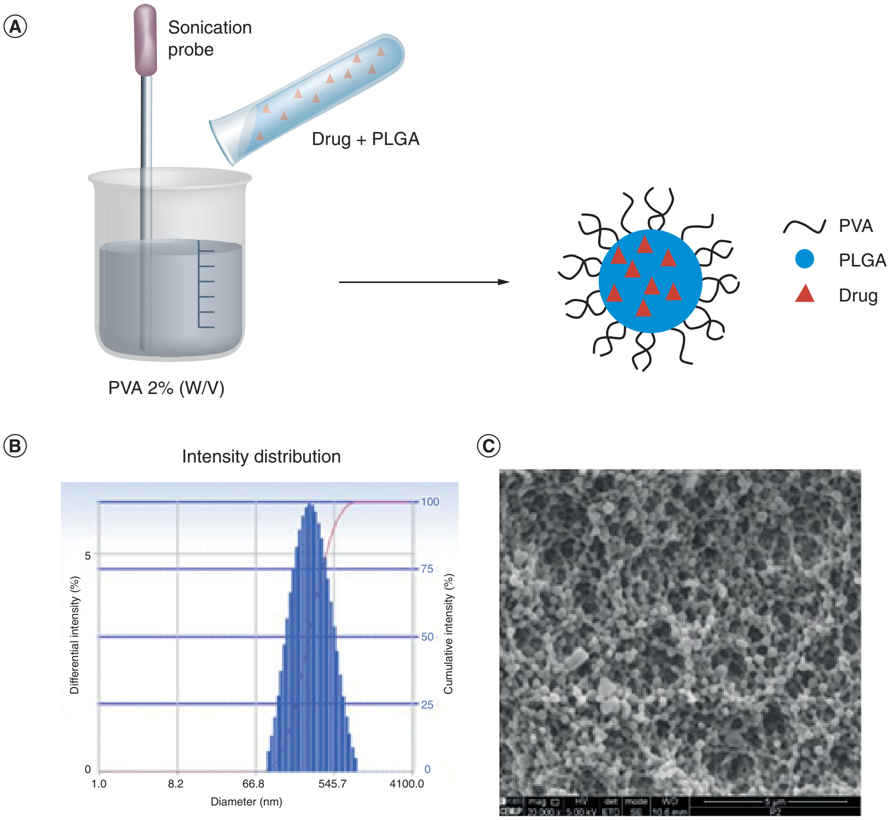

QA16-loaded PLGA Np

QA16-loaded PLGA Np (SEM)

Ⓓ

Formulation	Size (nm)	PdI
Unloaded nanoparticles	248 ± 7	0.19 ± 0.01
Loaded nanoparticles	322 ± 26	0.25 ± 0.02

Figure 4. Preparation of poly(lactic-co-glycolic acid) encapsulated nanoparticle. (A) Scheme to produce QA-**16** loaded PLGA nanoparticles. **(B)** Intensity distribution size of drug loaded PLGA NPs (QA-**16**-NPS s). The horizontal scale shows the diameter (nm) of the QA-**16**-NPs and the vertical scale shows the percentage of differential and cumulative intensities. **(C)** SEM microphotograph of QA-**16**-NPs **(D)** Particle characterization by DLS including size (nm) and PdI of unloaded NPs and loaded nanoparticle (QA-**16**-NPs).
DLS: Dynamic light scattering; NP: Nanoparticle; PLG: Poly(lactic-co-glycolic acid); QA: Quinic acid; SEM: Scanning electron microscope.

hence the influence of QA-**16**-NPs was assessed in glioblastoma cell lines. The results revealed that the QA-**16** and QA-**16**-NPs treated LN229 cells showed up to 1.6- and 1.7-fold increase in caspase3/7 activity, whereas SNB19 cells have 0.46- and 0.4-fold increase (Figure 7A). Thus, QA derivatives may induce apoptosis in LN229 than SNB19 cells by increasing the activation of caspase 3/7 pathway. Also, estimation on the amount of reactive oxygen species serves as a reliable source of oxidative stress. Upon treatment of LN229 with QA-**16** and QA-**16**-NPs, it showed a significance fold change of about 2.9 when compared with the control (H_2O_2). QA-**16**-NPs treated

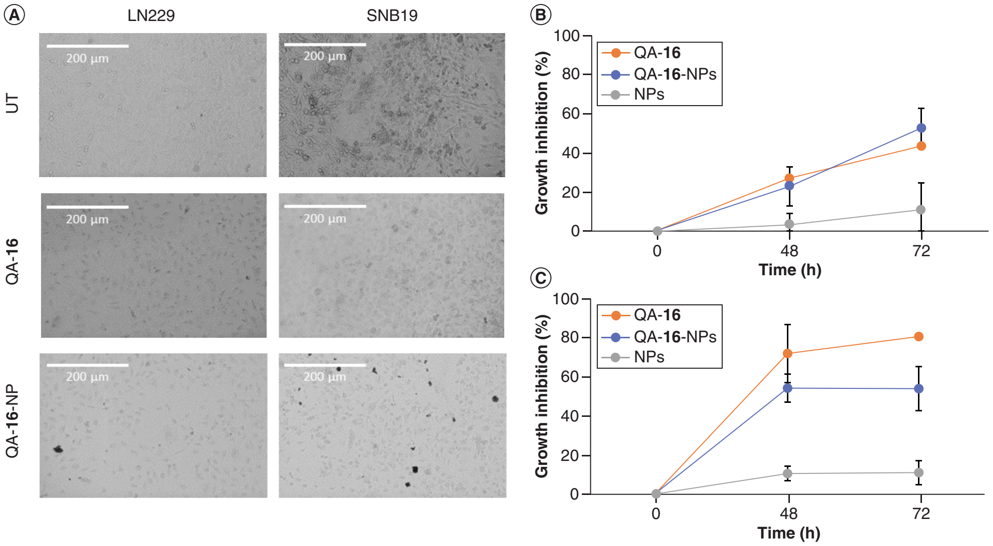

Figure 5. Cytotoxicity effect of QA-16-Nps on glioblastoma cell lines. (A) Microscopic images of untreated (control) LN229 and SNB19 cells on treatment with the IC_{50} concentration QA-**16** and QA-**16**-NPS s. **(B)** Percentage of cell growth inhibition of LN229 cells and **(C)** in SNB19 cells treated with IC_{50} concentration QA-**16** and QA-**16**-NPs versus control groups (NPs alone) at different time points. The significant differences between treated and controls groups are shown as $*p < 0.05$.

IC_{50}: Half maximal inhibitory concentration; NP: Nanoparticle; QA: Quinic acid.

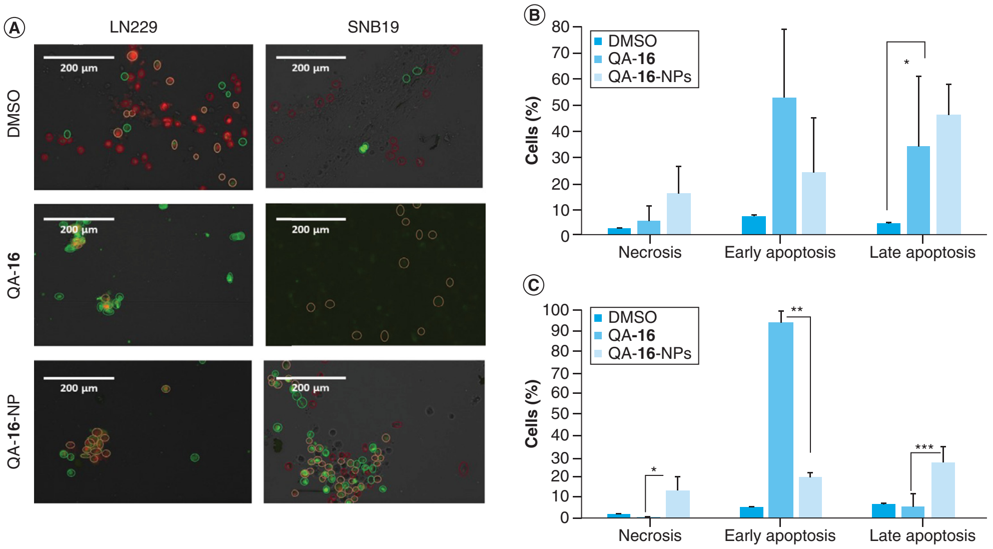

Figure 6. Apoptosis induction by QA-16-NPs by annexin V/PI stained glioblastoma cells. (A) Microscopic images of LN229 and SNB19 cells treated with DMSO (negative control), IC_{50} concentration of QA-**16**, QA-**16**-NPs; necrosis (nucleus is red), apoptosis (cell membrane is strongly stained with green and/or red) and live (cells with less or no fluorescence). **(B)** Percentage of apoptosis and necrosis in LN229 and **(C)** in SNB19 cells. The significant differences between treated and controls groups are shown as $*p < 0.05$.

DMSO: Dimethyl sulfoxide; NP: Nanoparticles; QA: Quinic acid.

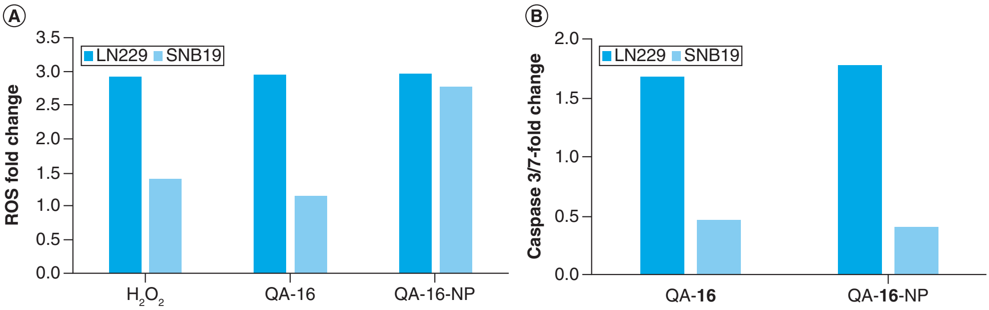

Figure 7. Activation of caspase 3/7 and reactive oxygen specie by QA-16-NPs. (A) Fold changes of caspase 3/7 in LN229 and SNB19 cells treated with IC_{50} concentration of QA-**16**, QA-**16**-NPs. **(B)** Fold changes of ROS in LN229 and SNB19 cells treated with IC_{50} concentration of QA-**16**, QA-**16**-NPs; H_2O_2 as the control. The significant differences between treated and controls groups are shown as $*p < 0.05$.
IC_{50}: Half maximal inhibitory concentration; NP: Nanoparticle; QA: Quinic acid; ROS: Reactive oxygen specie.

SNB19 cells has about 2.7-fold change with the difference of 1.6-fold in QA-**16** and 1.3-fold in H_2O_2 (Figure 7B). These experiments suggest that the cell death is induced not only by caspase 3/7 but also ROS mediated apoptosis. It is noted that NPs might be selectively toxic for particular cancerous cells lines [39,40]. Thus, the selective toxicity of QA-**16**-NPs against GS cell line might depend on cell type dependent intracellular responses.

Discussion

With recent advances in the biomedical field for the treatment of various types of cancers including GS, quinic acid derivatives has gained more attention as a pharmaceutically important chemical compound. It is nontoxic in nature and found to possess potent antioxidant, anti-viral, anti-microbial, anti-vascular, anti-inflammatory [41] and anticancer properties [14,16,42–44]. 3,5-dicaffeoyl-epi-quinic acid (DCEQA), which is a bioactive derivative of caffeoylquinic acid found to possess anti-obesity [45] and anti-photoaging abilities [46].

With such motivation, we have studied the potential use of chemically synthesized quinic acid derivatives against GS. By understanding its mechanism of action, the top lead compounds can be combined along with the available therapeutic agents for better treatment strategy.

Our results demonstrated that out of 16 novel derivatives, QA-**16** showed the best inhibitory effect on glioblastoma cell lines. Impairing the flexibility of the quinic acid core in the form of lactone is detrimental for the cytotoxic activity as seen for series **3–5**. Noticeably, such lack of cytotoxicity does not seem to be caused by electronic effects considering the moderate activity observed for the other carbonyl containing compounds **7–12**, although the presence of the tertiary hydroxyl group seems beneficial. The sulfate group is also detrimental given the lack of cytotoxicity of **3** and **13** against GS cell lines. Apart from the sulfates **3** and **13**, all compounds bearing a tertiary hydroxyl group (**7–12** and **16**) showed moderate to excellent cytotoxicity. Notably, the introduction of silyl ether groups, not only increased the lipophilicity but also the cytotoxic activity. Indeed, the presence of more lipophilic *tert*-butyldiphenylsilyl substituents increased the cytotoxic effect of the nonlactones when compared with its *tert*-butyldimethylsilyl analogues (**14** vs **15**).

The inhibitory concentration of QA-**16** against glioma cells was higher than the standard chemotherapeutic agent, TMZ. Multiple GS cell lines are found to be resistant to TMZ due to the overexpression of O^6-MGMT and/or lack of a DNA repair pathway [47]. Interestingly, the cytotoxicity effect of QA-targeted GS cells significantly more than nontumorous cells. Thus, QA-**16** selectively inhibits the cancer cells which might be by interfering with a specific molecule or signal transduction pathways overexpressed in cancer cells [48]. Similarly, several studies show promising anti-cancer activity such as 3,5-dicaffeoyl-epi-quinic acid (DCEQA) with matrix MMP inhibitory properties [49] and 3-Caffeoyl, 4-dihydrocaffeoylquinic acid from *Salicornia herbacea* prevents tumor cell invasion by inhibiting transcription factor AP-1 and regulating protein kinase C-δ-dependent matrix metalloproteinase-9 expression [50].

We have elucidated the effects of QA-**16** on cellular migration, where the migration rate was greatly reduced in GS cells over time. The ability of the compound to reduce the migration of cells is considered a vital process, where the deregulated cell migration might contribute to many pathological conditions such as inflammation and cancer metastasis [51–53]. Thus, QA-**16** might function as a potent drug on inhibiting the metastasis condition in the tumor microenvironment.

The development of synthetic nanoparticles using PLGA and PLA is preferred for the long-term sustainable delivery of drugs (days or even weeks) than the natural polymers. Also, it has been reported that new brain targeted polymeric PLGA-NPs modified with g7-NPs)successfully creates interaction with blood–brain barrier (BBB) and efficiently cross it [54]. The comparative cytotoxicity efficacy of QA-**16**-NPs against GS cells was analyzed, that showed higher toxicity to LN229 followed by SNB19. Thus, PLGA as a highly stable biocompatible polymer helps in the release of the drug for inducing cytotoxicity.

The ability to trigger apoptosis in tumor cells is an important cellular process for cancer treatment. Considering this fact, we have studied the apoptosis in the glioma cells, where the QA-**16**-NPs have enforced the apoptotic process at a faster rate with the cells to enter the late apoptosis having compromised cell membrane. Similar investigation on oral squamous cancer cells identified the role of QA in inducing apoptosis by reducing the expression of Bcl-2 and BAX [4]. The apoptotic conditions may be achieved due to the release of proinflammatory intracellular contents like caspase and ROS. Typically, ROS accumulation disturbs the cell cycle progression through regulatory proteins like cyclins, Cdks and Cdk inhibitors leading to apoptosis [55]. Thus, QA-**16**-NPs was found to induced Caspase 3/7, a proapoptotic protein and ROS to a significant fold higher level, thus substantiating the strategy of apoptosis.

Conclusion

This study has provided preliminary evidence that the quinic acid derivative QA-**16** could potentially function as a cytotoxicity agent against glioblastoma. Nanoencapsulation of QA-**16** also have similar cytotoxicity effect against the GS cells. QA-**16** and QA-**16**-NPs could be a chemotherapeutic agent that induces programmed cell death through Caspase 3/7 and ROS mediated pathway. Thus, with the in-vitro analysis, the safety of nanoparticle in treating glioblastoma has been proven as a promising vehicle for deployment of anti-glioblastoma drugs.

Future perspective

The study clearly demonstrated that the cytotoxicity properties of quinic acid as a better drug candidate. The comparative analysis with the known chemotherapeutic agent, temozolomide, emphasize the greater drug potential and higher toxicity of quinic acid, illustrated the application of newly synthesized QA-**16** ([1R,3R,4S,5R]-4,5-bis([*tert*-butyldiphenylsilyl]oxy)-1-(hydroxymethyl)cyclohexane-1,3-diol) as one of the future anti-glioblastoma drug. Our results support that QA-**16**-NP can exploit the interaction with cell membrane and deliver anticancer drugs to tumors to induce cell death. In the future, a more complete *in-vivo* optimization of QA-**16**-NP could be done which will make the discovery of novel anti-glioma drug candidates to prevent the metastasis.

Summary points

- Quinic acid (QA)-**16**, a quinic acid-derived triol with a primary, secondary and tertiary hydroxyl groups was identified as a top lead compound with higher cytotoxicity.
- QA-**16** exerts highest cytotoxicity effect specifically against glial cells and patients 'derived cell lines than normal cells.
- QA-**16** affects proliferation and migration of glioblastoma cells in a dose- and time-dependent manner.
- Poly(lactide-co-glycolide) encapsulated QA-**16** (QA-**16**-NPs) and QA-**16** exerts similar growth inhibition in GS cells.
- QA-**16** and QA-**16**-NPs induces apoptosis through caspase 3/7 and ROS mediated signaling pathway.

Supplementary data

To view the supplementary data that accompany this paper please visit the journal website at: www.future-science.com/doi/suppl/10.4155/fmc-2020-0194

Financial & competing interests disclosure

The Academy of Finland is duly acknowledged for financial support to NRC (no. 326487 and 326486), Finnish Cultural Foundation is acknowledged for financial support to S Holmstedt (no. 00190336). A Murugesan and O Yli-Harja acknowledge the Academy of Finland for the project grant support (no. 297200). This study received Portuguese national funds from FCT – Foundation for Science and Technology through projects UIDB/04326/2020, UIDB/04565/2020 and UIDB/50006/2020. The authors have no

other relevant affiliations or financial involvement with any organization or entity with a financial interest in or financial conflict with the subject matter or materials discussed in the manuscript apart from those disclosed.

No writing assistance was utilized in the production of this manuscript.

References

1. Stupp R, Mason W, van den Bent MJ *et al.* Radiotherapy plus concomitant\nand adjuvant temozolomide for glioblastoma. *N. Engl. J. Med.* 352, 987–996 (2005).
2. Davis ME. Glioblastoma: overview of disease and treatment. *Clin. J. Oncol. Nurs.* 20(Suppl. 5), S2–S8 (2016).
3. Nurgali K, Jagoe RT, Abalo R. Editorial: adverse effects of cancer chemotherapy: anything new to improve tolerance and reduce sequelae? *Front. Pharmacol.* 9, 245 (2018).
4. Singh A, Chauhan SS, Tripathi V. Quinic acid attenuates oral cancer cell proliferation by downregulating cyclin D1 expression and Akt signaling. *Pharmacogn. Mag.* 14(55), 14 (2018).
5. Viswanathan A, Kute D, Musa A *et al.* 2-(2-(2,4-dioxopentan-3-ylidene)hydrazineyl)benzonitrile as novel inhibitor of receptor tyrosine kinase and PI3K/AKT/mTOR signaling pathway in glioblastoma. *Eur. J. Med. Chem.* 166, 291–303 (2019).
6. Viswanathan A, Musa A, Murugesan A *et al.* Battling glioblastoma: a novel tyrosine kinase inhibitor with multi-dimensional anti-tumor effect (running title: cancer cells death signalling activation). *Cells.;* 8(12), 1624 (2019).
7. Doan P, Musa A, Murugesan A *et al.* Glioblastoma multiforme stem cell cycle arrest by alkylaminophenol through the modulation of EGFR and CSC signaling pathways. *Cells* 9(3), 681 (2020).
8. Padmini E, Inbathamizh L. Quinic acid as a potent drug candidate for prostate cancer - a comparative pharmacokinetic approach. *Asian J. Pharm. Clin. Res.* 6(4), 106–112 (2013).
9. Fiuza SM, Gomes C, Teixeira LJ *et al.* Phenolic acid derivatives with potential anticancer properties – a structure–activity relationship study. Part 1: methyl, propyl and octyl esters of caffeic and gallic acids. *Bioorg. Med. Chem.* 12(13), 3581–3589 (2004).
10. Candeias NR, Assoah B, Simeonov SP. Production and synthetic modifications of shikimic acid. *Chem. Rev.* 118(20), 10458–10550 (2018).
11. Pero RW. Health consequences of catabolic synthesis of hippuric acid in humans. *Curr. Clin. Pharmacol.* 5(1), 67–73 (2010).
12. Karin M. NF-kappaB as a critical link between inflammation and cancer. *Cold Spring Harb. Perspect. Biol.* 1(5), a000141 (2009).
13. Zeng K, Thompson KE, Yates CR, Miller DD. Synthesis and biological evaluation of quinic acid derivatives as anti-inflammatory agents. *Bioorganic Med. Chem. Lett. [Internet].* 19(18), 5458–5460 (2009).
14. Toutounchian JJ, Steinle JJ, Makena PS *et al.* Modulation of radiation injury response in retinal endothelial cells by quinic acid derivative KZ-41 involves p38 MAPK. *PLoS ONE* 9(6), e100210 (2014).
15. He H, Weir RL, Toutounchian JJ *et al.* The quinic acid derivative KZ-41 prevents glucose-induced caspase-3 activation in retinal endothelial cells through an IGF-1 receptor dependent mechanism. *PLoS ONE* 12(8), e0180808 (2017).
16. Zanello PR, Koishi AC, Rezende Junior Cde O *et al.* Quinic acid derivatives inhibit dengue virus replication *in vitro*. *Virol. J.* 12, 223 (2015).
17. Laubli H, Borsig L. Selectins promote tumor metastasis. *Semin. Cancer Biol.* 20(3), 169–177 (2010).
18. Kaila N, Somers WS, Thomas BE *et al.* Quinic acid derivatives as sialyl Lewisx-mimicking selectin inhibitors: design, synthesis, and crystal structure in complex with E-selectin. *J. Med. Chem.* 48(13), 4346–4357 (2005).
19. Girard C, Dourlat J, Savarin A *et al.* Sialyl Lewisx analogs based on a quinic acid scaffold as the fucose mimic. *Bioorganic Med. Chem. Lett. [Internet].* 15(13), 3224–3228 (2005).
20. Shamay Y, Paulin D, Ashkenasy G, David A. Multivalent display of quinic acid based ligands for targeting E-selectin expressing cells. *J. Med. Chem.* 52(19), 5906–5915 (2009).
21. Huang S, Wang LL, Xue NN *et al.* Chlorogenic acid effectively treats cancers through induction of cancer cell differentiation. *Theranostics* 9(23), 6745–6763 (2019).
22. Amoozgar Z, Park J, Lin Q, Weidle JH, Yeo Y. Development of quinic acid-conjugated nanoparticles as a drug carrier to solid tumors. *Biomacromolecules* 14(7), 2389–2395 (2013).
23. Schwendeman SP. Recent advances in the stabilization of proteins encapsulated in injectable PLGA delivery systems. *Crit. Rev. Ther. Drug Carrier Syst.* 19(1), 73–98 (2002).
24. Mohamed F, Van Der Walle CF. Engineering biodegradable polyester particles with specific drug targeting and drug release properties. *J. Pharm. Sci.* 24(1), 71–87 (2008).
25. Ramalho MJ, Sevin E, Gosselet F *et al.* Receptor-mediated PLGA nanoparticles for glioblastoma multiforme treatment. *Int. J. Pharm.* 545(1-2), 84–92 (2018).
26. Jain A, Chasoo G, Singh SK, Saxena AK, Jain SK. Transferrin-appended PEGylated nanoparticles for temozolomide delivery to brain: *in vitro* characterisation. *J. Microencapsul.* 28(1), 21–28 (2011).

27. Marucci G, Lammi C, Buccioni M *et al.* Comparison and optimization of transient transfection methods at human astrocytoma cell line 1321N1. *Anal. Biochem.* 414(2), 300–302 (2011).
28. Attardi LD, de Vries A, Jacks T. Activation of the p53-dependent G1 checkpoint response in mouse embryo fibroblasts depends on the specific DNA damage inducer. *Oncogene* 23(4), 973–980 (2004).
29. Xu W, Baribault H, Adamson ED. Vinculin knockout results in heart and brain defects during embryonic development. *Development* 125(2), 327–337 (1998).
30. Chung I-M, Kim M-Y, Park W-H, Moon H-I. Quinic acid derivatives from *Saussurea triangulata* attenuates glutamate-induced neurotoxicity in primary cultured rat cortical cells. *J. Enzym. Inhib. Med. Chem.* 24(1), 188–191 (2009).
31. Lee MW Jr, Sevryugina Y V, Khan A, Ye SQ. Carboranes increase the potency of small molecule inhibitors of nicotinamide phosphoribosyltranferase. *J. Med. Chem.* 55(16), 7290–7294 (2012).
32. Fonte P, Soares S, Sousa F *et al.* Stability study perspective of the effect of freeze-drying using cryoprotectants on the structure of insulin loaded into PLGA nanoparticles. *Biomacromolecules* 15(10), 3753–3765 (2014).
33. Paci A, Veal G, Bardin C *et al.* Review of therapeutic drug monitoring of anticancer drugs part 1 – cytotoxics. *Eur. J. Cancer* 50(12), 2010–2019 (2014).
34. Chang MC. Areca nut extract and arecoline induced the cell cycle arrest but not apoptosis of cultured oral KB epithelial cells: association of glutathione, reactive oxygen species and mitochondrial membrane potential. *Carcinogenesis* 22(9), 1527–1535 (2001).
35. Assoah B, Veiros LF, Afonso CAM, Candeias NR. Biomass-based and oxidant-free preparation of hydroquinone from quinic acid. *European J. Org. Chem.* (22), 3856–3861 (2016).
36. Díaz B, Sánchez-Espinel C, Arruebo M *et al.* Assessing methods for blood cell cytotoxic responses to inorganic nanoparticles and nanoparticle aggregates. *Small* 4(11), 2025–2034 (2008).
37. Nan A, Bai X, Son SJ, Lee SB, Ghandehari H. Cellular uptake and cytotoxicity of silica nanotubes. *Nano Lett.* 8(8), 2150–2154 (2008).
38. Chang JS, Chang KLB, Hwang DF, Kong ZL. *In vitro* cytotoxicitiy of silica nanoparticles at high concentrations strongly depends on the metabolic activity type of the cell line. *Environ. Sci. Technol.* 41(6), 2064–2068 (2007).
39. Namvar F, Rahman HS, Mohamad R *et al.* Cytotoxic effects of biosynthesized zinc oxide nanoparticles on murine cell lines. *Evidence-based Complement. Altern. Med.* 1–11 (2015).
40. SL M, VM E. Cytotoxicity in MCF-7 and MDA-MB-231 breast cancer cells, without harming MCF-10A healthy cells. *J. Nanomed. Nanotechnol.* 7(2), 1–11 (2016).
41. Peng W, Ming QL, Han P *et al.* Anti-allergic rhinitis effect of caffeoylxanthiazonoside isolated from fruits of *Xanthium strumarium L.* in rodent animals. *Phytomedicine* 21(6), 824–829 (2014).
42. Roleira FMF, Tavares-Da-Silva EJ, Varela CL *et al.* Plant derived and dietary phenolic antioxidants: anticancer properties. *Food Chem.* 183, 235–258 (2015).
43. Jang SA, Park DW, Kwon JE *et al.* Quinic acid inhibits vascular inflammation in TNF-α-stimulated vascular smooth muscle cells. *Biomed. Pharmacother.* 96, 563–571 (2017).
44. He X, Rui HL. Cranberry phytochemicals: isolation, structure elucidation, and their antiproliferative and antioxidant activities. *J. Agric. Food Chem.* 54(19), 7069–7074 (2006).
45. Oh JH, Lee JI, Karadeniz F, Seo Y, Kong CS. 3,5-dicaffeoyl-epi-quinic acid isolated from edible halophyte atriplex gmelinii inhibits adipogenesis via AMPK/MAPK pathway in 3T3-L1 adipocytes. *Evidence-based Complement. Altern. Med.* 2018, 1–8 (2018).
46. Oh JH, Lee JI, Karadeniz F, Park SY, Seo Y, Kong CS. Antiphotoaging rffects of 3,5-dicaffeoyl-epi-quinic acid via inhibition of matrix metalloproteinases in UVB-irradiated human keratinocytes. *Evidence-based Complement. Altern. Med.* 2020, 1–10 (2020).
47. Lee SY. Temozolomide resistance in glioblastoma multiforme. *Genes Dis.* 3(3), 198–210 (2016).
48. Darzynkiewicz Z. Novel strategies of protecting non-cancer cells during chemotherapy: are they ready for clinical testing? *Oncotarget.* 2(3), 107–108 (2011).
49. Lee JI, Kil JH, Yu GH *et al.* 3,5-Dicaffeoyl-epi-quinic acid inhibits the PMA-stimulated activation and expression of MMP-9 but not MMP-2 via downregulation of MAPK pathway. *Z. Naturforsch. C.* 75(3–4), 113–120 (2020).
50. Hwang YP, Yun HJ, Choi JH *et al.* 3-Caffeoyl, 4-dihydrocaffeoylquinic acid from Salicornia herbacea inhibits tumor cell invasion by regulating protein kinase C-δ-dependent matrix metalloproteinase-9 expression. *Toxicol. Lett.* 198(2), 200–209 (2010).
51. Van Helvert S, Storm C, Friedl P. Mechanoreciprocity in cell migration. *Nat. Cell Biol.* 20, 8–20 (2018).
52. Charras G, Sahai E. Physical influences of the extracellular environment on cell migration. *Nat. Rev. Mol. Cell Biol.* 15, 813–824 (2014).
53. Mayor R, Etienne-Manneville S. The front and rear of collective cell migration. *Nat. Rev. Mol. Cell Biol.* 17, 97–109 (2016).
54. Tosi G, Bortot B, Ruozi B *et al.* Potential use of polymeric nanoparticles for drug delivery across the blood–brain barrier. *Curr. Med. Chem.* 20(17), 2212–2225 (2013).
55. Verbon EH, Post JA, Boonstra J. The influence of reactive oxygen species on cell cycle progression in mammalian cells. *Gene* 511(1), 1–6 (2012).